

University of Warwick institutional repository: <http://go.warwick.ac.uk/wrap>

A Thesis Submitted for the Degree of PhD at the University of Warwick

<http://go.warwick.ac.uk/wrap/57457>

This thesis is made available online and is protected by original copyright.

Please scroll down to view the document itself.

Please refer to the repository record for this item for information to help you to cite it. Our policy information is available from the repository home page.

**Isolation of environmental lignin-
degrading bacteria and identification of
extracellular enzymes**

By

Charles Robert Taylor

A thesis submitted in partial fulfillment of the requirements for the
degree of Doctor of Philosophy

Department of Chemistry, University of Warwick

April 2013

Table of Contents

Table of Contents	2
List of Figures	9
List of Tables	22
List of Abbreviations	27
Acknowledgements	31
Declaration	32
Abstract	33
Chapter 1: Introduction	34
1.1. Renewable energy and biorefining	34
1.2. First and second-generation biofuels	35
1.3. Lignocellulose	36
1.3.1. Cellulose	37
1.3.2. Hemicellulose	38
1.3.3. Lignin	39
1.3.4. Cellulosic bioethanol production	40
1.3.5. Existing pre-treatment methods	42
1.3.5.1. Physical methods	42
1.3.5.2. Chemical methods	43
1.3.5.3. Biological methods	46
1.4. Lignin	47
1.4.1. Lignin Biosynthesis	50
1.4.2. Characterization of lignin	53
1.5. Microbial breakdown of lignin	55

1.5.1. Degradation of lignin by fungi	56
1.5.2. Bacterial degradation of lignin	64
1.5.2.1. Breakdown patterns	64
1.5.2.2. Bacterial lignin degradation pathways	65
1.5.2.3. Thermotolerant lignin-degrading bacteria	72
1.6. Assays for monitoring lignin breakdown	72
1.6.1. Nitrated lignin assays	74
1.7. Project aims	77
Chapter 2: Screening for environmental lignin-degrading bacteria	79
2.1. Introduction	79
2.2. Development of nitrated lignin assays	80
2.2.1. Development of a novel nitration method for the preparation of nitrated lignin solution	80
2.2.2. UV/visible nitrated lignin assays for nitrated MWL samples A, B and C with previously studied lignin-degrading bacteria	81
2.2.3. Development of the nitrated lignin spray assay	83
2.3. Screening for lignin-degrading bacteria from soil samples	85
2.3.1. Sourcing of samples and enrichment of bacteria	85
2.3.2. Nitrated lignin spray assay for soil isolates	86
2.3.3. UV/visible nitrated lignin assays for isolated soil bacteria	89
2.3.3.1. 'Active' isolates from the spray assay	89

2.3.3.2. 'Inactive' isolates from the spray assay	92
2.3.3.3. Validation of the nitrated lignin assays	94
2.3.4. Identification of isolated lignin-degrading bacteria	95
2.4. Screening for thermotolerant lignin-degrading bacteria	96
2.4.1. Nitrated lignin spray assay for thermotolerant isolates	97
2.4.2. UV/visible nitrated lignin assay for thermo- tolerant isolates	99
2.5. Conclusions	100
Chapter 3: Characterization of environmental lignin-degrading bacteria	103
3.1. Introduction	103
3.2. Growth in liquid media	104
3.2.1. LB broth	104
3.2.2. M9 salts supplemented with glucose and yeast extract	105
3.2.3. M9 salts supplemented with Kraft lignin and/or glucose, and yeast extract	107
3.3. Temperature-dependent growth of thermo- tolerant isolates	111
3.4. Growth on aromatic carbon sources, glucose and cellulose	112

3.5. Transmission Electron Microscopy of	116
<i>Sphingobacterium sp.</i>	
3.6. Biotransformation of Kraft lignin	117
3.6.1. Size-fractionation of Kraft lignin	117
3.6.2. Inoculation of previously studied lignin- degrading bacteria with size-fractionated Kraft lignin	118
3.6.3. Incubation of environmental lignin-degrading bacteria with size-fractionated Kraft lignin.	120
3.7. Bioconversion of lignin-containing feedstocks	126
3.7.1. Bioconversion of wheat straw	128
3.7.2. Bioconversion of Organosolv lignin	138
3.7.3. Bioconversion of Kraft lignin	145
3.8. Conclusions	151
Chapter 4: Purification of extracellular	153
lignin-degrading enzymes from <i>M.</i>	
<i>phyllosphaerae</i> and <i>Sphingobacterium sp.</i>	
4.1. Introduction	153
4.2. Purification of extracellular lignin-degrading	156
enzymes from <i>M. phyllosphaerae</i>	
4.2.1. Anion exchange chromatography	156
4.2.2. Hydrophobic interaction chromatography	159
4.3. Purification of extracellular lignin-degrading	162
enzymes from <i>Sphingobacterium sp.</i>	
4.3.1. Anion exchange chromatography	164

4.3.2. Hydrophobic Interaction chromatography of SAE 1	167
4.3.3. Hydrophobic Interaction chromatography of SAE 2	176
4.3.3.1. Purification of SAE 2 fraction 18 via gel filtration FPLC	179
4.4. Conclusions	186
Chapter 5: Conclusions and future work	189
Chapter 6: Experimental	192
6.1. Screening for environmental lignin-degrading bacteria	192
6.1.1. Preparation of nitrated MWL solution	192
6.1.2. Sourcing and enrichment of cultures	192
6.1.3. UV/visible nitrated lignin assay for nitrated MWL samples A, B and C	193
6.1.4. Media Recipes	194
6.1.5. Nitrated lignin spray assay	195
6.1.6. UV/visible nitrated lignin assays for environmental lignin-degrading bacteria	196
6.1.7. Identification of environmental lignin-degrading bacteria	196
6.2. Characterization of environmental lignin-degrading bacteria	197
6.2.1. Growth in liquid media	197

6.2.2. Growth on aromatic carbon sources and cellulose	197
6.2.3. Temperature-dependent growth of thermo-tolerant strains	197
6.2.4. Transmission Electron Microscopy	198
6.2.5. Fractionation of Kraft lignin by aqueous gel filtration chromatography	198
6.2.6. Incubation of size-fractionated Kraft lignin with lignin-degrading bacteria	198
6.2.7. Bioconversion of lignin and lignocellulose	199
6.2.7.1. Estimation of CFU composition of each sample	200
6.2.7.2. Determination of soluble phenolic content	200
6.2.7.3. Determination of total reducing sugar content	201
6.2.7.4. pH measurements	202
6.2.7.5. FT–IR measurements	202
6.3. Purification of extracellular enzymes	203
6.3.1. Collection of culture supernatant for enzyme purification	203
6.3.2. Ammonium sulfate precipitation	203
6.3.3. Q-sepharose anion exchange column chromatography	204
6.3.4. TCA precipitation	204
6.3.5. Concentration and desalting of protein samples	205

6.3.6. UV/visible nitrated lignin assays for samples of partially purified enzyme	205
6.3.7. ABTS assays	206
6.3.8. Protein characterization by SDS–PAGE	206
6.3.8.1. Preparation of polyacrylamide gels	206
6.3.8.2. Preparation of protein samples	207
6.3.8.3. Electrophoresis	207
6.3.8.4. Coomassie Brilliant Blue–R250 staining	207
6.3.8.5. Silver Staining	208
6.3.9. Phenyl-sepharose hydrophobic interaction chromatography	209
6.3.10. Gel filtration FPLC	209
6.3.11. Determination of protein concentration	209
6.3.12. Identification of proteins by tryptic digest and nano LC–ESI–MS/MS	210
6.3.13. Solution-based tryptic digest and protein identification by nano LC–ESI–MS/MS	211
References	212

List of Figures

Figure 1.1. Biorefinery concept of the National Renewable Energy Laboratory (NREL).	34
Figure 1.2. Structural arrangement of the lignocellulose polymer matrix in vascular plants.	36
Figure 1.3. Structure of the repeating unit of cellulose	38
Figure 1.4. Chemical structures of xylan (1) and mannan (2), two different forms of hemicellulose.	38
Figure 1.5. Chemical structures of the primary precursors of lignin: <i>trans-p</i> -coumaryl alcohol (1), <i>trans</i> -coniferyl alcohol (2) and <i>trans</i> -sinapyl alcohol (3).	39
Figure 1.6. Stages in the production of bioethanol and other products from lignocellulose. The energy-intensive pre-treatment step is discussed in the text.	41
Figure 1.7. α -aryl ether cleavage in phenolic aryl-propane units during the Kraft pulping process.	45
Figure 1.8. Mechanistic detail of β -aryl ether cleavage in non-phenolic aryl-propane units during the Kraft pulping process.	45
Figure 1.9. Chemical structure of lignin derived from Beech as suggested by Nimtz.	48
Figure 1.10. Chemical structures of the dominant units	49

of the lignin polymer: β -O-4' (1), 5-5' (2), β -5' (3), β - β' (4) and β -1' (5).

Figure 1.11. Structural component of lignin, with the low-stability α -aryl ether linkages indicated by dotted circles **50**

Figure 1.12. Conversion of phenylalanine into cinnamic acid by phenylalanine lyase (PAL). **50**

Figure 1.13. Chemical structures of H-, G- and S-type monolignols. **51**

Figure 1.14. Various stages in the natural biosynthesis of the dominant structural units β - β , β -5 and β -O-4 from G-, H- and S-type monolignols, which are derived from phenylalanine. **52**

Figure 1.15. Acetyl derivatization of lignin by acetyl bromide for solubility under acidic conditions. **55**

Figure 1.16. Chemical structures of the characteristic lignin oxidation products *p*-hydroxyl (4), vanillyl (5) and syringyl (6). **56**

Figure 1.17. Oxidative cleavage of the lignin structure by lignin peroxidase (LiP). **57**

Figure 1.18. Crystal structure of lignin peroxidase (LiP) from *P. chrysosporium*. **58**

Figure 1.19. An illustration of the general catalytic cycle of peroxidases. **58**

Figure 1.20. Catalytic mechanism of manganese peroxidase (MnP).	59
Figure 1.21. Oxidation of catechol by laccase.	60
Figure 1.22. Crystal structure of the laccase active site, illustrating the mononuclear and trinuclear Cu sites.	61
Figure 1.23. Mechanistic detail of the side chain cleavage of a phenolic β -O-4-lignin model compound by laccase from <i>C. versicolor</i> .	62
Figure 1.24. Reactions occurring for oxalate.	63
Figure 1.25. Suggested reactions for the abiotic decomposition of malonate.	63
Figure 1.26. Biphenyl ring cleavage pathway.	66
Figure 1.27. β -aryl ether cleavage pathway in <i>S. paucimobilis</i> SYK-6 and subsequent catabolic pathways.	67
Figure 1.28. β -keto adipate pathway	68
Figure 1.29. Ferulic acid catabolic pathway in <i>B. coagulans</i> BK07.	68
Figure 1.30. Catalytic cycle of DyP B, in which β -aryl ether (1) is converted into vanillin (2) or guaiacol (3)	70
Figure 1.31. Nitration of lignin via reaction with tetranitromethane, the molecular basis of the nitrated lignin assays.	75

- Figure 1.32.** Nitrated lignin spray assay, showing yellow coloration for *P. putida* mt-2 (centre-left) and *R. jostii* RHA1 (centre-right), and no coloration for non-degraders *B. subtilis* (far-left) and *L. mesenteroides* (far-right), after 24 hr incubation at 30 °C. **76**
- Figure 2.1.** Change in absorbance at 430 nm from 0–20 min for reaction of the culture supernatant of known lignin-degrading bacteria *P. putida* mt-2 and *R. jostii* RHA1 and non lignin-degrader *B. subtilis* with nitrated MWL samples A, B and C in the presence of 2 mM H₂O₂. An additional control experiment was performed in which the culture supernatant was replaced with 113 mM Tris buffer (pH 7.4) containing 7.5 mM NaCl. **81**
- Figure 2.2.** Nitrated lignin spray assay for soil isolates. **87**
- Figure 2.3.** Change in absorbance at 430 nm from 0–20 min following reaction of the culture supernatant of isolates that appeared to be active towards lignin degradation in the nitrated lignin spray assay, with 2 mM H₂O₂ and nitrated MWL. **90**
- Figure 2.4.** Change in absorbance at 430 nm from 0–20 min following reaction of the culture supernatants of isolates that appeared ‘inactive’ towards lignin degradation in the nitrated lignin spray assay, with 2 **93**

mM H₂O₂ and nitrated MWL.

Figure 2.5. Validation of the screening protocol for **94**

lignin-degradation activity, via relative activity of ‘active’ and ‘inactive’ isolates from the nitrated lignin spray assay, using the UV/visible nitrated lignin assay.

Activity in the presence of 2 mM H₂O₂ (y-axis) is plotted against activity in the absence of H₂O₂ (x-axis).

Figure 2.6. Nitrated lignin spray assay for **98**

thermotolerant strain *Sphingobacterium sp.* The left-hand plate, sprayed with nitrated MWL solution, shows a significant yellow colouration compared with the unsprayed right-hand plate.

Figure 2.7. Change in absorbance at 430 nm from 0– **99**

20 min following reaction of nitrated MWL solution with the culture supernatants of the thermotolerant strains and previously studied lignin-degrading bacteria *P. putida* mt-2 and *R. jostii* RHA1, in the presence and absence of 2 mM H₂O₂.

Figure 3.1. OD₆₀₀ of cultures of environmental lignin- **104**

degrading bacteria, grown in LB broth, at various time points: 24 hr, 48 hr, 72 hr, 96 hr and 120 hr.

Figure 3.2. OD₆₀₀ of liquid cultures of environmental **105**

lignin-degrading bacteria grown in M9 salt solution supplemented with glucose (2.0 % v/v) and yeast extract (0.5 % w/v) for 24 hr, 48 hr, 72 hr, 96 hr and

120 hr.

- Figure 3.3.** OD₆₀₀ of liquid cultures of environmental lignin-degrading bacteria in M9 salts supplemented with: a) glucose (2.0 % v/v) and yeast extract (0.5 % w/v) and b) Kraft lignin (2.0 % w/v), glucose (2.0 % v/v) and yeast extract (0.5 % w/v). Readings were taken every 24 hours for a total period of 336 hours. **108**
- Figure 3.4.** Structures of carbon sources: biphenyl (1), vanillic acid (2), veratryl alcohol (3), *m*-cresol (4), *p*-cresol (5), ferulic acid (6) and cellulose (7). **112**
- Figure 3.5.** Transmission electron micrograph of *Sphingobacterium sp.*, grown in LB broth at 45 °C. Scale bar (bottom left) 1 μmol⁻¹, courtesy of Dr. E. Hardiman. **116**
- Figure 3.6.** Absorbance of various size-fractions of Kraft lignin at 280 nm. The molecular weight decreases from high (fraction 1) to low (fraction 16). **118**
- Figure 3.7.** Gel filtration HPLC analysis of the breakdown of size-fractionated high-molecular weight (A) and low-molecular weight (B) forms of Kraft lignin by *Sphingobacterium sp.*, in the presence of M9 salts at 45 °C. **121**
- Figure 3.8.** Gel filtration HPLC analysis of the breakdown of high-molecular weight (A, C) and low-molecular weight (B, D) forms of Kraft lignin by *M.* **123**

marinilacus (left) and *M. phyllosphaerae* (right), in the presence of M9 salts at 30 °C.

Figure 3.9. Gel filtration HPLC analysis of the **125**

breakdown of high-molecular weight (A, C) and low-molecular weight (B, D) forms of Kraft lignin by *M. oxydans* (left) and *R. erythropolis* (right), in M9 salt solution at 30 °C.

Figure 3.10. Number of CFUs per ml in samples of **128**

wheat straw (2.5 % w/v) treated with *M. phyllosphaerae*, *R. erythropolis* and *Sphingobacterium sp.* in the presence of fish meal or CSL, taken after 48, 96, 168, 240 and 336 hr.

Figure 3.11. Soluble phenol content of samples of **129**

wheat straw (2.5 % w/v) treated with *M. phyllosphaerae*, *R. erythropolis* and *Sphingobacterium sp.* in the presence of fish meal or CSL, taken after 48, 96, 168, 240 and 336 hr.

Figure 3.12. Reducing sugar content of samples of **131**

wheat straw lignocellulose (2.5 % w/v) treated with *M. phyllosphaerae*, *R. erythropolis* and *Sphingobacterium sp.* in the presence of fish meal or CSL, taken after 48, 96, 168, 240 and 336 hr.

Figure 3.13. pH of samples of wheat straw (2.5 % w/v) **132**

treated with *M. phyllosphaerae*, *R. erythropolis* and *Sphingobacterium sp.* in the presence of fish meal or

CSL, taken after 48, 96, 168, 240 and 336 hr.

Figure 3.14. FT–IR (ATR) spectra of the liquid **133**

fractions of *Sphingobacterium sp.* (A), *M. phyllosphaerae* (B) and *R. erythropolis* (C) inoculated in M9 salts supplemented with wheat straw (2.5 % w/v) and CSL (2 % w/v). Samples taken after 96, 168 and 336 hr were measured along with untreated wheat straw in the same medium.

Figure 3.15. FT–IR (ATR) analysis of the solid **136**

fractions of *Sphingobacterium sp.* (A), *M. phyllosphaerae* (B) and *R. erythropolis* (C) inoculated in M9 salts supplemented with wheat straw (2.5 % w/v) and CSL (2 % w/v). Samples taken after 96, 168 and 336 hr were measured along with untreated wheat straw in the same medium.

Figure 3.16. Hypothetical cleavage at different **137**

positions in the lignin polymer to yield solid and liquid fractions.

Figure 3.17. Number of CFUs per ml in samples of **138**

Organosolv lignin (2.5 % w/v) treated with *M. phyllosphaerae* and *Sphingobacterium sp.* in the presence of fish meal or CSL (2 % w/v), taken after 48, 96, 168, 240 and 336 hr.

Figure 3.18. Soluble phenol content of samples of **139**

Organosolv lignin (2.5 % w/v) treated with *M.*

phyllosphaerae and *Sphingobacterium sp.* in the presence of fish meal or CSL, taken after 48, 96, 168, 240 and 336 hr.

Figure 3.19. Reducing sugar content of samples of **140**
Organosolv lignin (2.5 % w/v) treated with *M.*

phyllosphaerae and *Sphingobacterium sp.* in the presence of fish meal or CSL, taken after 48, 96, 168, 240 and 336 hr.

Figure 3.20. pH of samples of Organosolv lignin (2.5 **141**
% w/v) treated with *M. phyllosphaerae* and

Sphingobacterium sp. in the presence of fish meal or CSL (2.0 % w/v), taken after 48, 96, 168, 240 and 336 hr.

Figure 3.21. FT-IR (ATR) analysis of the liquid **142**
fractions of *Sphingobacterium sp.* (A) and *M.*

phyllosphaerae (B) inoculated in M9 salts supplemented with Organosolv lignin (2.5 % w/v) and CSL (2 % w/v). Samples taken after 96, 168 and 336 hr were measured along with untreated Organosolv lignin in the same medium.

Figure 3.22. FT-IR (ATR) analysis of the solid **144**
fractions of *Sphingobacterium sp.* (A) and

M. phyllosphaerae (B) inoculated in M9 salts supplemented with Organosolv lignin (2.5 % w/v) and CSL (2 % w/v). Samples taken after 96, 168 and 336

hr were measured along with untreated Organosolv lignin in the same medium.

Figure 3.23. Number of CFUs per ml in samples of **145**

Kraft lignin (2.5 % w/v) treated with *M.*

phyllosphaerae, *R. erythropolis* and *Sphingobacterium*

sp. in the presence of fish meal or CSL (2.0 % w/v),

taken after 48, 96, 168, 240 and 336 hr.

Figure 3.24. Soluble phenol content of samples of **146**

Kraft lignin (2.5 % w/v) treated with *M.*

phyllosphaerae, *R. erythropolis* and *Sphingobacterium*

sp. in the presence of fish meal or CSL (2.0 % w/v),

taken after 48, 96, 168, 240 and 336 hr.

Figure 3.25. pH of samples of Kraft lignin (2.5 % w/v) **148**

treated with *M. phyllosphaerae*, *R. erythropolis* and

Sphingobacterium sp. in the presence of fish meal or

CSL (2.0 % w/v), taken after 48, 96, 168, 240 and

336 hr.

Figure 3.26. FT-IR (ATR) analysis of fractions of **149**

Sphingobacterium sp. (A), *M. phyllosphaerae* (B) and

R. erythropolis (C) inoculated in M9 salts

supplemented with Kraft lignin (2.5 % w/v) and CSL

(2 % w/v). Samples taken after 96, 168 and 336 hr

were measured along with untreated Kraft lignin in the

same medium.

Figure 4.1. Change in absorbance at 430 nm over 20 **157**

min following treatment of nitrated MWL with *M. phyllosphaerae* enzyme fractions 1 – 26 eluted from the Q-sepharose anion exchange column, with increasing [NaCl] of the mobile phase from 0 M (fraction 1) to 2 M (fraction 26) in 20 mM Tris buffer (pH 7.4). Fraction 27 is a control experiment in which 20 mM Tris buffer (pH 7.4) was used rather than a sample of enzyme.

Figure 4.2. Coomassie Brilliant Blue–R250-stained SDS–PAGE gel for AE 1, 2 and 3 from the Q-sepharose anion exchange column. **158**

Figure 4.3. Time-dependent change in absorbance at 430 nm for fractionated enzyme samples 1 – 25 from AE 1, with decreasing [(NH₄)₂ SO₄] from 2 M (fraction 1) to 0 M (fraction 25). Fraction 26 represents a control experiment, which contained 20 mM Tris buffer (pH 7.4) instead of a sample of enzyme. **159**

Figure 4.4. Purification of extracellular enzymes from the culture supernatant of *Sphingobacterium sp.* via ammonium sulfate precipitation followed by a series of chromatographic steps. **163**

Figure 4.5. Specific activity (top) and units of activity (bottom) of the re-suspended enzyme sample, following ammonium sulfate precipitation, and purified enzyme samples SAE 1 and SAE 2 towards **166**

nitrated Organosolv lignin, nitrated MWL and ABTS
in the presence of, and in the absence of 2 mM H₂O₂

Figure 4.6. Specific activity of the unpurified **168**
extracellular enzymes from *Sphingobacterium sp.*,
SAE 1, SAE 2 and fractionated enzyme samples from
SAE 1 of differing hydrophobic strength. Fractions 1 –
21 were eluted over a [(NH₄)₂ SO₄] gradient of 2 M (Fr
1) to 0 M (Fr 21). A peak in activity is generally
defined as any sample (s) of purified enzyme that
exhibit a specific activity of at least 200 units mg⁻¹ in
one or more assays.

Figure 4.7. Coomassie Brilliant Blue–R250 stained **170**
SDS–PAGE loaded with SAE 1, SAE 2 and Fr 1 – 3
and 10 – 12 from hydrophobic interaction
chromatography of SAE 1.

Figure 4.8. Coomassie Brilliant Blue–R250-stained **171**
SDS–PAGE gel loaded with fractions 15 – 22 purified
from SAE 1 via hydrophobic interaction
chromatography.

Figure 4.9. Specific activity of the unpurified **178**
extracellular enzymes from *Sphingobacterium sp.*,
SAE 1, SAE 2 and fractionated enzyme samples from
SAE 2 of differing hydrophobic strength. Fractions 1 –
21 were eluted over a [(NH₄)₂ SO₄] gradient of 2 M
(Fr1) to 0 M (Fr 21).

- Figure 4.10.** Absorbance of fractions 1 – 29, purified from SAE 2 fraction 18 via gel filtration FPLC, using a Superdex 200 column. **179**
- Figure 4.11.** Change in absorbance at 430 nm over 20 min for purified enzyme fractions 1 – 29 (45 % v/v) in the presence of ABTS (50 % v/v) and H₂O₂ (5 % v/v). Activity peaks 1 (Fr 1), 2 (Fr 5), 3 (Fr 8), 4 (Fr 11), 5 (Fr 14, 15), 6 (Fr 16, 17), 7 (Fr 18 – 20), 8 (Fr 24) and 9 (Fr 28) are discussed in the text. Fraction 30 is a control, containing 20 mM Tris buffer (pH 7.4) rather than a sample of enzyme. **180**
- Figure 4.12.** Silver-stained SDS–PAGE gel loaded with enzyme samples 2 – 7, purified from SAE 2 Fr 18 via gel filtration FPLC. **182**
- Figure 4.13.** Coomassie Brilliant Blue–R250-stained SDS–PAGE gel loaded with enzyme samples 8 – 14, purified from SAE 2 Fr 18 via gel filtration FPLC. Bands 9.1 – 14.3 are discussed in the text. **183**
- Figure 4.14.** Conversion of the superoxide anion radical to O₂ and H₂O₂ by manganese superoxide dismutase (MnSOD). **187**

List of Tables

<p>Table 1.1. Percentage content of cellulose, hemicellulose and lignin in common varieties of lignocellulose and waste materials.</p>	<p>37</p>
<p>Table 1.2. Overview of various physical and chemical lignocellulose pre-treatment methods.</p>	<p>47</p>
<p>Table 1.3. Percentage composition of the major lignin units in softwood and hardwood species.</p>	<p>49</p>
<p>Table 2.1. Change in absorbance at 430 nm from 0 – 20 min following treatment of nitrated MWL samples A, B and C with the culture supernatant of lignin-degrading bacteria <i>P. putida</i> mt-2 and <i>R. jostii</i> RHA1, non-degrader <i>B. subtilis</i> and a control experiment in which the culture supernatant was replaced with 113 mM Tris buffer (pH 7.4) containing 7.5 mM NaCl. Assays were performed in the presence of 2 mM H₂O₂.</p>	<p>82</p>
<p>Table 2.2. Degree of yellow colouration of colonies of <i>R. jostii</i> RHA1 and <i>P. putida</i> mt-2 and <i>B. subtilis</i> on agar-solidified LB following spraying with nitrated MWL solution (sample C) diluted 10- or 25-fold in 750 mM Tris buffer (pH 7.4) containing 50 mM NaCl, 20 mM Tris buffer (pH 7.4) and dH₂O. += no observed colouration, ++ = faint yellow colouration, +++ = clear yellow colouration.</p>	<p>84</p>

Table 2.3. Number of bacterial isolates from each enriched soil sample, diluted 1000-fold in 20 mM Tris buffer (pH 7.4) along with their IDs and the approximate number of CFUs per ml in each enriched culture.	86
Table 2.4. Source of each bacterial isolate, its assigned ID and the degree of yellow colouration observed following the spraying of colonies on agar-solidified LB with nitrated MWL sample C.	88
Table 2.5. % Identity of isolated lignin-degrading soil bacteria over 500 – 1400 aligned nucleotides, and the bacterial family of each strain.	95
Table 2.6. % Identity of thermotolerant lignin-degrading bacteria, isolated from composted wheat straw, over 650 – 1,000 aligned nucleotides and the bacterial family of each strain.	97
Table 2.7. Level of growth of thermotolerant isolates on agar-solidified LB (++++ = good growth, +++ = moderate growth) and the degree of yellow colouration observed upon spraying colonies with nitrated MWL solution (+ = no colour change, ++ = faint yellow colouration, +++ = clear yellow colouration). Yellow colouration of colonies of <i>Rhizobiales sp.</i> was unclear due to the yellow colour of colonies formed by this strain.	98

- Table 3.1.** Maximum OD₆₀₀ reached by cultures of environmental lignin-degrading bacteria grown for 120 or 336 hr in LB broth and M9 salt solution supplemented with 2.0 % (w/v) glucose and/or 2.0 % (w/v) Kraft lignin with 0.5 % (w/v) yeast extract. OD₆₀₀ values outlined in bold indicate the medium in which the highest OD₆₀₀ was reached and numbers in brackets indicate the number of hours of inoculation. **110**
- Table 3.2.** Level of growth of thermotolerant isolates *Rhizobiales sp.* T1 and *Sphingobacterium sp.* T2 on agar-solidified LB after 48 and 168 hr of incubation at 30, 37, 45, 50 and 55 °C. **111**
- Table 3.3.** Level of growth of environmental lignin-degrading bacterial strains on different carbon sources biphenyl (1.0 g l⁻¹), *m*-cresol (0.22 g l⁻¹), *p*-cresol (0.22 g l⁻¹), ferulic acid (1.0 g l⁻¹), vanillic acid (1.0 g l⁻¹), veratryl alcohol (0.84 g l⁻¹) and cellulose (0.5 g l⁻¹), after 240 hr at 30 or 45 °C. **114**
- Table 3.4.** Degree of growth of previously studied lignin-degrading bacteria on high-, medium- and low-molecular weight forms of Kraft lignin observed after incubation in the presence of M9 salts at 30 °C for 72, 168 and 192 hr. **119**
- Table 3.5.** Growth patterns of environmental lignin-degrading bacteria on high-, medium- and low- **120**

molecular weight forms of Kraft lignin after 72 and 192 hr of inoculation.

Table 3.6. IR peaks observed in literature studies of lignin, and their appearance in the observed data. **134**

Numbers in brackets indicate the observations in the solid (s) or liquid (l) FT–IR (ATR) analysis.

Table 3.7. IR peaks observed in literature studies of lignin [191 – 193], and their appearance in the **143**

observed data. Numbers and letters in brackets alongside the frequency values indicate the state of the fraction.

Table 3.8. Tentative assignment of peaks 1 – 8 from the FT–IR (ATR) analysis of treated and untreated **150**

Kraft lignin (Fig. 3.27), based on literature assignments [191 – 193]. Numbers in brackets alongside the frequency values indicate the peak number.

Table 4.1. Suggested identities of proteins present in purified enzyme samples HI 1, HI 3 and HI 5. **161**

Table 4.2. Identity and predicted molecular weight of proteins from purified enzyme fractions 1, 12, 17 and **174**

20, and the approximate molecular weight of the Coomassie Brilliant Blue–R250-stained SDS–PAGE bands from which they were identified.

Table 4.3. Identity and predicted molecular weight of **175**

the different proteins present in fraction 1, a low-hydrophobic strength enzyme sample purified from SAE 1 via hydrophobic interaction chromatography.

Table 4.4. Identity and predicted molecular weight of proteins identified in enzyme fractions 9, 11, 12, 13 and 14, purified from SAE 2 fraction 18 via gel filtration chromatography. Samples 9.4 and 13.1 contained keratin, and identical peptides were observed in 14.3 and 14.4, therefore they were not considered. **185**

Table 6.1. Volumes of gallic acid solution ($10 \mu\text{g } \mu\text{l}^{-1}$) and dH_2O used in the preparation of each calibration standard solution. **201**

Table 6.2. Volumes of glucose (1 mg ml^{-1}) and dH_2O used in the preparation of each calibration solution. **202**

Table 6.3. Volumes of Bio-rad protein dye concentrate and 1 mg ml^{-1} BSA used in the construction of the calibration graph. All measurements were carried out in triplicate. **210**

List of Abbreviations

AAO	aryl alcohol oxidase
ABTS	2,2'-azino-bis (3-ethylbenzothiazoline-6-sulfonic acid)
APS	ammonium persulfate
ATR	attenuated total reflectance
AU	arbitrary unit
<i>B. subtilis</i>	<i>Bacillus subtilis</i>
BLAST	Basic Local Alignment Search Tool
BSA	Bovine Serum Albumin
CFU	colony-forming unit
CIMV	Compagnie Industrielle Matter Plant
CoA	Co-enzyme A
CSL	corn steep liquor
Da	Dalton
dH ₂ O	distilled H ₂ O
DHPB	dihydroxybiphenyl
DNA	deoxyribonucleic acid
DNS	3,5-dinitrosalicylic acid
DyP	dye-decolourizing peroxidase
E.C.	enzyme classification
E.R.S.	enzyme resting state
ESI-MS	electrospray ionization mass spectrometry
FAD	flavin adenine dinucleotide

FC	Folin-Ciocalteu
FPLC	fast protein liquid chromatography
FT-IR	Fourier transform infrared
G-	guaiacyl
H-	hydroxyphenyl
HPLC	high performance liquid chromatography
HRI	Horticultural Research Institute
IR	infrared
<i>L. mesenteroides</i>	<i>Leuconostoc mesenteroides</i>
LB	Luria Bertani
LC-MS	liquid chromatography-mass spectrometry
LiP	lignin peroxidase
<i>M. luteus</i>	<i>Micrococcus luteus</i>
<i>M. marinilacus</i>	<i>Microbacterium marinilacus</i>
<i>M. oxydans</i>	<i>Microbacterium oxydans</i>
<i>M. phyllosphaerae</i>	<i>Microbacterium phyllosphaerae</i>
MALDI	matrix-assister laser desorption/ionization
mAU	milli arbitrary unit
Me	methyl
MnP	manganese peroxidase
MW	molecular weight
MWL	milled wood lignin
NAD	nicotinamide adenine dinucleotide
NMR	nuclear magnetic resonance

nm	nanometers
NREL	National Renewable Energy Laboratory
<i>O. pseudogrignonense</i>	<i>Ochrobactrum pseudogrignonense</i>
<i>O. rhizosphaerae</i>	<i>Ochrobactrum rhizosphaerae</i>
OD ₆₀₀	optical density at 600 nm
<i>o</i> -	<i>ortho</i> -
<i>P. putida</i> mt-2	<i>Pseudomonas putida</i> mt-2
PAL	phenylalanine ammonia lyase
PCA	protocatechuic acid
PCR	polymerase chain reaction
<i>R. erythropolis</i>	<i>Rhodococcus erythropolis</i>
<i>R. jostii</i> RHA1	<i>Rhodococcus jostii</i> RHA1
rRNA	ribosomal RNA
S-	syringyl
<i>S. paucimobilis</i>	<i>Sphingomonas paucimobilis</i>
<i>S. viridosporus</i>	<i>Streptomyces viridosporus</i>
SDS-PAGE	sodium dodecyl sulfate polyacrylamide gel electrophoresis
SEC	size-exclusion chromatography
SOD	superoxide dismutase
TCA	trichloroacetic acid
TEMED	tetramethylethylenediamine
UK	United Kingdom
UV	ultraviolet

VA	veratryl alcohol
°C	degrees celsius
ϵ_{300}	molar extinction coefficient at 300 nm

Acknowledgements

Firstly, I would like to thank my supervisor, Prof. Tim Bugg for allowing me the chance to do a PhD in this field of research and for his endless enthusiasm and advice, which has been invaluable throughout the project. I am also grateful to several other members of academic staff from the University of Warwick, particularly Prof. Liz Wellington and Dr. Paul Norris for their microbiology-related support and for providing access to their facilities in the department of Life Sciences, and to Dr. Claudia Blindauer, Dr. Ann Dixon and Prof. Peter Sadler for their advice in recent years. Prof. David Pink, Dr. Kerry Burton and Dr. Guy Barker (Warwick HRI) must also be acknowledged for their support and provision of the composted wheat straw in the early days.

Special recognition must go to Dr. Gordon Allison (IBERS, Aberystwyth) for his enthusiasm and openness to collaborative work and allowing me to use his FT-IR facilities, and to the research group of Prof. Lindsay Eltis (University of British Columbia) for their cooperation and interest in the lignin project. I am also very grateful to Sue Slade for her help with the proteomics, Matt Mitchell for providing the milling machines, Cerith Harries and Mark Ward for their assistance with the media preparation and Phil Aston for help with Mass Spectrometry. I would also like to thank Liz Hardiman, Helena Wright, Darren Braddick, Ludovic Laigle, Mark Ahmad and Rahman Rahmanpour for their lab-based support over the years.

I would like to express my gratitude to my sponsors at Fondation Tuck, Paris France for funding the project and for their hospitality during my visits. Finally, I would like to thank my family and friends for their support and encouragement over the past 3 years.

Declaration

I confirm that the work presented in this thesis is my own work unless otherwise acknowledged, and has not been submitted for a degree at any other academic institution. Some of the work presented in Chapters 2 and 3 has recently been published:

Development of novel assays for lignin degradation: comparative analysis of bacterial and fungal degraders; M. Ahmad, C.R. Taylor, D. Pink, K. Burton, G. Bending and T.D.H. Bugg, *Molecular Biosystems*, 2010, **6**, 815–821.

Isolation of bacterial strains able to metabolize lignin from screening of environmental samples; C.R. Taylor, E.M. Hardiman, M. Ahmad, P.D. Sainsbury, P.R. Norris and T.D.H. Bugg, *Journal of Applied Microbiology*, 2012, **3**, 521–530.

Abstract

A novel screening method for detecting lignin-degradation activity on agar plates was developed using nitrated lignin. Using this method, ten lignin-degrading bacteria have been isolated from environmental sources, including seven mesophilic soil bacteria and three thermotolerant strains from composted wheat straw. All of the isolates have demonstrated activity towards lignin degradation in the assays, the most active strain being a thermotolerant *Sphingobacterium* strain from the Bacteroidetes family.

The ability of each strain to degrade a variety of aromatic carbon sources and size-fractionated Kraft lignin has been examined by laboratory-scale growth experiments and gel filtration chromatography respectively, and the bioconversion of different lignin-containing feedstocks by three of the most active strains has been examined in a series of laboratory-scale fermentation experiments.

Purification of extracellular lignin-degrading enzymes from the culture supernatant of *Sphingobacterium sp.* has highlighted several different enzyme activities and possible lignin-degrading enzymes.

Chapter 1: Introduction

1.1. Renewable energy and biorefining

Accelerating global energy demands are exhausting the supply of finite resources such as fossil fuels, leading to adverse socioeconomic and environmental effects that could be reduced by utilizing renewable energy resources such as plant biomass [1]. Referring to biological material derived from living or recently living organisms such as plants and trees [2], biomass is the World's largest and most sustainable energy resource with a global availability of 220 billion open dry ton per year [3]. The processes that convert biomass feedstocks into a range of commercial products and renewable energy are termed 'biorefining'. Biorefineries (Fig. 1.1) are amalgamated bio-based industries that employ a range of processes to produce biofuels, chemicals, biomaterials, food and power [4 – 7]. Such industries can potentially convert several forms of biomass into an extensive range of products, maximizing the value derived from the renewable feedstocks.

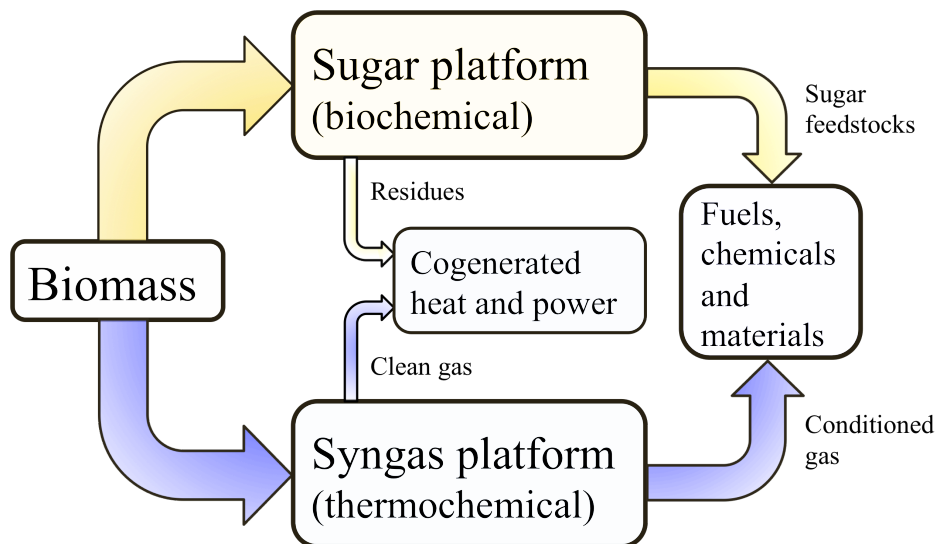


Figure 1.1. Biorefinery concept of the National Renewable Energy Laboratory (NREL) [8].

The NREL biorefinery concept is based on two different platforms: the sugar platform, which is based on biochemical processing and focuses on the fermentation of sugars derived from biomass feedstocks; and the syngas platform, which is based on thermochemical processing and focuses on the gasification of biomass [8]. An example of a sugar platform-based biorefinery process is the conversion of lignocellulosic biomass into second-generation bioethanol, which is fundamental to the sustained use of renewable energy.

1.2. First- and second-generation biofuels

Fossil fuels are a non-renewable energy source having adverse socioeconomic and environmental effects [9, 10] such as increased consumer prices and high atmospheric CO₂ levels, which are directly linked to global warming [9, 10]. Production of biofuels from renewable resources such as plant biomass could facilitate a reduction in the global dependence on fossil fuels and minimize CO₂ production since the plant material used as a feedstock would consume CO₂ upon growth [9].

First-generation bioethanol is produced by converting sugars from crops, e.g. sugar cane, into bioethanol via fermentation [10, 11], and is commercially available with an annual production volume of around 50 billion litres. Despite leading to reduced atmospheric CO₂ levels and offering a greener alternative to fossil fuels [11], the long-term use of first-generation bioethanol is sustainable only in a few Countries [12]; this is largely due to the feedstocks, which compete with food crops and in turn increase food prices [12]. Second-generation bioethanol offers a distinct advantage since the lignocellulosic feedstocks constitute the majority of abundant, inexpensive and unused plant biomass, which does not directly compete with food crops. Lignocellulosic biomass

includes forestry residues, agricultural waste, wood products and animal waste [13 – 15]. There is a great deal of scope to use this material as a feedstock for second-generation bioethanol since it is available in large quantities and is much less expensive than corn and sugar cane. Despite this advantage the commercialization of second-generation bioethanol is not yet economically viable due the chemical and structural complexity of lignocellulose, which requires a great deal of energy to break down [16].

1.3. Lignocellulose

Lignocellulose is a polymer matrix composed of carbohydrate and lignin polymers (Fig. 1.2). The carbohydrate component consists of cellulose and hemicellulose polysaccharides that contain pentose (C5) and hexose (C6) sugars. In plant cell walls the polysaccharides are strongly bound to lignin, which fills the spaces between them [17].

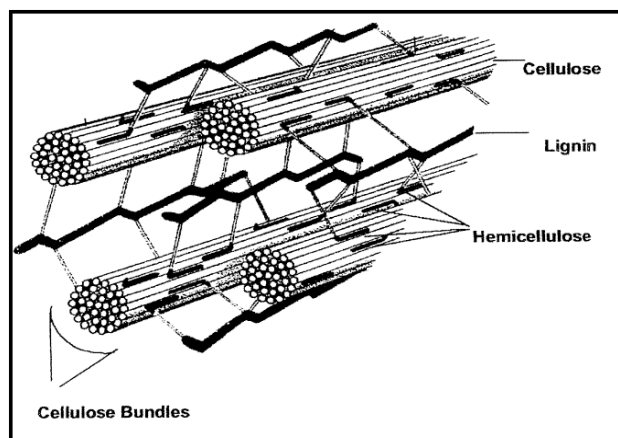


Figure 1.2. Structural arrangement of the lignocellulose polymer matrix in vascular plants [18].

Chemical analyses suggest that lignocellulose contains around 15 – 30 % lignin and 35 – 65 % carbohydrate [19], with varied composition of cellulose,

hemicellulose and lignin in different types of biomass. The lignin content is generally higher in wood than in grasses, of which cellulose forms the primary component (Table 1.1).

Table 1.1. % composition of cellulose, hemicellulose and lignin in common varieties of lignocellulose and waste materials [20, 21].

Biomass	% Cellulose	% Hemicellulose	% Lignin
Corn cobs	45	35	15
Switch grasses	45	31	12
Hardwood stems	40–55	24–40	18–25
Wheat straw	30	50	15
Softwood stems	45–50	25–35	25–35
Primary wastewater solids	42	22	27
Pulping waste	60–70	10–20	5–10

1.3.1. Cellulose

Cellulose is a linear, repeating polymer (Fig. 1.3) composed of D-glucose units linked by β (1 \rightarrow 4) glycosidic bonds, and its chemical properties are mostly determined by the degree of polymerization, which is highly dependent on the plant species (15, 000 in cotton compared to around 10, 000 in wood). Alignment of the polymers leads to the formation of crystalline sections in native cellulose [22], which is a semi-crystalline polymer. These crystalline sections are held together by strong hydrogen bonds and Van der Waals forces between the planes [23].

Cellulose is generally arranged into a matrix of microfibrils [22, 23], which are each 3 to 6 μ m in diameter and contain several glucan chains of very high glucose content, offering a great deal of rigidity to the plants.

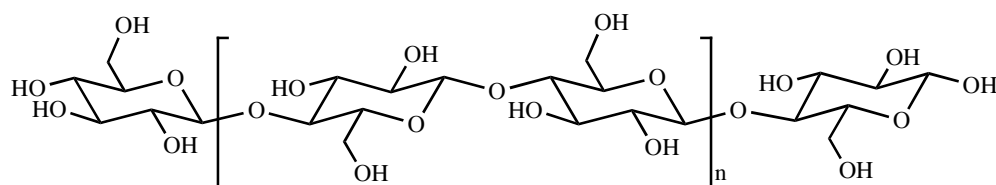


Figure 1.3. Structure of the repeating unit of cellulose [24].

1.3.2. Hemicellulose

‘Hemicellulose’ refers to a wide variety of heteropolysaccharides including arabinoxylans (1→3) and (1→4)-β-glucans, gluco- and galacto-mannans, pectins and xyloglucans, all of which vary in their degree of polymerization [25], the composition of monosaccharides and glycosidic linkages, and the substitution pattern. The structural features of hemicellulose affect physical properties such as crystallinity, enzymatic degradability, porosity, solubility and viscosity. Different chemical forms of include xylan and mannan (Fig. 1.4) [26].

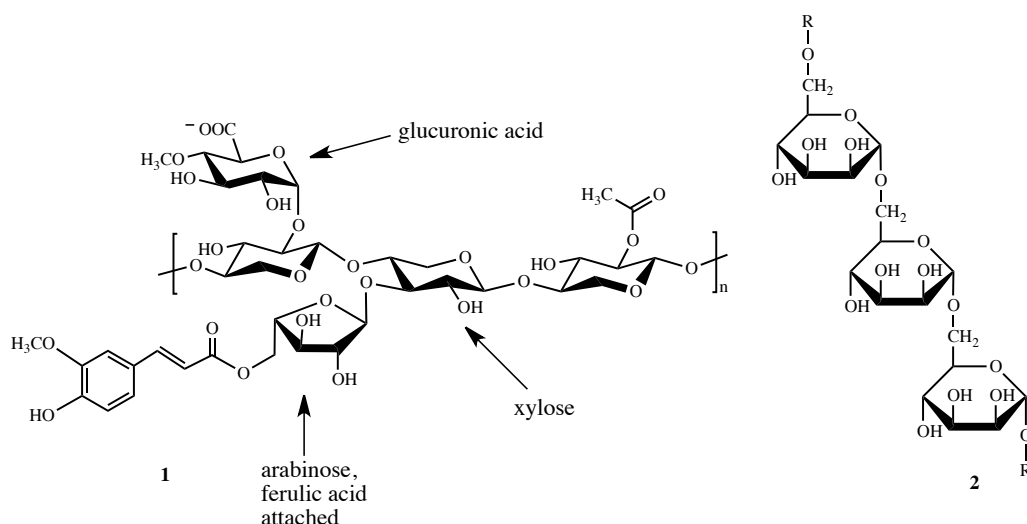


Figure 1.4. Chemical structures of xylan (1) and mannan (2), two different forms of hemicellulose [27].

In contrast to cellulose, hemicellulose is easier to break down due to its shorter, more random structure, and can be broken down by acids or hemicellulases to

dispense the C5 and C6 sugar components, which include arabinose (C5), galactose (C6), glucose (C6), mannose (C6) and xylose (C5) [27]. The C6 sugars can be readily fermented into ethanol by several microorganisms whereas very few organisms can ferment C5 sugars, generally resulting in low yields. Since a significant proportion of lignocellulose is composed of C5 sugars, particularly xylose, the efficient utilization of these sugars is fundamental to the economic viability of lignocellulosic bioethanol production.

1.3.3. Lignin

Behind cellulose, lignin is the second most abundant natural organic polymer, and is generally defined as polymeric natural products derived from enzyme-induced dehydrogenative polymerization of three primary precursors: *trans-p*-coumaryl, *trans*-coniferyl and *trans*-sinapyl alcohol [28] (Fig. 1.5).

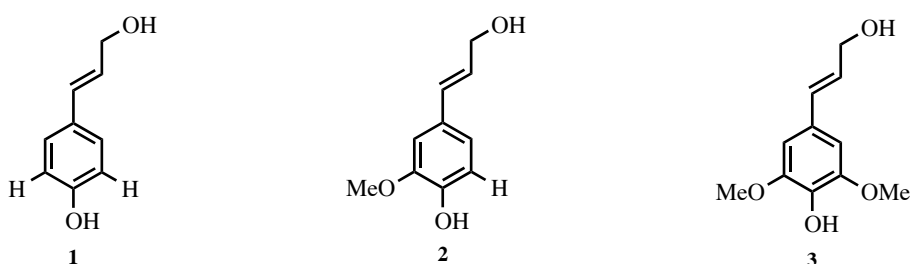


Figure 1.5. Chemical structures of the primary precursors of lignin: *trans-p*-coumaryl alcohol (1), *trans*-coniferyl alcohol (2) and *trans*-sinapyl alcohol (3) [29].

Lignin is located with hemicellulose between cellulose microfibrils in primary and secondary cell walls (Fig. 1.2) [30], and is covalently linked to hemicellulose via a network of benzyl-ester and phenyl-glycoside bonds. Lignin performs an essential role in the transport of water and nutrients by hindering the permeation of water across the cell walls of xylem tissue [30].

In contrast to cellulose and hemicellulose, lignin is a highly recalcitrant, non-repeating polymer [31, 32] that cannot be utilized in fermentation processes

although it can be broken down into a variety of low-molecular weight aromatic chemical products such as vanillin (4-hydroxy-3-methoxybenzaldehyde), which is responsible for the flavour of vanilla and can be used in the synthesis of a range of pharmaceuticals [33, 34]. Approximately 85 % of the World's vanillin is synthesized from guaiacol, with the remainder from lignin [35]. Production of vanillin via lignin breakdown is a greener alternative to the guaiacol method that requires petroleum-derived compounds. The structure of lignin and its breakdown mechanisms are discussed in detail later in this chapter.

1.3.4. Cellulosic bioethanol production

Cellulosic bioethanol is produced from lignocellulose via a series of stages (Fig. 1.6). The first major step involves pre-treatment in which cellulose and hemicellulose are separated from the lignin and the hemicellulose is converted into C5 sugars [9]. This is followed by the enzymatic hydrolysis of cellulose into fermentable sugars [36]. The C5 and C6 sugars are then converted into ethanol via fermentation [37], and the ethanol is recovered via distillation.

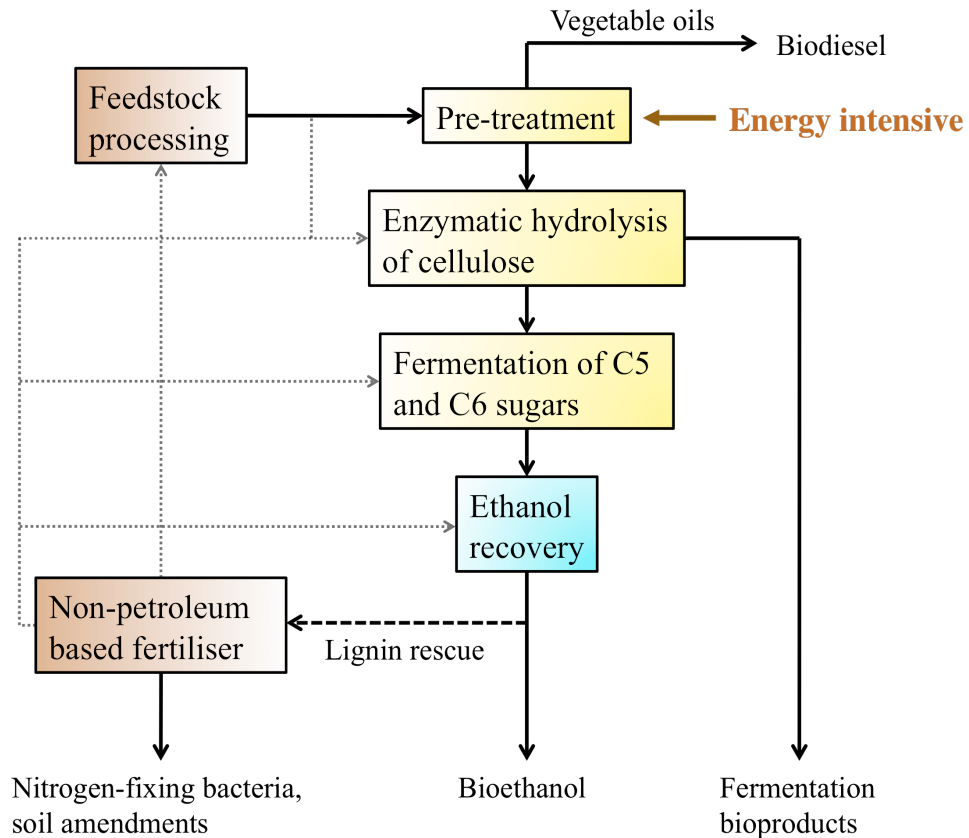


Figure 1.6. Stages in the production of bioethanol and other products from lignocellulose. The energy-intensive pre-treatment step is discussed in the text [38, 39].

Since sugars required for the production of bioethanol are trapped inside the cross-linked lignocellulose matrix (Fig. 1.2), a form of pre-treatment [40] is required for their release.

Pre-treatment refers to a procedure that converts native lignocellulose into a form that contains cellulose of sufficient bioavailability to be hydrolyzed [40]. This process alters the biomass structure, its microscopic and macroscopic size and also the submicroscopic chemical and structural composition. The modifications made during pre-treatment increase the accessibility of enzyme binding sites and the surface area available to water, which is otherwise prevented by cellulose microfibrils [41].

Pre-treatment methods are generally classed as physical, chemical or biological, all of which are very expensive since they require high temperatures to

completely solubilize and remove the highly recalcitrant lignin component [41]. Without using a pre-treatment method, yields of bioethanol and fermentation bioproducts would otherwise be too low to commercially compete with petroleum-derived products.

Following pre-treatment, cellulose and hemicellulose are hydrolyzed into sugar monomers, which are then fermented into ethanol by ethanol-producing microbes [41].

1.3.5. Existing pre-treatment methods

Several different pre-treatment methods exist, which are generally classed as physical, chemical or biological [42, 43]. Though many of these methods are effective, they are very energy-intensive since high temperatures are often required to completely solubilize and remove the lignin.

1.3.5.1. Physical methods

Physical methods include pyrolysis, mechanical size reduction, microwave oven and electron beam irradiation.

Pyrolysis involves treatment of lignocellulose at temperatures above 300 °C, at which the decomposition of cellulose produces H₂ and CO gases as well as residual char [44 – 46]. Further treatment of the residual char is carried out by leaching with water or mild acid, which contains sufficient carbon source to induce microbial growth for bioethanol production since glucose is the main component of water leachate [47]. A 55 % weight reduction of biomass takes place during water leaching, and an 80 – 85 % conversion of cellulose to

reducing sugars has been demonstrated by Fan *et. al.*, [48] with more than 50 % glucose through mild acid leaching.

Mechanical size reduction is the initial step in bioethanol production from agricultural solid wastes, and involves chipping, grinding or milling. These methods reduce the crystallinity of cellulose and enhance the efficiency of downstream processes [49]. The energy consumption depends on the initial and final particle sizes, moisture content and the nature of the material, i.e. softwood or hardwood [49, 50]. The advantage of size reduction is that it may provide better results, although very fine particle size may cause problems in subsequent steps such as channelling [51, 52].

1.3.5.2. Chemical methods

The most efficient chemical pre-treatment methods at present include treatment with organic solvents, ionic liquids and Kraft pulping, all of which are very expensive [41].

Organosolv pre-treatment is a favourable method of eliminating the recalcitrance of lignocellulosic biomass [53 – 55] since it does not require an additional size-reduction step and can readily convert hardwood and softwood feedstocks into a bioavailable cellulosic material that can be readily broken down by cellulases, leading to an efficient conversion into glucose (90 – 100 %) and production of sulfur-free lignin that can be converted into commercially-useful products. The pre-treatment is generally carried out at temperatures between 140 and 200 °C for around 30 – 60 min [56, 57], with the ethanol concentration ranging from 40 – 60 %. An organic or aqueous organic solvent mixture with organic acid catalysts, such as HCl or H₂SO₄, is used to cleave the

lignin and hemicellulose linkages. Organic solvents include acetone, ethanol, ethylene glycol, methanol, tetrahydrofurfuryl alcohol and triethylene glycol. Organic acids such as acetylsalicylic, oxalic and salicylic acid can also be used as catalysts in the process. Solvents are usually recycled to minimize costs, and must be removed since they may inhibit the growth of organisms, enzymatic hydrolysis and fermentation [56, 57].

Ionic liquids have been found to be efficient in the solubilization of wood, lignin and crystalline cellulose [58 – 60] and improving the rates of subsequent saccharification [61]. Their use as a pre-treatment is advantageous since they are non-flammable and can be recycled [62, 63]. Recent reports also suggest that treatment of maple wood with several ionic liquids enhances the yields of cellulose saccharification as a result of lignin extraction [64].

Kraft pulping: The chemical pulping process is a physiochemical method of pre-treatment, which is one of the most prevalent, removing a sufficient amount of lignin to isolate individual cellulose fibres, which produces a pulp that is applicable to manufacturing paper and other materials. The dominant chemical pulping process in many Countries is the Kraft process, which involves reacting wood chips with an aqueous solution of sodium hydroxide and sodium sulfide under high pressure at a temperature of around 170 °C for approximately 2 hours [65].

Although the stable C–C linkages are generally unaffected by the Kraft process, hydroxide and hydrosulfide ions react with the lignin polymer and fragment it into smaller water-soluble fractions. This process is initiated by cleavage of the α - and β -aryl ether linkages between the phenyl propane units (see section 1.4),

which in turn generates free phenolic hydroxyl groups [66]. The induction of these hydroxyl groups increases the water solubility of the lignin.

Cleavage of the α -aryl and β -aryl ether linkages are the dominant lignin-breakdown reactions that take place during Kraft pulping [67, 68], and the reactivity of these linkages is dependent upon the moiety present at the *para* position in relation to the propane side chain [69, 70].

α -aryl ether linkages in the phenolic units are cleaved via conversion of the phenolate unit into a quinone methide intermediate (Fig. 1.7).

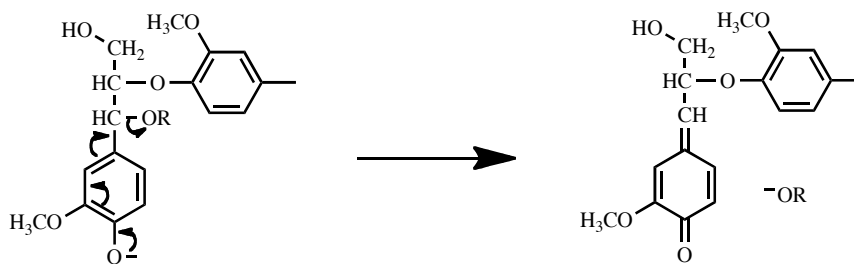


Figure 1.7. α -aryl ether cleavage in phenolic aryl-propane units during the Kraft pulping process [67–70].

β -aryl ether linkages in the non-phenolic units are cleaved via attack of an ionized hydroxyl group located on the α - or γ - carbon (Fig. 1.8).

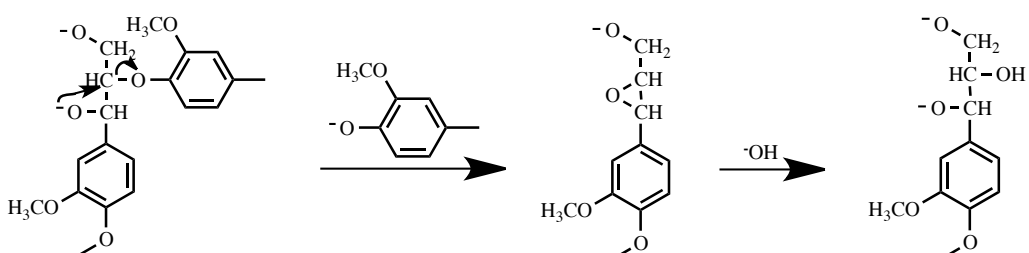


Figure 1.8. Mechanistic detail of β -aryl ether cleavage in non-phenolic aryl-propane units during the Kraft pulping process [67, 68, 70].

1.3.5.3. Biological methods

Lignocellulose can be pre-treated by microorganisms such as fungi and bacteria. In comparison to physical and chemical methods, biological pre-treatments are safer and much less energy-intensive since they require no chemical and less mechanical treatment [71 – 73]. Despite these advantages, biological pre-treatments are hindered by low rates of hydrolysis and low yields. The process of lignin removal via these processes is usually slow. As a novel biological pre-treatment, the enzymatic hydrolysis of lignocellulose by lignin-degrading bacterial strains or enzymes would be more environmentally friendly, produce greater yields with fewer byproducts and also yield a variety of useful low-molecular weight aromatic chemical byproducts e.g. vanillin [33, 34].

Table 1.2. Overview of various physical and chemical lignocellulose pre-treatment methods [44 – 50, 56 – 65].

Method	Conditions	Yield	Products
Pyrolysis	400–600 °C, under vacuum	20–25 % (residual char), 40–60 % (tar), 15–20 % (levoglucosan isomers), 30–35 % (reducing sugars)	Residual char (derived mainly from lignin), Tar (which can be broken down into levoglucosan isomers pyranose and furanose) and reducing sugars
Mechanical size reduction	Wet and dry milling, vibratory ball milling. Ball milling is advised for hardwoods and cutter milling for softwoods	N/A, power input depends on initial and final particle sizes, moisture content and the nature of the feedstock (softwood or hardwood)	Feedstocks of reduced particle size and crystallinity for more efficient downstream processing
Organosolv	140–200 °C, 30–60 min, 30–60 % ethanol	20–30 % (lignin), 40–55 % (cellulose), 20–25 % (hemicellulose)	Lignin, cellulose, hemicellulose
Kraft pulping	Reaction of feedstocks in aqueous solution of NaCl and Na ₂ S under high pressure at 170 °C for 2 hr	40–50 % (softwoods), 45–55 % (hardwoods)	Water-soluble lignin
Ionic liquids	< 100 °C, solution-based organic salts consisting of an organic cation and an inorganic anion	N/A, ability to dissolve lignocellulose depends on the physical and chemical properties of the ions.	Precipitated cellulose (amorphous and porous), lignin and hemicellulose

1.4. Lignin

Lignin is a non-repeating amorphous polymer [74] of high-molecular weight that is highly cross-linked and optically inactive (Fig. 1.9). The heterogeneous polymeric structure is composed of phenylpropanoid units linked by an array of stable C–C and hydrolysis-resistant ether linkages [75]. These features, together

with insolubility and lack of stereo-regularity, offer high resistance towards microbial degradation [76].

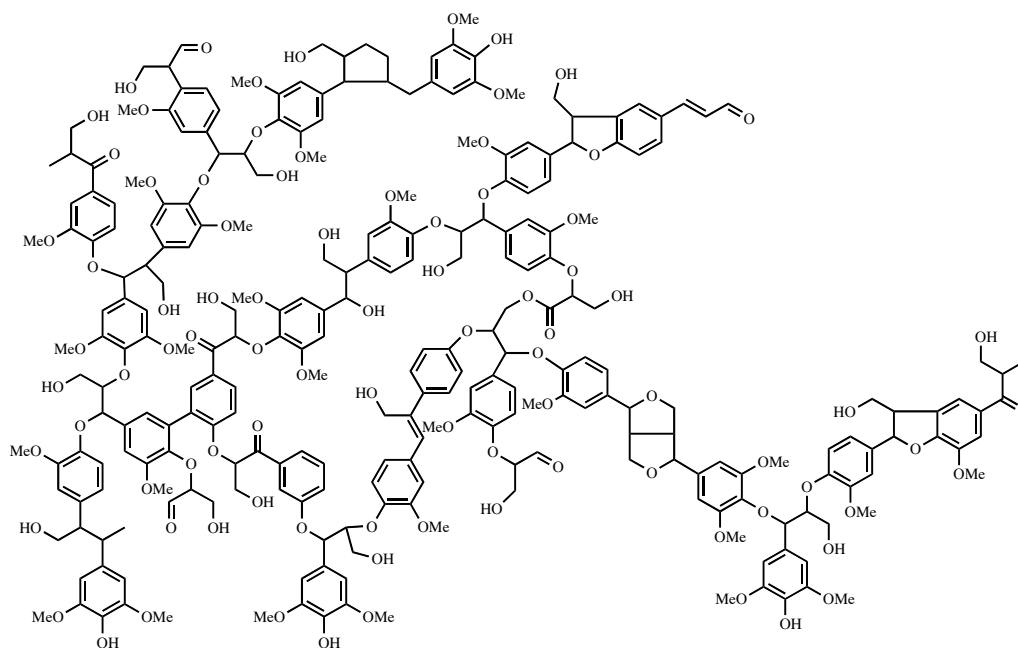


Figure 1.9. Chemical structure of lignin derived from Beech as suggested by Nimtz [77].

The three different monomeric units that make up the lignin polymer are termed H-, G- and S-units and the variation in their composition in different forms of wood leads to a wide variety of different lignin structures (see 1.4.1.).

β -aryl ether (β -O-4')-linked dimers are the predominant structural units, constituting around 50 % of the total number of units, followed by biphenyl (5-5'), phenylcoumaran (β -5'), resinol (β - β) and spirodienone (β -1') (Fig. 1.10).

Previous studies suggest that the structure of lignin is racemic [78], meaning that a simple β -O-4-linked dimer that contains two asymmetric carbon atoms exists in four stereo-isomeric forms. The vast increase in the number of stereoisomers with increasing numbers of lignin subunits confers an extremely complex, non-repeating, three-dimensional polymer.

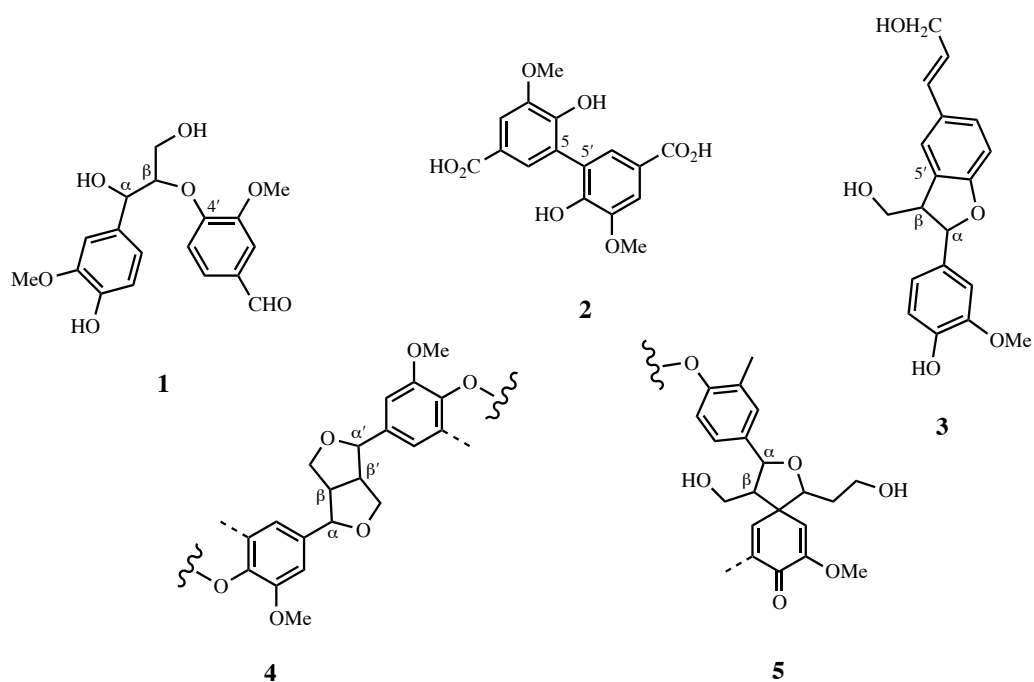


Figure 1.10. Chemical structures of the dominant units of the lignin polymer: β -O-4' (**1**), 5-5' (**2**), β -5' (**3**), β - β' (**4**) and β -1' (**5**) [78].

Table 1.3. Percentage composition of the major lignin units in softwood and hardwood species [78 – 83].

Structural unit	% of total linkages	
	Softwood	Hardwood
β -aryl ether	50	60
phenylcoumaran	9 – 12	6
biphenyl	10 – 11	5
diaryl ether	4	7
other	22 – 27	22

The only relatively weak linkage in lignin that can be readily hydrolyzed is the α -aryl ether linkage (Fig. 1.11) [79]. Cleavage of the more stable ether bonds requires harsh conditions.

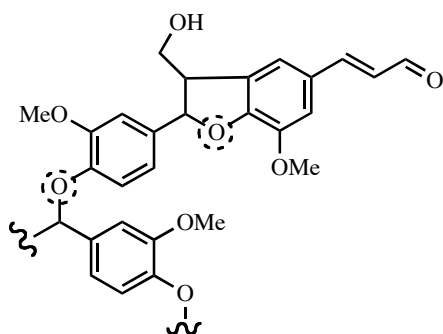


Figure 1.11. Structural component of lignin, with the low-stability α -aryl ether linkages indicated by dotted circles [79].

1.4.1. Lignin Biosynthesis

Phenylpropanoids are a family of organic compounds that include hydroxycinnamic acids, cinnamic aldehydes, flavonoids and stilbenoids, all of which are derived from phenylalanine via the action of phenylalanine ammonia lyase (PAL) (Fig. 1.12) [84].

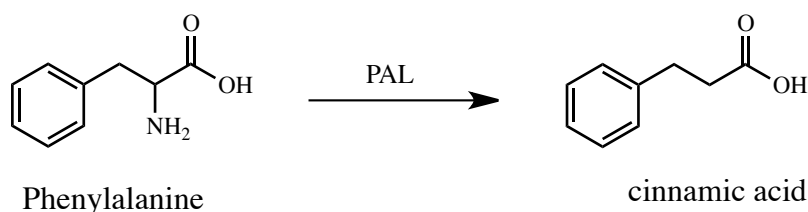


Figure 1.12. Conversion of phenylalanine into cinnamic acid by phenylalanine ammonia lyase (PAL) [84].

Subsequent hydroxylations and methylations lead to coumaric acid, caffeic acid, ferulic acid, 5-hydroxyferulic acid and sinapic acid [84]. Reduction of the carboxylic acid functional groups in cinnamic acids yields the corresponding aldehydes and further reduction yields monolignols such as coumaryl alcohol, coniferyl alcohol and sinapyl alcohol, which vary in degree of methoxylation (Fig. 1.13) [85].

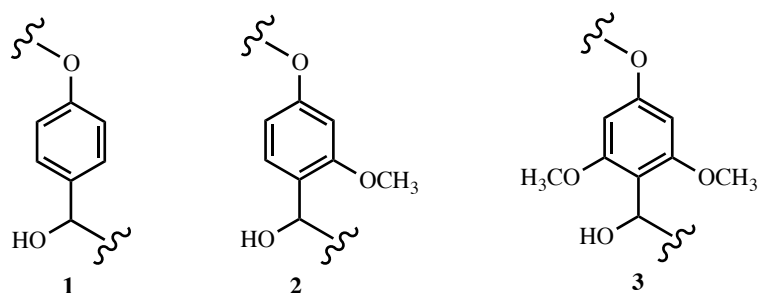


Figure 1.13. Chemical structures of H-, G- and S-type monolignols [85].

The composition of the various monolignols can vary among species, individuals and cell types within an organism. The most common types are *p*-hydroxyphenyl (H), guaiacyl (G) and syringyl (S), and lignins are generally classed as either G or G-S. Hardwood (gymnosperm) lignins are mostly composed of G-lignins, whereas softwood (angiosperm) lignins are mostly composed of G-S-lignins, though both types of lignin can coexist within the same plant. G-lignins only contain H- and G-propane units, whereas G-S-lignins also contain S-propane units [85].

Lignins are synthesized via oxidative coupling between monolignols [84, 86], which, upon secretion to the extracellular environment are radicalized by extracellular peroxidases and laccases, an in situ process. The radicals are then capable of forming a variety of different ether or carbon-carbon bonds to form larger structural units (Fig. 1.14).

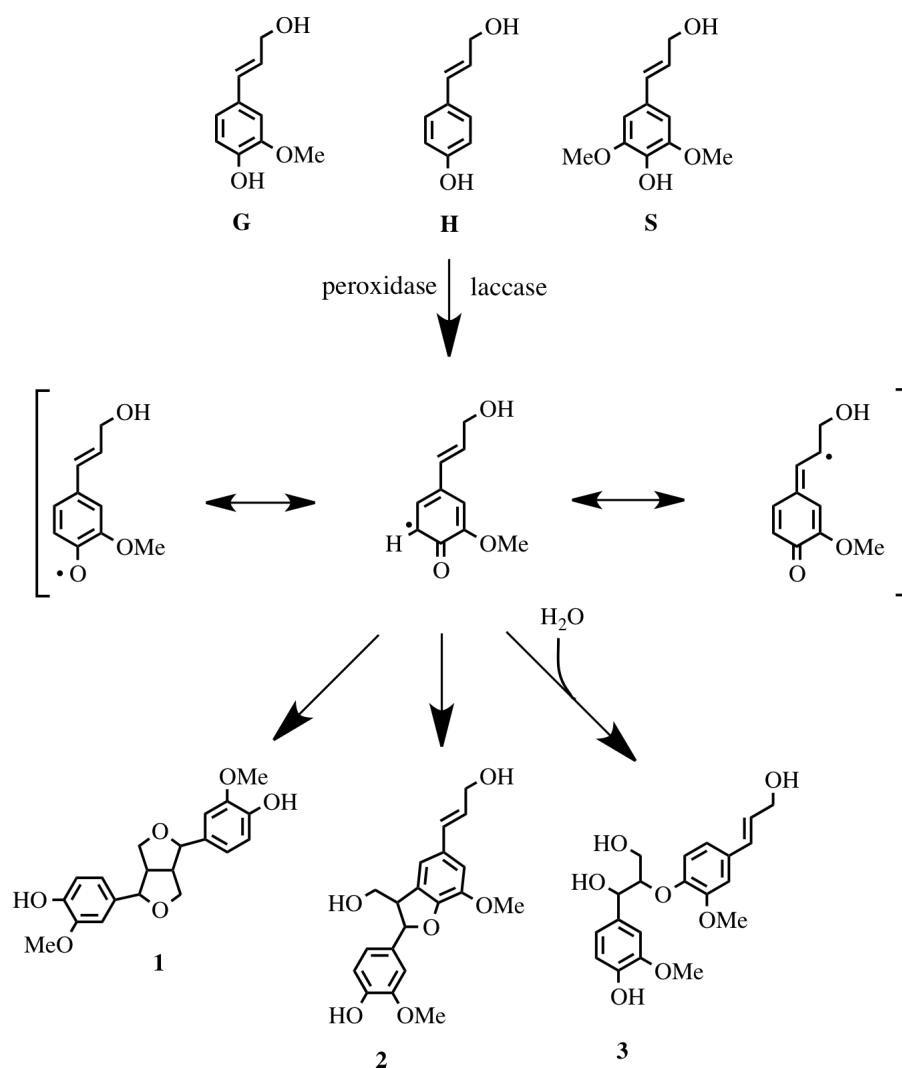


Figure 1.14. Various stages in the natural biosynthesis of the dominant structural units β - β (**1**), β -5 (**2**) and β -O-4 (**3**) from G-, H- and S-type monolignols, which are derived from phenylalanine [84].

Most of the enzymes for lignin biosynthesis are known [87]: phenylalanine ammonia lyase (PAL), cinnamate 4-hydroxylase (C4H), 4-coumarate-CoA ligase (4CL), shikimate hydroxycinnamoyl transferase (HCT), coumarate 3-hydroxylase (C3H), caffeoyl-CoA 3-O-methyl-transferase (CCoAOMT), cinnamoyl-CoA reductase (CCR), cinnamyl alcohol dehydrogenase (CAD), ferulate 5-hydroxylase (F5H) and caffeic acid/5-hydroxyferulic acid O-methyltransferase (COMT).

Since the bonds formed between the lignin monomers are significantly more stable than those present in other biological polymers, it is difficult for them to be broken down by a single enzyme. Advances in the understanding of lignin biosynthesis allows the development of novel lignin modification methods that can enable it to be solubilized at lower temperatures, hence minimizing the pre-treatment costs [84–87].

1.4.2. Characterization of lignin

Since lignin is structurally very complex, it is difficult to thoroughly characterize, though solid-state NMR, FT-IR, ESI-MS, MALDI-MS and microanalysis are reported to partially characterize lignin [88–99].

Solid-state ^{13}C -NMR has been used since the 1980s to identify the substitution patterns of the aromatic rings in the lignin polymer, and more recently to assess the structural changes induced during the extraction process [88 – 90]. The dipolar interactions between carbon atoms and protons are used to cause dephasing of the signals, and selection of an appropriate time during which the dipolar interactions are allowed to affect can allow the detection of only quaternary carbons since their rate of decay is slower than the protonated carbon signals [91, 92]. The ability of this technique to characterize both lignin and the wood from which it is extracted is of considerable use in distinguishing between natural structural changes and those induced during the extraction processes e.g. the milling of wood in the production of milled wood lignin [93]. In contrast, solution-based NMR cannot be used to evaluate the structural features of lignin in untreated wood. Additional advantages of Solid-state ^{13}C -NMR include the

ability to detect free and ether-linked phenolic units by the dipolar dephasing method.

Infrared spectroscopy is a widely used technique in lignin research, and monitors the absorption by molecules at particular frequencies, which are specific to particular bonds that vibrate within the structure (e.g. O–H, C=O) [94]. In recent years IR spectroscopy has been revolutionized by the development of Fourier transform instruments and enhanced sample presentation techniques. FT–IR spectroscopy has been used to study the chemical composition of wood [94–96] and analyze chemical changes induced by fungal degradation, more specifically to monitor the structural changes in beech wood induced by white-rot fungi [97] and the effects of brown-rot fungi on Scots pine [98]. Advantages of this method include high sensitivity, rapid analysis time and the requirement of low amounts of sample [99].

The proportion of lignin in a sample of lignocellulosic biomass can also be quantified via the acetyl bromide method [100–103], a rapid process involving the dissolution of finely ground lignocellulose in 25 % acetyl bromide in concentrated acetic acid at 50 – 70 °C. Acetyl derivatization of the lignin polymer enhances its solubility under acidic conditions (Fig. 1.15), and the lignin concentration of the resulting solution is determined by monitoring the change in absorbance at 280 nm [100–103]. This method is advantageous since low sample volumes are required although it needs to be referenced to a standard curve constructed using known concentrations of standard lignin extracted from similar plant material with acetyl bromide [101] or acidic dioxane [102].

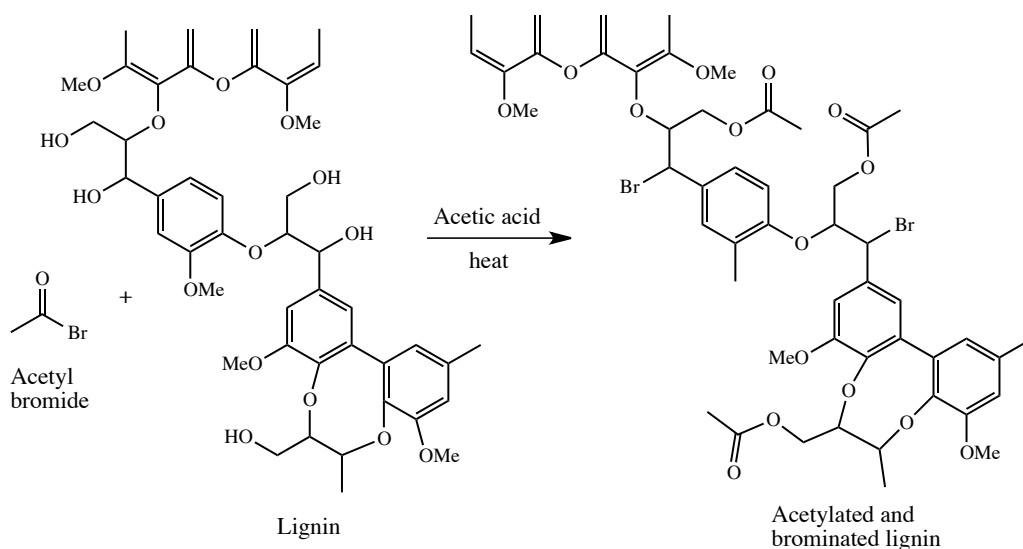


Figure 1.15. Acetyl derivatization of lignin by acetyl bromide for solubility under acidic conditions [100].

A further method for quantifying lignin is the Klason method [103], which is based on gravimetry and involves treatment of the sample with 72 % sulfuric acid followed by heating with dilute acid to hydrolyze the polysaccharides and solubilize the products. The solid fraction is then washed, dried and weighed. Although this is a reliable method for determining the total lignin content, it faces several limitations including lack of accuracy for hardwood samples due to the varying content of acid-soluble lignin [103].

1.5. Microbial breakdown of lignin

Fungi and bacteria contribute to the natural biodegradation of lignin. Although fungal species have been found to produce enzymes that are very efficient in depolymerizing lignin, their poor stability under extreme environmental conditions such as pH and temperature limits their industrial use [104]. In contrast, several bacteria are stable under such conditions and there is a great deal of scope for the use of thermotolerant bacteria in industrial lignin

breakdown processes. In the past 35 years there has been an increased interest in bacterial lignin breakdown and several lignin-degrading bacteria have been reported [105 – 112].

In addition to the possibility of isolating extremophilic lignin-degrading bacteria, other potential advantages of studying lignin-degrading bacteria rather than lignin-degrading fungi include easier gene cloning and more advanced protein expression. Despite these advantages, knowledge of bacterial lignin-degradation mechanisms is limited. The two main oxidants that depolymerize lignin are O_2 and H_2O_2 , and typical products of lignin oxidation include *p*-hydroxyl, vanillyl and syringyl groups (Fig. 1.16) [85].

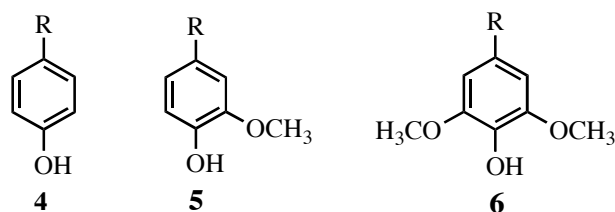


Figure 1.16. Chemical structures of the characteristic lignin oxidation products *p*-hydroxyl (**4**), vanillyl (**5**) and syringyl (**6**) [85].

1.5.1. Degradation of lignin by Fungi

Fungi depolymerize lignin via an enzymatic procedure performed by lignolytic enzymes including manganese peroxidase (MnP) [113], lignin peroxidase (LiP) [113] and laccase [114–118]. Wood-rotting fungi are generally divided into two broad classes: brown-rot fungi and white-rot fungi [113]. White-rot fungi are more effective towards lignin degradation and the most extensively studied since they are capable of completely oxidizing both lignin and cellulose to carbon dioxide and water. In contrast, brown-rot fungi generally only attack the cellulose [113].

White-rot fungi secrete a variety of extracellular oxidative enzymes that collaboratively break down lignin. A well-studied example is *Phanerochaete chrysosporium* [114], a Basidiomycete that releases extracellular peroxidase enzymes LiP and MnP to break down the lignin structure into smaller components [119].

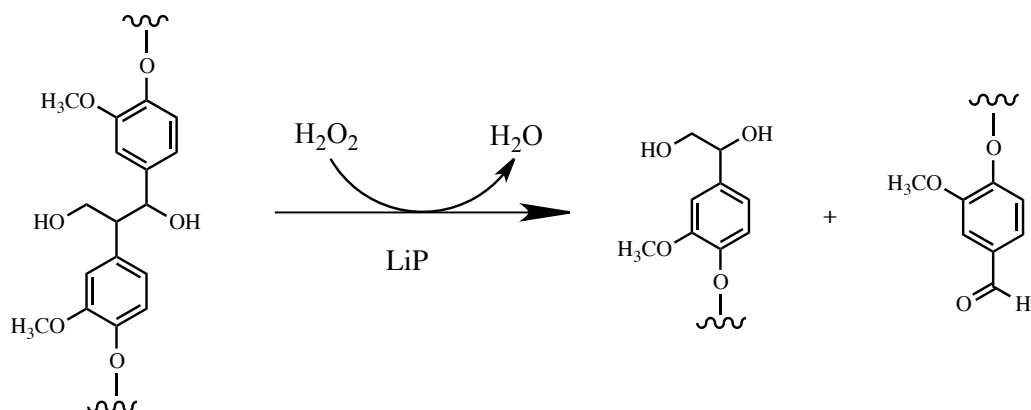


Figure 1.17. Oxidative cleavage of the lignin structure by lignin peroxidase (LiP) [114].

Lignin peroxidases (LiPs) are unique in their ability to oxidize non-phenolic substrates such as carbon-carbon and ether bonds. They are globular and largely helical heme-containing enzymes (Fig 1.18) that catalyze the oxidation of lignin and several other non-phenolic aromatic compounds (Fig. 1.17) in the presence of H₂O₂, a pre-requisite for activity [113, 114]. Reactions catalyzed by LiP include ring-opening reactions, side-chain cleavages, demethoxylations and benzylic alcohol oxidations, all of which are concordant with a mechanism involving the one-electron oxidation of aromatic compounds to initially produce aryl cation radicals that can undergo subsequent non-enzymatic, substituent-dependent reactions to yield an array of final products [113].

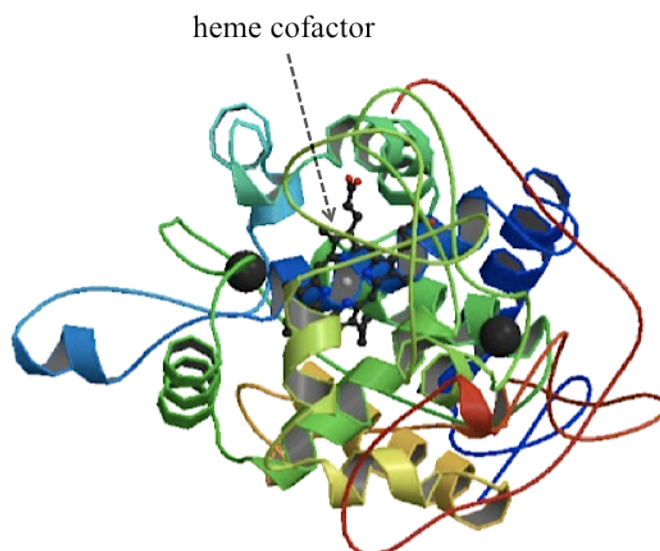


Figure 1.18. Crystal structure of LiP from *P. chrysosporium* [114].

The H_2O_2 -induced catalytic cycling involves substrate reduction of enzyme intermediates known as compound I and compound II (Fig. 1.19). The first step in the mechanism involves the formation of compound I, which stores two oxidizing equivalents from H_2O_2 as an oxyferryl iron centre and a radical, either on the porphyrin ring or on a solvent exposed tryptophan residue, Trp171. This process involves an acid-base mechanism, and it is widely believed that the conserved distal histidine in the active site of heme peroxidases is the acid-base catalyst that induces the heterolytic cleavage of H_2O_2 [113, 114].

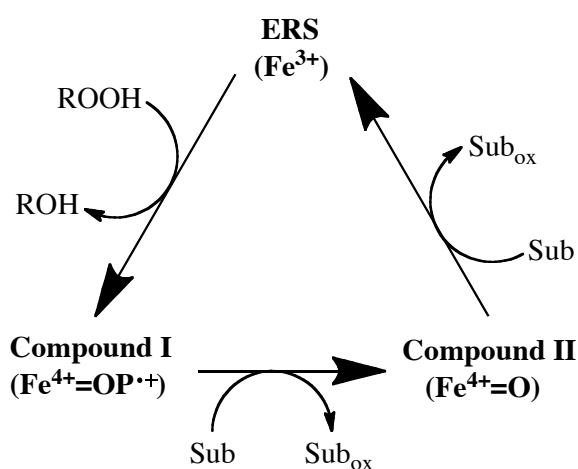


Figure 1.19. An illustration of the general catalytic cycle of peroxidases [113].

Hyperperoxide (ROOH) causes the two-electron oxidation of the enzyme resting state (ERS) to yield compound I containing Fe^{4+} and a porphyrin cation radical ($\text{P}^{\cdot+}$). Two single-electron reductions of this compound lead to compound II, which contains $\text{Fe}^{4+}=\text{O}$ after porphyrin reduction. Consecutive oxidation of two substrate molecules, e.g. low-redox potential phenols or Mn^{2+} in case of MnP, leads to the enzyme resting state.

Manganese peroxidases (MnPs) oxidize lignin, several phenolic compounds and Mn (II) to Mn (III) [115], a process that is dependent on the availability of H_2O_2 and the free manganous ion, Mn (II), which acts as a diffusible redox couple [113].

Mn (II) is the primary reducing substrate in the MnP catalytic mechanism (Fig. 1.20) [113], readily reducing $\text{MnP}_{(\text{compound 1})}$ to $\text{MnP}_{(\text{compound 2})}$, which in turn oxidises the organic substrate.

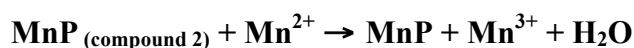
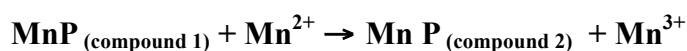


Figure 1.20. Catalytic mechanism of manganese peroxidase (MnP) [113].

P. chrysosporium activates the MnP oxidative reaction by secreting organic acids such as malonate and oxalate that chelate and stabilize the Mn (III) [114, 115], thereby enabling it to diffuse from the enzyme's surface and oxidize the phenolic substrate. Mn (III) can also oxidize an additional redox mediator such as veratryl alcohol, which can break down non-phenolic compounds.

In contrast to LiP and MnP that contain Fe in their active sites, laccases (*p*-diphenol:dioxygen oxidoreductases E.C.1.10.3.2), are multicopper oxidases [115 – 118] that catalyze the one-electron oxidation of a variety of substrates, including diamines, *ortho*- and *para*- diphenols (Fig. 1.21), amino- and methoxy- substituted phenols, and a variety of lignin model compounds [115, 116]. The one-electron reduction process is associated with the four-electron reduction of O₂ to H₂O [116]. Examples of reactions catalyzed by laccases include side-chain cleavage of β-O-4 phenolic lignin and C-C_β cleavage of phenolic lignin compounds [120]. In order to degrade lignin and other bulky substrates, mediators are required [115], e.g. TEMPO (2,2,6,6-tetramethyl-piperidine-N-oxyl radical), which are promptly oxidized by laccases.

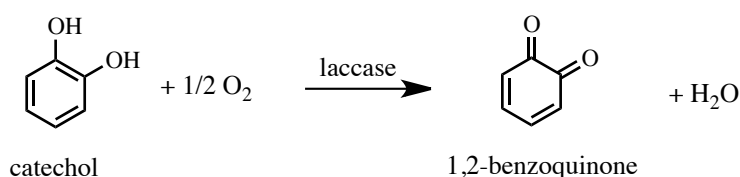


Figure 1.21. Oxidation of catechol by laccase [121].

The catalytic activity of laccases requires four Cu atoms of three different types (Fig. 1.22), distinguishable by their spectroscopic properties [117]. The oxidation of the organic substrate occurs at the mononuclear type-1 Cu (T1) site, whilst the reduction of O₂ occurs at the trinuclear site that is composed of one type-2 (T2) Cu and two type-3 (T3 and T3') Cu's [117]. An electron is extracted from the phenolic substrate to the T1 Cu, and is then transferred to the trinuclear site, which is separated from the mononuclear site by a distance of approximately 12 – 13 Å [117].

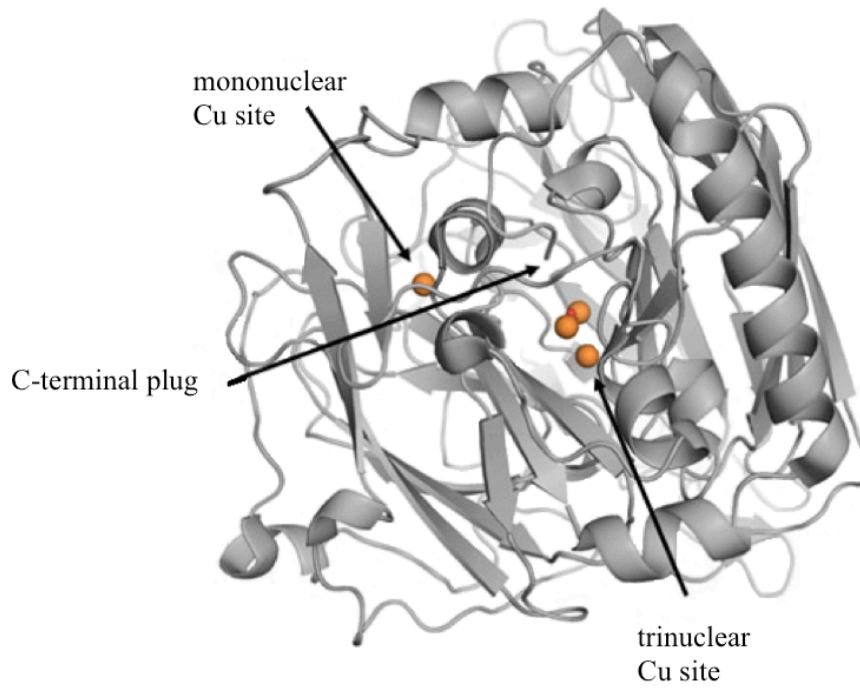


Figure 1.22. Crystal structure of laccase, illustrating the mononuclear and trinuclear Cu sites [122].

An extracellular laccase is produced by many white-rot fungi during primary metabolism [113], but not by *P. chrysosporium* which suggests that it degrades lignin via a different mechanism to that of many other white rot fungi.

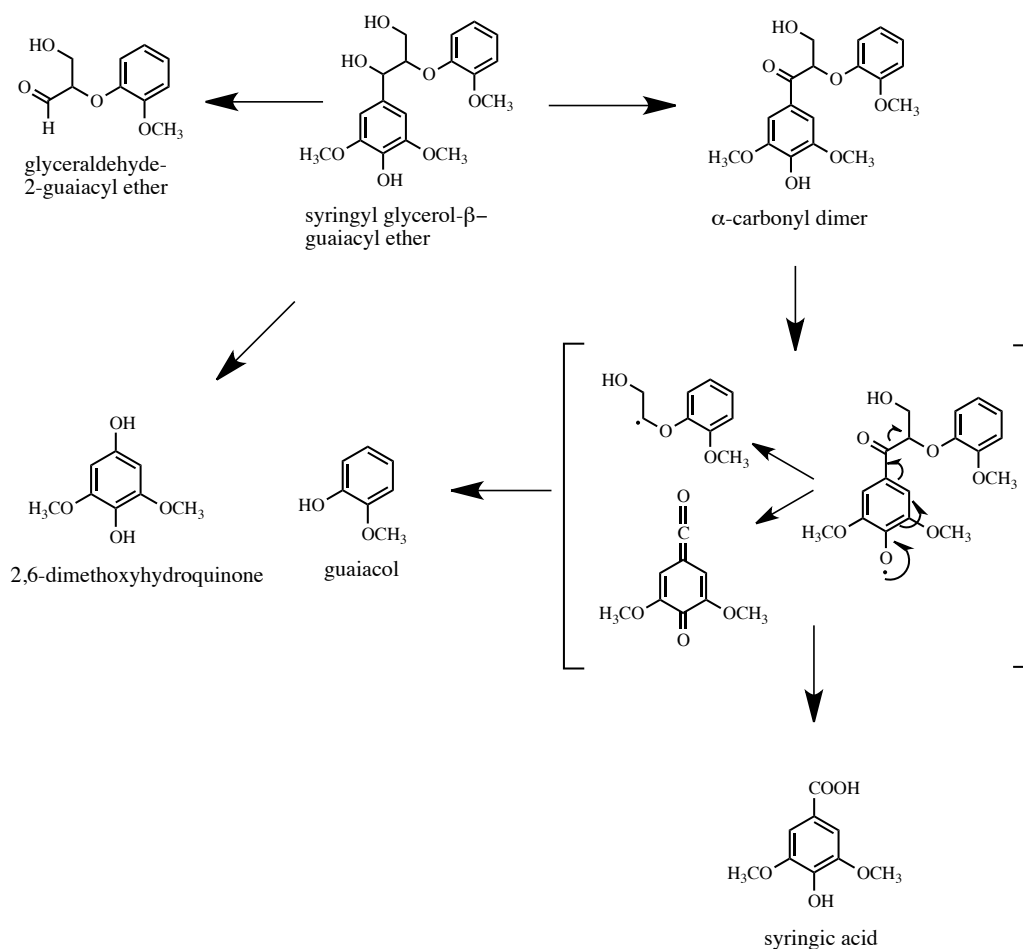


Figure 1.23. Mechanistic detail of the side chain cleavage of a phenolic β -O-4-lignin model compound by laccase from *C. versicolor* [115].

In the past decade it has been discovered that a laccase is capable of oxidizing Mn (II) to Mn (III) in the presence of Mn chelators oxalate, malonate and pyrophosphate [123, 124]. Schlosser and Hofer discovered that the presence of oxalate or malonate led to the formation of H_2O_2 and the reduction of tetranitromethane, indicating the presence of the superoxide anion radical, $\text{O}_2^{\cdot-}$ [125]. These reactions were found to be more rapid in the presence of oxalate compared to malonate, and the observations suggest that laccase reactions involve enzyme catalyzed Mn (II) oxidation in the presence of oxalate or malonate chelators, which are broken down by the resulting Mn (III), leading to

the formation of superoxide and its consecutive reduction to H₂O₂, which is required by lignin peroxidases for activity towards lignin degradation.

H₂O₂ is formed via oxidation of hydroquinones by lignolytic enzymes and auto-oxidation of the corresponding semiquinone products concurrently reducing O₂ to superoxide anion radical [126, 127]. Mn (II) reduces superoxide to H₂O₂ and is oxidized to Mn (III) [127, 128], and superoxide may dismutate to H₂O₂ and O₂. Oxidation of oxalate (Fig. 1.24) and malonate (Fig. 1.25) by Mn (III) is also believed to be a source of H₂O₂ [123, 124].

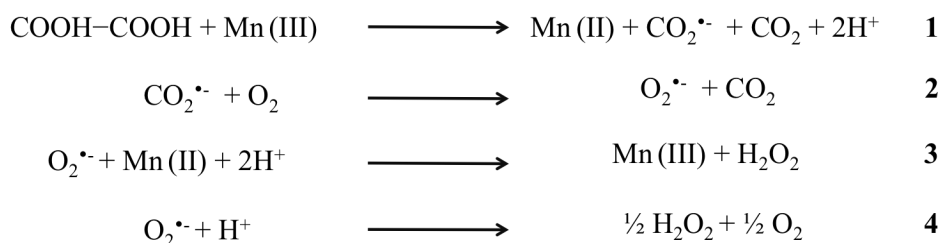


Figure 1.24. Reactions occurring for oxalate [123, 129].

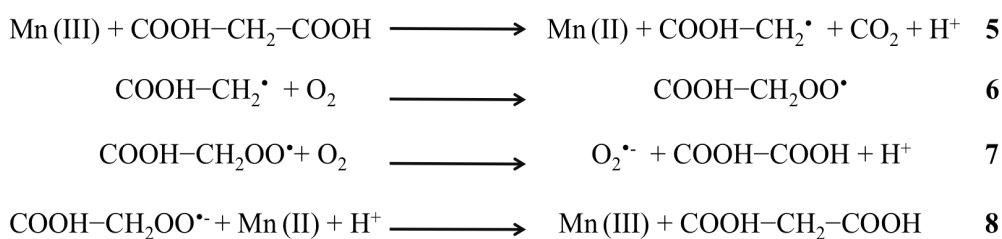


Figure 1.25. Suggested reactions for the abiotic decomposition of malonate [124].

The superoxide and oxalate produced in reaction 7 can subsequently contribute to reactions 1 and 4.

1.5.2. Bacterial degradation of lignin

A significant amount of research in the past few decades has supported the theory that bacteria break down lignin as well as discovering bacterial strains that degrade specific lignin components [105, 119]. By the mid-1980s, developments in the understanding of bacterial lignin-degradation mechanisms were obtained from work with Gram-positive Actinomycetes and *Pseudomonas* species.

Reported lignin-degrading bacteria [105 – 112] include Actinomycetes such as *Nocardia*, *Rhodococcus*, *Sphingomonas paucimobilis* SYK-6 and *Streptomyces viridosporus* T7A which, when grown on lignocellulose, produces extracellular peroxidases that degrade both the lignin and carbohydrate components of lignocellulose [130]. In the past 5 years a new family of peroxidases, known as the dye-decolourizing peroxidase (DyP) family, has been identified [131]. The first characterized recombinant bacterial lignin peroxidase, DyP B, has since been reported from this category [132].

1.5.2.1. Breakdown patterns

Three structural patterns of cell wall breakdown by bacteria have been reported: cavitation, erosion and tunnelling [133 – 135]. Cavitation bacteria are located in the lumen of wood cells and are known to utilize breakdown products [133]. Erosion bacteria attack the cell wall from the lumen into the secondary cell walls either solely or as part of a collaborative process [134]. They perform the dominant type of bacterial lignin degradation in undisturbed waterlogged wood and are active in anaerobic environments. In morphological terms, erosion bacteria are generally rod-shaped. In contrast, tunnelling bacteria are much

more aerobic, requiring a plentiful supply of oxygen, although they are known to produce microscopic tunnels through the cell wall [135].

1.5.2.2. Bacterial lignin-degradation pathways

Lignin is broken down into a more soluble, lower-molecular weight material via oxidative pathways [130] as indicated by the characterization of a *Streptomyces*-degraded softwood lignin. A variety of single-ring aromatic intermediates yielded from the breakdown of hardwood, softwood and grass lignins by *S. viridosporus* have also been identified [130].

Significant steps in lignin degradation include cleavage of the biphenyl ring (Fig. 1.26), β -aryl ether cleavage (Fig. 1.27) [136], 3-O-methyl gallate (3MGA) catabolic pathways, the β -keto adipate pathway (Fig. 1.28), the ferulic acid catabolic pathway (Fig. 1.29), the protocatechuate (PCA) catabolic pathway and O-demethylation of syringate and vanillate [137].

Biphenyl ring cleavage:

Several biphenyl-degrading bacteria have been reported, including *Pseudomonas putida* mt-2 and *Rhodococcus jostii* RHA1 [138], which grow on biphenyl (1) and in turn oxidize it via a catabolic pathway. Enzymes involved in the breakdown of biphenyl are termed *bph* [138, 139], a gene cluster that includes four different genes (*bphA*, *bphB*, *bphC* and *bphD*), each of which encodes a different biphenyl-degrading enzyme.

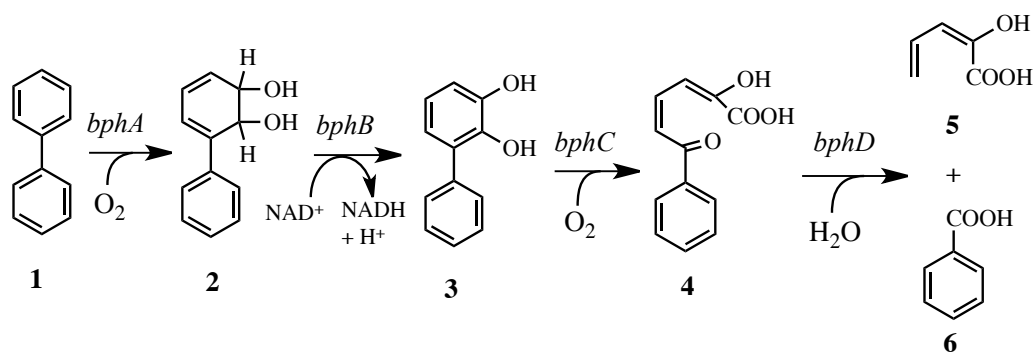


Figure 1.26. Biphenyl ring cleavage pathway [137–139].

The bacterial degradation of biphenyl (1) proceeds via a dioxygenase-catalyzed reaction [138], initiated by conversion into a dihydrodiol compound, 2,3-dihydroxyl-1-phenylcyclohexa-4,6-diene (2), by biphenyl dioxygenase (*bphA*); this hydroxylation reaction destabilizes the aromatic ring and initiates the ring cleavage pathway [139]. Dihydrodiol dehydrogenase (*bphB*) then converts this compound into 2,3-DHBP (3), which is subsequently cleaved at the 1, 2-position by 2,3-DHBP dioxygenase (*bphC*) to produce a *meta*-cleavage compound, 2-hydroxy-6-oxo-6-phenylhexa-2, 4-dienoic acid (4). Hydrolysis of compound 4 by *meta*-cleavage compound hydrolase (*bphD*) generates 2-hydroxypenta-2, 4-dienoic acid (5) and benzoic acid (6) [138].

The biphenyl ring cleavage pathway has been found to be similar in different bacteria such as *Achromobacter* [140], *Arthrobacter*, *Pseudomonas* and *Rhodococcus* [138], irrespective of whether they are Gram-positive or Gram-negative [138].

Possibly the most prevalent lignin-degradation pathway is the reductive cleavage of the β -aryl ether since it constitutes approximately 50 % of linkages in lignin [136, 137] and leads to the production of vanillin [113]. *S. paucimobilis* SYK-6 secretes specific enzymes to break down the lignin, which include O-demethylases, β -etherases and dioxygenases for ring cleavage [136].

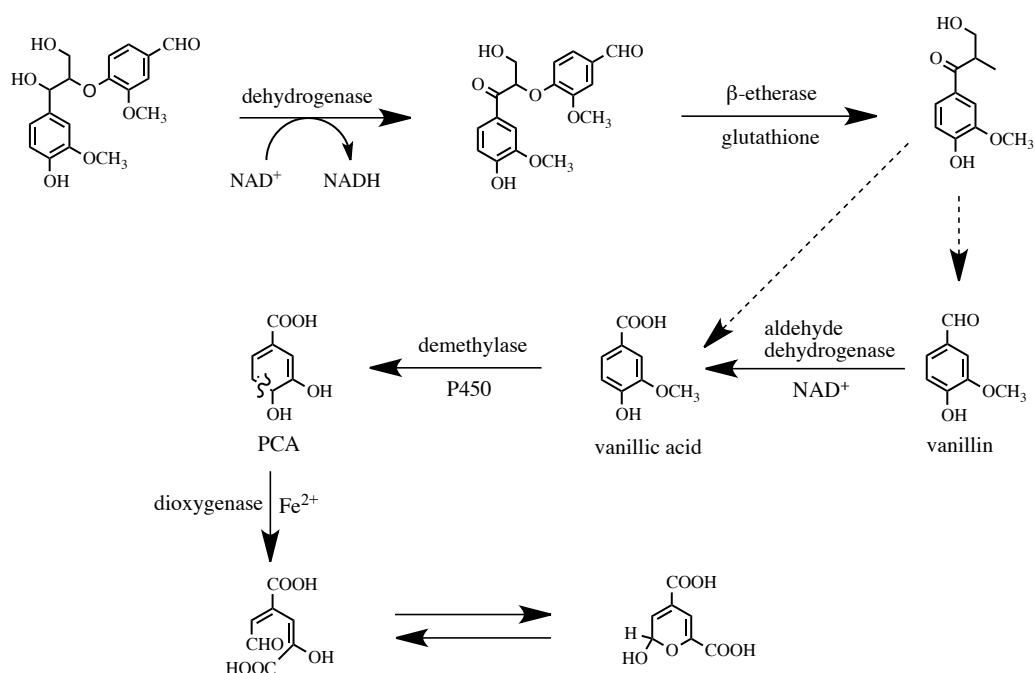
β -aryl ether cleavage:

Figure 1.27. β -aryl ether cleavage pathway in *S. paucimobilis* SYK-6 and subsequent catabolic pathways [136, 137].

Studies on the dominant pathways for bacterial degradation of aromatic compounds have shown that a small number of central intermediates [136, 137, 141] such as protocatechuic acid (PCA) and catechol are produced. These intermediates subsequently undergo *ortho*-cleavage or *meta*-cleavage. Non-substituted aromatic and chloro-aromatic compounds are generally broken down via *ortho*-cleavage, whilst the ring-opening reactions of methyl-substituted aromatic substrates occur via *meta*-cleavage, a process catalyzed by catechol-2,3-dioxygenase [142, 143].

Vanillate (4-hydroxy-3-methoxybenzoate) and PCA are important intermediates in the catabolic process [141], and two different vanillate demethylation pathways have been reported; one being catalyzed by vanillate demethylase, and the other by tetrahydrofolate-dependent O-demethylase [137]. The ring-opening

reaction of PCA is catalyzed by a dioxygenase enzyme, supposedly 3,4-dioxygenase, 4,5-dioxygenase or 2,3-dioxygenase [141].

The downstream pathway reported in *S. viridosporus*, known as the β -ketoadipate pathway [144] (Fig 1.28), is reported to be induced by PCA and 4-hydroxybenzoate.

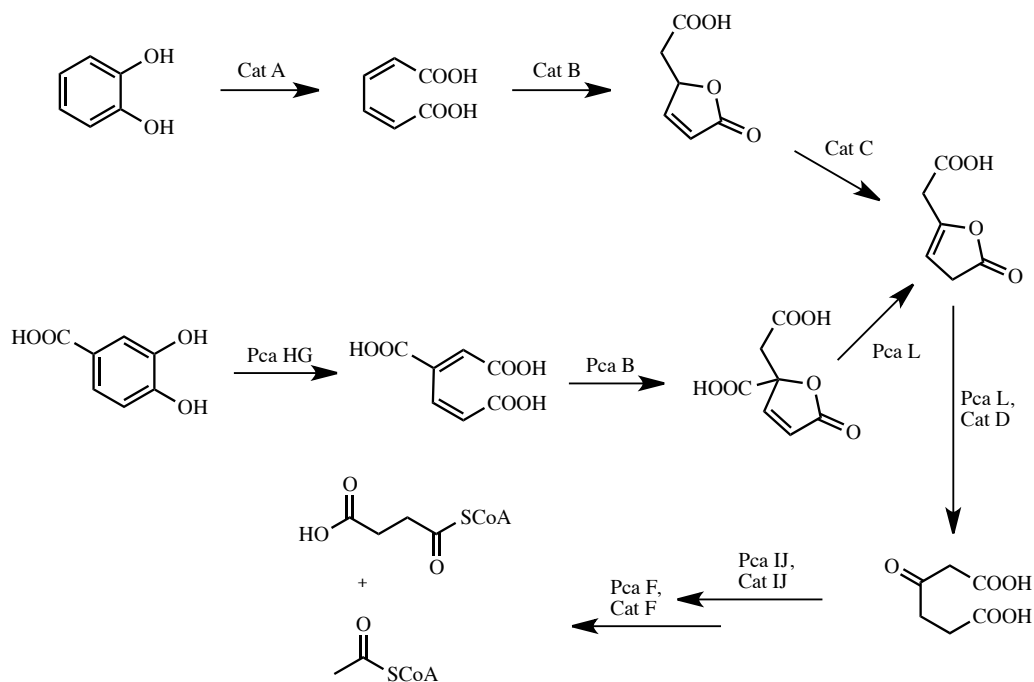


Figure 1.28. β -ketoadipate pathway [144].

Previous studies have found that *S. viridosporus*-induced modifications to lignin are consistent with the activity of enzymes in the β -ketoadipate pathway.

Ferulic acid catabolic pathway:

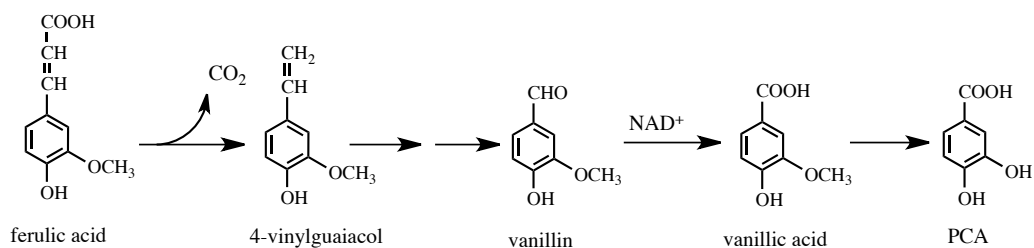


Figure 1.29. Ferulic acid catabolic pathway in *B. coagulans* BK07 [145].

Ferulic acid, a cinnamic acid derivative, contributes to the cross-linking of cell walls, and is the precursor for lignin biogenesis [137]. Ferulic acid (Fig. 1.29) is a renewable and abundant precursor of aromatic compounds [146], and its catabolism to yield desirable compounds such as vanillin and PCA has been reported in fungi and bacteria [146]. Early studies reported an oxidative side-chain cleavage in *Pseudomonas acidovorans* [147] to produce acetic acid, and more recent studies have discovered a coenzyme-A-dependent pathway, yielding vanillin [148]. However, a much faster rate of ferulic acid catabolism was reported by Karmakar *et. al* [145], who isolated a novel bacterial strain that converts ferulic acid to vanillic acid and PCA via 4-vinylguaiacol and vanillin (Fig. 1.29).

DyP peroxidases:

Bioinformatic studies identified two genes of interest in the secretome of *Rhodococcus jostii* RHA1, which had previously been found to be capable of degrading lignin [132]. These genes encoded dye-decolourizing peroxidases, which are known as DyP A and DyP B and contain a heme prosthetic group as well as possessing distinctive primary and tertiary structures, which result in catalytic mechanisms that are unique among the peroxidases. Gene deletion studies found that a Δ DyP B deletion mutant was much less active towards lignin degradation in the nitrated lignin assay (see 1.6.1), whilst a Δ DyP A deletion mutant did not result in activity loss [132]. DyP B was also found to be active towards a variety of lignin dimers and was discovered to directly interact with Kraft lignin via stopped flow experiments, an observation that had previously been unique to lignin peroxidases [132]. Other interesting observations include

the enhancement of activity of DyP B in the presence of Mn (II) and its specificity for the β -aryl ether component of lignin (Fig. 1.30). The combination of these observations highlighted DyP B as the most active of the two DyP peroxidases towards lignin degradation, and it is the first recombinant bacterial lignin peroxidase to be characterized kinetically.

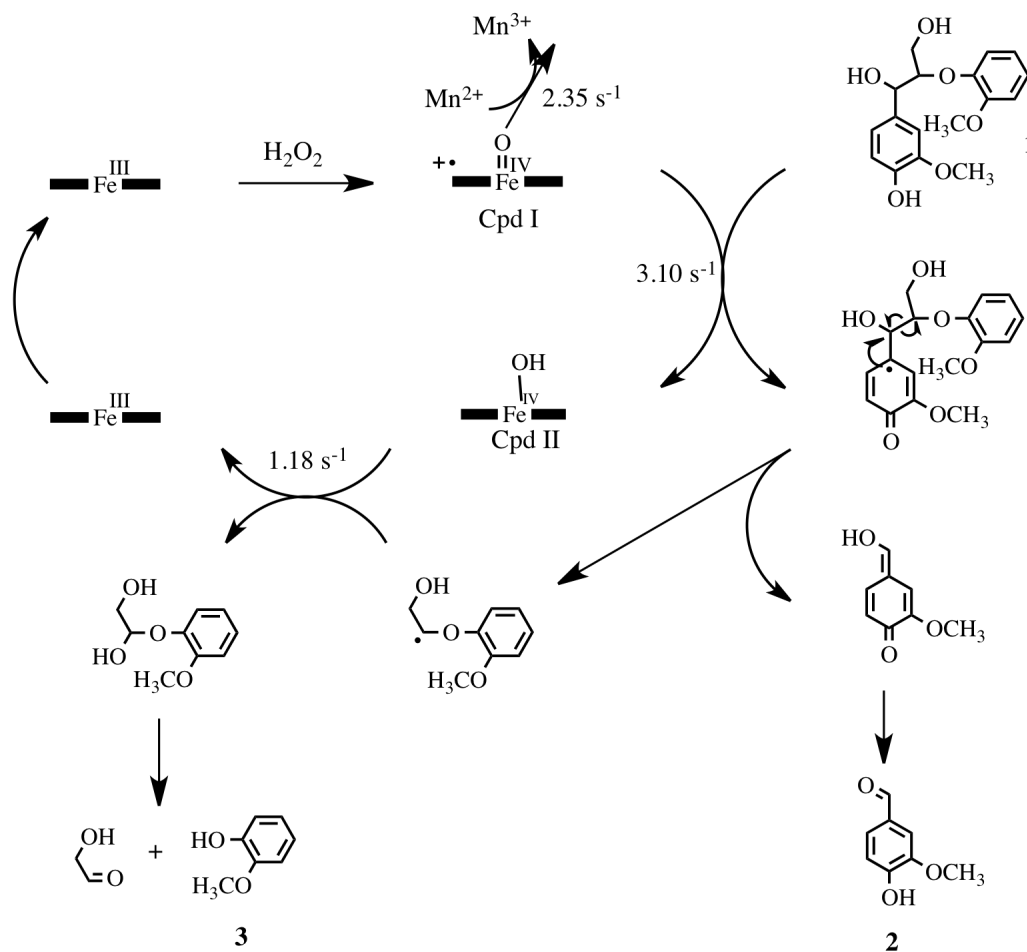


Figure 1.30. Catalytic cycle of DyP B, in which β -aryl ether (**1**) is converted into vanillin (**2**) or guaiacol (**3**) [132].

The catalytic cycle of DyP B (Fig. 1.30) is initiated by the reaction of the ferric enzyme with H₂O₂ to yield compound I, which is two reducing equivalents more oxidized than the ferric resting state. Compound I then reacts with one equivalent of the reducing substrate to yield compound II, which in turn reacts

with a second equivalent of the reducing substrate to yield the resting state Fe^{III} peroxidase [132].

In addition to peroxidases there are several reports of bacterial laccases, one of which has been found to be active towards the degradation of low-molecular weight aromatic compounds and was purified from *γ-proteobacterium* JB [109], a moderately thermotolerant and alkali-tolerant strain that exhibited optimal activity at 55 °C and was stable for 60 days over the pH range 4 – 10. This enzyme has also been found to be capable of decolourizing dyes, including soda pulp [109, 149], a process that requires the removal of the residual lignin from cellulose fibers. Despite the stability of this enzyme, its large-scale industrial use is not commercially viable since it requires 2,2'-azino-bis (3-ethylbenzthiazoline-6-sulfonic acid) [ABTS] as a mediator [150].

A catalase-peroxidase enzyme from unsequenced lignin-degrading soil bacterium *Amycolatopsis* sp. 75iv2 has recently been identified by Chang *et. al* [151] via a novel approach involving functional analysis of the secretome to identify the oxidative enzymes of interest. On the basis of their abundance and activity, two extracellular heme-containing peroxidases Amyco 1 and Amyco 2 were purified to homogeneity and their respective functions class as a bifunctional catalase-peroxidase. Further experiments found that Amyco 1 was capable of degrading unprotected phenolic sites within the lignin polymer, with each active site being capable of oxidizing two phenolic equivalents in each reaction cycle [151].

1.5.2.3. Thermotolerant lignin-degrading bacteria

Bacteria adapted to survive at high temperatures secrete enzymes that are active under similar conditions to those adopted in industrial processes. Performing such processes at elevated temperatures offers several advantages, including the increased bioavailability and solubility of organic compounds and reduced risk of contamination [152]. Reactions that involve hydrophobic substrates that are highly resistant to biodegradation (e.g. lignin) are of significant interest in the planning of future biorefinery processes since their bioavailability can be enhanced at high temperatures.

Although several thermotolerant cellulases and xylanases have been cloned, purified and characterized [153, 154], reports of thermotolerant lignin-degrading enzymes produced by bacteria are less common. Moderately thermotolerant peroxidases and laccases produced by wood-rotting fungi are reported to be most active over temperature ranges of 30 – 55 °C and 55 – 60 °C respectively [152]. Peroxidases produced by bacteria have been examined for lignin-degradation activity but results have been inconclusive.

1.6. Assays for monitoring lignin degradation

Early studies on bacterial lignin degradation led to unreliable results, largely due to limitations in the experimental methods used. In the 1970s the experimental methodologies were revolutionized by the development of an assay method based on the use of ^{14}C -labelled lignin [155], which was used to detect lignin-degradation activity of *Streptomyces*, *Rhodococcus* and *Nocardia* strains. This method involves quantitatively measuring the production of $^{14}\text{CO}_2$ [155], resulting from the oxidation of ^{14}C -lignin-labelled materials. However, this

method is rather slow as it is usually carried out over periods of at least ten days. Other limitations include the laborious techniques required for production of ^{14}C -labelled lignin substrates and to trap and quantify the $^{14}\text{CO}_2$ produced.

Alternative assay methods used to evaluate lignin peroxidase activity were based on the oxidation of β -O-4 model compounds [156], requiring substrate synthesis, and the production of ethylene by the one-electron oxidation of 2-keto-4-methiolbutyric acid (KMB) by *P. chrysosporium*, which was performed using gas chromatography. These laborious methods were generally limited by poor efficiency. A more efficient, widely adopted method involves assessing lignin peroxidase activity by monitoring the conversion of milli molar concentrations of veratryl alcohol to veratraldehyde, which is indicated by a change in absorbance at 310 nm [157]. There are also several limitations to this method, in particular the poor specificity due to the very strong absorbance of other phenolic and lignin-related aromatic compounds at 310 nm and high optical dispersion at 310 nm, resulting in increased sensitivity to turbidity than a method that monitors absorbance in the visible region.

In the early 1990s a more robust method for monitoring lignin peroxidase activity was introduced, which is based on the breakdown of azo and heterocyclic waste dyes from the textile industry and involves measuring the disappearance of the dye by monitoring the absorbance at 651 nm [158]. This is more reliable than the veratryl alcohol method since Azure B, unlike veratryl alcohol, is not oxidized by non-phenolic alcohol oxidases, lignin peroxidase has a much stronger preference for Azure B than veratryl alcohol and Azure B is only decolourized under atypical physical or biological conditions. Despite these improvements, the efficiency of the dye-based assay is hindered by the

necessity to produce a standard curve and to eliminate any dye-decolourizing agents present in the enzyme samples [158].

1.6.1. Nitrated lignin assays

In work leading up to this project, a novel spectrophotometric assay involving chemically nitrated lignin [159] was developed to monitor lignin degradation, and hence detect lignin-degrading bacteria. This method involves measuring the time-dependent change in absorbance at 430 nm over a 20-minute period [159]; breakdown of nitrated lignin releases nitrated phenols (Fig. 1.31), which lead to an increase in absorbance at 430 nm, hence giving an indication of the rate of lignin breakdown. This assay method was examined using *S. viridosporus*, *R. jostii* RHA1 and *P. putida* mt-2, lignin-degrading bacteria, and *Bacillus subtilis* and *Leuconostoc mesenteroides*, non lignin-degrading bacteria, and is performed with and without H₂O₂, allowing us to detect whether the bacteria use extracellular lignin peroxidases or laccases. Time-dependent absorbance increases of 1 – 3 mAU were observed over 20 min for the lignin-degrading bacteria, whereas a decrease or no change in absorbance was observed for the non-degraders. *S. viridosporus* was much less active in the absence of H₂O₂, whilst *P. putida* mt-2 and *R. jostii* RHA1 still appeared to be active without H₂O₂, suggesting that they can utilize O₂ for lignin degradation [159].

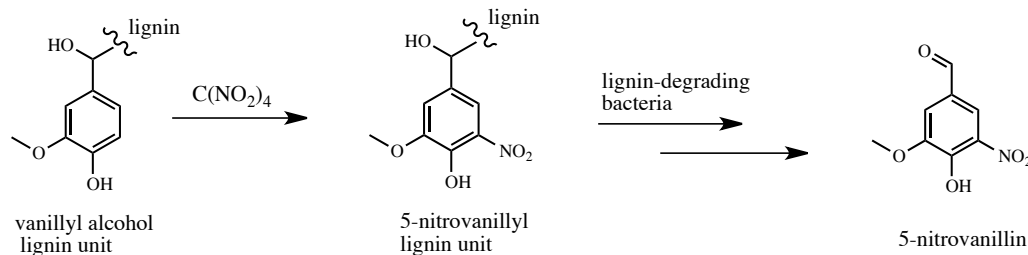


Figure 1.31. Nitration of lignin via reaction with tetranitromethane, the molecular basis of the nitrated lignin assays [159].

The molecular basis for the observed time-dependent increases was examined by preparing liquid cultures of the known lignin-degrading bacteria and *B. subtilis* in the presence of nitrated milled wood lignin (MWL) overnight and examining the resulting solution by reverse phase HPLC. Several new peaks absorbing at 430 nm were observed. In the solutions containing *S. viridosporus* and *R. jostii* RHA1, a peak of identical retention time and UV/visible spectrum to 5-nitrovanillin was observed, and a range of other peaks absorbing at 430 nm were formed by treatment with *R. jostii* RHA1 and *P. putida* mt-2. In contrast, no new peaks were formed by treatment with *B. subtilis*. Verification that the absorbance increases were not due to the breakdown of cellulose and glucose was achieved by reacting *R. jostii* RHA1 and *P. putida* mt-2 with glucose and cellulose, which were nitrated under the same conditions as MWL. No time-dependent change in absorbance at 430 nm was observed in any of the experiments [159].

The nitrated lignin assay has also been used to demonstrate the activity of DyP B towards lignin degradation. Recombinant DyP A and DyP B proteins were examined in the presence and in the absence of H₂O₂. DyP B was found to be active in the presence of H₂O₂, but not in its absence, whereas DyP A showed no activity with or without H₂O₂. These observations suggest that only DyP B

exhibits lignin peroxidase activity, consistent with results from gene knockout experiments [132, 159].

M. Ahmad (University of Warwick) observed a yellow coloration upon spraying of agar-plated cultures of *Pseudomonas fluorescens* and *R. jostii* RHA1 with nitrated lignin solution at a concentration of $25 \mu\text{g ml}^{-1}$, ten-fold higher than the concentration used for the UV/visible microtitre plate assay method (Fig. 1.32).

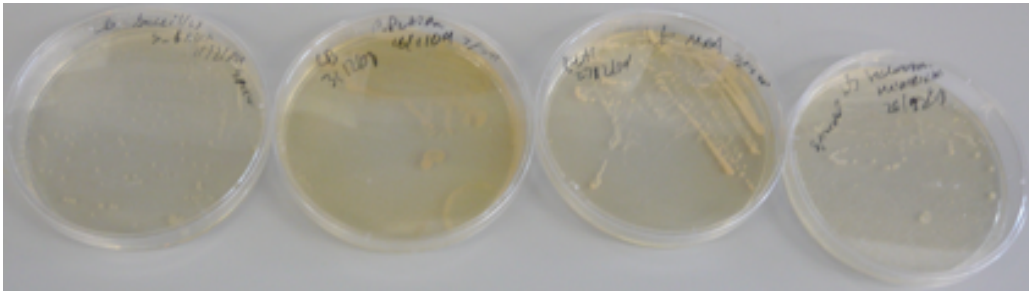


Figure 1.32. Nitrated lignin spray assay, showing yellow coloration for *P. putida* mt-2 (centre-left) and *R. jostii* RHA1 (centre-right), and no coloration for non-degraders *B. subtilis* (far-left) and *L. mesenteroides* (far-right), after 24 hr incubation at 30 °C.

The yellow coloration was observed following incubation of the cultures at 30 °C for 24 – 48 hr. In contrast, no colour change was observed on agar plates containing *B. subtilis* and *L. mesenteroides*. These observations suggested that it might be possible to use this ‘spray’ assay as a screening method for the isolation of novel lignin-degrading bacteria from environmental samples.

1.7. Aims of the Project

The aims of this project are to isolate lignin-degrading bacteria from environmental sources, purify the extracellular enzymes and examine their ability to degrade various lignin-containing feedstocks:

- The nitrated lignin assays [159] will be modified via alterations to parameters and tested using a variety of different types of nitrated lignin with previously studied lignin-degrading bacteria and non lignin-degrading bacteria. The optimized assays will be used to screen a large collection of environmental bacteria for activity towards lignin degradation. Mesophilic strains will be isolated from soil samples collected from forestry locations, and thermotolerant strains from composted wheat straw. The strains that exhibit activity in the nitrated lignin assays will be identified by analysis of the 16S rRNA gene sequence.
- The ability of the environmental lignin-degrading bacteria to grow in different liquid media, lignin-related aromatic compounds and cellulose will be examined.
- The strains will be inoculated with high- and low-molecular weight forms of Kraft lignin, size-fractionated via aqueous gel filtration chromatography, and gel filtration HPLC analysis will reveal any modifications to the molecular weight distribution resulting from treatment with each strain..
- The most 'active' strains towards lignin degradation will be examined for their ability to break down different lignin-containing feedstocks in a series of laboratory-scale fermentation experiments. Degradation of the

feedstock will be monitored via measurement of soluble phenol content, colony-forming units, reducing sugar content and pH. The treated and untreated material will also be studied by FT-IR.

- Extracellular enzymes will be purified from the culture supernatant of the most active strains using regular protein purification methods. Nitrated lignin and ABTS assays will be used to monitor activity of the purified enzymes, and Mass Spectrometry used to acquire internal peptide sequence data.

Chapter 2: Screening for environmental lignin-degrading bacteria

2.1. Introduction

As discussed in Chapter 1, the use of bacterial enzymes rather than fungal enzymes to break down the lignin component of lignocellulose in a novel biological pre-treatment process offers several advantages. Since relatively little is understood about bacterial lignin-degradation pathways and few bacterial lignin-degrading enzymes have been identified there is a great deal of scope to identify environmental bacteria that are capable of naturally degrading lignin. Such bacteria are likely to exist in soils in forestry locations and also in wood-digesting insects such as termites [160, 161], whilst thermotolerant bacteria are more likely to exist in geothermal environments such as hot springs, compost piles and fermentations of lignocellulosic material. In order to isolate lignin-degrading bacteria from environmental sources it is essential to develop an efficient method to screen a wide range of isolates for activity towards lignin degradation. The preliminary results obtained using the nitrated lignin [159] assay suggest that this could be used as the basis of a new screening method.

2.2. Development of nitrated lignin assays

2.2.1. Development of a novel nitration method for the preparation of nitrated lignin solution

In work leading up to the project, the nitrated lignin assay was initially developed using samples of milled wood lignin (MWL), nitrated with tetranitromethane [159]. However, inconsistent results were obtained and so the assay was modified using concentrated nitric acid rather than tetranitromethane. In order to determine the degree of nitration towards which known lignin-degrading bacteria exhibit optimum activity, 5 mg MWL from wheat straw, prepared by M. Ahmad [159], was mixed with glacial acetic acid and varying volumes of concentrated nitric acid: 100 μ l (A), 200 μ l (B) and 300 μ l (C).

Analysis of samples A, B and C by UV/visible spectroscopy indicated the presence of a new peak at 430 nm, corresponding to the nitrated product, and a shift from 280 nm (un-nitrated MWL) to 300 nm (nitrated MWL) was observed in the UV/visible analysis, which indicates the presence of nitrated aromatic rings. The degree of nitration of sample C, which was most sensitive to the lignin-degradation activity of extracellular enzymes secreted by *R. jostii* RHA1 and *P. putida* mt-2 (Fig. 1), was estimated from the ratio of absorbance at 300 nm to 280 nm to be 41 – 47 % of phenolic rings compared to 35 % for the nitrated MWL prepared by M. Ahmad via the tetranitromethane method [159]. ESI mass spectrometry of the nitrated and un-nitrated MWL samples indicated a similar molecular weight distribution for nitrated and un-nitrated MWL in the range m/z 540 – 1500.

2.2.2. UV/visible nitrated lignin assays for nitrated MWL samples A, B and C with previously studied lignin-degrading bacteria

In order to determine the sample of maximum sensitivity towards activity of lignin-degrading enzymes, the culture supernatants of previously studied lignin-degrading bacteria *R. jostii* RHA1 and *P. putida* mt-2 were reacted with nitrated MWL samples A, B and C in the presence of 2 mM H₂O₂ and the absorbance at 430 nm monitored over 20 min. The culture supernatant of *B. subtilis*, a previously studied non lignin-degrading strain was also reacted with each sample of nitrated MWL solution in a negative control experiment.

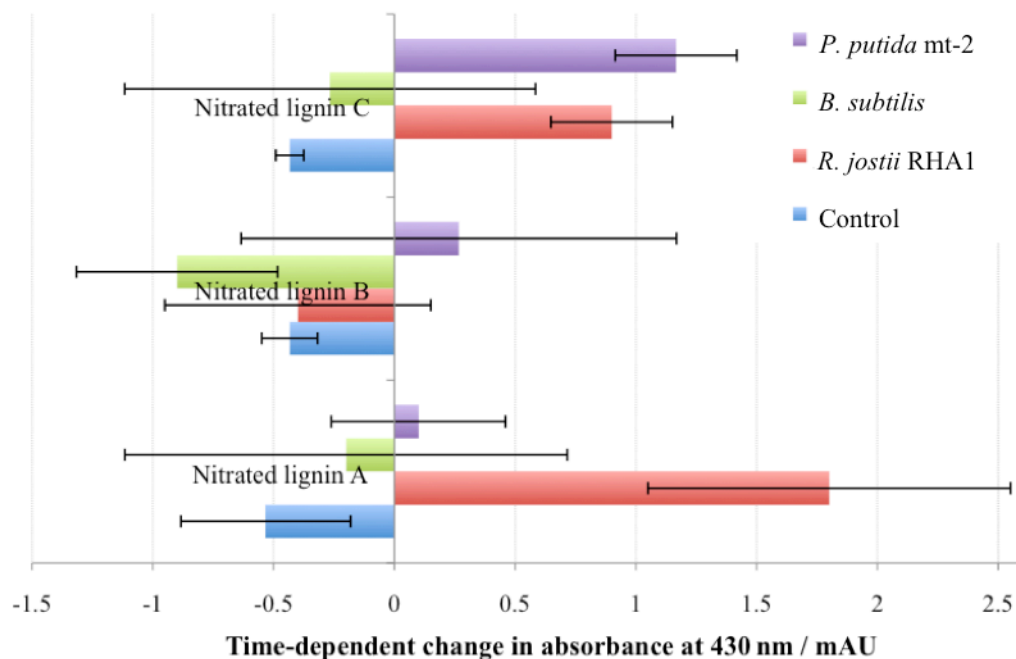


Figure 2.1. Change in absorbance at 430 nm from 0 – 20 min for reaction of the culture supernatant of known lignin-degrading bacteria *P. putida* mt-2 and *R. jostii* RHA1 and non lignin-degrader *B. subtilis* with nitrated MWL samples A, B and C in the presence of 2 mM H₂O₂. An additional control experiment was performed in which the culture supernatant was replaced with 113 mM Tris buffer (pH 7.4) containing 7.5 mM NaCl. Assays were carried out in technical triplicate.

In the UV/visible nitrated lignin analysis (Fig. 2.1), sample C showed the greatest increase in absorbance at 430 nm of 1.2 mAU following treatment with the culture supernatant of *P. putida* mt-2 compared to 0.1 mAU for sample A

and 0.3 mAU for sample B. Sample A was most sensitive towards the culture supernatant of *R. jostii* RHA1, exhibiting a time-dependent absorbance increase of 1.7 mAU compared to 1.2 mAU for sample C, though it was least sensitive to *P. putida* mt-2. Sample B failed to detect the activity of *R. jostii* RHA1, exhibiting a decrease in absorbance (– 0.2 mAU) and was much less sensitive towards *P. putida* mt-2 than sample C, which is consistent with results obtained using the tetranitromethane-nitrated MWL from wheat straw and is consistent with literature reports that suggest *P. putida* mt-2 and *R. jostii* RHA1 are capable of degrading lignin and *B. subtilis* is not capable of lignin degradation.

Table 2.1. Change in absorbance at 430 nm from 0 – 20 min following treatment of nitrated MWL samples A, B and C with the culture supernatant of lignin-degrading bacteria *P. putida* mt-2 and *R. jostii* RHA1, non-degrader *B. subtilis* and a control experiment in which the culture supernatant was replaced with 113 mM Tris buffer (pH 7.4) containing 7.5 mM NaCl. Assays were performed in the presence of 2 mM H₂O₂ and carried out in technical triplicate.

Bacterial strain	Time-dependent change in absorbance at 430 nm / mAU		
	Sample A	Sample B	Sample C
<i>R. jostii</i> RHA1	+ 1.8	– 0.4	+ 0.9
<i>P. putida</i> mt-2	+ 0.1	+ 0.3	+ 1.2
<i>B. subtilis</i>	– 0.2	– 0.9	– 0.3
Control	– 0.5	– 0.4	– 0.4

None of the samples detected any lignin-degradation activity in the control experiment (113 mM Tris buffer, pH 7.4) or activity of *B. subtilis*, exhibiting decreases in absorbance in all cases (see Table 2.1). Since relatively low activity was observed following treatment of samples A and B by *P. putida* mt-2 in comparison to sample C and sample B failed to detect any lignin-degradation activity of *R. jostii* RHA1, these samples were not used in subsequent nitrated lignin assays. Sample C, which detected activity of both previously studied lignin-degrading bacteria was instead used and although it only exhibited a time-

dependent absorbance increase of 0.9 mAU with *R. jostii* RHA1 compared to 1.5 mAU observed by M. Ahmad [159], it was much more sensitive to *P. putida* mt-2, for which absorbance increases of < 0 mAU were observed following treatment of nitrated MWL from wheat straw synthesized via the tetranitromethane nitration method [159].

2.2.3. Development of the nitrated lignin spray assay

Development of the nitrated lignin spray assay was carried out using nitrated MWL sample C and *R. jostii* RHA1, *P. putida* mt-2, and *B. subtilis*, a negative control. The assay was initially performed using nitrated MWL solution diluted 25-fold in 750 mM Tris buffer (pH 7.4) containing 50 mM NaCl. Since no colour change was observed following the spraying of colonies of *R. jostii* RHA1 and *P. putida* mt-2 and 96 hr of incubation of the culture at 30 °C, the dilution factor was reduced to 10-fold and the assay repeated, though no colour changes were observed. Following these observations, modifications were made to the concentration and ionic strength of the Tris buffer, which was lowered to 20 mM with no supplementation with NaCl. A slight yellow colouration was observed upon spraying colonies of *P. putida* mt-2 with nitrated MWL solution diluted 10-fold in 20 mM Tris buffer (pH 7.4), but not with the less concentrated solution, diluted 25-fold. No colouration was observed upon spraying colonies of *R. jostii* RHA1 at either substrate concentration. It was then discovered that the nitrated MWL solution that had been diluted 10-fold in dH₂O reacted more sensitively with *P. putida* mt-2 since a more distinct yellow colouration of colonies was observed (see Table 2.2). This suggests that the presence of Tris buffer may have inhibitory effects on the activity of *P. putida* mt-2 towards

nitrate MWL, therefore nitrated lignin solution for all subsequent assays was diluted in dH₂O, 10-fold for spray assays and 25-fold for UV/visible assays.

Table 2.2. Degree of yellow colouration of colonies of *R. jostii* RHA1 and *P. putida* mt-2 and *B. subtilis* on agar-solidified LB following spraying with nitrated MWL solution (sample C) diluted 10- or 25-fold in 750 mM Tris buffer (pH 7.4) containing 50 mM NaCl, 20 mM Tris buffer (pH 7.4) and dH₂O. += no observed colouration, ++ = faint yellow colouration, +++ = clear yellow colouration.

Strain	Degree of yellow colouration of sprayed colonies					
	750 mM Tris buffer		20 mM Tris buffer		dH ₂ O	
	10-fold	25-fold	10-fold	25-fold	10-fold	25-fold
<i>R. jostii</i> RHA1	+	+	++	+	+++	++
<i>P. putida</i> mt-2	+	+	+	+	++	+
<i>B. subtilis</i>	+	+	+	+	+	+

In contrast to *P. putida* mt-2, colouration of colonies of *R. jostii* RHA1 was only observed using nitrated MWL diluted 10-fold in dH₂O, indicating a significant variation in the sensitivity of this method to the different lignin-degrading bacteria. No colour changes were observed upon spraying colonies of *B. subtilis*, which is consistent with results from the UV/visible assay (Fig. 2.1). The spray assay was repeated using nitrated MWL samples A and B instead of C, though no colour changes were observed following the spraying of any all strains with each sample. These observations further suggest that sample C is much more sensitive to bacterial lignin-degrading enzymes than samples A and B, though it is intriguing that no yellow colouration was observed after spraying colonies of *R. jostii* RHA1 with sample A, which was more sensitive to this strain in the UV/visible assay than sample C.

Since the alternative nitrated lignin assay conditions involving dilution of nitrated MWL in dH₂O rather than 750 mM Tris buffer (pH 7.4) was capable of detecting lignin-degradation activity of *P. putida* mt-2 and *R. jostii* RHA1 in the

spray assay it was used in subsequent screening studies to isolate lignin-degrading bacteria from soil samples and composted wheat straw.

2.3. Screening for lignin-degrading bacteria from soil samples

2.3.1. Sourcing of samples and enrichment of bacteria

Soil samples were collected from woodland locations in Warwickshire and woodland and heathland locations in Hampshire, United Kingdom. Each sample was enriched for 21 days at 30 °C in M9 salts (Na_2HPO_4 : 12.8 g l⁻¹, KH_2PO_4 : 3.0 g l⁻¹, NaCl : 0.5 g l⁻¹, NH_4Cl : 1.0 g l⁻¹) supplemented with wheat straw (2.0 % w/v). Aliquots were then spread onto agar-solidified medium of the same composition, although nutrient agar was used to enhance growth. After 72 hours of incubation at 30 °C, rapid bacterial growth had occurred on all plates with up to 2.5×10^6 colony forming units (CFUs) per ml observed, so a dilution series of each enriched culture in 20 mM Tris buffer (pH 7.4) was carried out and 1000-fold dilutions were required to observe single colonies. The number of colonies from each sample that had grown after 72 hours of incubation was estimated and used to calculate the approximate composition of CFUs in each enriched sample (see Table 2.3).

Table 2.3. Number of bacterial isolates from each enriched soil sample, diluted 1000-fold in 20 mM Tris buffer (pH 7.4) along with their IDs and the approximate number of CFUs per ml in each enriched culture.

Source of soil sample	Approximate number of colonies on agar plates	CFUs ml ⁻¹	Total number of strains isolated	IDs of isolates
Hampton Lucy, Warwickshire (Sample 1)	200	1.0 x 10 ⁶	13	A1–6
Hampton Lucy, Warwickshire (Sample 2)	100	5.0 x 10 ⁵	12	B1–6
Lyndhurst, Hampshire	150	7.5 x 10 ⁵	13	C1–6
Emery Down, Hampshire	500	2.5 x 10 ⁶	8	D1–6
Beaulieu, Hampshire	5	2.5 x 10 ⁴	4	E1–3

2.3.2. Nitrated lignin spray assay for soil isolates

In order to selectively pick colonies from strains capable of degrading lignin, cultures were grown on agar-solidified medium composed of M9 salts supplemented with wheat straw (2.0 % w/v) for 72 hr, and then sprayed with nitrated MWL solution (sample C, diluted 10-fold in dH₂O). The six most yellow colonies, or clusters of colonies, were picked and re-streaked onto agar-solidified medium composed of M9 salts supplemented with glucose (2.0 % w/v) and yeast extract (0.5 % w/v). Each different colony was then re-streaked onto agar-solidified medium of the same composition until pure cultures had been achieved, and then labelled (see Tables 2.3 and 2.4). Pure cultures of each isolate were then sprayed with nitrated MWL solution once more in order to distinguish the ‘active’ isolates towards lignin degradation from the ‘inactive’ ones.

Following the spraying of colonies and incubation for 48 hr at 30 °C, yellow colouration of colonies of some of the isolates was observed with no further

colouration after 96 hr. Out of the 44 different isolates, 18 had become more yellow after spraying (see Table 2.4) and the degree of yellow colouration of colonies of certain isolates was more distinct than observed using other isolates, suggesting that these isolates were possibly capable of degrading lignin. Colouration of some strains was accompanied by a visible change in the consistency of the culture (Fig. 2.2).

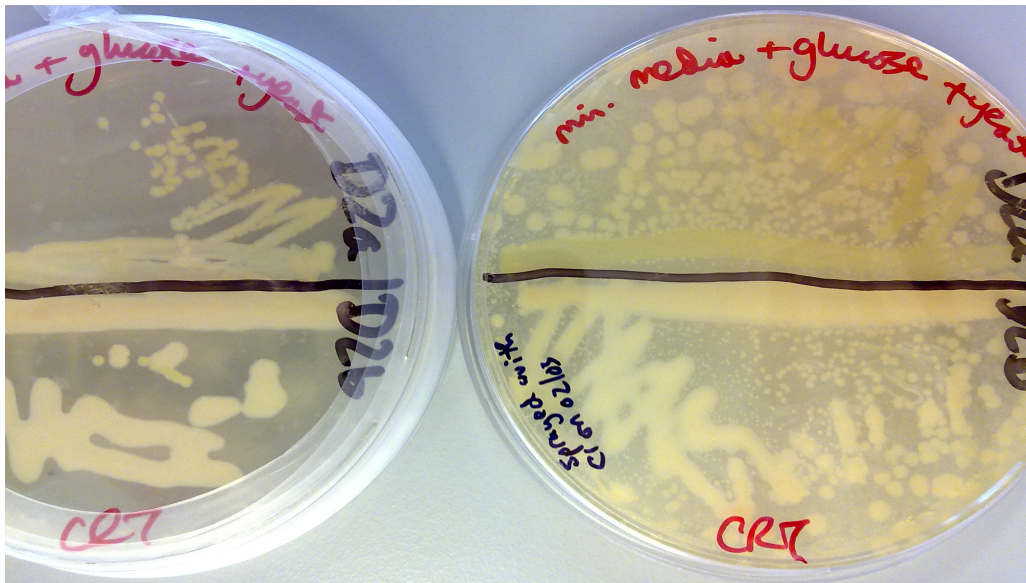


Figure 2.2. Nitrated lignin spray assay for soil isolates. The right-hand plate was sprayed with nitrated MWL solution, whilst the left-hand plate was unsprayed. The culture on the upper half of the plate appears to be ‘active’, due to the yellow colouration, whilst the culture on the lower half of the plate seems to be ‘inactive’ since no colour change is observed.

It is worth noting that some isolates (e.g. A2.1) formed bright yellow colonies, therefore yellow colouration of these strains in the spray assay was difficult to observe. Following this observation, combined with the poor sensitivity of the spray assay towards *R. jostii* RHA1 (see section 2.2.3), the UV/visible nitrated lignin assay was performed on all strains regardless of observations in the nitrated lignin spray assay.

Table 2.4. Source of each bacterial isolate, its assigned ID and the degree of yellow colouration observed following the spraying of colonies on agar-solidified LB with nitrated MWL sample C. += no colour change, ++ = faint yellow colouration, +++ = distinctive yellow colouration.

Source of bacteria isolate	ID	Degree of yellow colouration in the nitrated lignin spray assay
Hampton Lucy, Warwickshire (sample 1)	A1.1	+++
	A1.2	++
	A2.1	+
	A3.1	++
	A4.1	+
	A4.2	+
	A4.3	+++
	A5.1	++
	A5.2	+++
	A6.1	++
	A6.2	+
	A6.3	++
Hampton Lucy, Warwickshire (sample 2)	B1.1	+
	B1.2	+
	B2.1	+++
	B2.2	+
	B3.1	+
	B4.1	+
	B5.1	++
	B5.2	+
	B5.3	++
	B5.4	+
B6.1	+	
B6.2	+	
Lyndhurst, Hampshire	C1.1	+
	C1.2	+
	C2.1	+
	C3.1	+
	C4.1	++
	C4.2	+
	C4.3	++
	C4.4	+
	C5.1	++
	C5.2	+
	C6.1	++
	C6.2	++
Emery Down, Hampshire	D1.1	+
	D2.1	+
	D4.1	+
	D4.2	+
	D5.1	++
Beaulieu, Hampshire	E1.1	++
	E1.2	+
	E3.1	+

2.3.3. UV/visible nitrated lignin assays for isolated soil bacteria

UV/visible nitrated lignin assays were performed using a similar procedure to that followed in 2.2, although the nitrated MWL stock solution was diluted 10-fold in dH₂O rather than 25-fold in 750 mM Tris buffer (pH 7.4) containing 50 mM NaCl.

2.3.3.1. 'Active' isolates from the spray assay:

Reaction of the culture supernatant of isolates exhibiting activity in the nitrated lignin spray assay with nitrated MWL solution in the presence and absence of 2 mM H₂O₂ was monitored in the UV/visible nitrated lignin assay, and the activity compared with known lignin-degrading bacteria *R. jostii* RHA1 and *P. putida* mt-2, and non lignin-degrader *B. subtilis*.

■ Activity in the absence of hydrogen peroxide ■ Activity in the presence of hydrogen peroxide

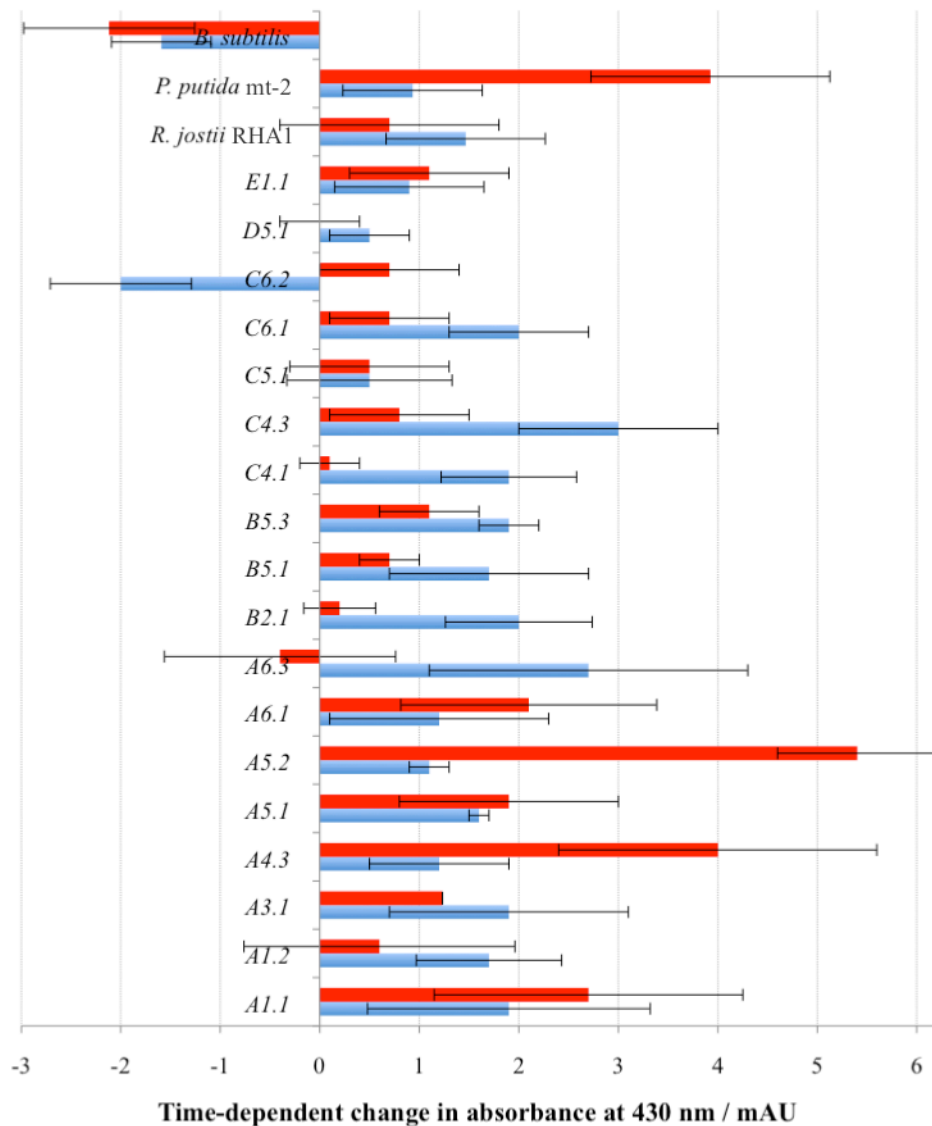


Figure 2.3. Change in absorbance at 430 nm from 0 – 20 min following reaction of the culture supernatant of isolates that appeared to be active towards lignin degradation in the nitrated lignin spray assay with 2 mM H₂O₂ and nitrated MWL. Controls include previously studied lignin-degrading *P. putida* mt-2 and *R. jostii* RHA1, and non-lignin degrader *B. subtilis*. Assays were performed in technical quadruplet.

The UV/visible nitrated lignin analysis for isolates that exhibited activity in the nitrated lignin spray assay (Fig. 2.3) suggests that many of these isolates are more active towards lignin degradation than previously studied lignin-degrading bacteria *R. jostii* RHA1 and *P. putida* mt-2 since significant time-dependent

increases in absorbance at 430 nm are observed in the presence and absence of 2 mM H₂O₂.

In contrast to the assay performed using nitrated MWL samples A, B and C, which were diluted in 750 mM Tris buffer (pH 7.4) containing 50 mM NaCl (Fig. 2.1), sample C was diluted 25-fold in dH₂O for use in this experiment. It is interesting that whilst *P. putida* mt-2 exhibited a higher time-dependent absorbance increase of 3.9 mAU in the presence of H₂O₂ compared to 1.2 mAU in the assay optimization experiment, *R. jostii* RHA1 exhibited a slightly lower absorbance increase of 0.7 mAU compared to 0.9 mAU. Although this small difference lies within the margin of experimental error, *P. putida* mt-2 appears to be 2–3-fold more active in the presence of dH₂O rather than 750 mM Tris buffer (pH 7.4), consistent with observations from the nitrated lignin spray assay.

With the exception of C5.1, C6.2 and D5.1, all of the isolates exhibited a greater activity towards nitrated MWL than *P. putida* mt-2 in the presence of H₂O₂ and many isolates were also more active than *R. jostii* RHA1 in the presence of H₂O₂. It is, however, interesting that the highest absorbance increases are observed in the absence of H₂O₂. A4.3 and A5.2 are of particular interest since time-dependent absorbance increases of 4.0 mAU and 5.4 mAU, respectively, are observed in the absence of H₂O₂, which are similar to, or slightly greater than the relatively high increase of 3.9 mAU observed for *P. putida* mt-2.

2.3.3.2. 'Inactive' isolates from the spray assay

In order to further examine the reliability of, and detect any active isolates that were not detected by the nitrated lignin spray assay, cultures of isolates that were not found to give a yellow colouration when sprayed with nitrated MWL solution were also grown in LB broth at 30 °C and the culture supernatants studied using the UV/visible assay.

The UV/visible nitrated lignin analysis (Fig. 2.4) shows that none of these isolates were as active as *P. putida* mt-2 in the absence of H₂O₂, although B5.4, B3.1, B2.2, B1.1, A4.2 and A4.1 appeared to be more active than *P. putida* mt-2 in the presence of H₂O₂. Of these isolates, only B3.1 and A4.2 appeared to be more active than *R. jostii* RHA1 in the presence of H₂O₂, though these differences lie within the range of experimental error.

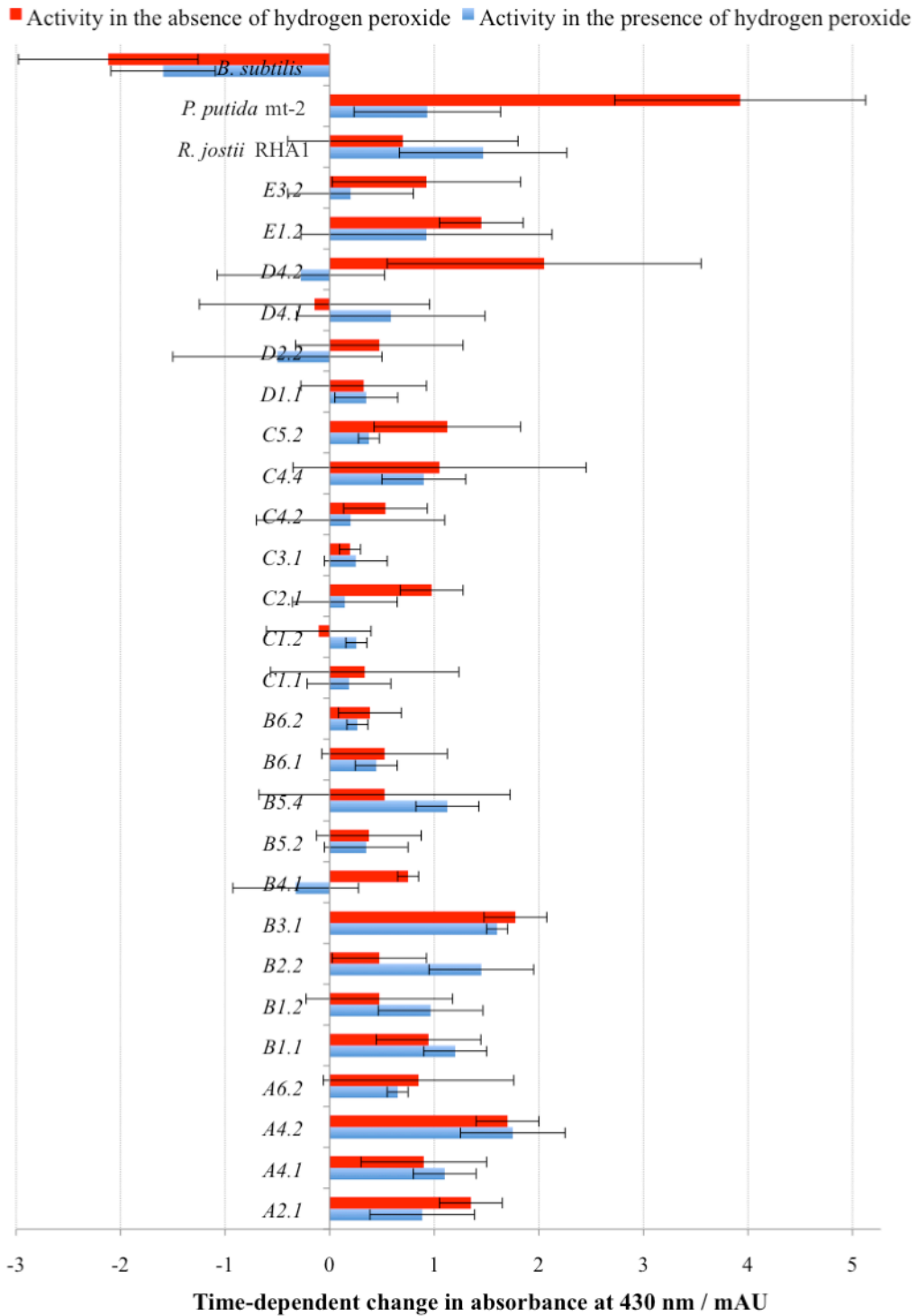


Figure 2.4. Change in absorbance at 430 nm from 0 – 20 min following reaction of the culture supernatants of isolates that appeared ‘inactive’ towards lignin degradation in the nitrated lignin spray assay, with 2 mM H₂O₂ and nitrated MWL. Control experiments include previously studied lignin-degrading bacteria *P. putida* mt-2 and *R. jostii* RHA1, and non lignin-degrader *B. subtilis*. Assays were performed in technical quadruplet.

2.3.3.3. Validation of the nitrated lignin assays

In order to clearly illustrate the consistency of observations in the spray and UV/visible nitrated lignin assays, the activity of each ‘active’ and ‘inactive’ isolate towards nitrated MWL in the presence and absence of H_2O_2 in the UV/visible assay was compared with the activity in the spray assay i.e. degree of yellow colouration.

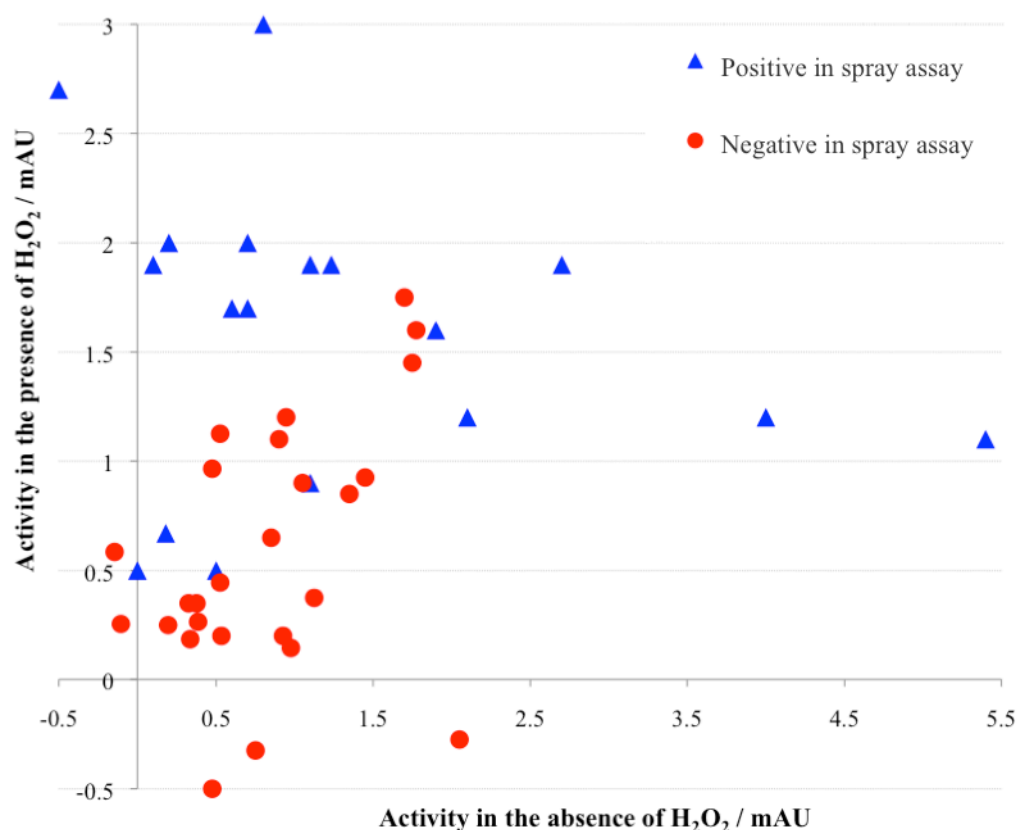


Figure 2.5. Validation of the screening protocol for lignin-degradation activity, via relative activity of ‘active’ and ‘inactive’ isolates from the nitrated lignin spray assay, using the UV/visible nitrated lignin assay. Activity in the presence of 2 mM H_2O_2 (y-axis) is plotted against activity in the absence of H_2O_2 (x-axis). The ‘active’ isolates are separated from the ‘inactive’ isolates. Assays were performed in technical quadruplet.

The results from the UV/visible microtitre plate assay are largely consistent with those from the spray assay as shown in Fig. 2.5 since the active strains from the spray assay exhibited greater activity overall with and without H_2O_2 than the inactive strains.

2.3.4. Identification of isolated lignin-degrading soil bacteria

The identity of each active bacterial isolate from the soil samples was determined by analysis of the 16S rRNA gene sequence, and 16S rRNA gene amplification was performed by colony PCR. Sequencing was carried out by Dr. P. Norris (Life Sciences, University of Warwick) and the Basic Level Alignment Search Tool (BLAST) used to identify known bacterial strains in the Genbank database that resemble the sequences of the isolates. The sequences of the isolates are almost identical to strains in the Genbank database (Table 2.5).

Table 2.5. % Identity of isolated lignin-degrading soil bacteria over 500 – 1400 aligned nucleotides, and the bacterial family of each strain.

Strain	Highest identity sequence match from 16S rRNA sequence	Sequence identity	Genbank accession no.	Bacterial family
A1.1 (identical to A6.1, A6.3, B2.1 & B5.1)	<i>Microbacterium phyllosphaerae</i>	100	NR025405	Actinobacteria
A1.2 (identical to A2.1, A3.1 and C5.1)	<i>Microbacterium marinilacus</i>	99.9	AB286020	Actinobacteria
A4.3	<i>Ochrobactrum pseudogrignonense</i>	99.8	HQ406749	α -proteobacteria
A5.1	<i>Rhodococcus erythropolis</i>	99.8	EU729738	Nocardioform
A5.2	<i>Microbacterium oxydans</i>	99.7	HQ202813	Actinobacteria
B5.3 (identical to E1.1)	<i>Micrococcus luteus</i>	100	FJ040810	Actinobacteria
C4.1 (identical to C6.1, D2.1, D3 & D5.1)	<i>Ochrobactrum rhizosphaerae</i>	100	AM490632	α -proteobacteria

After elimination of duplicates and highly similar sequences, seven different types of strain were identified, as illustrated in Table 2.5. These strains include seven Actinobacteria (three *Microbacterium* strains, one *Micrococcus* strain and one *Rhodococcus* strain) and two Alphaproteobacteria (*Ochrobactrum* strains). Five of the strains were isolated from enrichment cultures from woodland soils in Warwickshire (*M. phyllosphaerae*, *M. marinilacus*, *M. oxydans*, *O. pseudogrignonense* and *R. erythropolis*) and the other two strains were isolated from heathland soils in Hampshire (*M. luteus* and *O. rhizosphaerae*). High levels of sequence identity, > 99.5 % over 500 – 1400 nucleotides, to isolates in the GenBank database were discovered (see Table 2.5), which had been obtained from a variety of phyllospheres, rhizospheres and sludge samples. The majority of isolates had highly similar 16S rRNA gene sequences to type strains to which they are most likely identical.

2.4. Screening for thermotolerant lignin-degrading bacteria

The screening methods used to isolate lignin-degrading bacteria from soil samples were repeated with enrichment cultures grown at 45 °C to isolate thermotolerant bacteria (T1–3, see Table 2.6) from samples of composted wheat straw obtained from a solid-state fermentation of wheat straw amended with 1 % w/v chicken manure, operating at 60 – 65 °C (provided by Dr. K. Burton, Warwick HRI). Aliquots of each sample were spread onto agar-solidified LB, followed by incubation at 45 °C for 72 hr. *Thermobifida fusca*, an extensively studied lignocellulose-degrading actinobacterium, was dominant on the plates and had 100 % 16S rRNA identity to the type strain.

Table 2.6. % identity of thermotolerant lignin-degrading bacteria, isolated from composted wheat straw, over 650–1,000 aligned nucleotides and the bacterial family of each strain.

Strain	Highest identity sequence match from 16S rRNA sequence	Sequence identity	Genbank accession no.	Bacterial family
T1	<i>Rhizobiales sp.</i>	100	NR025405	α -proteobacteria
T2	<i>Sphingobacterium sp.</i>	100	AB286020	Bacteroidetes
T3	<i>Thermobifida fusca</i>	100	HQ406749	Actinobacteria

Analysis of the 16S rRNA gene sequences (Table 2.6) suggested that T1 has an identical sequence to that of an unnamed *Rhizobiales* strain and was less related (< 96 % sequence identity) to named strains of *Nitratireductor*, *Mesorhizobium* and *Phyllobacterium* e.g. 96 % sequence identity to *Phyllobacterium trifolii* (NR-043193). The sequence of T2 was highly identical to an unnamed strain of *Sphingobacterium*, though it was less identical to the most closely related type strain, *Sphingobacterium composti* (NR-041363), with which it shared 92 % sequence identity. Activity of each thermotolerant isolate towards lignin degradation was confirmed using the nitrated lignin assays.

2.4.1. Nitrated lignin spray assay for thermotolerant isolates

In order to confirm activity towards lignin degradation, cultures of each thermotolerant strain on agar-solidified LB were sprayed with nitrated MWL solution and incubated at 45 °C for 24 hr at which point yellow colouration had occurred.

Table 2.7. Level of growth of thermotolerant isolates on agar-solidified LB (++++ = good growth, +++ = moderate growth) and the degree of yellow colouration observed upon spraying colonies with nitrated MWL solution (+ = no colour change, ++ = faint yellow colouration, +++ = clear yellow colouration). Yellow colouration of colonies of *Rhizobiales sp.* was unclear due to the yellow colour of colonies formed by this strain.

Strain	Growth on agar-solidified LB	Activity in the spray assay
<i>Rhizobiales sp.</i>	++++	+, unclear (yellow colonies)
<i>Sphingobacterium sp.</i>	++++	+++
<i>T. fusca</i>	+++	++

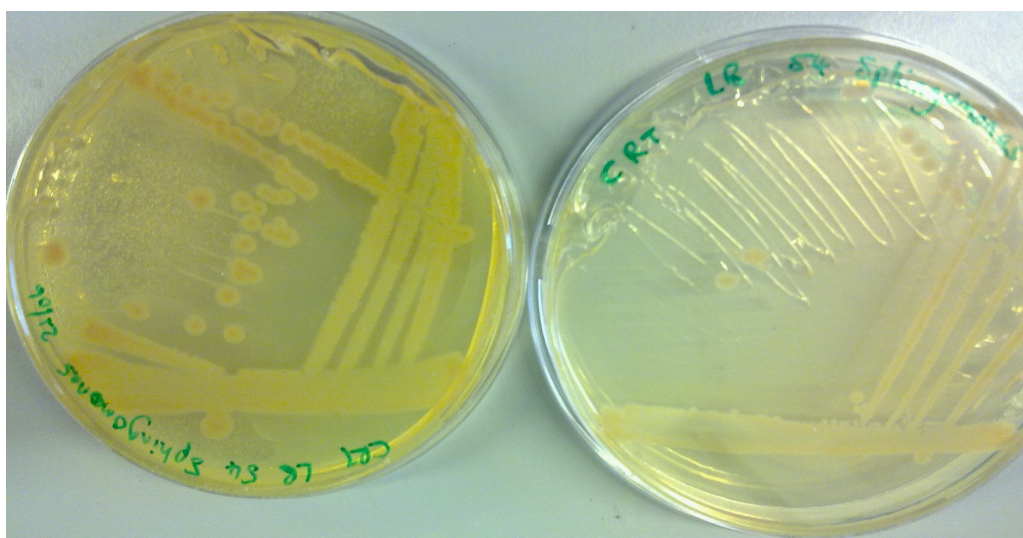


Figure 2.6. Nitrated lignin spray assay for thermotolerant strain *Sphingobacterium sp.* The left-hand plate, sprayed with nitrated MWL solution, shows a significant yellow colouration compared with the unsprayed right-hand plate.

A yellow colouration of colonies of *Sphingobacterium sp.* and *T. fusca* was observed following spraying with nitrated MWL solution and incubation at 45 °C for 48 hr, suggesting that these strains are potentially active towards lignin degradation. Yellow colouration of colonies of *Rhizobiales sp.* was unclear since the colonies were yellow in appearance prior to spraying with nitrated MWL solution. The greatest degree of yellow colouration was observed on sprayed cultures of *Sphingobacterium sp.* (Fig. 2.6).

2.4.2. UV/visible nitrated lignin assay for thermotolerant isolates

The culture supernatants of *Sphingobacterium sp.* and *Rhizobiales sp.* were reacted with nitrated MWL solution and the UV/visible nitrated lignin analysis (Fig. 2.7) is defined by a very high time-dependent absorbance increase at 430 nm of 9.5 mAU for *Sphingobacterium sp.* in the presence of H₂O₂ and 34.0 mAU in the absence of H₂O₂. These values are approximately ten-fold higher than those observed for *P. putida mt-2* under the same conditions. *Rhizobiales sp.* appeared to be much less active towards lignin degradation than *Sphingobacterium sp.*, exhibiting a much lower activity, with a time-dependent absorbance increase of 4.3 mAU in the absence of H₂O₂, and did not appear to be active in the presence of H₂O₂ since a slight decrease in absorbance at 430 nm was observed.

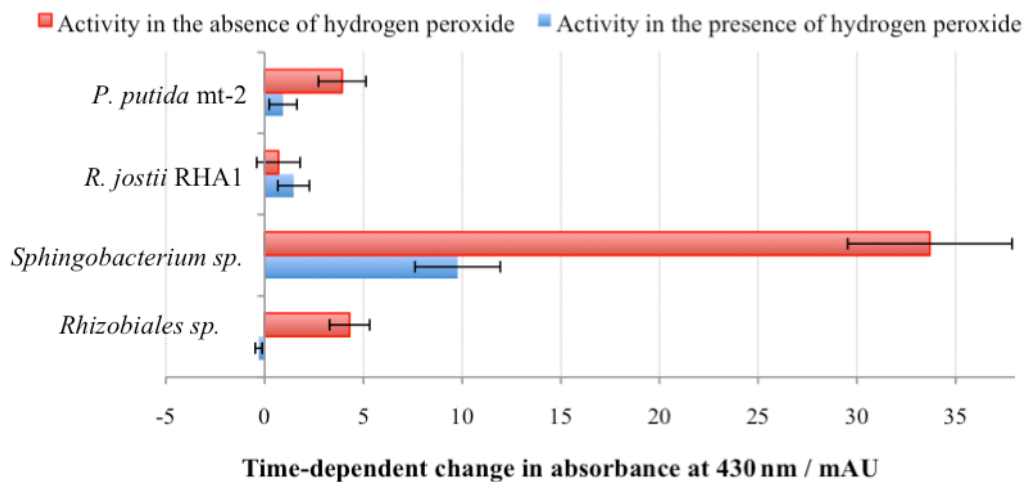


Figure 2.7. Change in absorbance at 430 nm from 0 – 20 min following reaction of nitrated MWL solution with the culture supernatants of the thermotolerant strains and previously studied lignin-degrading bacteria *P. putida mt-2* and *R. jostii RHA1*, in the presence and absence of 2 mM H₂O₂. Assays were performed in technical quadruplet.

Despite an observed yellow colouration of colonies after spraying with nitrated MWL solution, *T. fusca* could not be studied in the UV/visible assay since the level of growth of liquid cultures in LB broth and M9 salts supplemented with glucose and yeast extract was very poor.

2.5. Conclusions

Several lignin-degrading bacteria have been isolated from a variety of environmental samples including woodland soil, heathland soil and composted wheat straw. Seven mesophilic strains were isolated from soils in two different regions of the United Kingdom and three thermotolerant strains from the composted wheat straw. The mesophilic isolates include three *Microbacterium* strains, a *Micrococcus* strain, a *Rhodococcus* strain (all Actinobacteria) and two *Ochrobactrum* strains (Alphaproteobacteria). The thermotolerant strains include two uncharacterized species of *Rhizobiales* and *Sphingobacterium*, and *Thermobifida fusca*. Application of the nitrated lignin assay found the *Sphingobacterium* strain to be the most active and the combination of the strong yellow colouration observed in the spray assay (Fig. 2.6) and the very high time-dependent absorbance increase in the UV/visible assay (Fig. 2.7) suggests that *Sphingobacterium sp.* may secrete extracellular enzymes that are highly efficient towards the degradation of lignin.

With the exception of *Sphingobacterium sp.*, almost all of these strains cluster into two families of bacteria, the Actinobacteria and the Alphaproteobacteria; an observation that is consistent with the classes of bacteria to which reported lignin-degrading strains belong: the Actinobacteria, Alphaproteobacteria and Gammaproteobacteria [162, 163]. The observations so far in this project,

combined with literature reports, suggest that strains in these bacterial families are metabolically capable of breaking down lignin. The Actinobacterium that has been observed most frequently in this project is *Microbacterium*, from which genus at least three different strains have been identified that exhibit activity towards lignin degradation. However, it is also interesting that a strain of *R. erythropolis* has been isolated since previous studies have shown that *R. jostii* RHA1, a degrader of polychlorinated biphenyls, is also capable of breaking down lignin [132, 159] and *Rhodococcus opacus* strains have recently been reported to degrade lignin model compounds [164]. Although no strains of *Microbacterium* and *Ochrobactrum* have been identified as degraders of lignin, there are reports of *Ochrobactrum* strains that have been found to degrade polychlorinated biphenyls [165] and polycyclic aromatic hydrocarbons [166], and it is interesting that *Microbacterium* and *Ochrobactrum* strains have been found in the gut of *Zootermopsis angusticollis* [167], a wood-penetrating termite. It is also intriguing that most bacteria found in termites and wood-penetrating insects cluster into the Actinobacteria, Alphaproteobacteria and Gammaproteobacteria [162].

Although strains of *Sphingobacterium* have previously been isolated from compost [168] and *Sphingobacterium composti* has been discovered in paper mill pulps [169], the only strain that is linked to lignin degradation is *Sphingobacterium sp.* ATM, which has recently been reported to produce an aryl alcohol oxidase [170]. Aryl alcohol oxidases have been found to catalyze the oxidation of aryl α - and α - β -unsaturated γ -alcohols to yield the corresponding aldehydes with concurrent reduction of O_2 to H_2O_2 , which is reported to be used in the regulation of peroxidase-catalyzed lignin degradation and to act as a

precursor for the hydroxyl free radical in white-rot fungi [171]. The aryl alcohol oxidase produced by *Sphingobacterium sp.* ATM was found to be most specific to veratryl alcohol, and its dye-decolourization ability links it to LiP, MnP and laccase, all of which are capable of decolourizing dyes as well as degrading lignin [172]. *Thermobifida fusca* is reported to be capable of breaking down plant cell walls in self-heating compost [173], although its activity towards lignin degradation was only monitored in the nitrated lignin spray assay so it cannot be classed as a lignin-degrading strain on the basis of results from this assay alone.

In summary, several environmental lignin-degrading bacterial strains have been isolated using the screening method reported in this chapter, which suggests that it is an efficient method for detecting lignin-degradation activity in environmental bacteria and that there is scope for further development of this method for future screening projects.

Chapter 3: Characterization of environmental lignin-degrading bacteria

3.1. Introduction

Several of the environmental lignin-degrading bacteria described in Chapter 2 demonstrated high activity in the nitrated lignin assays, with thermotolerant *Sphingobacterium sp.* being far more active than all other strains. In order to determine the optimum growth conditions and develop the understanding of the pathways via which these strains degrade lignin and/or lignocellulose, a series of experiments have been carried out based on:

- Ability to grow in a variety of liquid media.
- Ability to grow on selected aromatic carbon sources and cellulose.
- Depolymerization of high- and low-molecular weight forms of Kraft lignin.
- Ability to degrade different lignin-containing feedstocks.

The degree of growth of each strain in LB broth and M9 salt solution supplemented with Kraft lignin and/or glucose with yeast extract was monitored via optical density (OD₆₀₀) measurements every 24 hours for 7 – 14 days, and the ability to grow on agar-solidified M9 salts supplemented with selected aromatic carbon sources and cellulose monitored via qualitative analysis of colony formation after 14 days of incubation.

A sample of commercially available Kraft lignin was size-fractionated via gel filtration chromatography and the high- and low-molecular weight forms treated with each strain for 8 days. Gel filtration HPLC analysis of the samples revealed modifications to the molecular weight distribution induced by each strain. Lignin-containing feedstocks wheat straw, Organosolv lignin and Kraft lignin

were treated with selected strains and changes to the soluble phenol content, reducing sugars content, number of CFUs and the pH of liquid fractions were monitored. FT-IR was used to study modifications to the solid and liquid fractions.

3.2. Growth in liquid media

Cultures of each strain were grown in liquid media of varying composition including LB broth and M9 salts supplemented with glucose (2.0 % v/v) and yeast extract (0.5 % w/v). Cell growth was monitored via measurement of OD₆₀₀ of the culture samples every 24 hours over a time course of 120 hours.

3.2.1. LB broth

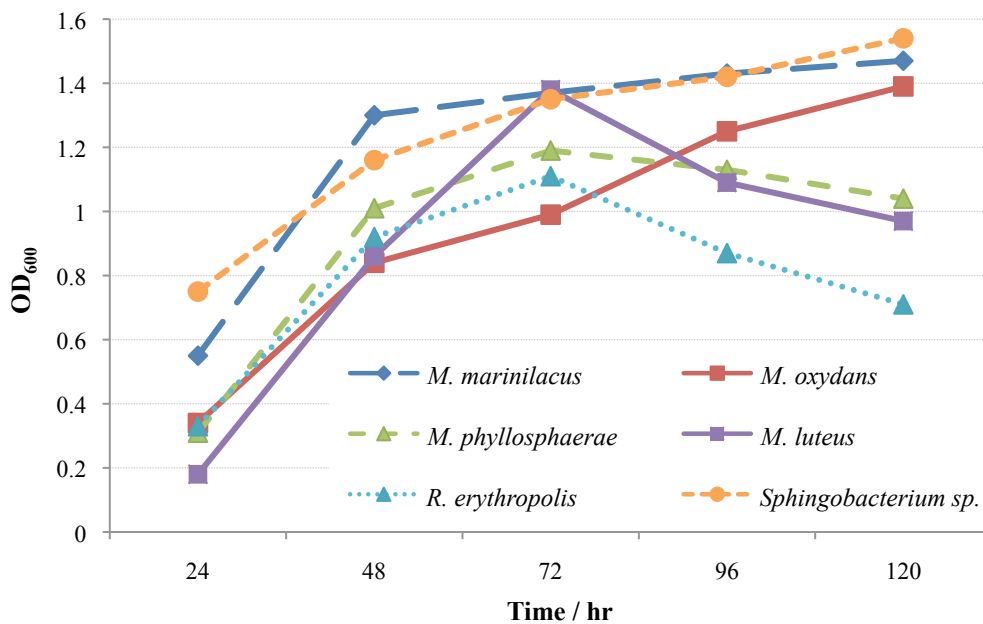


Figure 3.1. OD₆₀₀ of cultures of environmental lignin-degrading bacteria, grown in LB broth, at various time points: 24 hr, 48 hr, 72 hr, 96 hr and 120 hr. Each strain was grown at 30 °C with the exception of *Spingobacterium sp.*, which was instead grown at 45 °C.

All of the strains exhibited good growth in LB broth, with the highest rate of growth (log phase) between 24 and 48 hr (Fig. 3.1), followed by slower growth between 48 and 72 hr. Cell death began at different times for the different strains, with the cells of *M. luteus*, *M. phyllosphaerae* and *R. erythropolis* beginning to die after 72 hr as the OD₆₀₀ decreased by 0.41, 0.15 and 0.40 from 72 – 120 hr respectively. In contrast, *M. marinilacus*, *M. oxydans* and *Sphingobacterium sp.* continued to grow steadily from 72 – 120 hr. *Sphingobacterium sp.*, closely followed by *M. marinilacus*, reached the highest OD₆₀₀ of all strains grown in this medium, with steady cell growth 48 hr after the beginning of cell death of *M. luteus*, *M. phyllosphaerae* and *R. erythropolis*.

3.2.2. M9 salts supplemented with glucose and yeast extract

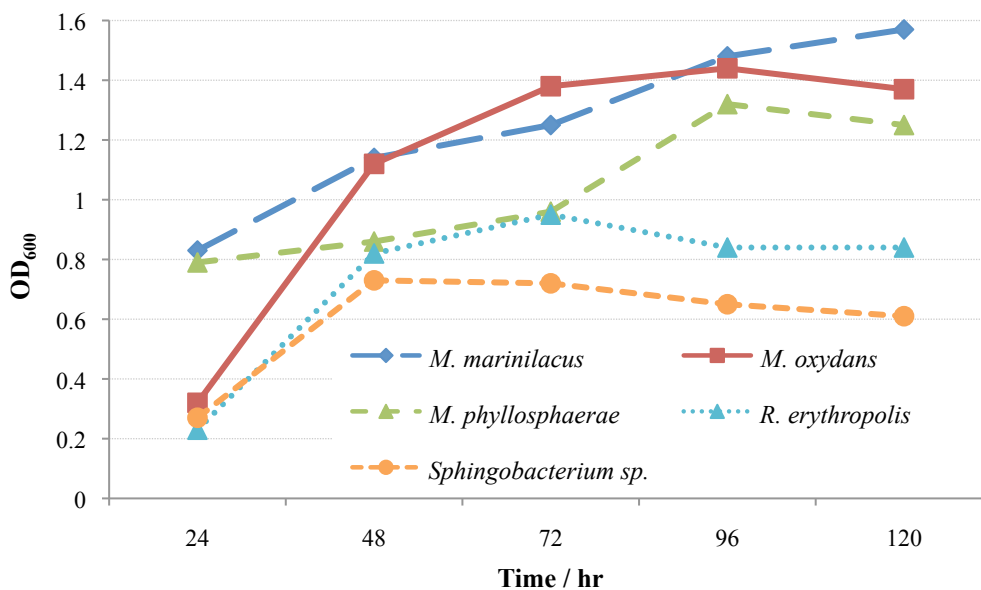


Figure 3.2. OD₆₀₀ of liquid cultures of environmental lignin-degrading bacteria grown in M9 salt solution supplemented with glucose (2.0 % v/v) and yeast extract (0.5 % w/v) for 24 hr, 48 hr, 72 hr, 96 hr and 120 hr. Each strain was grown at 30 °C with the exception of *Sphingobacterium sp.*, which was instead grown at 45 °C.

In contrast to LB broth, *M. luteus* did not appear to grow in M9 salt solution supplemented with glucose and yeast extract although it had been isolated, and exhibited good growth on agar plates of the same composition.

Whilst all strains were capable of good growth in LB broth and M9 salts supplemented with glucose and yeast extract some strains grew much more rapidly in LB broth and vice versa. *Sphingobacterium sp.* grew much less rapidly in enriched M9 media than in LB broth, reaching an OD₆₀₀ of 0.30 after 24 hr and 0.65 after 120 hr (Fig. 3.2), compared to 0.75 and 1.50 respectively in LB broth (Fig. 3.1). In contrast to growth in LB, which sees the cell density of *Sphingobacterium sp.* continually increase over 120 hr, the cell density in glucose and yeast extract slowly decreases from a peak of 0.70 at 48 hr to 0.65 at 120 hr, suggesting that growth of this strain in the presence of glucose is limited. After reaching an identical OD₆₀₀ in LB and M9 media containing glucose with yeast extract after 24 hr of inoculation, *M. oxydans* grew much more rapidly in M9 media containing glucose and yeast extract from 24 – 120 hr, reaching OD₆₀₀ values of 1.12 after 48 hr and 1.38 after 72 hr compared to 0.84 and 0.99 respectively in LB broth at the same time points.

It is interesting that *M. phyllosphaerae* grew twice as rapidly in M9 salts supplemented with glucose and yeast extract in the first 24 hours compared to LB broth, and the maximum cell density of 1.30 was reached when grown in M9 media containing glucose and yeast extract for 96 hr compared to a lower reading of 1.20 after 72 hours of incubation in LB broth. Similar to the observations for *Sphingobacterium sp.*, a higher cell density is observed for cultures of *R. erythropolis* in LB broth compared to M9 media containing glucose and yeast extract at each time point, though the cell density is much

more stable in the latter medium from 72 – 120 hr (a sharp decrease is observed over the same interval in LB broth).

M. marinilacus grew rapidly in both types of media, though a slightly higher optical density was reached after 120 hr of growth in M9 salts supplemented with glucose and yeast extract.

In summary, the observed growth patterns in LB broth and glucose and yeast extract suggest that whilst *M. marinilacus* and *R. erythropolis* exhibited good growth in both media, cultures of *Sphingobacterium sp.*, *M. oxydans* and *M. phyllosphaerae* should be prepared in M9 salts supplemented with glucose (2.0 % v/v) and yeast extract (0.5 % w/v) rather than in LB broth for rapid growth.

3.2.3. M9 salts supplemented with Kraft lignin and/or glucose, and yeast extract

In order to detect whether or not the strains were capable of degrading Kraft lignin, cultures of each strain were grown in M9 salts supplemented with 2.0 % (w/v) Kraft lignin and 0.5 % (w/v) yeast extract for 336 hours, and the OD₆₀₀ of each culture monitored every 24 hours. The experiments were also carried out using the same medium supplemented with 2.0 % (w/v) glucose to examine whether cell growth was inhibited or promoted by glucose and/or Kraft lignin.

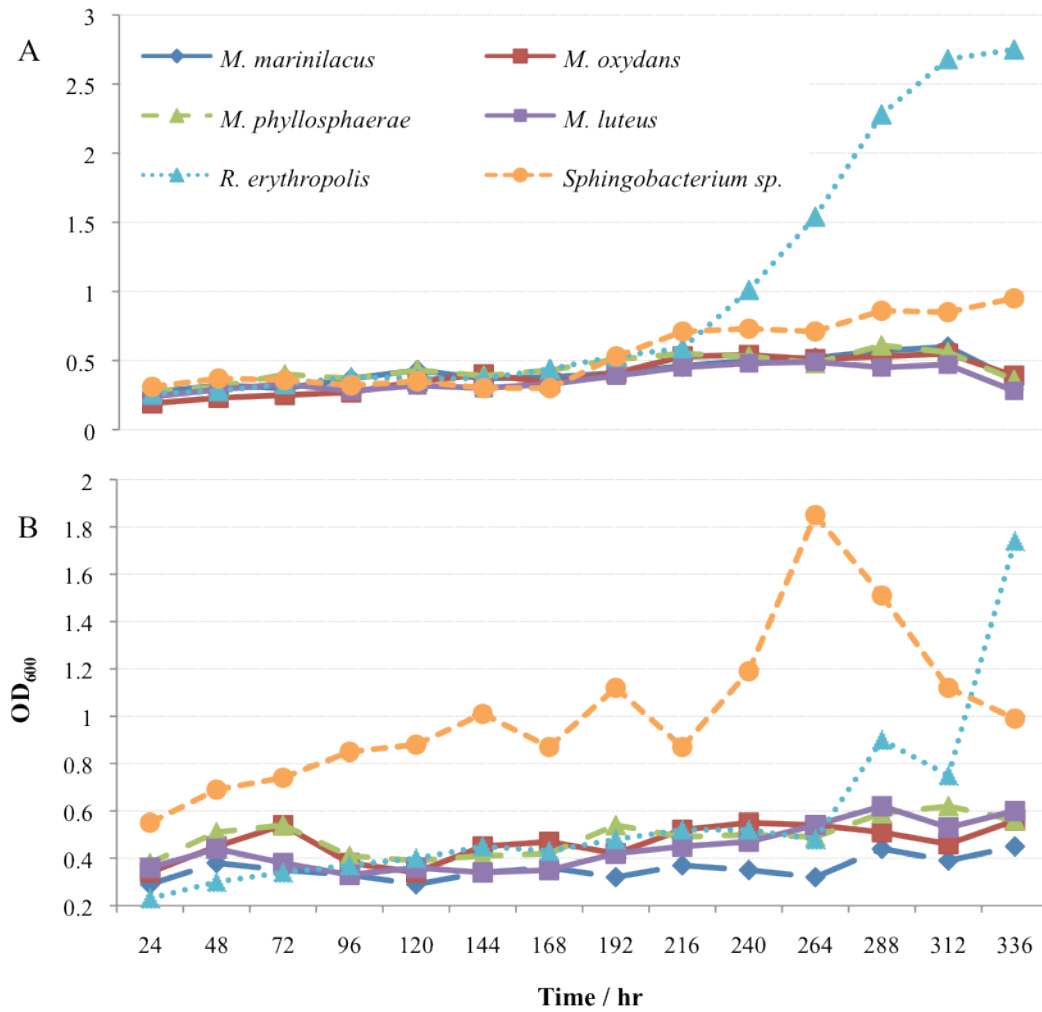


Figure 3.3. OD₆₀₀ of liquid cultures of environmental lignin-degrading bacteria in M9 salts supplemented with: A) glucose (2.0 % v/v) and yeast extract (0.5 % w/v) and B) Kraft lignin (2.0 % w/v), glucose (2.0 % v/v) and yeast extract (0.5 % w/v). Readings were taken every 24 hours for a total period of 336 hours. Each strain was grown at 30 °C with the exception of *Sphingobacterium sp.*, which was instead grown at 45 °C.

The OD₆₀₀ analyses for strains grown in the presence of Kraft lignin (Fig. 3.3) show lower levels of growth at all time points than observed using only M9 salts supplemented with glucose and yeast extract as a growth medium (Fig. 3.2), which suggests that growth inhibitors may be present in the Kraft lignin. The pre-hydrolysis liquor, produced in the Kraft pulping process, is known to contain furfural [174], which is a reported inhibitor of bacterial cell growth, which may explain the limited growth of most strains. However, growth of *Sphingobacterium sp.* was significantly enhanced in the presence of Kraft lignin,

reaching an OD₆₀₀ of 0.88 after 120 hr compared with 0.61 in the absence. The optimum cell density of 1.85 for *Sphingobacterium sp.* was reached after 264 hr, which is much greater than around 0.50 reached by most of the other strains at that time point. It is interesting that after 264 hours of relatively slow growth *R. erythropolis* began to grow rapidly, which could either be the result of some contamination or degradation of any inhibitors to yield products that this strain can metabolize more efficiently, e.g. less potent phenolic compounds [175, 176]. The combination of rapid growth of *R. erythropolis* and cell death of *Sphingobacterium sp.* between 264 and 336 hr could suggest that the two strains may metabolize Kraft lignin and any lower-molecular weight breakdown products via different pathways: whilst the presence of Kraft lignin may inhibit the growth of *R. erythropolis*, it significantly enhances growth of *Sphingobacterium sp.*, which may be an indication of more rapid metabolism of Kraft lignin by *Sphingobacterium sp.* compared to *R. erythropolis*. Since none of the other strains reach an OD₆₀₀ above 0.60 it is clear that their metabolic capabilities are limited in the absence of glucose.

Whilst a similar pattern of limited growth in Kraft lignin-supplemented growth medium was observed for most isolates in the presence and absence of glucose it is striking that the growth rate of *Sphingobacterium sp.* was significantly reduced in the absence of glucose throughout the time-course and that the strain grew optimally in media containing glucose and Kraft lignin, rather than solely glucose or Kraft lignin. The maximum OD₆₀₀ reached by cultures of *Sphingobacterium sp.* in the presence of glucose and Kraft lignin was almost double the level reached in Kraft lignin alone (see Table 3.1). *R. erythropolis*

grew much more rapidly in the absence of glucose, reaching an OD₆₀₀ of 2.75 after 336 hr compared to 1.74 in the same medium supplemented with glucose.

Table 3.1. Maximum OD₆₀₀ reached by cultures of environmental lignin-degrading bacteria grown for 120 or 336 hr in LB broth and M9 salt solution supplemented with 2.0 % (w/v) glucose and/or 2.0 % (w/v) Kraft lignin with 0.5 % (w/v) yeast extract. OD₆₀₀ values outlined in bold indicate the medium in which the highest OD₆₀₀ was reached and numbers in brackets indicate the number of hours of inoculation. Each strain was grown at 30 °C with the exception of *Sphingobacterium sp.*, which was instead grown at 45 °C.

Strain	Maximum OD ₆₀₀ reached in each growth medium			
	LB broth	Glucose + yeast extract	Kraft lignin + glucose + yeast extract	Kraft lignin + yeast extract
<i>M. luteus</i>	1.38 (72)	No growth	0.62 (288)	0.49 (264)
<i>M. marinilacus</i>	1.47 (120)	1.57 (120)	0.45 (336)	0.60 (312)
<i>M. oxydans</i>	1.39 (120)	1.44 (96)	0.56 (336)	0.55 (312)
<i>M. phyllosphaerae</i>	1.19 (72)	1.32 (96)	0.62 (312)	0.61 (288)
<i>R. erythropolis</i>	1.11 (72)	0.95 (72)	1.74 (336)	2.75 (336)
<i>Sphingobacterium sp.</i>	1.54 (120)	0.73 (48)	1.85 (264)	0.95 (336)

Although most strains exhibited good growth in LB broth or M9 salt solution supplemented with glucose and yeast extract it is interesting that cell growth of *Sphingobacterium sp.* and *R. erythropolis*, two of the most active strains in the UV/visible nitrated lignin assays, reached an optimum in the media supplemented with Kraft lignin. The maximum OD₆₀₀ reached by *R. erythropolis* in M9 salts supplemented with Kraft lignin and yeast extract was almost 250 % of that reached in LB broth, although the time taken to reach this high OD₆₀₀ was relatively long (264 – 336 hr). By contrast, the maximum OD₆₀₀ of *Sphingobacterium sp.* reached in Kraft lignin, glucose and yeast extract was only 120 % of that reached in LB broth in a much shorter inoculation time. These results are fairly consistent with observations from the UV/visible nitrated lignin assays (see Chapter 2) since they also highlight *Sphingobacterium sp.* as

being particularly active towards lignin degradation. It is not surprising that *R. erythropolis* grows optimally in the presence of Kraft lignin since this strain has previously been found to exhibit metabolic activity towards synthetic lignin-derived compounds [175, 176].

3.3. Temperature-dependent growth of thermotolerant isolates

The optimum growth temperature of thermotolerant strains *Sphingobacterium sp.* and *Rhizobiales sp.* was determined by assessing the level of growth of each strain on agar-solidified LB at various temperatures in the range 30 – 55 °C after 48 and 168 hr of growth.

Table 3.2. Level of growth of thermotolerant isolates *Rhizobiales sp.* T1 and *Sphingobacterium sp.* T2 on agar-solidified LB after 48 and 168 hr of incubation at 30, 37, 45, 50 and 55 °C. += no growth, ++ = poor growth, +++ = moderate growth and ++++ = good growth.

Strain	Level of growth at various temperatures									
	30 °C		37 °C		45 °C		50 °C		55 °C	
	48 hr	168 hr	48 hr	168 hr	48 hr	168 hr	48 hr	168 hr	48 hr	168 hr
T1	++	+++	+++	++++	++++	++++	++++	++++	+	++
T2	++	+++	+++	++++	++++	++++	++++	++++	++	+++

Although the thermotolerant strains were enriched and isolated at 45 °C they evidently grow efficiently between 37 and 50 °C (Table 3.2), with inhibited growth outside this temperature range.

3.4. Growth on aromatic carbon sources, glucose and cellulose

In order to develop the understanding of the metabolic capabilities of each lignin-degrading bacterial strain, the ability to degrade a variety of aromatic compounds was examined by carrying out growth experiments in M9 salt solution supplemented with an aromatic compound or cellulose as the sole carbon source (0.02–0.1 % w/v). The aromatic compounds used (Fig. 3.4) were biphenyl, vanillic acid, veratryl alcohol, *m*-cresol, *p*-cresol and ferulic acid. Growth in vanillic acid (2.0 % w/v) was initially monitored in liquid media, though growth was severely limited with only very slow growth of some of the strains in glucose after 336 hours. By comparison, growth on agar plates of identical media composition was faster with the appearance of colonies after 168 hours, therefore the remainder of the experiments were performed on agar plates.

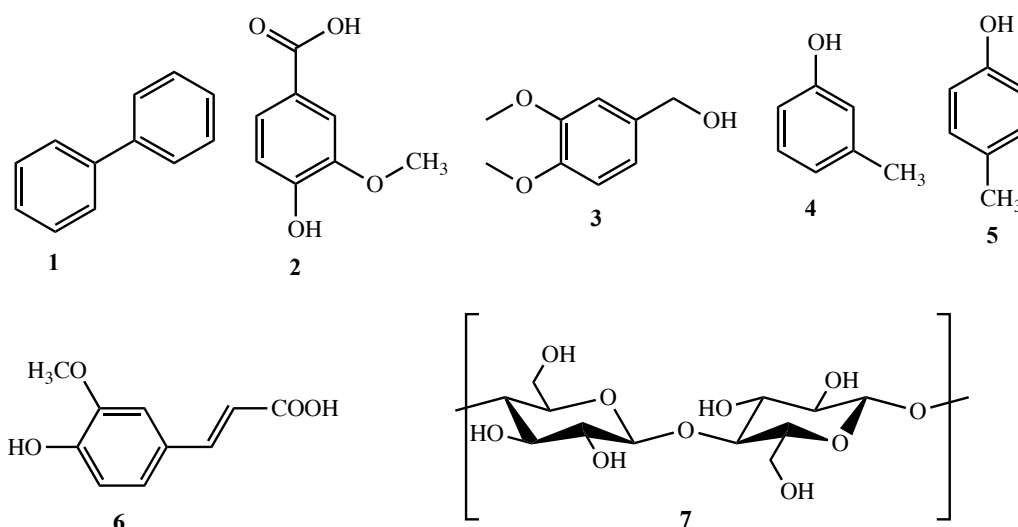


Figure 3.4. Structures of carbon sources: biphenyl (1), vanillic acid (2), veratryl alcohol (3), *m*-cresol (4), *p*-cresol (5), ferulic acid (6) and cellulose (7).

The ability of the strains to grow on biphenyl and vanillic acid was of significant interest since biphenyl is a component of lignin [77] and *R. jostii* RHA1, a recently studied lignin-degrading strain, has been identified as a degrader of biphenyl [177]. Vanillic acid is an intermediate on the β -aryl ether cleavage pathway in *S. paucimobilis* SYK-6 [137]. Growth on veratryl alcohol was also of interest since an enzyme purified from *Sphingobacterium* sp. ATM was found to be specific towards this compound [170]. Growth on cellulose was monitored in order to examine the selectivity of the strains and find out whether they grow selectively on the lignin-related aromatic compounds in preference to cellulose, or they are also capable of metabolizing cellulose.

Another reason for carrying out the growth experiments is to examine the reliability of the sequence data by examining the growth patterns of different isolates that have identical BLAST results, e.g. the two *M. phyllosphaerae* strains A1.1 and A1.2. Note that strains A4.3 and C4.1 were not characterized further since *O. anthropi*, which has a sequence is highly similar to *O. pseudogrignonense* was discovered to be a Category 2 organism that is a potential opportunistic pathogen.

Table 3.3. Level of growth of environmental lignin-degrading bacterial strains on different carbon sources biphenyl (1.0 g l⁻¹), *m*-cresol (0.22 g l⁻¹), *p*-cresol (0.22 g l⁻¹), ferulic acid (1.0 g l⁻¹), vanillic acid (1.0 g l⁻¹), veratryl alcohol (0.84 g l⁻¹) and cellulose (0.5 g l⁻¹), after 240 hr at 30 or 45 °C. += no growth, ++ = poor growth, +++ = moderate growth and ++++ = good growth. ND = not determined.

Strain	biphenyl (1)	vanillic acid (2)	veratryl alcohol (3)	<i>m</i>-cresol (4)	<i>p</i>-cresol (5)	ferulic acid (6)	cellulose (7)
<i>Microbacterium phyllosphaerae</i> A1.1	++	++++	+	+	+	+++	++
<i>Microbacterium phyllosphaerae</i> A1.2	++	++++	+++	+	+	+++	++
<i>Microbacterium marinilacus</i> A2.1	++	+++	+	+	+	++	+++
<i>Microbacterium marinilacus</i> A3.1	++	+	+	+	+	++	+++
<i>Ochrobactrum pseudogrignonense</i> A4.3	+	++	+++	+++	+	ND	ND
<i>Rhodococcus erythropolis</i> A5.1	++++	+++	+++	+++	+++	+	++++
<i>Microbacterium oxydans</i> A5.2	+	+	+	+	+	++	++
<i>Micrococcus luteus</i> B5.3	++	+++	+++	+++	+++	+++	+
<i>Ochrobactrum rhizosphaerae</i> C4.1	+++	+++	+	+	+	ND	ND
<i>Microbacterium marinilacus</i> C5.1	+++	+++	+++	+	+	+++	+++
<i>Ochrobactrum rhizosphaerae</i> D5.1	+++	+++	+++	+	+	+	ND
<i>Micrococcus luteus</i> E1.1	+++	+++	+++	+++	+++	+++	+
<i>Sphingobacterium</i> sp.	++++	++++	+++	++	+	++	+
<i>Rhizobiales</i> sp.	++	++	++	++	++	+	+

After 240 hours of incubation at 30 or 45 °C all strains had grown on one or more of the aromatic carbon sources (Table 3.3), though most were selective for specific compounds. Good growth on biphenyl was observed for *Sphingobacterium sp.* and *R. erythropolis*, whilst growth of the *Microbacterium* strains was limited. A different pattern of growth was observed on vanillic acid, which was readily metabolized by the *Microbacterium* strains and *Sphingobacterium sp.* in addition to *R. erythropolis*. The good growth of *Sphingobacterium sp.* on biphenyl, vanillic acid and veratryl alcohol but not on cellulose suggests that this organism is selective for metabolism of the lignin component of lignocellulose. It is not surprising that *R. erythropolis* grew well on vanillic acid and biphenyl since *R. jostii* RHA1 is known to degrade biphenyl [177] and *Rhodococcus* strains are reported to degrade phenolic compounds [175, 176]. The moderate growth of the *Ochrobactrum* strains on biphenyl is also consistent with previous studies, which found that *Ochrobactrum* strains are capable of degrading polychlorinated biphenyls and polycyclic aromatic hydrocarbons [178, 179].

The identical *M. phyllosphaerae* strains A1.1 and A1.2 exhibited almost the same level of growth, the only difference being the moderate growth of A1.2 on veratryl alcohol in comparison with A1.1. The same degree of similarity in the results was observed with the two *M. luteus* strains B5.3 and E1.1 and the two *M. marinilacus* strains A2.1 and A3.1. However, the other *M. marinilacus* strain, C5.1, grew more readily on biphenyl and veratryl alcohol than A2.1 and A3.1. This slight difference in growth rate could be due to experimental error, since growth was monitored qualitatively, and/or a result of the difference in environmental conditions; C5.1 was isolated from heathland soil in a different

geographical region to A2.1 and A3.1, which were both isolated from soil in woodland locations.

It is clear that all strains have difficulty in degrading *m*-cresol and *p*-cresol; this observation is not striking since cresol-degradation pathways have been characterized in only a small number of isolates from environmental samples, mainly *Pseudomonas* species [162]. It is not surprising that *R. erythropolis* showed moderate growth on the cresols since *Rhodococcus* strains have also been reported to degrade phenolic compounds [175, 176].

3.5. Transmission Electron Microscopy of *Sphingobacterium sp.*

Transmission electron microscopy was used to study the cells of *Sphingobacterium sp.*, and showed that the strain formed filaments that contain small branches (Fig. 3.5). This is an unusual observation since sphingobacteria are usually rod-shaped [112].

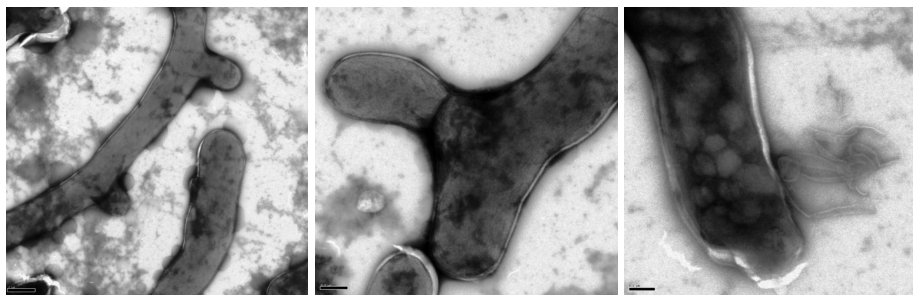


Figure 3.5. Transmission electron micrograph of *Sphingobacterium sp.*, grown in LB broth at 45 °C. Scale bar (bottom left) 1 μmol^{-1} , courtesy of Dr. E. Hardiman.

3.6. Biotransformation of Kraft lignin

Determination of the molecular weight distribution of lignin, which defines its physiochemical properties and reactivity [180 – 182], is fundamental to the understanding of lignin breakdown processes, and the design of industrial lignins for specific applications. Studies on the molecular weight distribution using various methodologies have been reported in the last 50 years, with gel filtration chromatography being one of the most effective methods [183, 184].

Aqueous-based gel filtration chromatography is a preferential method for size-fractionation of Kraft lignin [183, 184], a major byproduct of the pulping industry (see Chapter 1). In comparison to most other forms of lignin, Kraft lignin has an enhanced reactivity and a greater solubility in water resulting from the separation of structural lignin units and the induction of hydrophilic groups during the pulping process (see Chapter 1).

3.6.1. Size-fractionation of Kraft lignin

In order to investigate whether the isolated strains were capable of depolymerizing high-molecular weight forms of Kraft lignin, or just the low-molecular weight forms, a sample of Kraft lignin (20 g l^{-1}) was size-fractionated by Ultrogel ACA-44 aqueous gel filtration chromatography. Sixteen fractions were collected in order of descending molecular weight, all of which absorb UV/visible light most strongly at 280 nm.

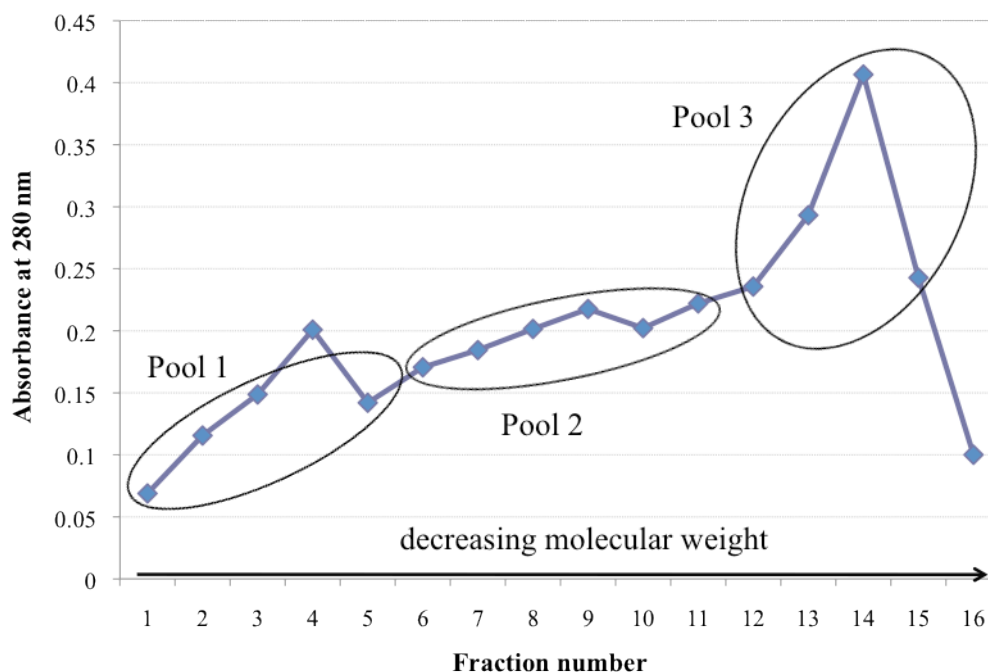


Figure 3.6. Absorbance of various size-fractions of Kraft lignin at 280 nm. The molecular weight decreases from high (fraction 1) to low (fraction 16).

The sixteen fractions were subsequently divided into three pools of fractions based on their absorbance at 280 nm (Fig. 3.6). These include pool 1 (fractions 1 – 3 and 5, high-molecular weight), pool 2 (fractions 6 – 11, medium-molecular weight) and pool 3 (fractions 12 – 15, low-molecular weight). Incubations of various bacterial strains with each fraction pool in the presence of M9 salts were carried out to assess their ability to break down high-, medium- and low-molecular weight forms of Kraft lignin.

3.6.2. Inoculation of previously studied lignin-degrading bacteria with size-fractionated Kraft lignin

Previously studied lignin-degrading bacteria *R. jostii* RHA1 and *P. putida* mt-2 were incubated with each molecular weight fraction in M9 salt solution at 30 °C. Aliquots were removed at 72, 168 and 192 hr, with growth observed in all cases after 72 hr.

Table 3.4. Degree of growth of previously studied lignin-degrading bacteria on high-, medium- and low-molecular weight forms of Kraft lignin observed after incubation in the presence of M9 salts at 30 °C for 72, 168 and 192 hr.

Strain	Growth on high-MW Kraft lignin			Growth on medium-MW Kraft lignin			Growth on low-MW Kraft lignin		
	72	168	192	72	168	192	72	168	192
<i>P. putida</i> mt-2	+	++	++	++	++	+++	+	++	+++
<i>R. jostii</i> RHA1	+	++	+++	+	++	+++	++	+++	+++

After 72 hours, *R. jostii* RHA1 had grown more readily than *P. putida* mt-2 in the presence of the low-molecular weight Kraft lignin. Interestingly, *P. putida* mt-2 grew more readily on medium-molecular weight than on low-molecular weight Kraft lignin over the same period. Similar growth patterns were observed after 168 and 192 hr, with *R. jostii* RHA1 growing most rapidly on the low-molecular weight form. Further growth was observed in the final 24 hr, with *P. putida* mt-2 growing most rapidly on the medium-molecular weight form and *R. jostii* RHA1 growing most rapidly on the low-molecular weight form of Kraft lignin.

The observations so far in this experiment suggest that although both strains are capable of depolymerizing high- and low-molecular weight forms of Kraft lignin, *R. jostii* RHA1 depolymerizes this material more efficiently than *P. putida* mt-2. Both strains generally grew more rapidly on the low- and medium-molecular weight material than on the high-molecular weight material, an observation that is expected since the structure of lignin should become easier to metabolize as the molecular weight decreases. It is also intriguing that *P. putida* mt-2 appears to grow most readily in the presence of medium-molecular weight lignin after 192 hours.

3.6.3. Incubation of environmental lignin-degrading bacteria with size-fractionated Kraft lignin.

Cultures of five of the most active bacterial strains isolated in this project (*Sphingobacterium sp.*, *M. marinilacus*, *M. oxydans*, *M. phyllosphaerae* and *R. erythropolis*, see Chapter 2) were grown in the presence of high- and low-molecular weight forms of Kraft lignin and M9 salts at 30 °C or 45 °C. Aliquots were removed after 72 and 192 hours and then centrifuged to give the culture supernatant, which was analyzed by gel filtration HPLC.

Table 3.5. Growth patterns of environmental lignin-degrading bacteria on high-, medium- and low-molecular weight forms of Kraft lignin after 72 and 192 hr of incubation.

Strain	Growth on high-MW Kraft lignin		Growth on medium-MW Kraft lignin		Growth on low MW - Kraft lignin	
	72 hr	192 hr	72 hr	192 hr	72 hr	192 hr
<i>Sphingobacterium sp.</i>	+	++	+	+++	++	+++
<i>M. marinilacus</i>	+	++	+	+++	++	++
<i>M. phyllosphaerae</i>	+	++	+	++	++	+++
<i>M. oxydans</i>	+	++	+	+++	++	+++
<i>R. erythropolis</i>	+	++	+	++	+	+++

The volume of each cell pellet after centrifugation was assessed to qualitatively monitor the level of cell growth (see Table 3.5). Similar growth patterns were observed for the different strains, which grew more rapidly on low- and medium- molecular weight forms of Kraft lignin than on the higher-molecular weight form.

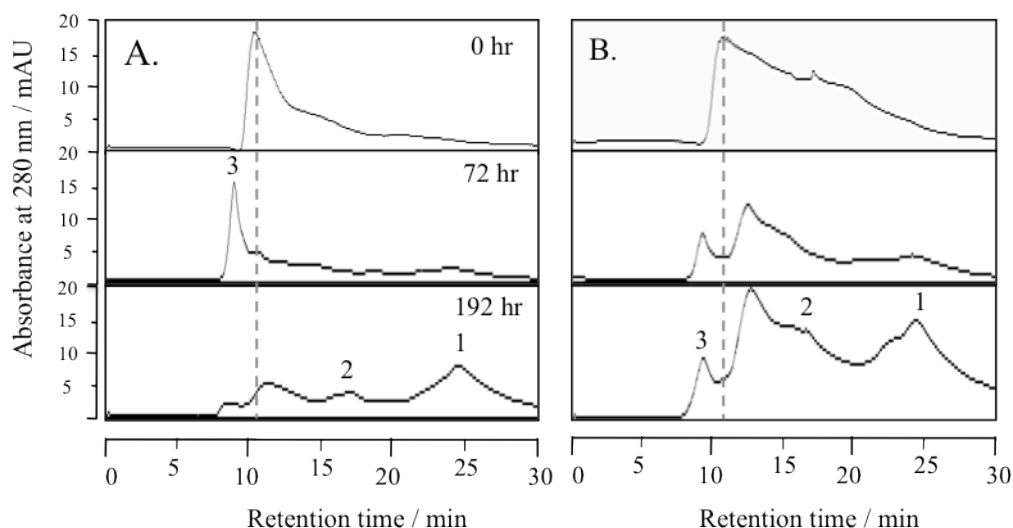


Figure 3.7. Gel filtration HPLC analysis of the breakdown of size-fractionated high-molecular weight (A) and low-molecular weight (B) forms of Kraft lignin by *Sphingobacterium sp.*, in the presence of M9 salts at 45 °C. The retention time for the high molecular weight lignin peak at 11 min is indicated with a dashed line. New peaks 1 (25 min), 2 (17 min) and 3 (9 min) are discussed in the text.

A peak at retention time 11 min is characteristic of the gel filtration HPLC analysis for the high-molecular weight Kraft lignin (Fig. 3.7). Following treatment with *Sphingobacterium sp.*, the intensity of this peak decreases vs. time, a reduction of approximately 75 % after 72 hr and disappearance after 192 hr. This reduced intensity correlates with the appearance of peak 1, which corresponds to depolymerization products of low molecular weight. The appearance of a low-intensity peak at 17 min corresponds to the formation of medium molecular-weight products. The formation of another new peak at 9 min suggests that a higher-molecular weight species has also been formed by treatment with *Sphingobacterium sp.*, which possibly arises from some repolymerization of the fragmented lignin to yield a higher-molecular weight polymer. The decrease in intensity of this peak after 192 hr suggests that the repolymerized material is broken down with increased levels of growth of *Sphingobacterium sp.*

The increase in intensity of the peak at 25 min is greater with *Sphingobacterium sp.* than with the mesophilic strains (Figures 3.8 and 3.9), suggesting that the low-molecular weight breakdown products that seem to be metabolized at different rates by the other strains are not metabolized by *Sphingobacterium sp.*

The analysis for the low-molecular weight form of Kraft lignin corresponds to a widespread peak over retention time period 11 – 20 min, which corresponds to lower molecular weight scattering. The intensity of this broad peak appears to decrease vs. time following incubation with *Sphingobacterium sp.* and as illustrated in Figure 3.7 A a new peak at retention time 24 min resembles lower-molecular weight products. Although these observations suggest that treatment of the low-molecular weight form of Kraft lignin with *Sphingobacterium sp.* induces modifications to the molecular weight distribution, it is evidently more efficient towards the depolymerization of the high-molecular weight form since the intensity of peak 3 is reduced from 15 mAU to 3 mAU in the analysis for treatment the high-molecular weight form (Fig. 3.7 A) compared with an increase of approximately 2 mAU for the low-molecular weight form of Kraft lignin (Fig. 3.7 B).

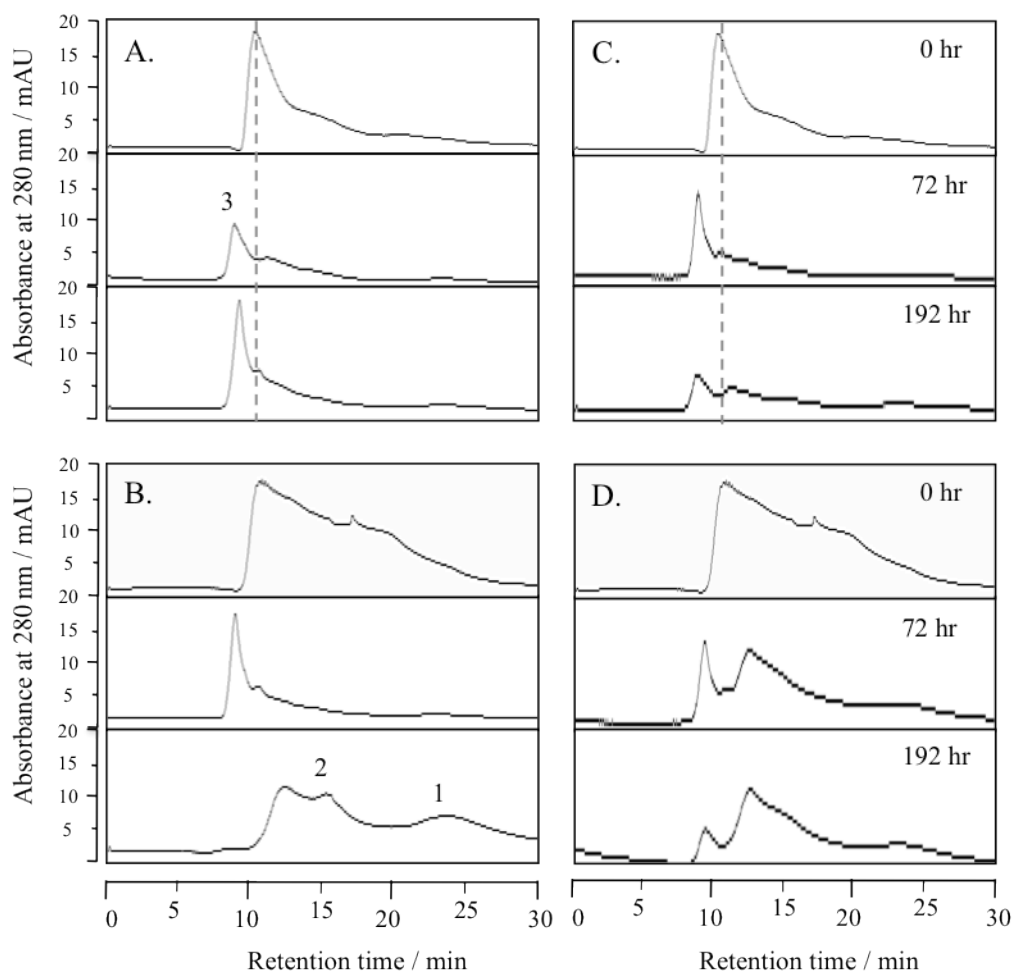


Figure 3.8. Gel filtration HPLC analysis of the breakdown of high-molecular weight (A, C) and low-molecular weight (B, D) forms of Kraft lignin by *M. marinilacus* (left) and *M. phyllosphaerae* (right), in the presence of M9 salts at 30 °C. The retention time for the high molecular weight lignin peak at 10–11 min is indicated with a dashed line and new peaks 1 (24 min), 2 (15 min), and 3 (9 min) are discussed in the text.

The gel filtration HPLC analysis (Fig. 3.8) indicates a reduced intensity of the peak at retention time 11 min following treatment of high-molecular weight Kraft lignin with *M. marinilacus* and *M. phyllosphaerae*, which suggests that both of these strains are capable of metabolizing this material; however the appearance of a peak at retention time 8 min after 72 hr indicates repolymerization, and is similar to the observations in the gel filtration HPLC analysis of the same samples treated with *Sphingobacterium sp.* (Fig. 3.7). *M. phyllosphaerae* seems to break down the higher-molecular weight

repolymerization product (s) after 192 hr to yield medium-molecular weight fragments, represented by the increased intensity of the peak at retention time 12 – 13 min (Figure 3.8 C). In contrast, *M. marinilacus* doesn't seem to be capable of breaking down the repolymerized material, as indicated by the increased intensity of the peak at retention time 9 min after 192 hours of treatment.

Repolymerization was also observed following treatment of low-molecular weight Kraft lignin with these strains, although the disappearance of the peak at 9 min (Figure 3.8 C) suggests that *M. marinilacus* is capable of depolymerizing this material more efficiently to yield low-molecular weight fragments.

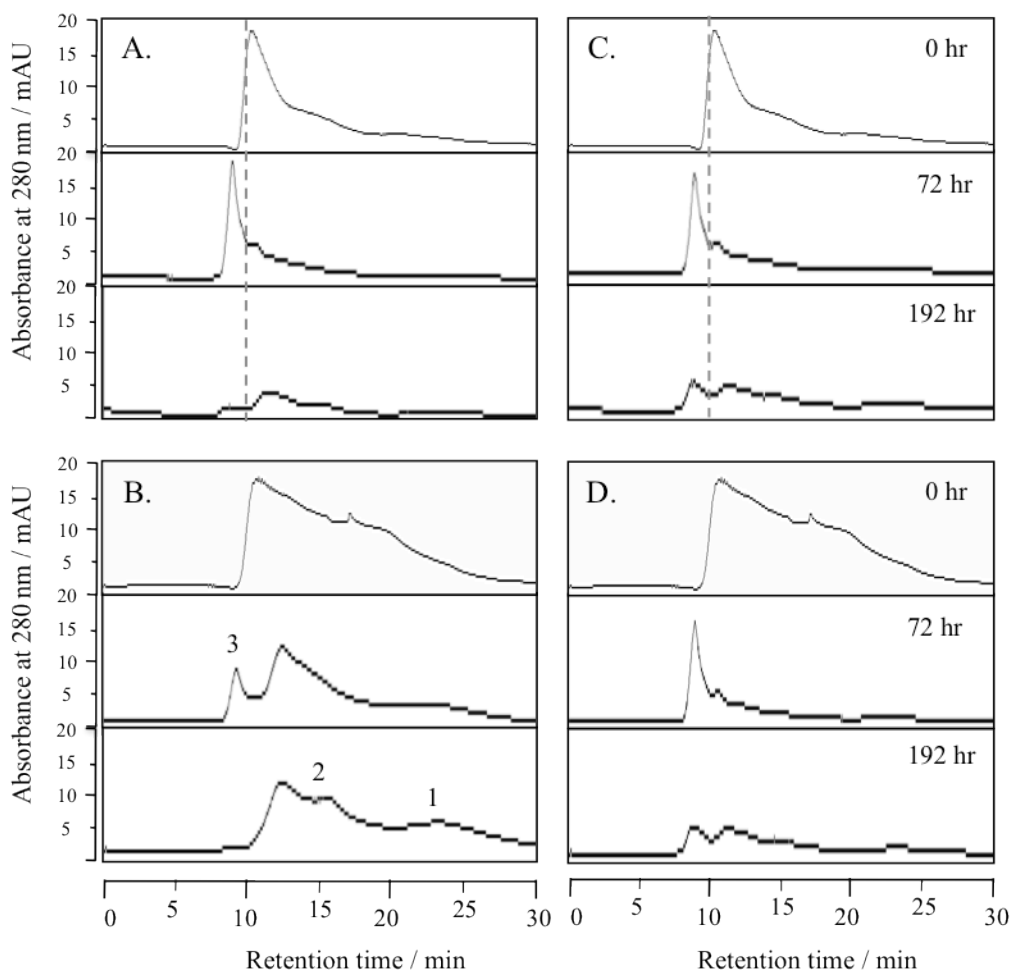


Figure 3.9. Gel filtration HPLC analysis of the breakdown of high-molecular weight (A, C) and low-molecular weight (B, D) forms of Kraft lignin by *M. oxydans* (left) and *R. erythropolis* (right), in M9 salt solution at 30 °C. The retention time for the high-molecular weight lignin peak at 11 min is indicated with a dashed line and new peaks 1 (24 min), 2 (15 min), and 3 (9 min) are discussed in the text.

The significantly reduced intensity of the peak at 11 min following treatment of high-molecular weight Kraft lignin by *M. oxydans* and *R. erythropolis* after 192 hr, combined with the absence of a peak corresponding to low-molecular weight products at 25 min (Fig. 3.9 A and C), suggests that these strains have not only depolymerized this material but have also metabolized any low-molecular weight products. These observations are similar to those in Fig. 3.8 (A and C), in which negligible peaks are seen at 25 min following treatment of the same

material with *M. marinilacus* and *M. phyllosphaerae* after 192 hr. In stark contrast, 192 hr of treatment of high-molecular weight material with *Sphingobacterium sp.* results in the accumulation of low-molecular weight products, indicated by the broad peak at 25 min of approximately 8 mAU in intensity. These observations suggest that the *Microbacterium* strains and *R. erythropolis* metabolize low-molecular weight lignin breakdown products much more rapidly than *Sphingobacterium sp.*

3.7. Bioconversion of lignin-containing feedstocks

The ability of *Sphingobacterium sp.*, *R. erythropolis* and *M. phyllosphaerae* to break down lignin was examined in more detail by examining their ability to degrade different forms of lignin and lignocellulose. *Sphingobacterium sp.* was of particular interest following the high activity observed in the nitrated lignin assays (see Chapter 2), *R. erythropolis* was selected for these experiments due to the very high level of growth observed in M9 salt solution supplemented with Kraft lignin and the recent identification of DyP B from *R. jostii* RHA1, and *M. phyllosphaerae* was chosen because it appeared to grow more readily on vanillic acid than the other *Microbacterium* strains. All three strains were found to depolymerize high-molecular weight Kraft lignin, although only *R. erythropolis* and *M. phyllosphaerae* seem to be capable of metabolizing the lower-molecular weight products. Starter cultures of each strain were grown in LB broth and then centrifuged to give the whole cells, which were washed with 20 mM potassium phosphate buffer (pH 7.0). The cells were then re-suspended in M9 salt solution (250 ml) supplemented with wheat straw, Organosolv lignin or Kraft lignin (2.5 % w/v) and a nitrogen supplement (2.0 % w/v), and the cultures incubated at 30

or 45 °C for 14 days. Aliquots were removed and filtered after 48, 96, 168, 240 and 336 hours of incubation and the liquid fractions were used to measure growth, soluble phenol content, reducing sugar content and pH. Growth was monitored via colony-forming unit (CFU) counts, soluble phenol content by Folin-Ciocalteu (FC) colorimetry [185, 186], and the total reducing sugar content measured by the dinitrosalicylic acid (DNS) method [187]. Samples of the solid and liquid fractions from each inoculation, removed after 96, 168 and 336 hours, were dried, powdered and then analyzed by FT-IR, collected by attenuated total reflectance (ATR) from 4000 – 500 cm⁻¹.

Since preliminary experiments found that the growth of each strain in M9 salts supplemented with only Kraft lignin, Organosolv lignin or wheat straw was limited in the absence of a nitrogen source, the media for the bioconversion experiments were supplemented with either corn steep liquor (2.0 % w/v) or fish meal (2.0 % w/v) in order to compare the growth rate and efficiency of each strain in the presence of each supplement. Corn steep liquor (CSL) is a byproduct of the wet milling of corn and is rich in vitamins, amino acids and other growth stimulants [188]. It can give rise to bacteria that are rich in proteins and poor in acidic polysaccharides. In addition to nitrogen content of 3.85 – 4.10 %, CSL also contains free reducing sugars (0.10 – 11.00 %), which make it an effective fermentation catalyst. Fish meal [189] is derived from fish waste and is composed of proteins (62 %), fat (9 %) and ash (18 %). Carrying out the bioconversion experiments using each different nitrogen source allowed the determination of the impact of each source, if any, on the activity of each strain towards lignin degradation.

3.7.1. Bioconversion of wheat straw

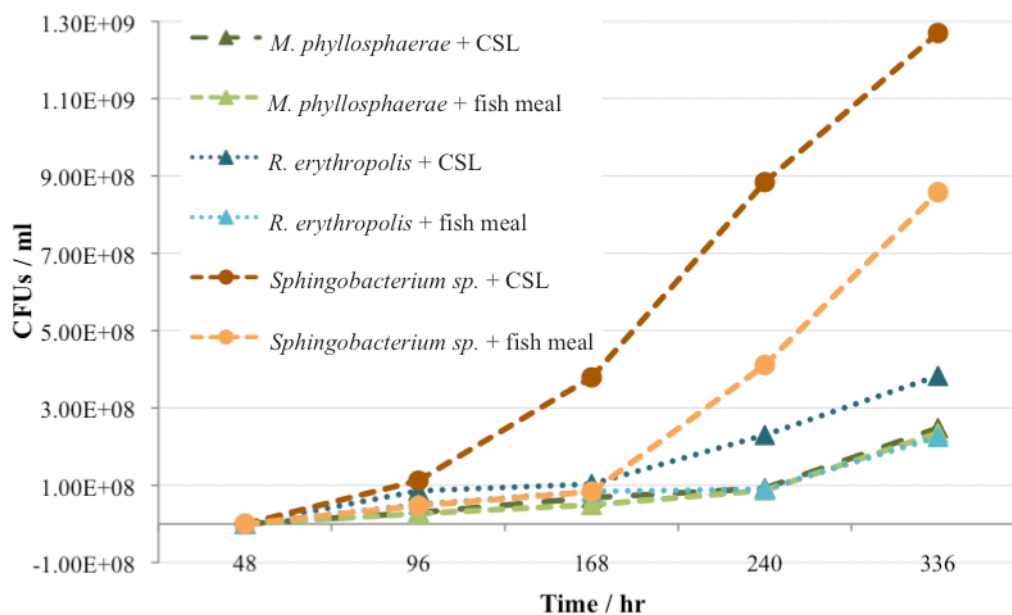


Figure 3.10. Number of CFUs per ml in samples of wheat straw (2.5 % w/v) treated with *M. phyllosphaerae*, *R. erythropolis* and *Sphingobacterium sp.* in the presence of fish meal or CSL, taken after 48, 96, 168, 240 and 336 hr.

All of the isolates showed a distinct increase in the composition of CFUs after 336 hr (Fig. 3.10). *Sphingobacterium sp.* grew much more rapidly than *R. erythropolis*, which exhibited a higher growth rate than *M. phyllosphaerae*. All strains grew more rapidly in the presence of CSL compared to fish meal. The observations for *Sphingobacterium sp.* are expected since this organism exhibited high activity towards lignin degradation in the UV/visible nitrated lignin assays (see Chapter 2), though it was not found to grow on cellulose. The relatively slow growth of *R. erythropolis*, which had exhibited good growth on cellulose, could be a result of the bioavailability of cellulose, which remains low until it is released from the lignocellulose polymer matrix upon the breakdown of lignin. It is expected that rapid growth of *R. erythropolis* would not be observed until the cellulose is released by breakdown of the lignin component of

wheat straw by *Sphingobacterium sp.*, which has the highest number of CFUs ml^{-1} after 336 hours.

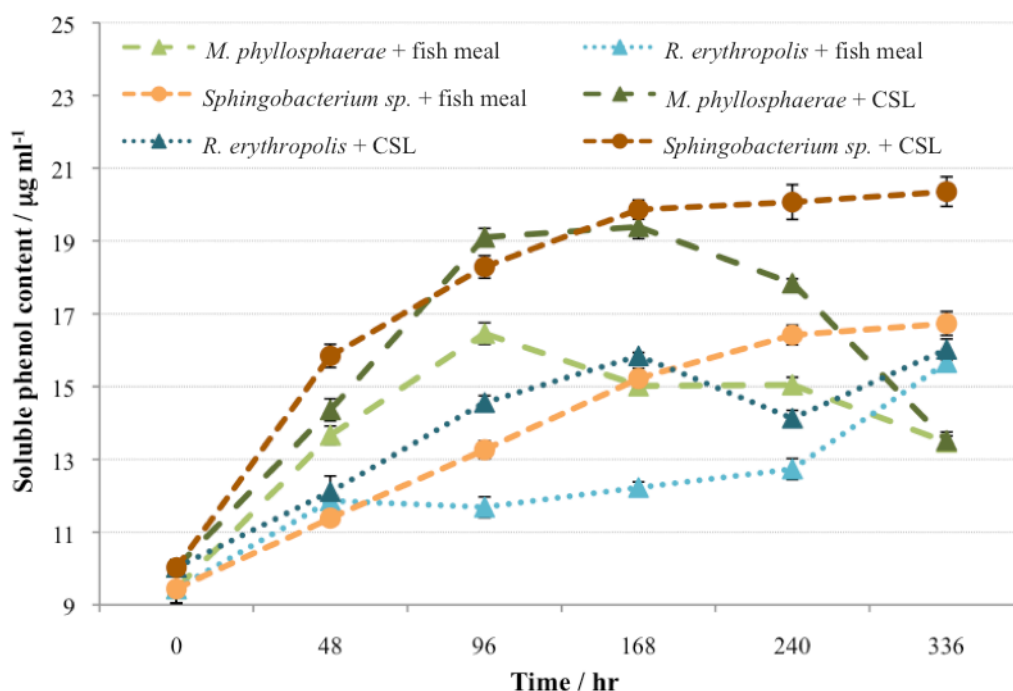


Figure 3.11. Soluble phenol content of samples of wheat straw (2.5 % w/v) treated with *M. phyllosphaerae*, *R. erythropolis* and *Sphingobacterium sp.* in the presence of fish meal or CSL, taken after 48, 96, 168, 240 and 336 hr. Experiments were performed in technical triplicate.

Analysis of samples for soluble phenol content (Fig. 3.11) indicates that treatment of wheat straw with each strain yields soluble phenols, though the extent of phenol production varies between the different bacteria and media composition. In many cases an initial increase in soluble phenol content is followed by a reduction or a slower increase, which could arise from the metabolism of the phenolic products by the bacteria. Two possible processes occur over the time course, which include the breakdown of lignin into low-molecular weight phenolic compounds, followed by further breakdown via primary metabolism (Equation 1).



Equation 1. Conversion of lignin into low-molecular weight phenolic compounds, which may be subsequently consumed by bacteria during primary metabolism.

The possible variation in the rates of k_1 and k_2 during the treatment of wheat straw by the different bacteria may explain the different patterns observed in Figure 3.11.

In comparison to *M. phyllosphaerae* and *R. erythropolis*, which seem to metabolize the phenolic products after 168 hr of inoculation with CSL, the phenol content remains stable following treatment with *Sphingobacterium sp.*, suggesting that it may either be inhibited by the phenol products or it is not metabolically capable of breaking them down. This observation is not surprising since reports of degradation of phenolic compounds by *Sphingobacterium* strains are sparse, though it is intriguing that the reduction in soluble phenol content following further treatment with *M. phyllosphaerae* after 168 hr is much greater than with *R. erythropolis*, since *Rhodococcus* strains have been reported to degrade a variety of phenolic compounds [175, 176].

In each case, CSL is the most effective nitrogen supplement for the strains since more rapid variation in soluble phenol content was observed.

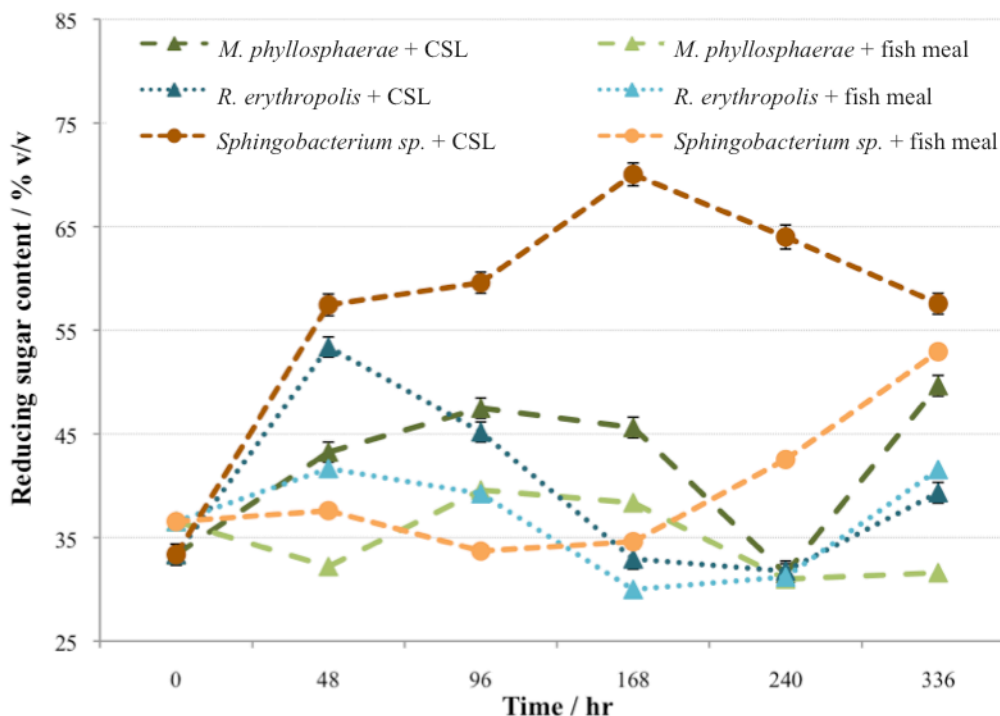


Figure 3.12. Reducing sugar content of samples of wheat straw lignocellulose (2.5 % w/v) treated with *M. phyllosphaerae*, *R. erythropolis* and *Sphingobacterium sp.* in the presence of fish meal or CSL, taken after 48, 96, 168, 240 and 336 hr. Experiments were performed in technical triplicate.

Analysis of aliquots for reducing sugar content (Fig. 3.12) shows that degradation of the wheat straw releases monosaccharides, which can subsequently be metabolized by the bacteria.



Equation 1. Depolymerization of cellulosic polysaccharides to release monosaccharide products, which may be subsequently consumed by bacteria during primary metabolism.

Treatment of wheat straw with each strain results in initial increases in the reducing sugar content (Fig. 3.12), which may correspond to the formation of monosaccharides (k_1). In many cases these increases are followed by a significant reduction in reducing sugar content. This suggests that the bacteria may be metabolizing the polysaccharides, which correlates with the increased number of CFUs per ml for *M. phyllosphaerae* and *R. erythropolis* (Fig. 3.10).

It is intriguing that treatment with *Sphingobacterium sp.* seems to depolymerize the cellulosic polysaccharides at a significantly enhanced rate in the presence of CSL compared to fish meal, which could be due to co-metabolism.

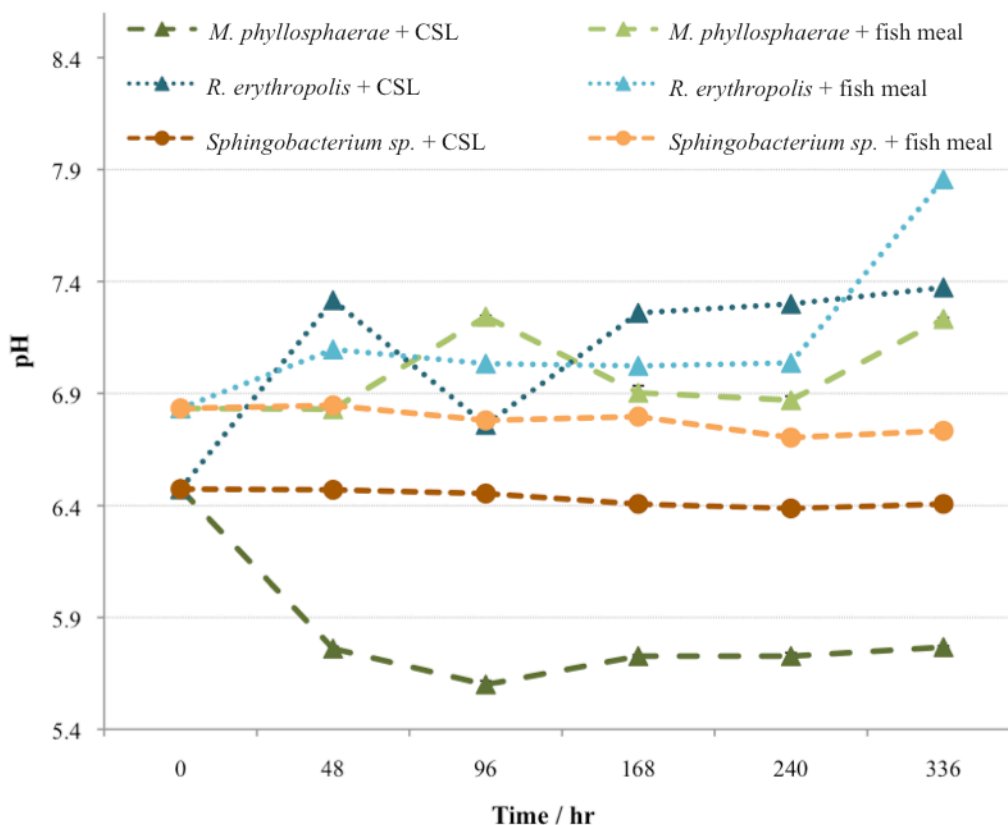


Figure 3.13. pH of samples of wheat straw (2.5 % w/v) treated with *M. phyllosphaerae*, *R. erythropolis* and *Sphingobacterium sp.* in the presence of fish meal or CSL, taken after 48, 96, 168, 240 and 336 hr. Experiments were performed in technical triplicate.

Analysis of the pH of aliquots vs. time shows some variation vs. time. Lignin breakdown products and intermediates include organic acids such as ferulic acid, oxalic acid and vanillic acid, which may explain the reduction in pH of 0.9 following treatment with *M. phyllosphaerae* in the presence of CSL, although the pH remained constant or increased in all other cases.

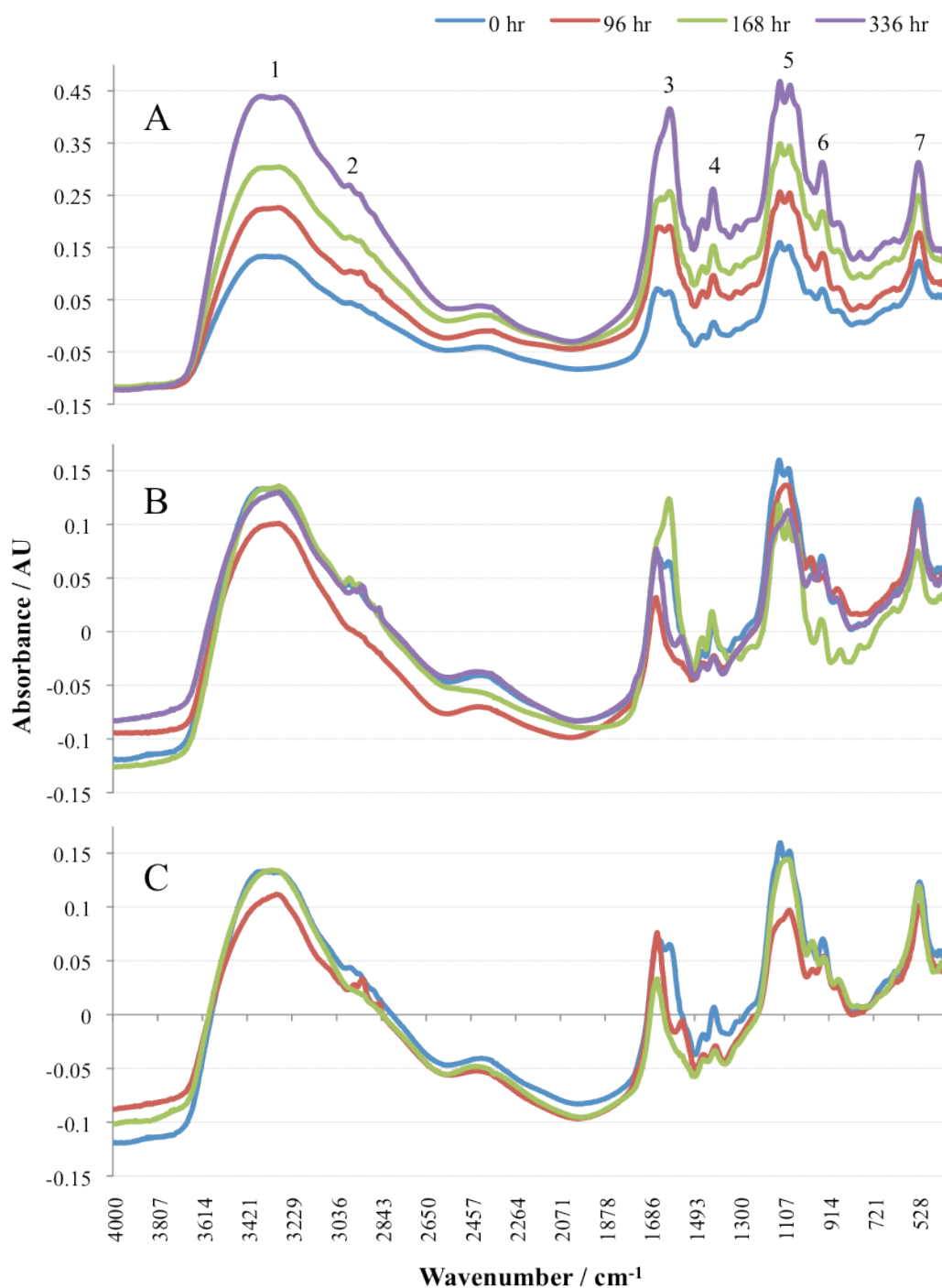


Figure 3.14. FT-IR (ATR) spectra of the liquid fractions of *Spingobacterium sp.* (A), *M. phyllosphaerae* (B) and *R. erythropolis* (C) inoculated in M9 salts supplemented with wheat straw (2.5 % w/v) and CSL (2 % w/v). Samples taken after 96, 168 and 336 hr were measured along with untreated wheat straw in the same medium. Peaks 1 – 4 are tentatively assigned in Table 3.6.

The FT-IR analysis of the solid and liquid fractions of treated and untreated wheat straw (Fig. 3.14 and 3.15) are defined by a broad peak from 3350 – 3200 cm^{-1} , sharper peaks of low to moderate intensity from 2980 – 2920 cm^{-1} and sharper peaks of low to high intensity in the regions of 1600 – 1500 cm^{-1} and 1200 – 1000 cm^{-1} . The peaks were numbered and tentatively assigned to bonds on the basis of literature reports (see Table 3.6).

Table 3.6. IR peaks observed in literature studies of lignin, and their appearance in the observed data (Fig. 3.14 and Fig. 3.15). Numbers in brackets indicate the observations in the solid (s) or liquid (l) FT-IR (ATR) analysis [191 – 193].

Peak	Observed frequency value or range / cm^{-1}	Probable interpretation	Literature range / cm^{-1}
1, 2	3356 – 3281 (1l); 3288 – 3238 (1s) 2986 – 2959 (2l); 2930 – 2920 (2s);	O–H stretch (phenolic and aromatic); C–H stretch (aromatic –OMe and side chain –CH ₂ and –CH ₃)	3500 – 2850
3	1653 – 1601 (l);	C=C stretch (guaiacyl aromatic ring); C–H bond deformation	1650 – 1600
4, 6	1416 – 1404 (4l) 1454 – 1410 (6s)	Aromatic skeletal stretches; C–O bond deformations from carbohydrate ring vibrations	1450 – 1400
5	1557 – 1517 (s);	C–H asymmetric deformation in –CH ₂ and –CH ₃	1600 – 1500
6	1454 – 1410 (s)	C–O stretch (carboxylic acid)	1450 – 1400
7	1319 – 1300 (s)	C–O stretch (downward direction); aromatic C–H deformation	1350 – 1300
8	1242 – 1235 (s)	(aromatic or secondary alcohol); aromatic C–H deformation	1350 – 1200
9, 10	1076 – 1054 (9s) 1038 – 1020 (10s)	C–O bond deformation (primary alcohol); C=O stretching vibration	1100 – 1000

Peak 1 ($3400 - 3200 \text{ cm}^{-1}$) corresponds to O–H stretches, possibly in low-molecular weight phenolic products, though this may also indicate the presence of low-molecular weight sugars produced from the wheat straw. Peak 2 ($3000 - 2850 \text{ cm}^{-1}$) corresponds to C–H bonds, possibly in low-molecular weight products [191]. Peak 3 ($1650 - 1600 \text{ cm}^{-1}$) corresponds to C=C stretches, possibly in the guaiacyl aromatic ring. Peaks 5, 7, 8 and 9 correspond to C–O stretches in low-molecular weight phenolic or sugar- products and peak 6 ($1450 - 1400 \text{ cm}^{-1}$) is likely to correspond to acidic C=O stretches. All peaks in the region $1500 - 1000 \text{ cm}^{-1}$ may also correspond to aromatic C=C stretches [191].

The intensity of all peaks appears to increase following bacterial treatment, and the increases in intensity appear to be greater in the analysis of the solid fractions (Fig. 3.15) compared to the liquid fractions (Fig. 3.14). Treatment of wheat straw with *Sphingobacterium sp.* leads to a significantly higher increase in intensity of all peaks in the FT–IR analysis of the liquid fractions compared to treatment with *R. erythropolis* and *M. phyllosphaerae*, which is consistent with the higher activity observed in the nitrated lignin assays, for which milled wood lignin from wheat straw was used in the preparation of nitrated lignin solution (see Chapter 2).

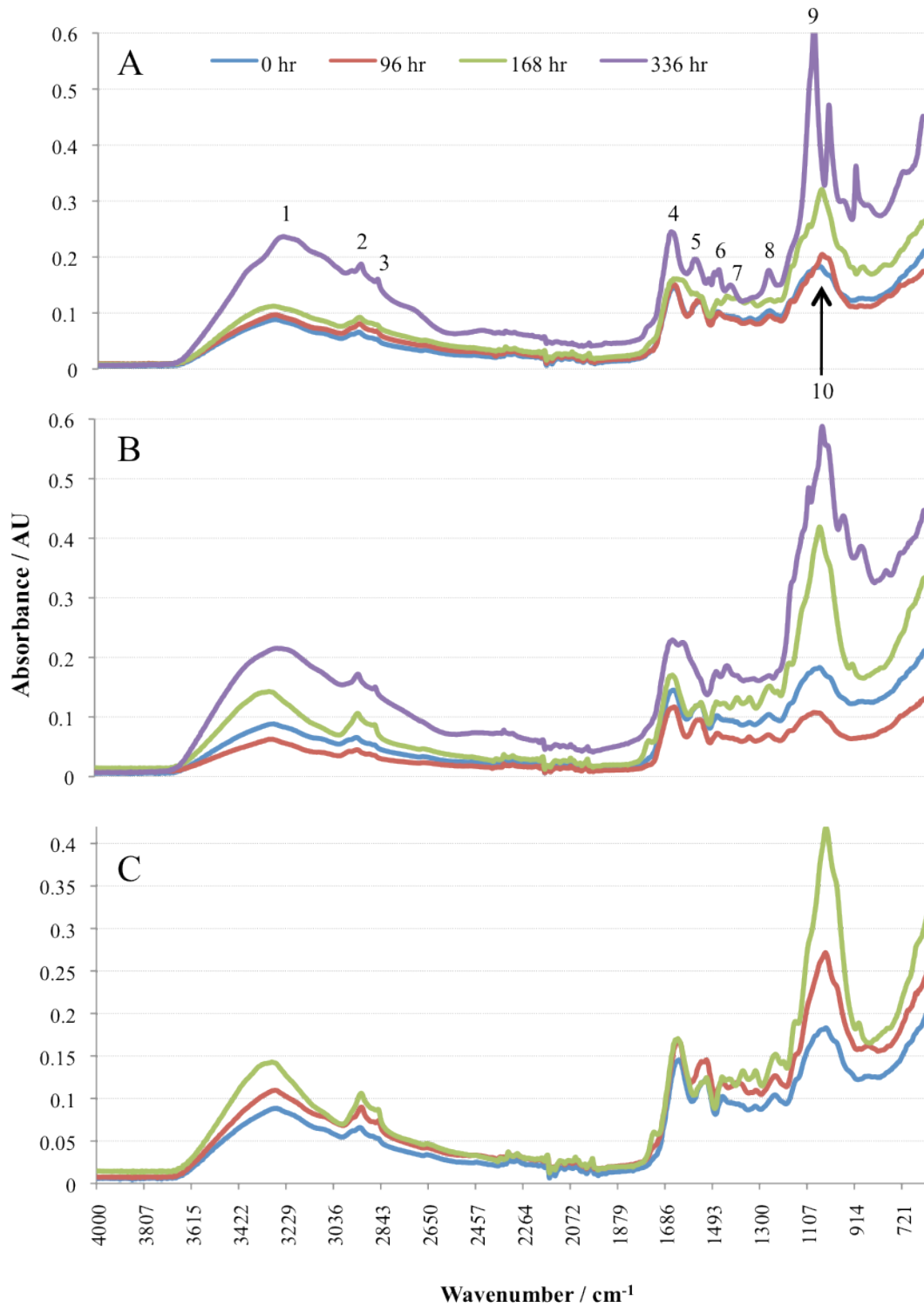


Figure 3.15. FT-IR (ATR) analysis of the solid fractions of *Spingobacterium sp.* (A), *M. phyllosphaerae* (B) and *R. erythropolis* (C) inoculated in M9 salts supplemented with wheat straw (2.5 % w/v) and CSL (2 % w/v). Samples taken after 96, 168 and 336 hr were measured along with untreated wheat straw in the same medium. Peaks 1 – 10 are tentatively assigned in Table 3.6.

The FT-IR analysis for the liquid and solid fractions (Fig. 3.14 and 3.15) both show an increase in the concentration of O-H stretches, which suggests that the breakdown of wheat straw by each strain results in the production of solid and solubilized phenolic compounds. The production of soluble and insoluble phenolic compounds from lignin may be a result of cleavage of the intramolecular linkages at different positions within the lignin polymer: cleavage at the ends of the structure possibly releases free, low-molecular weight phenols which are of high solubility, whilst cleavage of bonds embodied in the polymeric structure may yield higher-molecular weight compounds of poor solubility (Fig. 3.16).

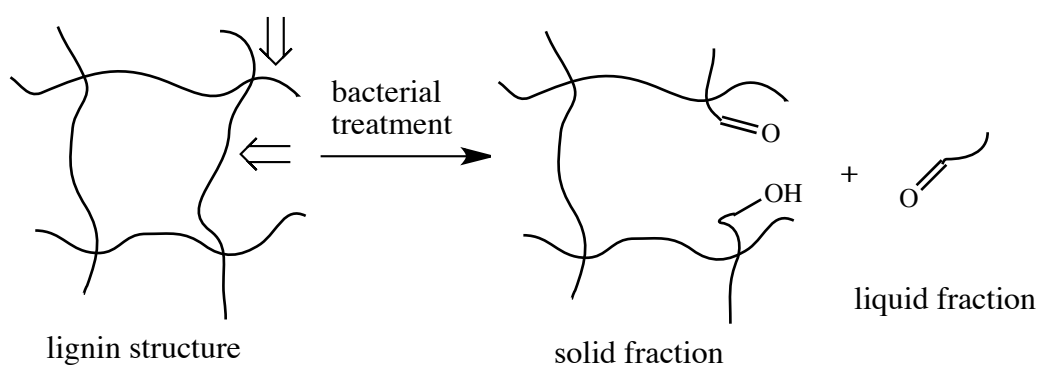


Figure 3.16. Hypothetical cleavage at different positions in the lignin polymer following bacterial treatment to yield solid and liquid fractions.

3.7.2. Bioconversion of Organosolv lignin

Treatment of Organosolv lignin from CIMV, France, by *Sphingobacterium sp.* and *M. phyllosphaerae* was monitored via the same experimental methods used to monitor the treatment of wheat straw.

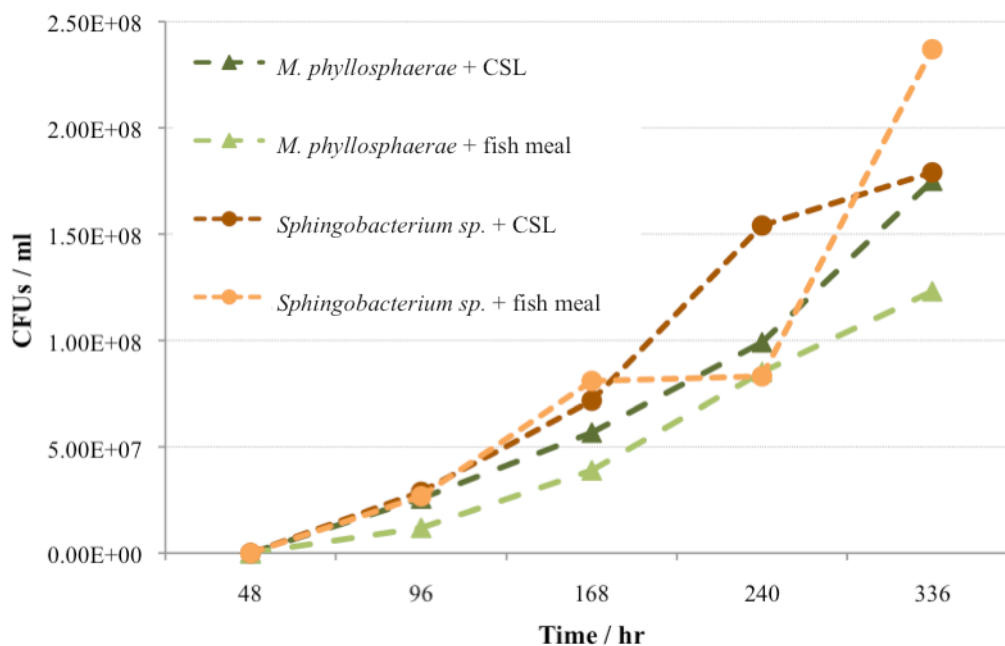


Figure 3.17. Number of CFUs per ml in samples of Organosolv lignin (2.5 % w/v) treated with *M. phyllosphaerae* and *Sphingobacterium sp.* in the presence of fish meal or CSL (2 % w/v), taken after 48, 96, 168, 240 and 336 hr.

Although *Sphingobacterium sp.* evidently grows slightly more readily than *M. phyllosphaerae* in the presence of fish meal and CSL, the difference in the degree of CFU formation by the two different strains, which peaks at approximately 5.0×10^7 CFUs ml⁻¹ after 240 hr (Fig. 3.17) is minute compared to the difference observed with the treatment of wheat straw (8.0×10^8 CFUs ml⁻¹, Fig. 3.10) and Kraft lignin (2.0×10^9 CFUs ml⁻¹, Fig. 3.23) at the same time points.

Both strains exhibited much lower rates of growth in the presence of Organosolv lignin compared to wheat straw and Kraft lignin (see 3.7.1 and 3.7.3).

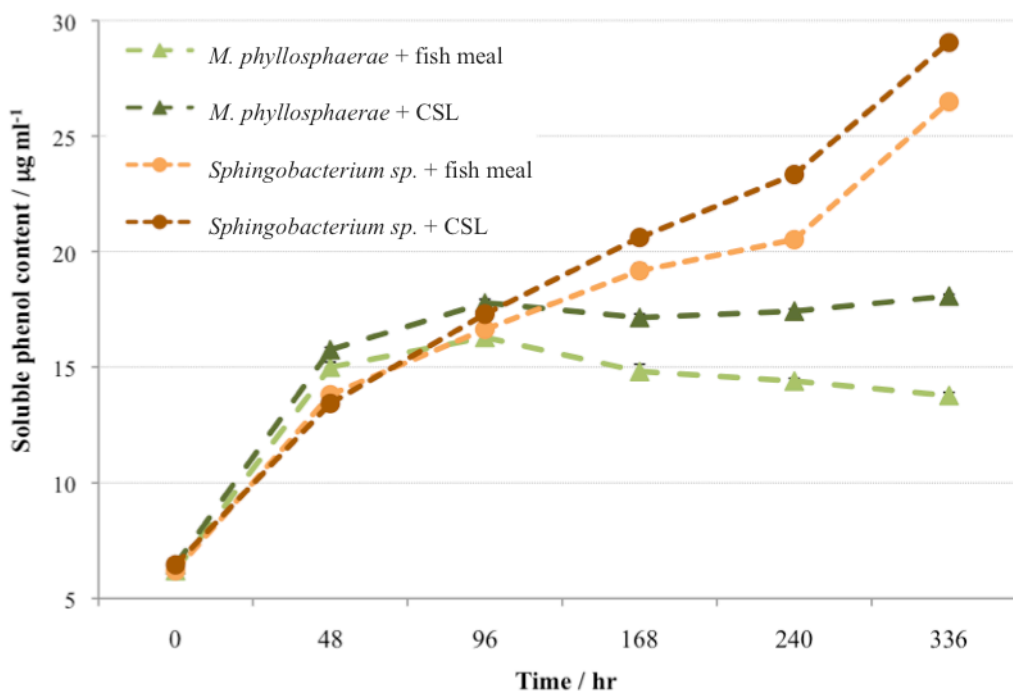


Figure 3.18. Soluble phenol content of samples of Organosolv lignin (2.5 % w/v) treated with *M. phyllosphaerae* and *Sphingobacterium sp.* in the presence of fish meal or CSL, taken after 48, 96, 168, 240 and 336 hr. Experiments were performed in technical triplicate.

Sphingobacterium sp. and *M. phyllosphaerae* are evidently capable of breaking down Organosolv lignin to yield low-molecular weight phenolic products, which correspond to approximately a three-fold increase in soluble phenol content after 48 hr (Fig. 3.18). These data suggest that *M. phyllosphaerae* is more active towards the degradation of low-molecular weight phenolic compounds than *Sphingobacterium sp.*, since the phenol content remains fairly stationary between 96 and 336 hr in the presence of *M. phyllosphaerae* compared to a further increase of approximately 12 – 13 µg ml⁻¹ (50 %) with *Sphingobacterium sp.* over the same time period.

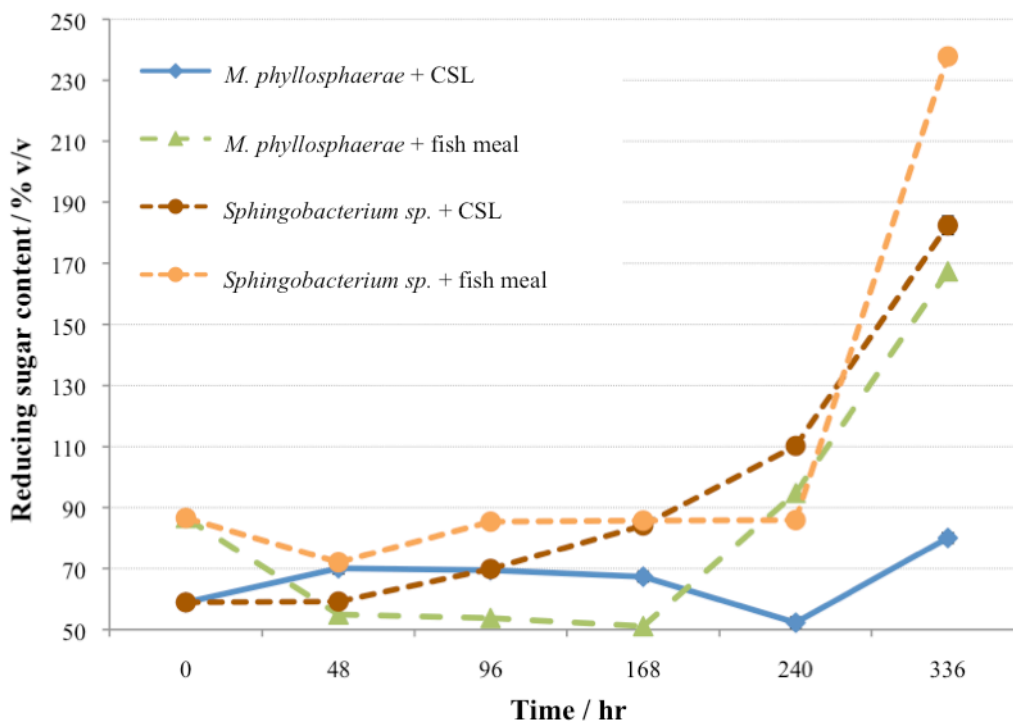


Figure 3.19. Reducing sugar content of samples of Organosolv lignin (2.5 % w/v) treated with *M. phyllosphaerae* and *Sphingobacterium sp.* in the presence of fish meal or CSL, taken after 48, 96, 168, 240 and 336 hr. Experiments were performed in technical triplicate.

The variation between the reducing sugar content of Organosolv lignin treated by *Sphingobacterium sp.* and *M. phyllosphaerae* in the presence of CSL and fish meal indicates that these supplements contain a significant amount of sugar, which is evidently metabolized by the bacteria. The significant increase from 240 – 336 hr is intriguing, indicating the presence of polysaccharides in the culture media. Previous studies have reported the sugar content of Organosolv lignin to be 2–8 % [190].

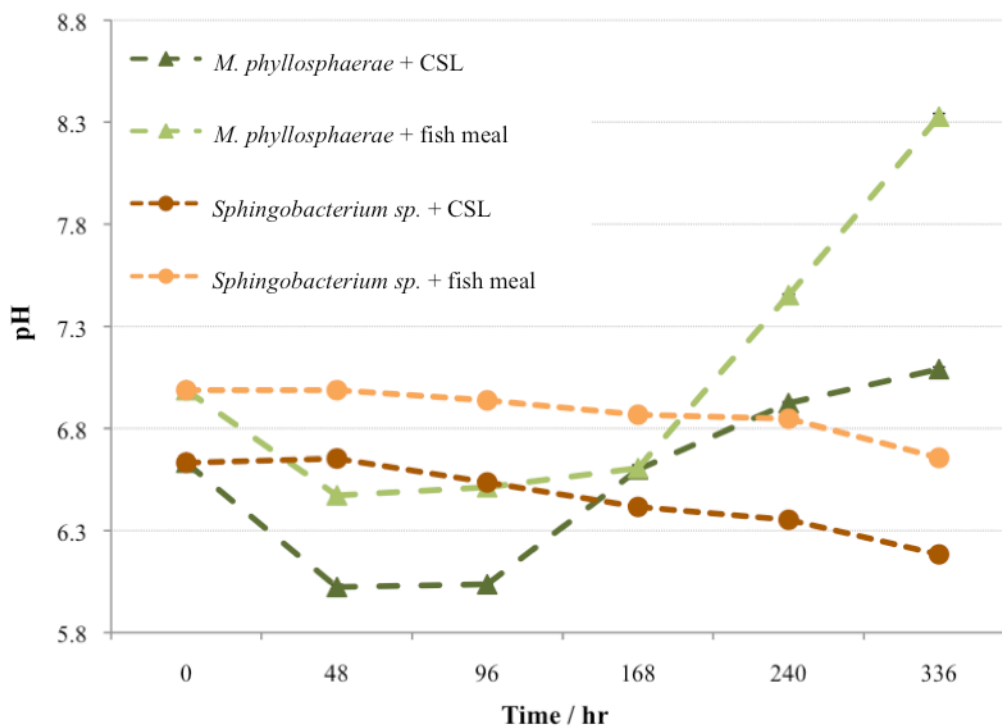


Figure 3.20. pH of samples of Organosolv lignin (2.5 % w/v) treated with *M. phyllosphaerae* and *Sphingobacterium sp.* in the presence of fish meal or CSL (2.0 % w/v), taken after 48, 96, 168, 240 and 336 hr. Readings were taken in technical triplicate.

The stark contrast in the pH change observed between cultures of *Sphingobacterium sp.* and *M. phyllosphaerae* suggests differences between the pathways via which they metabolize lignin. Treatment with *Sphingobacterium sp.* leads to a gradual reduction in pH of approximately 0.5 over 336 hr. In contrast, treatment with *M. phyllosphaerae* results in rapid decreases in pH of 0.5 – 0.6 in the first 48 hours, suggesting that organic acid intermediates are produced, which are subsequently metabolized by this organism after 96 hr.

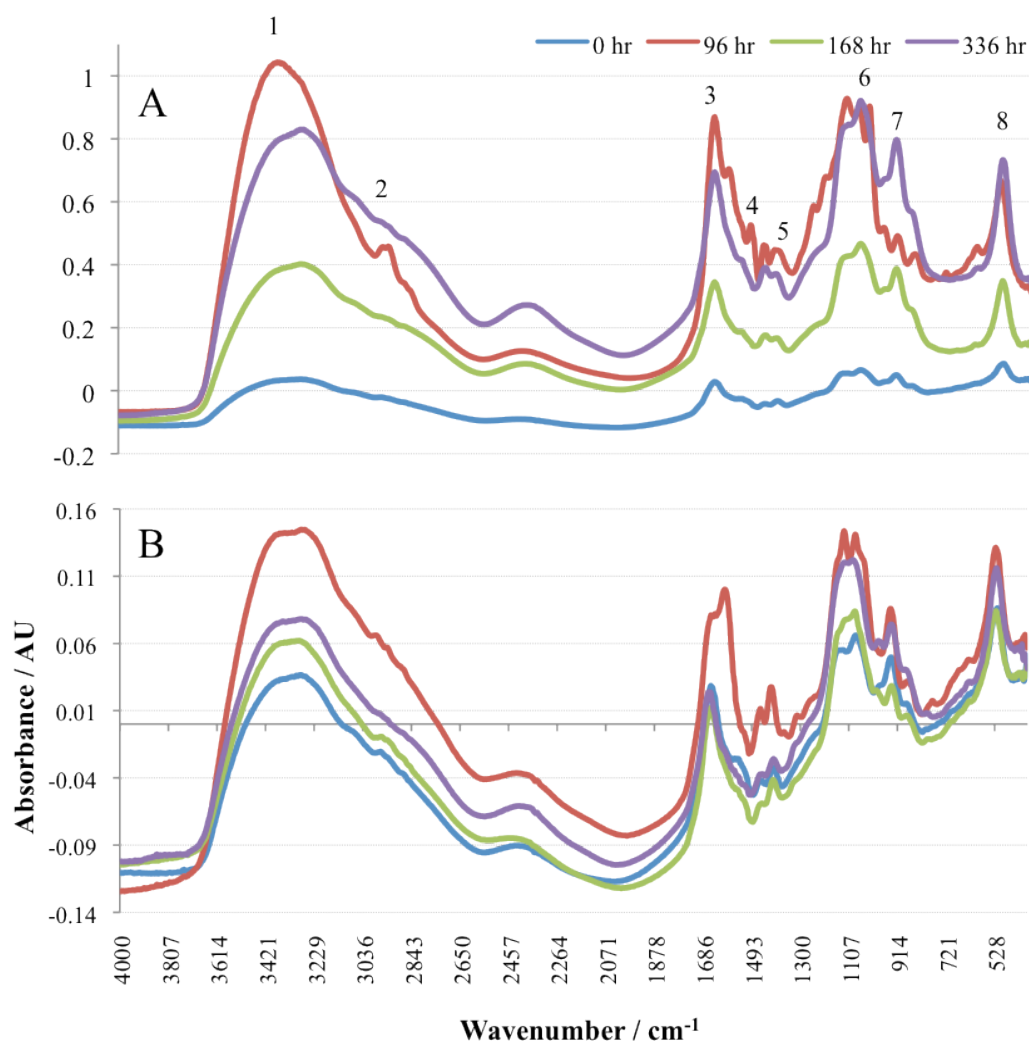


Figure 3.21. FT-IR (ATR) analysis of the liquid fractions of *Sphingobacterium sp.* (A) and *M. phyllosphaerae* (B) inoculated in M9 salts supplemented with Organosolv lignin (2.5 % w/v) and CSL (2 % w/v). Samples taken after 96, 168 and 336 hr were measured along with untreated Organosolv lignin in the same medium. Peaks 1 – 8 are tentatively assigned in Table 3.7.

Analysis of the solid and liquid fractions of treated and untreated Organosolv lignin (Fig. 3.21) is similar to treated and untreated wheat straw (Fig. 3.14 and 3.16). In similarity to the bacterial treatment of wheat straw, the intensity of the peaks increase following treatment with *Sphingobacterium sp.* (Fig. 3.21A) and *M. phyllosphaerae* (Fig. 3.21B), although treatment with *Sphingobacterium sp.* led to an increase in intensity approximately ten-fold higher than treatment with *M. phyllosphaerae* over 96 hours, which seems to correlate with the FT-IR analysis of treated wheat straw (3.14) and the nitrated lignin assay data for these

strains (see Chapter 2). It is intriguing that in both cases the intensity of all peaks fluctuates from 96–336 hr.

Table 3.7. IR peaks observed in literature studies of lignin [191–193], and their appearance in the observed data (Fig. 3.21 and Fig. 3.22). Numbers and letters in brackets alongside the frequency values indicate the state of the fraction (l = liquid, s = solid).

Peak	Observed frequency value or range / cm^{-1}	Type of vibration	Literature range / cm^{-1}
1–3	3375–3279 (1l); 3287–3267 (1s); 2985–2939 (2l); 2932–2920 (2s); 2857–2851 (3s)	O–H stretch (phenolic and aromatic); C–H stretch (aromatic –OMe and side chain –CH ₂ and –CH ₃) C=O stretch (conjugated <i>p</i> -substituted aryl ketone)	3500–2850
3, 4	1662–1599 (3l); 1645–1599 (4s)	C=C stretch (guaiacyl aromatic ring); C–H bond deformation	1650–1600
5	1541–1514 (s)	Asymmetric C–H deformation in –CH ₂ and –CH ₃	1600–1500
4, 6	1462–1406 (4l) 1456–1450 (6s)	Asymmetric C–H deformation in –OMe; C–O stretch (guaiacyl –OMe);	1460–1400
5, 7	1419–1406 (5l); 1423–1369 (7s)	C–O stretch (carboxylic acid)	1450–1400
8	1234–1217	C–O bond deformation (aromatic or secondary alcohol)	1350–1200
6, 9	1090–1080 (6l); 1034–1028 (9s)	C–O bond deformation (primary alcohol)	1100–1000

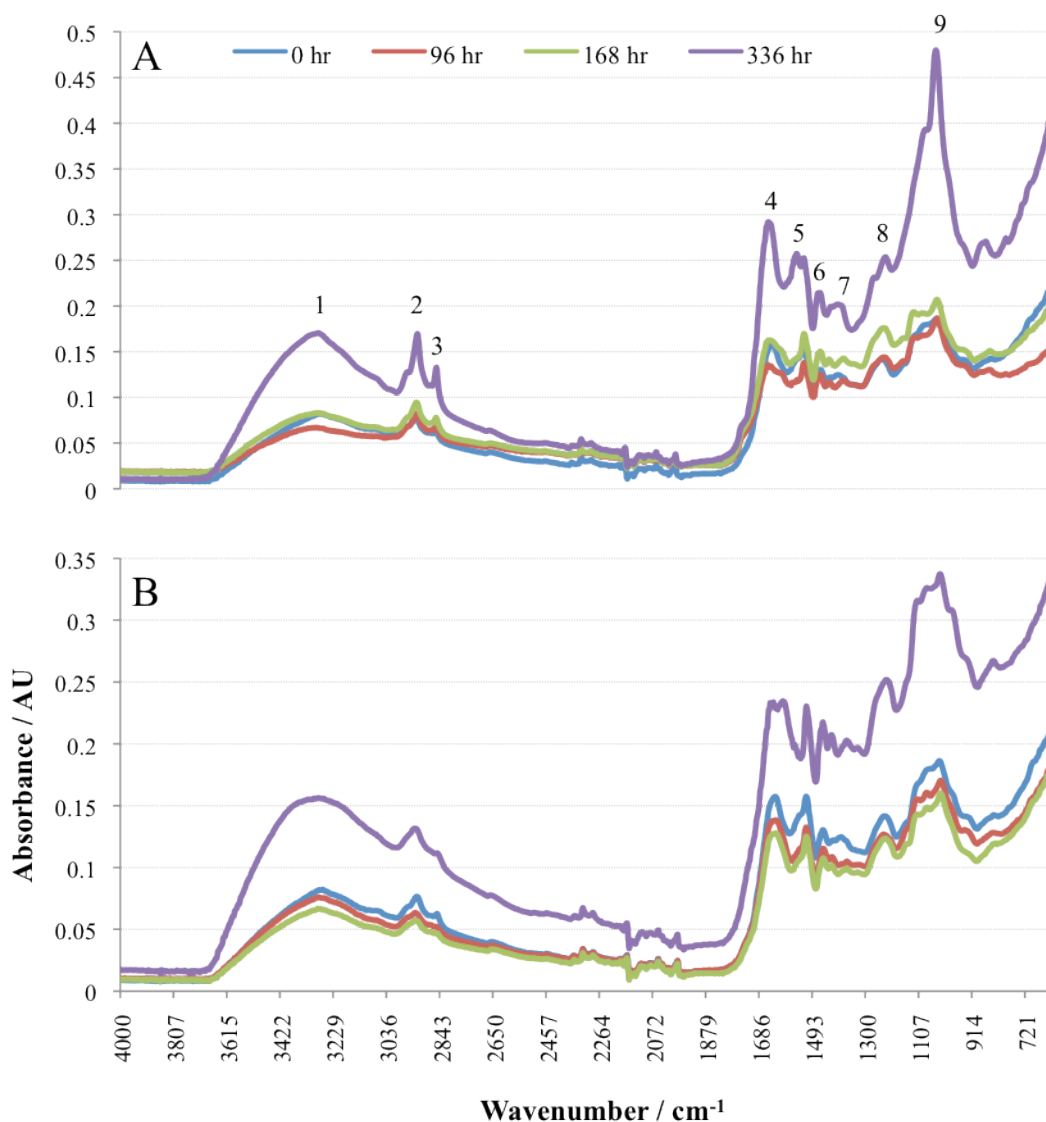


Figure 3.22. FT-IR (ATR) analysis of the solid fractions of *Sphingobacterium sp.* (A) and *M. phyllosphaerae* (B) inoculated in M9 salts supplemented with Organosolv lignin (2.5 % w/v) and CSL (2 % w/v). Samples taken after 96, 168 and 336 hr were measured along with untreated Organosolv lignin in the same medium. Peaks 1 – 9 are tentatively assigned in Table 3.7.

The FT-IR analysis of the solid fractions of Organosolv lignin treated with *Sphingobacterium sp.* and *M. phyllosphaerae* (Fig. 3.22) indicates an increase in absorbance of all peaks following treatment with each strain, although a slightly higher increase of 0.09 AU is observed following treatment with *Sphingobacterium sp.* compared to 0.07 AU with *M. phyllosphaerae*. Similar to the analysis for treated wheat straw (Fig. 3.14), greater increases in absorbance are observed in the analyses of the liquid fractions than for the solid fractions,

indicating a greater rate of increase in the concentration of free, soluble phenols than higher-molecular weight insoluble phenols (see Fig. 3.16).

3.7.3. Bioconversion of Kraft lignin

Analysis of Kraft lignin treated with *Sphingobacterium sp.*, *R. erythropolis* and *M. phyllosphaerae* was performed using the same techniques as for wheat straw and Organosolv lignin, although all samples were in liquid form since the Kraft lignin was completely dissolved in the media.

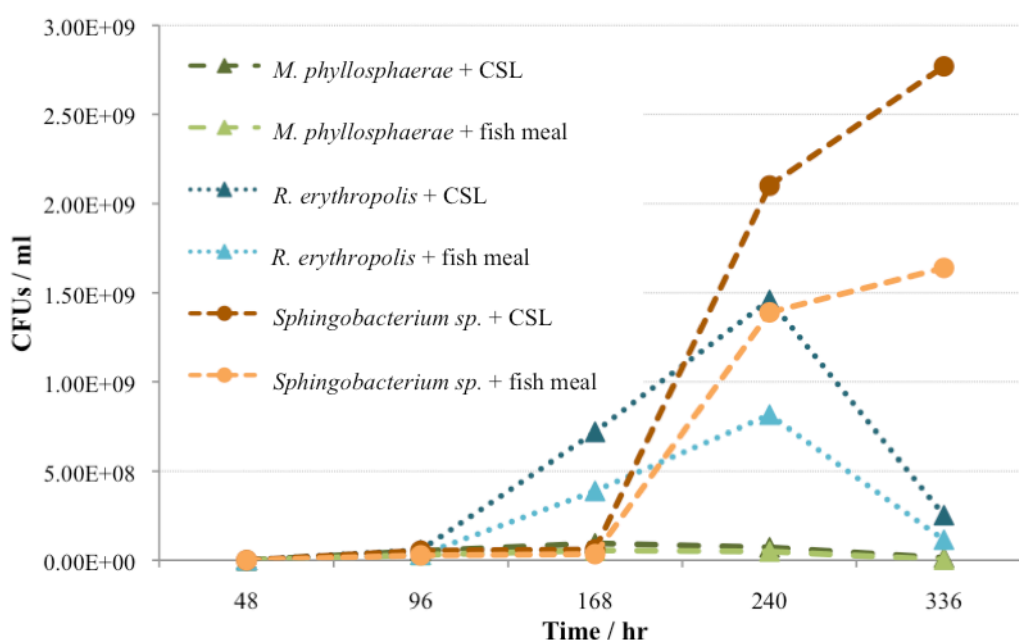


Figure 3.23. Number of CFUs per ml in samples of Kraft lignin (2.5 % w/v) treated with *M. phyllosphaerae*, *R. erythropolis* and *Sphingobacterium sp.* in the presence of fish meal or CSL (2.0 % w/v), taken after 48, 96, 168, 240 and 336 hr.

Despite a significant variation in the level of growth of each strain with the two different nitrogen-containing supplements, fish meal and CSL, *Sphingobacterium sp.* and *R. erythropolis* grew much more rapidly in the presence of Kraft lignin than *M. phyllosphaerae*. In the presence of CSL, 2.10×10^9 and 1.45×10^9 CFUs ml⁻¹ were observed at 240 hr for *Sphingobacterium sp.* and *R. erythropolis* respectively, compared to only 5.0×10^7 for *M.*

phyllosphaerae. These observations are consistent with those from the earlier growth experiments in M9 salts supplemented with Kraft lignin and yeast extract (Fig. 3.3), which also show limited growth of *M. phyllosphaerae* in the presence of Kraft lignin. Another similarity with the observations from the growth experiments in Kraft lignin (Fig. 3.3) is the limited growth of *Sphingobacterium sp.* and *R. erythropolis* in the initial 7 days of inoculation, followed by rapid growth between 7 and 14 days. It is interesting that *Sphingobacterium sp.* grew more rapidly than *R. erythropolis* between 168 and 336 hr in the presence of fish meal and CSL since growth of *Sphingobacterium sp.* was limited in the presence of Kraft lignin and yeast extract, requiring a glucose supplement for good growth (Fig. 3.3).

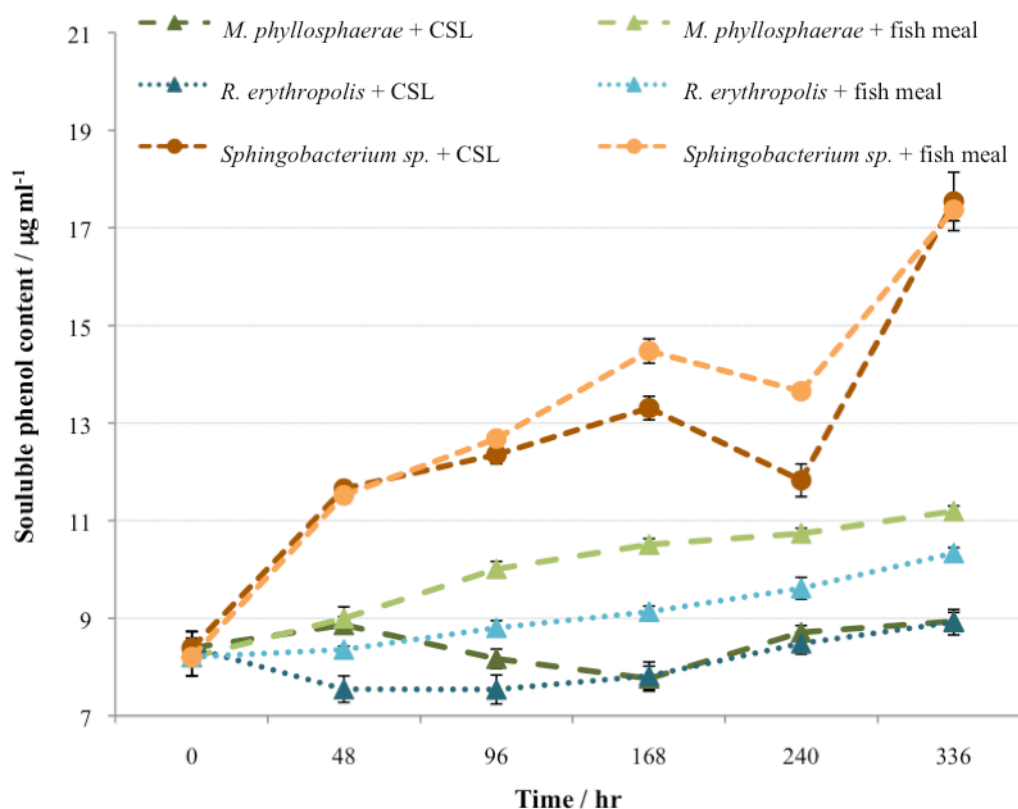


Figure 3.24. Soluble phenol content of samples of Kraft lignin (2.5 % w/v) treated with *M. phyllosphaerae*, *R. erythropolis* and *Sphingobacterium sp.* in the presence of fish meal or CSL (2.0 % w/v), taken after 48, 96, 168, 240 and 336 hr, and performed in technical triplicate.

Although the soluble phenol content increased in the initial 48 hours of treatment with *Sphingobacterium sp.*, only a minor increase was observed following treatment with *M. phyllosphaerae* and the soluble phenol content decreases following treatment with *R. erythropolis* supplemented with CSL. These reduced rates of increase in soluble phenol content and decreases could correspond to repolymerization of the phenolic products in the first 48 hours, which was indicated in the gel filtration HPLC analysis of high- and low-molecular weight forms of Kraft lignin following 72 hours of treatment with all of these strains (Fig. 3.7–3.9).

The higher content of soluble phenols in *Sphingobacterium sp.*-treated Kraft lignin fractions compared to Kraft lignin treated with the other two strains is also consistent with gel filtration HPLC data from the size-fractionation experiments, which showed an intense broad peak corresponding to low-molecular weight products following treatment with *Sphingobacterium sp.* (Fig. 3.7). This peak was of a significantly lower intensity in the analysis of high- and low-molecular weight Kraft lignin treated by *M. phyllosphaerae* (Fig. 3.8) and *R. erythropolis* (Fig. 3.9). The consistency of these observations further suggests that *M. phyllosphaerae* and *R. erythropolis* are much more capable of metabolizing low-molecular weight products from lignin degradation than *Sphingobacterium sp.*

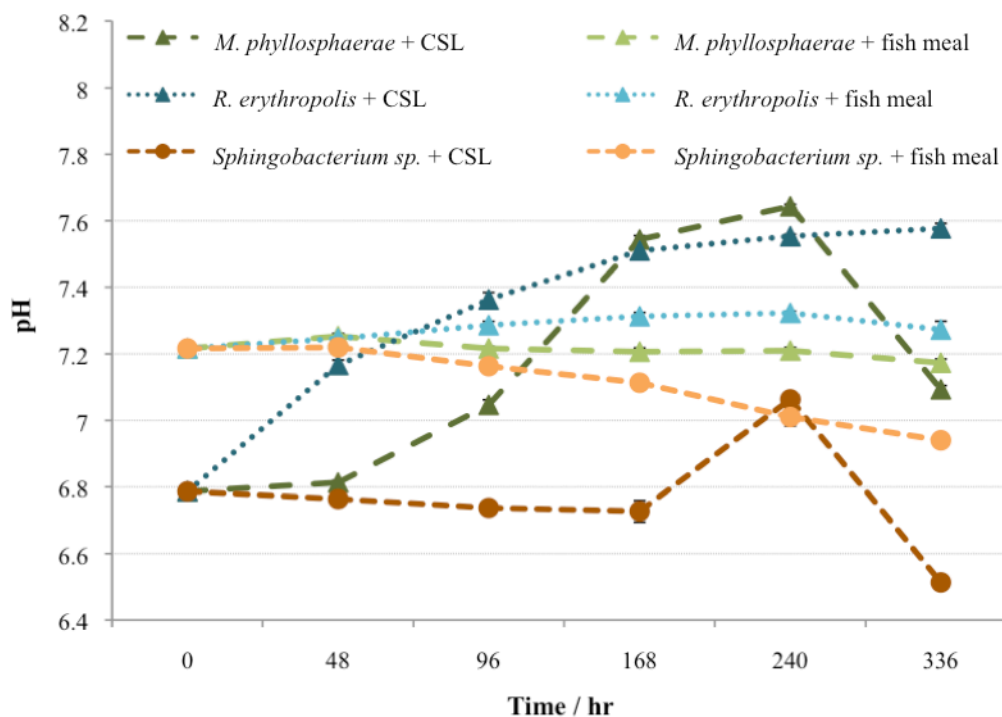


Figure 3.25. pH of samples of Kraft lignin (2.5 % w/v) treated with *M. phyllosphaerae*, *R. erythropolis* and *Sphingobacterium sp.* in the presence of fish meal or CSL (2.0 % w/v), taken after 48, 96, 168, 240 and 336 hr. Readings were taken in technical triplicate.

The pH analysis of treated and untreated Kraft lignin in the presence of CSL shows an overall decrease of 0.3 following inoculation with *Sphingobacterium sp.* at 336 hr, compared to increases of 0.8 and 0.3 for *R. erythropolis* and *M. phyllosphaerae* respectively. It is interesting that the pH changes fluctuated greatly from 168–336 hr in the presence of CSL, but not with fish meal.

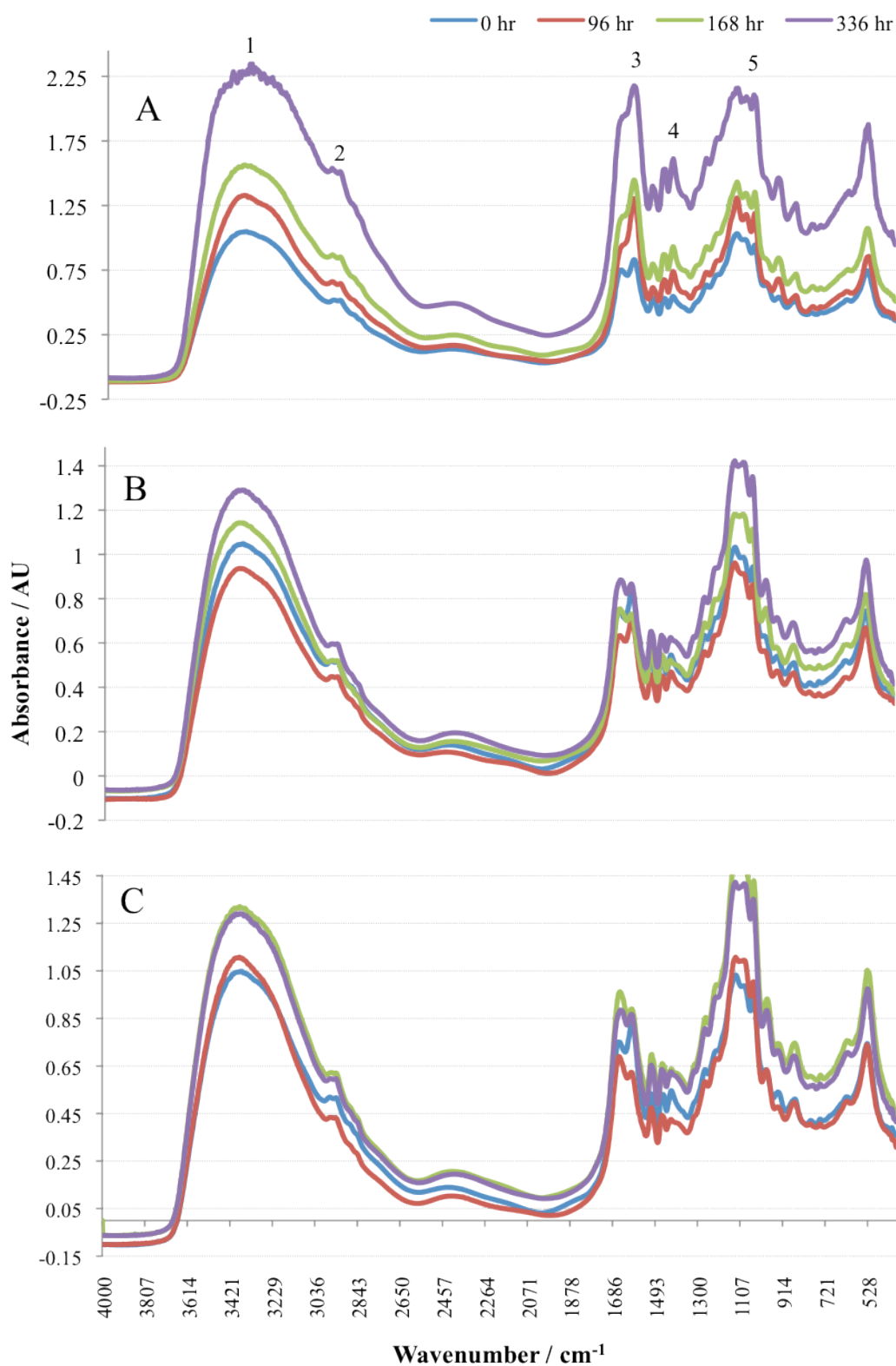


Figure 3.26. FT-IR (ATR) analysis of fractions of *Spingobacterium* sp. (A), *M. phyllosphaerae* (B) and *R. erythropolis* (C) inoculated in M9 salts supplemented with Kraft lignin (2.5 % w/v) and CSL (2 % w/v). Samples taken after 96, 168 and 336 hr were measured along with untreated Kraft lignin in the same medium. Peaks 1 – 5 are tentatively assigned in Table 3.8.

Table 3.8. Tentative assignment of peaks 1 – 5 from the FT–IR (ATR) analysis of treated and untreated Kraft lignin (Fig. 3.27), based on literature assignments [191 – 193]. Numbers in brackets alongside the frequency values indicate the peak number.

Peak	Observed frequency value or range / cm^{-1}	Probable interpretation	Literature range / cm^{-1}
1, 2	3400 – 3352 (1); 2978 – 2941 (2)	O–H stretch (phenolic and aromatic); C–H stretch (aromatic –OMe and side chain –CH ₂ and –CH ₃)	3500 – 2850
3	1657 – 1597	C=O stretch (conjugated <i>p</i> -substituted aryl ketone)	1650 – 1600
4	1462 – 1418	C=C stretch (guaiacyl aromatic ring); C–H bond deformation	1460 – 1400
5	1130 – 1090	Asymmetric C–H deformation in –CH ₂ and –CH ₃ ; aromatic skeletal vibration	1150 – 1100

Since the Kraft lignin was completely dissolved in the growth media the FT–IR analysis contains peaks of a greater intensity than for separate solid and liquid analyses for wheat straw and Organosolv lignin. Although the analysis for Kraft lignin is defined by similar peaks to those features in the analyses for wheat straw and Organosolv lignin (Fig. 3.14, 3.15, 3.21, 3.22), peak 1, which represents phenolics lies from 3400 – 3352 cm^{-1} , which is slightly higher in frequency than the ranges of 3356 – 3238 cm^{-1} and 3375 – 3267 cm^{-1} for wheat straw and Organosolv lignin respectively. A similar trend is seen for peak 2, which also lies at a higher frequency in the FT–IR analysis of Kraft lignin.

Consistent with the FT–IR analysis for treated and untreated wheat straw and Organosolv lignin, a much greater increase in intensity from 0 – 336 hr is observed during treatment with *Sphingobacterium sp.* compared to *R. erythropolis* and *M. phyllosphaerae*, which further suggests that *Sphingobacterium sp.* is the most active of the isolated lignin-degrading bacteria.

3.8. Conclusions

All of the strains grew rapidly in LB broth and in M9 salts supplemented with glucose and yeast extract, with the exception of *M. luteus*, though growth in minimal medium supplemented with Kraft lignin was much slower and more strain-specific. *R. erythropolis* and *Sphingobacterium sp.* seem to grow much more rapidly in media containing Kraft lignin than all of the other isolates, which reach a peak optical density much lower than that observed following incubation in LB broth.

Despite very poor growth in liquid media composed of M9 salts and a lignin-related aromatic compound as the sole carbon source, the strains were also found to grow moderately well on agar plates of the same composition, with most strains being selective for specific substrates. *Sphingobacterium sp.* and *R. erythropolis* were found to grow most readily on lignin-related aromatic compounds, with *Sphingobacterium sp.* found to be selective for the lignin-related aromatic compounds and not cellulose. In contrast, *R. erythropolis* and the *Microbacterium* strains also grew moderately well on cellulose as well as the aromatic compounds.

The isolates were also found to be capable of depolymerizing high- and low-molecular weight forms of Kraft lignin into lower-molecular weight material, and also showed activity towards the breakdown of wheat straw, Organosolv lignin and Kraft lignin into soluble and insoluble phenolic products. A variety of structural changes induced by the treatment of each type of lignin by *Sphingobacterium sp.*, *M. phyllosphaerae* and *R. erythropolis* were monitored by FT-IR, which suggested an increase in the concentration of soluble and insoluble phenolic compounds following treatment of wheat straw, Organosolv

lignin and Kraft lignin, and more specifically a greater rate of production of low-molecular weight soluble phenols than higher-molecular weight insoluble phenols. The observed increase in soluble phenol content is consistent with the molecular hypothesis for the nitrated lignin assays [159], which is based on the production of low-molecular weight, soluble phenolic compounds from the degradation of lignin. The FT-IR analyses of treated and untreated wheat straw, Organosolv lignin and Kraft lignin highlight *Sphingobacterium sp.* to be the most active strain towards lignin degradation due to the relatively high increases in intensity of peaks corresponding to phenolic compounds in comparison to treatment with *R. erythropolis* and *M. phyllosphaerae*. As discussed earlier in this chapter, these observations are largely consistent with the nitrated lignin assay data in Chapter 2. The very high activity of *Sphingobacterium sp.* towards lignin degradation, combined with the degradation of Kraft lignin and low-molecular weight aromatic compounds in a different manner to *R. erythropolis* and *M. phyllosphaerae*, suggests that it may produce different extracellular lignin-degrading enzymes compared to those produced by the mesophilic strains, which highlights the need to purify and identify the lignin-degrading enzymes secreted by these organisms to develop our understanding of the different metabolic pathways via which they may degrade lignin.

Chapter 4: Purification of extracellular lignin-degrading enzymes from *M. phyllosphaerae* and *Sphingobacterium sp.*

4.1. Introduction

The extracellular enzymes secreted by most of the environmental bacteria described in Chapter 2 exhibited activity towards lignin degradation, particularly *Sphingobacterium sp.*, *M. phyllosphaerae* and *R. erythropolis*, which were also found to be capable of breaking down wheat straw, Organosolv lignin and Kraft lignin into soluble and insoluble phenolic products or intermediates, as seen in Chapter 3. Although *Sphingobacterium sp.* seemed to be the most efficient strain, it appeared less able to metabolize the low-molecular weight phenolic products from the depolymerization of lignin. These different observations suggest that there are significant differences between the metabolic capabilities of the extracellular lignin-degrading enzymes secreted by *Sphingobacterium sp.* and those produced by *M. phyllosphaerae* and *R. erythropolis*, therefore it is essential to study the extracellular enzymes from these different strains in order to examine their structure, function and the different pathways via which they degrade lignin. Since bacterial enzymes from *R. jostii* RHA1 have recently been extensively studied (Chapter 1), attempts to purify lignin-degrading enzymes from the secretome of *Sphingobacterium sp.* and *M. phyllosphaerae* were prioritized over *R. erythropolis*, though it would be interesting to study the differences between the lignin-degrading enzymes secreted by *R. erythropolis* and *R. jostii* RHA1 in the future.

The techniques used for protein purification are based on their distinct physiochemical and biological properties such as net charge, hydrophobicity, molecular mass and ligand features.

A three-phase protocol was used, which included anion exchange chromatography as the capture step, hydrophobic interaction chromatography as the intermediate step and gel filtration chromatography as the final step.

After each stage of column chromatography each sample of partially purified enzyme was concentrated via ultrafiltration, the final protein concentration estimated using the Bradford method [194] and lignin-degradation activity monitored in assays involving nitrated lignin [159] and/or ABTS [195]. SDS-PAGE was used to assess the number of different proteins in these fractions, along with their approximate molecular weight. Each gel was stained with Coomassie Brilliant Blue-R250, or silver stain depending on the intensity of protein bands, which correlates with the amount of protein in the sample. In most cases the protein concentration of partially purified enzyme samples was very low, requiring silver staining.

4.2. Purification of extracellular lignin-degrading enzymes from *M. phyllosphaerae*

Liquid cultures of *M. phyllosphaerae* were grown in LB broth for 40 hr at 30 °C and whole cells removed by centrifugation (5,000 rev min⁻¹, 30 min) to give the culture supernatant. The purification of extracellular enzymes from the culture supernatant of *M. phyllosphaerae* was initiated by ammonium sulfate precipitation to 70 % saturation, followed by anion exchange chromatography.

4.2.1. Anion exchange chromatography

Following ammonium sulfate precipitation the enzyme was re-suspended in 20 mM potassium phosphate buffer (pH 7.4), applied to a Q-sepharose anion exchange column and eluted with a NaCl gradient of 0 – 2 M in 20 mM Tris buffer (pH 7.4). The activity of each of the 26 eluted fractions towards lignin degradation in the presence and absence of H₂O₂ was monitored in the nitrated lignin assay, using nitrated MWL (Fig. 4.1).

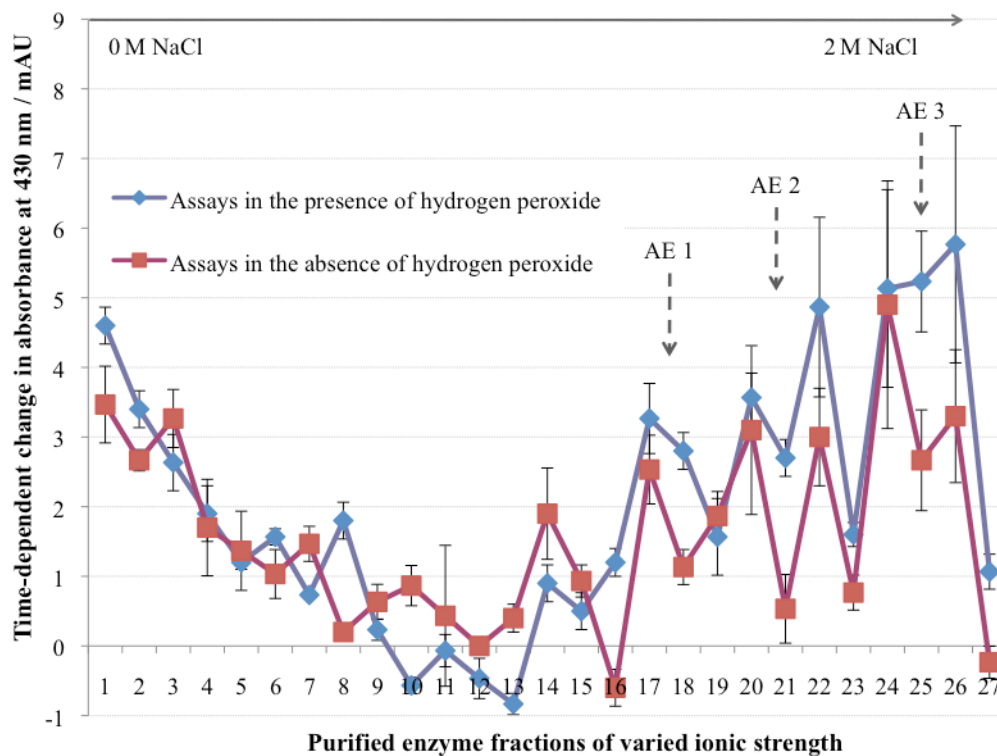


Figure 4.1. Change in absorbance at 430 nm over 20 min following treatment of nitrated MWL with *M. phyllosphaerae* enzyme fractions 1 – 26 eluted from the Q-sepharose anion exchange column, with increasing [NaCl] of the mobile phase from 0 M (fraction 1) to 2 M (fraction 26) in 20 mM Tris buffer (pH 7.4). Fraction 27 is a control experiment in which 20 mM Tris buffer (pH 7.4) was used rather than a sample of enzyme. Samples AE 1 – AE 3 are discussed in the text. Assays were performed in the presence and absence of 2 mM H₂O₂, and carried out in technical triplicate.

The UV/visible nitrated lignin analysis (Fig. 4.1) suggests that activity of the enzymes, purified from *M. phyllosphaerae*, towards lignin degradation increases at higher salt concentrations (fractions 17 – 26) with slightly higher activity in the presence of H₂O₂, indicating that some of the lignin-degrading enzymes have anionic properties and may be H₂O₂-dependent. Fractions of similar ionic strength and enzyme activity were pooled to create three samples of partially purified enzyme: AE 1 (17–18), AE 2 (20–22) and AE 3 (24–26).

Samples AE 1 – 3 were concentrated approximately ten-fold and the final concentration of protein in each sample estimated via the Bradford method [194] to be $0.34 \pm 0.073 \text{ mg ml}^{-1}$, $0.26 \pm 0.094 \text{ mg ml}^{-1}$ and $0.25 \pm 0.114 \text{ mg ml}^{-1}$ for

samples AE 1, AE 2 and AE 3 respectively. Each sample was loaded onto an SDS-PAGE gel and Coomassie Brilliant Blue-R250-staining revealed several bands of low intensity in the region 50–250 kDa (Fig. 4.2), the concentration of proteins in AE 3 being much higher than in AE 1 and AE 2. The most intense band appears to have a molecular weight of 70 kDa and appears to be present in all samples.

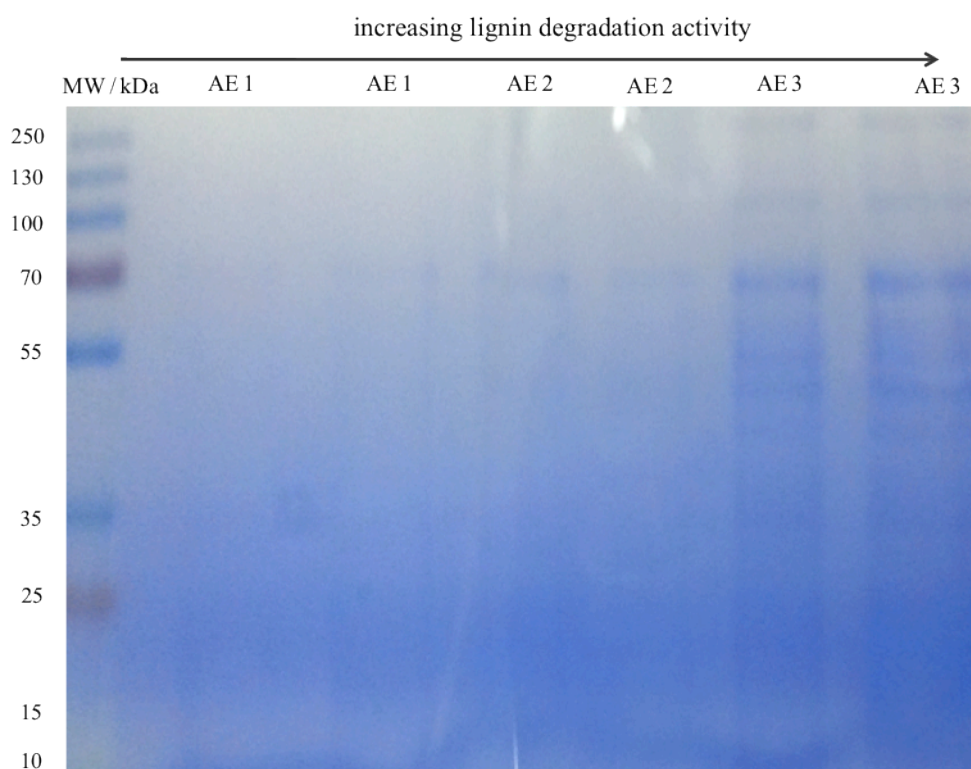


Figure 4.2. Coomassie Brilliant Blue-R250-stained SDS-PAGE gel for AE 1, 2 and 3 from the Q-sepharose anion exchange column.

Since AE 3 appears to contain the enzymes that are most active towards lignin degradation, further purification of these enzymes was attempted by phenyl-sepharose hydrophobic interaction chromatography.

4.2.2. Hydrophobic interaction chromatography

Sample AE 1, composed of high-ionic strength enzyme fractions 24 – 26 from the Q-sepharose anion exchange column, was fractionated by phenyl-sepharose hydrophobic interaction chromatography and divided into 25 fractions of high-medium- and low-hydrophobicity based on their order of elution over a $[(\text{NH}_4)_2\text{SO}_4]$ gradient of 2 – 0 M in 20 mM Tris buffer (pH 7.4). The activity of each fraction was monitored in the UV/visible nitrated lignin assay in the presence and absence of H_2O_2 .

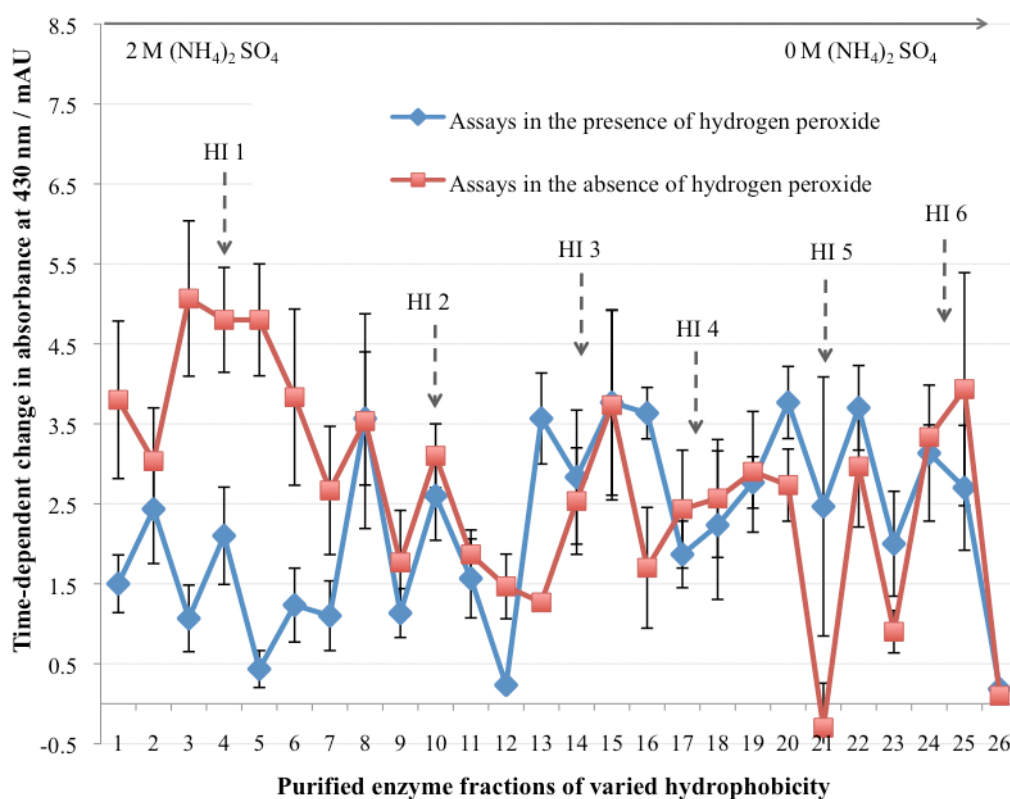


Figure 4.3. Time-dependent change in absorbance at 430 nm for fractionated enzyme samples 1 – 25 from AE 1, with decreasing $[(\text{NH}_4)_2\text{SO}_4]$ from 2 M (fraction 1) to 0 M (fraction 25). Fraction 26 represents a control experiment, which contained 20 mM Tris buffer (pH 7.4) instead of a sample of enzyme. Samples HI 1 – 6 are discussed in the text. Assays were performed in the presence and absence of 2 mM H_2O_2 , and carried out in technical triplicate.

The UV/visible nitrated lignin assay analysis (Fig. 4.3) is defined by several broad peaks in activity at various hydrophobic strengths. The observed increase in absorbance at 430 nm following treatment of nitrated MWL with these fractions generally ranges from 2 – 4 mAU. The fractions were combined on the basis of activity, and five different fraction pools were created, including two pools of negative activity for control purposes: HI 1 (fractions 1 – 8), HI 2 (fractions 9 – 12, negative control), HI 3 (fractions 13 – 16), HI 4 (fractions 17 – 18, negative control), HI 5 (fractions 19 – 22) and HI 6 (fractions 23 – 25). HI 1 appears to be active towards lignin degradation without H₂O₂, suggesting that the activity could be O₂-dependent. HI 2 and HI 4 do not appear to be very active, so were classed as negative controls. HI 3, HI 5 and HI 6 are active with and without H₂O₂, suggesting that activity could be due to a combination of peroxidase and laccase activity. It is interesting that the active enzymes of low hydrophobicity appear to be O₂-dependent, compared to the more hydrophobic enzymes, which exhibit similar activity in the presence and absence of H₂O₂.

Each sample was concentrated to a final volume of 500 – 1000 µl and the final concentration of protein in each sample determined by the Bradford method [194] to be 0.17 ± 0.057 mg ml⁻¹ (HI 1), 0.16 ± 0.050 mg ml⁻¹ (HI 2), 0.12 ± 0.021 mg ml⁻¹ (HI 3), 0.14 ± 0.031 mg ml⁻¹ (HI 4), 0.13 ± 0.026 mg ml⁻¹ (HI 5) and 0.17 ± 0.038 mg ml⁻¹ (HI 6). All samples were loaded onto an SDS-PAGE gel, although no bands were revealed by staining with Coomassie Brilliant Blue R-250. Few bands of very low intensity in each sample were revealed by silver staining. HI 1, HI 3 and HI 5 were analyzed via in-solution tryptic digest and proteins identified by nano LC-ESI-MS/MS.

Table 4.1. Suggested identities of proteins present in purified enzyme samples HI 1, HI 3 and HI 5.

Sample	Protein identity	Parent bacterial strain	MW / kDa
HI 1	Chain E, leech-derived tryptaseinhibitor TRYPSIN COMPLEX		24.14
	Hypothetical protein CHGG_02127	<i>Chaetomium globosum</i> CBS 148.51	24.09
	Predicted protein	<i>Physcomitrella patens</i> <i>subsp.patens</i>	9.69
	Putative transcriptional regulator	<i>Streptomyces albus</i> J1074	40.43
	Transcriptional regulator	<i>Streptosporangium roseum</i> DSM 43021	54.00
HI 3	Hypothetical protein PsyrpaN_02270	<i>Pseudomonas syringae</i> pv. <i>aesculi</i> str. NCPPB 3681	51.14
	Putative polar amino acid ABC transporterpermease	<i>Clavibacter michiganensis</i> <i>subsp. Michiganensis</i> NCPP B382	24.38
	Hybrid polyketide synthase and non ribosomal peptide synthetase	<i>Lysobacter enzymogenes</i>	34.27
	Hypothetical protein Dret_1806	<i>Desulfohalobium retbaense</i> DSM 5692	29.05
HI 5	Sigma S4 interacting domain protein	<i>Hyphomicrobium denitrificans</i> ATCC 51888	125.10
	Hypothetical protein PsyrpaN_02270	<i>Pseudomonas syringae</i> pv. <i>aesculi</i> str. NCPPB 3681	51.14
	Putative polar amino acid ABC transporterpermease	<i>Clavibacter michiganensis</i> <i>subsp. Michiganensis</i> NCPP B382	24.38
	Major outer membrane lipoprotein 1	<i>Pseudomonas oleovorans</i>	8.85
	Outer membrane lipoprotein Opr 1	<i>Azotobacter vinelandii</i> DJ	8.79
	Hybrid polyketide synthase and non ribosomal peptide synthetase	<i>Lysobacter enzymogenes</i>	34.27
	Hypothetical protein Dret_1806	<i>Desulfohalobium retbaense</i> DSM 5692	29.05

Unfortunately, no proteins from *Microbacterium*-related bacteria were identified (Table 4.1). This suggests that the lignin-degrading enzymes present in HI 1, HI 3 and HI 5 were not identified as a result of the very low protein concentration in each sample. In view of the very low protein concentration and the loss of activity vs. time, efforts were focused on thermotolerant strain *Sphingobacterium sp.*

4.3. Purification of extracellular lignin-degrading enzymes from *Sphingobacterium sp.*

Purification of extracellular enzymes from the culture supernatant of *Sphingobacterium sp.* was performed in various stages including ammonium sulfate precipitation, anion exchange chromatography, hydrophobic interaction chromatography and size-exclusion chromatography (Fig. 4.4).

Following the difficulties in the purification of extracellular lignin-degrading enzymes from *M. phyllosphaerae*, the scale of purification of extracellular enzymes from *Sphingobacterium sp.* was increased by preparing 3 litres of liquid culture of *Sphingobacterium sp.* compared to 1.5 litres of *M. phyllosphaerae*.

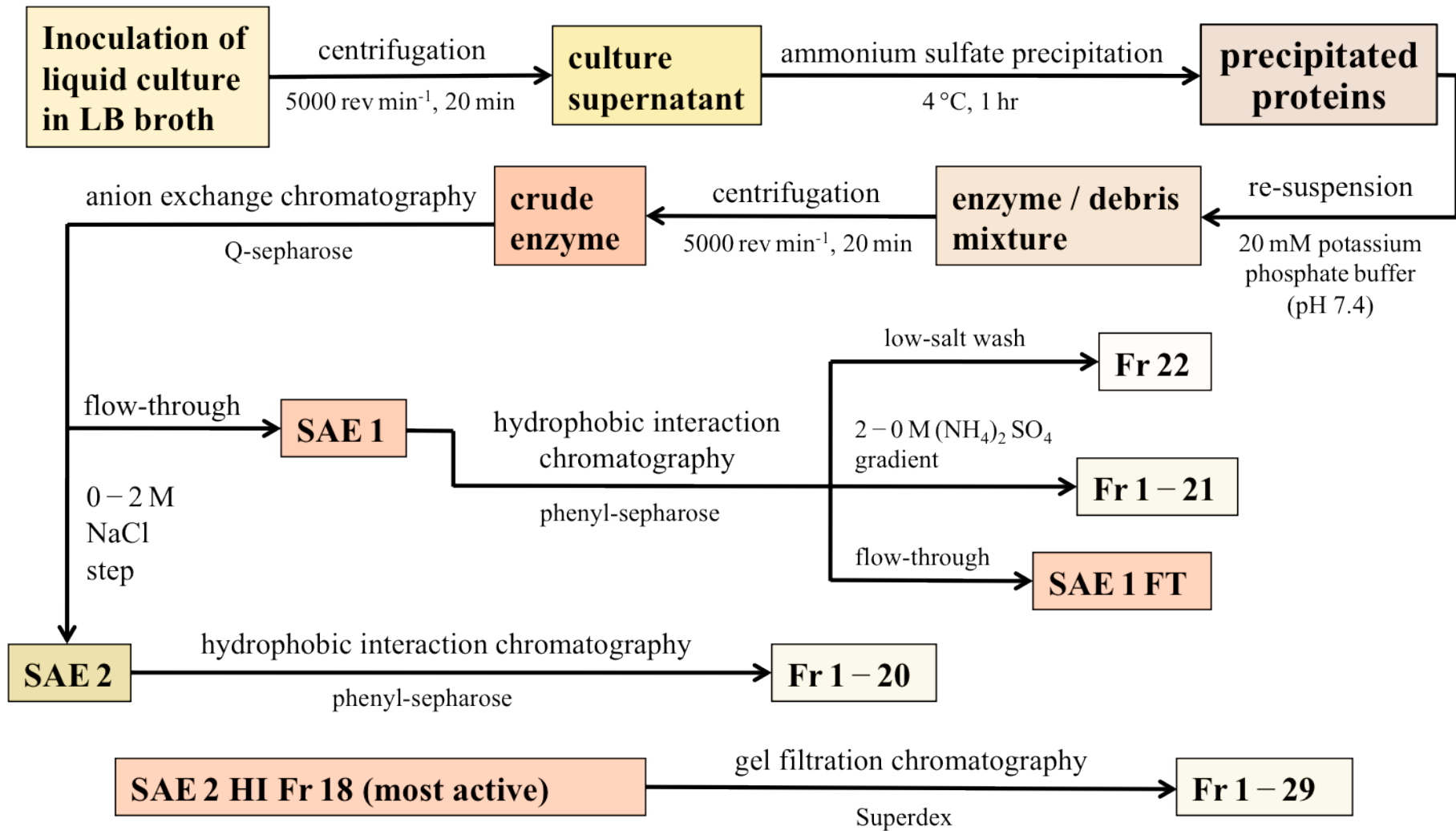


Figure 4.4. Purification of extracellular enzymes from the culture supernatant of *Sphingobacterium sp.* via ammonium sulfate precipitation followed by a series of chromatographic steps. Purified enzyme samples SAE 1 and SAE 2 are discussed in the text.

4.3.1. Anion exchange chromatography

Following ammonium sulfate precipitation to 70 % saturation the enzyme pellets were re-suspended in 20 mM potassium phosphate buffer (pH 7.4) and fractionated by Q-sepharose anion exchange chromatography. Upon loading the re-suspended enzyme onto the anion exchange column and washing with 20 mM Tris buffer (pH 7.4), the majority of the protein did not bind to the Q-sepharose resin and flowed through the column. In contrast, the protein that bound to the column did not elute until the column was washed with 20 mM Tris buffer (pH 7.4) containing 2 M NaCl. These observations suggest that the extracellular enzymes produced by *Sphingobacterium sp.* are either cationic (SAE 1) or strongly anionic (SAE 2). Samples SAE 1, SAE 2 and the crude enzyme were concentrated and the protein concentration estimated via the Bradford method [194] to be 1.64, 0.14 and 0.21 mg ml⁻¹ respectively.

In addition to measuring the activity of samples of partially purified enzyme towards nitrated lignin, an additional assay method was used to examine enzyme activity. This alternative method involves the use of 2,2'-azino-bis (3-ethylbenzothiazoline-6-sulfonic acid) [ABTS], which is commonly used as a substrate with H₂O₂ to study the reaction kinetics of peroxidase enzymes and in the absence of H₂O₂ for laccase enzymes [195]. The parallel use of the two assay methods will ensure detection of lignin-degradation activity in enzyme samples with maximum sensitivity.

The activity of SAE 1 and SAE 2 was monitored using the ABTS and UV/visible nitrated lignin assay methods. All assays were carried out in the presence of, and in the absence of H_2O_2 and two different types of chemically nitrated lignin were used in the nitrated lignin assays: nitrated Organosolv lignin and nitrated MWL.

Since the concentrations of protein in the crude enzyme, SAE 1 and SAE 2 were very different, it was essential to monitor enzyme activity in relation to the concentration of protein in each enzyme sample, hence the time-dependent increases in absorbance observed in the nitrated lignin and ABTS assays were converted into total activity (in units) and specific activity (in units mg^{-1}). Since the time-dependent absorbance increases were typically in the range of milli absorbance units, one unit of activity was defined as an increase of one milli absorbance unit per minute, and the specific activity of each sample defined as the number of units of activity per milligram of protein.

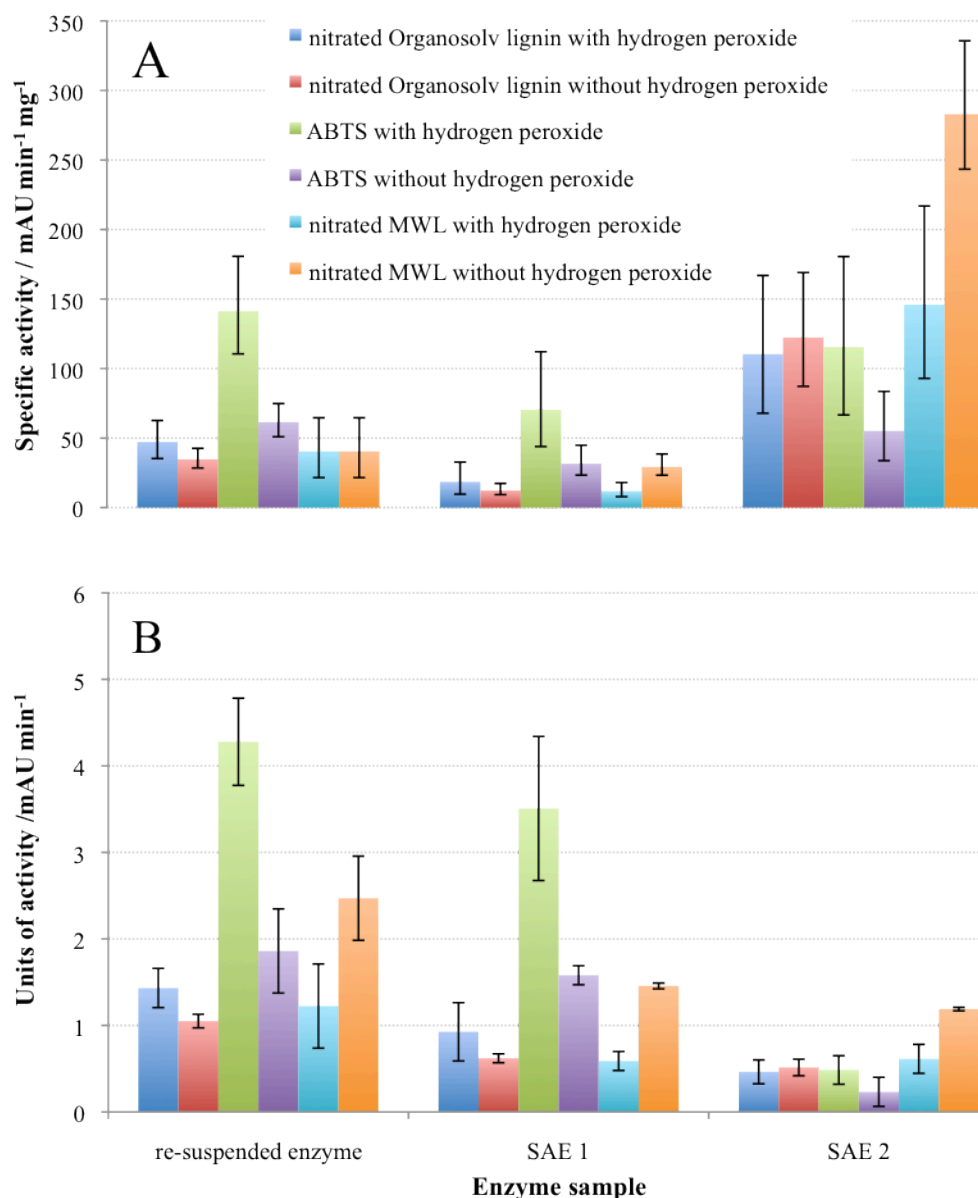


Figure 4.5. Specific activity (A) and units of activity (B) of the re-suspended enzyme sample, following ammonium sulfate precipitation, and purified enzyme samples SAE 1 and SAE 2 towards nitrated Organosolv lignin, nitrated MWL and ABTS in the presence of, and in the absence of 2 mM H₂O₂. Assays were performed in technical triplicate. The data for each sample are discussed in the text.

Although the number of units of activity exhibited by SAE 1 were up to seven-fold higher than SAE 2 in the ABTS assays and up to two-fold higher in the nitrated lignin assays (Fig. 4.5), SAE 2 exhibited a much higher specific activity than SAE 1 in all assays, particularly in the nitrated MWL assays, which show the specific activity of SAE 2 to be approximately ten-fold higher than SAE 1 in

the presence and absence of H₂O₂. The greater specific activity for SAE 2 compared to SAE 1 suggests that some of the most active lignin-degrading enzymes secreted by *Sphingobacterium sp.* are strongly anionic. Almost all of the enzyme assays show the specific activity of SAE 2 to be significantly higher than the crude enzyme, indicating 2 – 5-fold purification, whereas SAE 1 shows no significant increase in specific activity.

Attempts were then made to further purify SAE 1 and SAE 2 via hydrophobic interaction chromatography.

4.3.2. Hydrophobic Interaction chromatography of SAE 1

Enzyme sample SAE 1 was applied to a phenyl-sepharose hydrophobic interaction column and eluted with a [(NH₄)₂SO₄] gradient of 2 – 0 M in 20 mM Tris buffer (pH 7.4). Each of the 25 eluted enzyme fractions were desalted and then concentrated approximately ten-fold to a final volume of 500 – 1000 µl and the final concentrations of protein in each fraction, estimated via the Bradford method [194], were in the range 0.1 – 0.4 mg ml⁻¹. The change in absorbance at 430 nm over 20 min following reaction of each enzyme fraction with nitrated MWL, nitrated Organolsolv lignin and ABTS was monitored in the presence and absence of H₂O₂ and then converted into specific activity using the estimated concentration of protein in each sample.

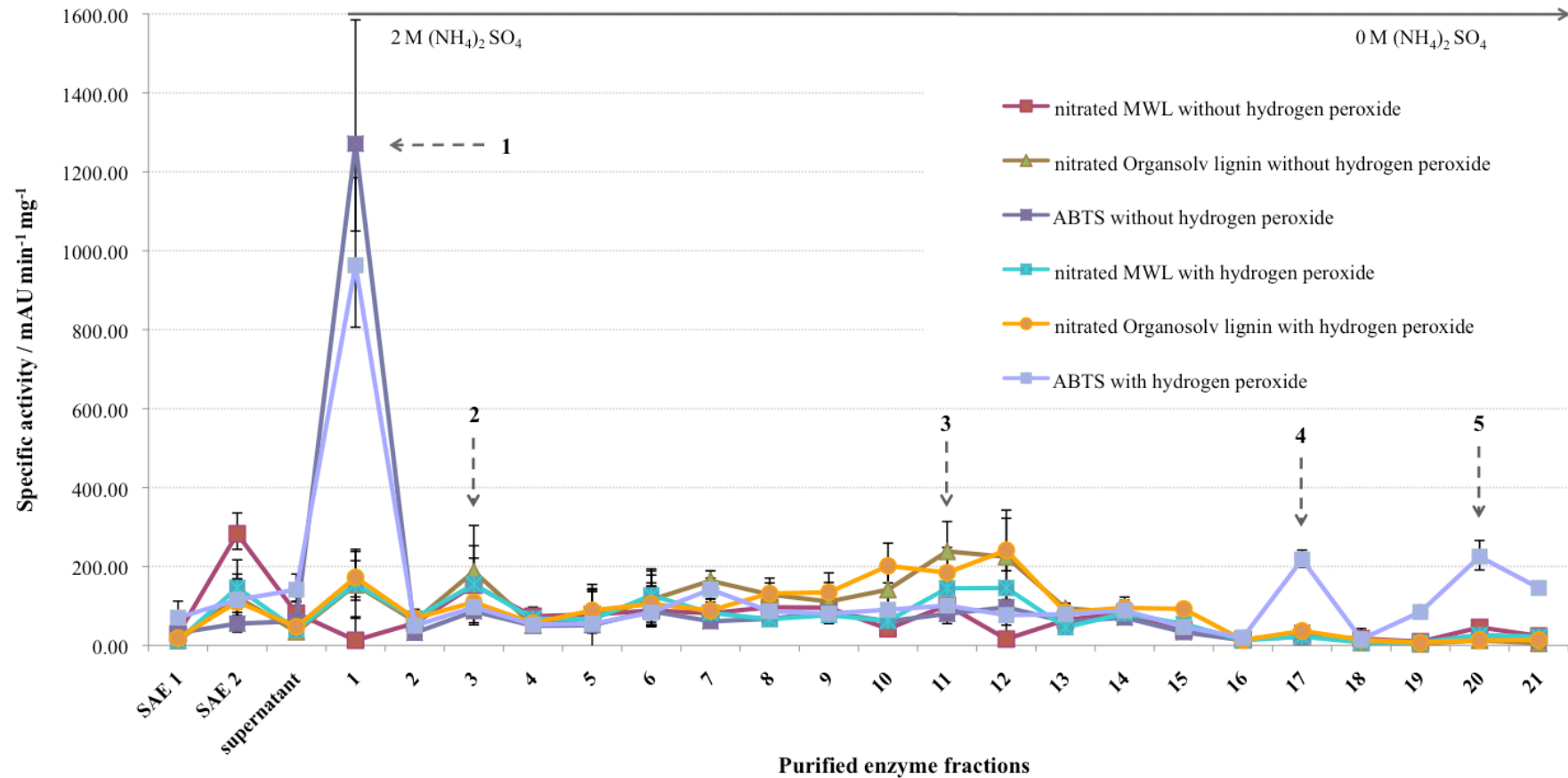


Figure 4.6. Specific activity of the unpurified extracellular enzymes from *Spingobacterium sp.*, SAE 1, SAE 2 and fractionated enzyme samples from SAE 1 of differing hydrophobic strength. Fractions 1–21 were eluted over a $[(\text{NH}_4)_2\text{SO}_4]$ gradient of 2 M (Fr 1) to 0 M (Fr 21). A peak in activity is generally defined as any sample (s) of purified enzyme that exhibit a specific activity of at least 200 units mg^{-1} in one or more assays. Peaks 1 (Fr 1), 2 (Fr 3), 3 (Fr 10–12), 4 (Fr 17), 5 (Fr 20) are discussed in the text. Assays were performed in the presence and absence of 2 mM H_2O_2 , and carried out in technical triplicate.

The ABTS and nitrated lignin analyses (Fig. 4.6) are defined by several peaks, which correspond to various proteins possessing surface residues of varying hydrophobic strength. Approximately 5 peaks in activity are apparent: peak 1 (Fr 1), peak 2 (Fr 3), peak 3 (Fr 10–12), peak 4 (Fr 17) and peak 5 (Fr 20). Peak 1, corresponding to enzymes of low hydrophobic strength, is distinctly the most active under all assay conditions, reaching a specific activity of $1280 \text{ units mg}^{-1}$ in the ABTS assay without H_2O_2 , which is approximately thirty-fold higher than that of SAE 1. The slightly higher specific activity of $1280 \text{ units mg}^{-1}$ in the absence of H_2O_2 compared to $960 \text{ units mg}^{-1}$ with H_2O_2 suggests that enzyme activity is inhibited rather than induced by H_2O_2 . It is interesting that the specific activity of fraction 1 towards ABTS is much greater than that shown towards nitrated Organosolv lignin, which in turn is greater than its activity towards nitrated MWL as a substrate.

Unlike fraction 1, which is approximately ten-fold more active towards ABTS than nitrated lignin, the specific activity of fractions 3 (peak 2) and 10–12 (peak 3) towards nitrated lignin is approximately double the activity towards ABTS. Fractions 10–12 appear to be more active towards Organosolv lignin than MWL and no peak in activity is observed following reaction of these fractions with ABTS. The reverse pattern is observed for fractions 17 and 20, which exhibit a specific activity of $200 \text{ units mg}^{-1}$ towards ABTS in the presence of H_2O_2 compared to a maximum of 50 units mg^{-1} towards nitrated MWL in the absence of H_2O_2 . The observations in Fig. 4.6 highlight the importance of the parallel use of the different assay methods to detect different patterns of lignin-degradation activity: fraction 1 (low hydrophobic strength) and relatively hydrophobic enzymes in fractions 17 and 18 are detected with far greater

sensitivity in the assays involving ABTS compared to those involving nitrated lignin. The reverse is true for fractions 10–12 of medium hydrophobic strength.

Following concentration and desalting of Fr 1 – 21, each fraction was loaded onto an SDS–PAGE gel along with the unpurified supernatant, SAE 1 and SAE 2. Staining with Coomassie Brilliant Blue–R250 revealed several bands corresponding to numerous proteins in each sample. Although no bands were observed in fractions 4 – 9, several bands of low to medium intensity were observed in Fr 1 – 3 and 10 – 12 (Fig. 4.7) and bands of low to high intensity observed in Fr 15 – 21 (Fig. 4.8).

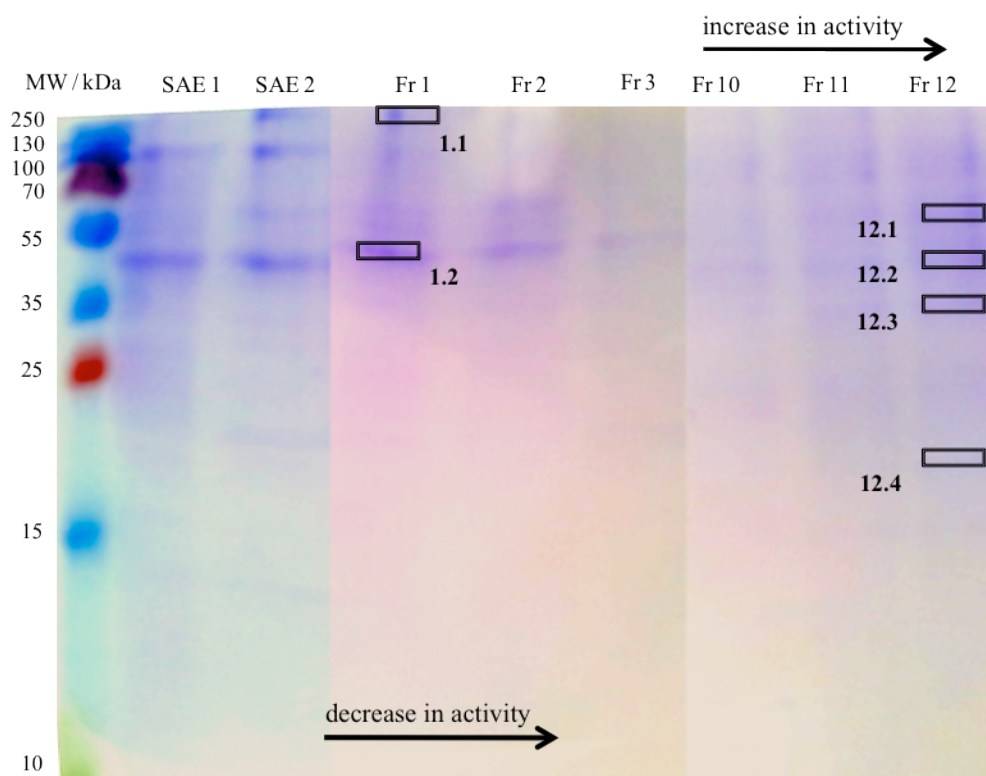


Figure 4.7. Coomassie Brilliant Blue–R250 stained SDS–PAGE loaded with SAE 1, SAE 2 and Fr 1 – 3 and 10 – 12 from hydrophobic interaction chromatography of SAE 1. Bands 1.1, 1.2, 12.1, 12.2, 12.3 and 12.4 are discussed in the text.

The presence of a reduced number of bands of relatively low intensity in SAE 1 and SAE 2 compared to the supernatant suggests that anion exchange chromatography had been an effective technique for the purification of extracellular lignin-degrading enzymes from *Sphingobacterium sp.* The SDS-PAGE analysis for fraction 1, the most active sample towards nitrated lignin and ABTS (Fig. 4.6) is defined by two bands of approximate molecular weights of 200 kDa (band 1.1) and 45 kDa (band 1.2).

Fraction 12, which exhibits the greatest activity of the fractions in peak 3, appears to contain several proteins at low concentration and the slightly higher intensity of bands 12.1 and 12.2 in this sample compared to fractions 10 and 11 correlates with a marginal increase in specific activity of 240 units mg^{-1} towards nitrated Organosolv lignin in the presence of H_2O_2 , compared to 200 and 190 units mg^{-1} for fractions 10 and 11 respectively.

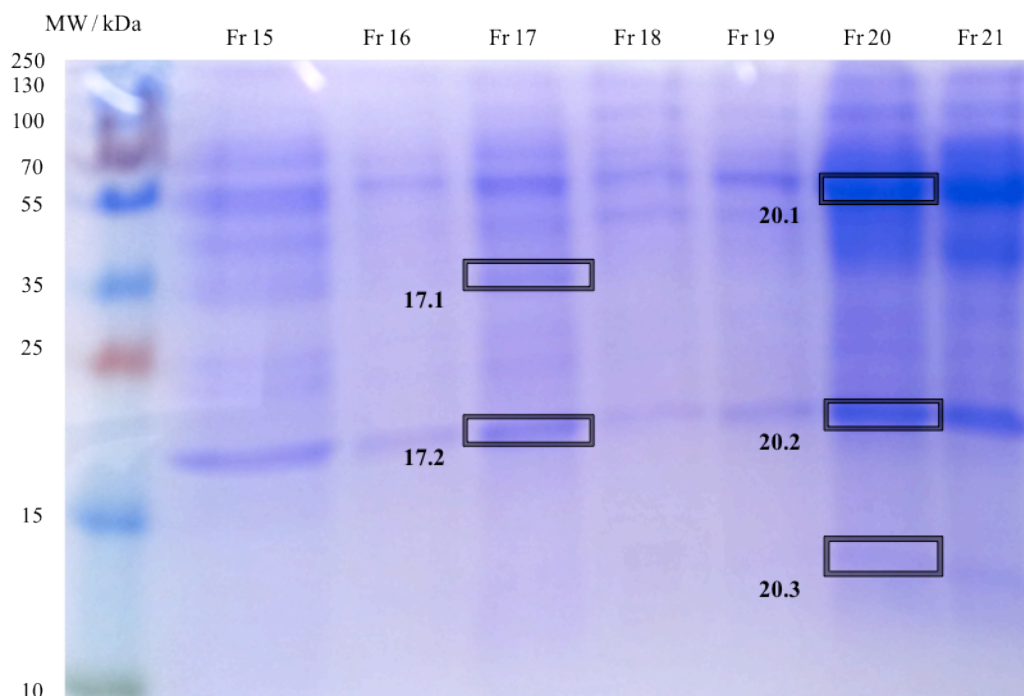


Figure 4.8. Coomassie Brilliant Blue-R250-stained SDS-PAGE gel loaded with fractions 15–22 purified from SAE 1 via hydrophobic interaction chromatography. Bands 17.1, 17.2, 20.1, 20.2 and 20.3 are discussed in the text.

Several bands are present in fractions 15 – 21, corresponding to a variety of proteins in the molecular weight range 13 – 250 kDa. The most active fractions in the assays (Fig. 4.6) are fractions 17, 20 and 21, which range from 150 – 200 mAU min⁻¹ mg⁻¹ in specific activity towards ABTS in the presence of H₂O₂. In comparison, fractions 15 and 19 exhibit approximately 80 and 100 mAU min⁻¹ mg⁻¹ towards nitrated Organosolv lignin and ABTS respectively, also in the presence of H₂O₂. Fractions 16 and 18 do not appear to be active towards any of the substrates.

Fractions 20 and 21 appear to contain a low-molecular weight protein of approximately 30 kDa (band 20.3), which is not visible in fractions 18 and 19 of lower activity although the concentration of protein in these samples of 0.10 and 0.17 mg ml⁻¹, respectively, is low compared to fraction 20, which contains 0.29 mg ml⁻¹ protein. Bands 20.1 and 20.2 in fraction 20 are of particular interest due to their reduced intensity in fraction 21, which is less active towards ABTS and has a higher protein concentration of 0.36 mg ml⁻¹.

Protein identification: Samples 1, 12, 17 and 20 were submitted for tryptic digest of the gel bands and nano LC–ESI–MS/MS. The observed molecular ion data for tryptic digests were compared with protein databases, and a number of matches were found with proteins ranging from 18 – 75 kDa in molecular weight (Table 4.2). The range of proteins identified include enolase, aldehyde dehydrogenase, two forms of superoxide dismutase and phosphoenolpyruvate carboxykinase, most of which are produced by *Sphingobacterium* or related strains. With the exception of the TonB-dependent receptor plug, the molecular

weights of the proteins identified generally match those observed on the in the SDS-PAGE analysis (Fig. 4.7, 4.8).

Table 4.2. Identity and predicted molecular weight of proteins from purified enzyme fractions 1, 12, 17 and 20, and the approximate molecular weight of the Coomassie Brilliant Blue–R250-stained SDS–PAGE bands from which they were identified.

Band ID	Protein name	Parent strain	Predicted MW / kDa	MW on gel / kDa
1.1	TonB-dependent receptor plug	<i>Leadbetterella byssophila</i> DSM 17132	24.93	130–250
1.2	Enolase	<i>Sphingobacterium spiritivorum</i> ATCC 33300	46.6	45
12.1	Putative uncharacterized protein	<i>Bacteroides</i> sp. D20	56.03	55
12.2	Possible M20/M25/M40 family peptidase	<i>Sphingobacterium spiritivorum</i> ATCC 33861	50.63	50
12.3	Aldehyde dehydrogenase (NAD ⁺)	<i>Sphingobacterium spiritivorum</i> ATCC 33861	38.66	35
12.4	Superoxide dismutase	<i>Sphingobacterium spiritivorum</i> ATCC 33861	22.28	20
17.1	Putative uncharacterized protein	<i>Sphingobacterium spiritivorum</i> ATCC 33861	61.99	60
17.2	Putative uncharacterized protein (Precursor)	<i>Sphingobacterium</i> sp. (strain 21)	22.35	18
20.1	Pyruvate dehydrogenase complex dihydrolipoamide acetyltransferase	<i>Sphingobacterium spiritivorum</i> ATCC 33861	57.06	58
20.2	Superoxide dismutase	<i>Chryseobacterium gleum</i> ATCC 35910	25.25	21
20.3	Phosphoenolpyruvate carboxykinase [ATP]	<i>Pedobacter heparinus</i> ATCC 13125	18.75	13

Following the observation of very high specific activity of fraction 1 towards ABTS in the presence and absence of H₂O₂ (Fig. 4.6), and lack of identified proteins of interest from bands 1.1 and 1.2 (Table 4.2), further identification of the proteins present in these samples was performed by solution-based tryptic digest and several additional proteins were identified (see Table 4.3).

Table 4.3. Identity and predicted molecular weight of the different proteins present in fraction 1, a low-hydrophobic strength enzyme sample purified from SAE 1 via hydrophobic interaction chromatography.

Identity of protein	Parent bacterial strain	Predicted MW / kDa
superoxide dismutase, manganese	<i>Sphingobacterium spiritivorum</i> ATCC33300	22.22
OmpA/MotB family protein	<i>Sphingobacterium spiritivorum</i> ATCC33300	49.65
Thrombospondin type 3 repeat-containing protein	<i>Pedobacter saltans</i> DSM 12145	32.00
superoxide dismutase	<i>Sulfurospirillum barnesii</i> SES-3	25.93
outer membrane lipoprotein OprI	<i>Azotobacter vinelandii</i> DJ	8.79

Additional proteins identified in fraction 1 include a further two forms of superoxide dismutase, the molecular weights of which lie in the range 22 – 26 kDa, which is also true for the superoxide dismutases identified in fractions 12 and 20 (see Table 4.2).

4.3.3. Hydrophobic Interaction chromatography of SAE 2

SAE 2 was also fractionated via phenyl-sepharose hydrophobic interaction chromatography using the same procedure as for SAE 1, with the collection of 21 fractions over a 2 – 0 M $[(\text{NH}_4)_2\text{SO}_4]$ gradient. The final concentration of each fraction after concentration and desalting was estimated via the Bradford method [194] to be in the range 0.03 – 0.20 mg ml⁻¹.

The activity of each fraction towards ABTS and nitrated MWL was monitored and the analysis (Fig. 4.9) is defined by seven peaks in activity towards ABTS and/or nitrated MWL. Peaks 1, 6 and 7 exhibit significantly higher activity towards ABTS whilst peaks 2, 3 and 4 show similar activity towards ABTS and nitrated MWL. The only peak exhibiting greater activity towards nitrated MWL than ABTS is peak 5, which exhibits a specific activity of 261 mAU min⁻¹ mg⁻¹ towards nitrated MWL compared to 160 mAU min⁻¹ mg⁻¹ towards ABTS in the presence of H₂O₂. It is interesting that, with the exception of fraction 10, the activity of all fractions is optimal in the presence of H₂O₂ since although the specific activity of SAE 2 towards ABTS was doubled in the presence of H₂O₂, activity of the same sample towards nitrated MWL was doubled in the absence of H₂O₂.

Peak 6, corresponding to proteins of high hydrophobic strength, is 2 – 3-fold more active towards ABTS than the other peaks, exhibiting a specific activity of 858 mAU min⁻¹ mg⁻¹ in the presence of H₂O₂. This compares to a lower value of 150 mAU min⁻¹ mg⁻¹ in the absence of H₂O₂, suggesting that enzymes present in this sample (e.g. lignin peroxidases) are strongly dependent on H₂O₂ to effectively degrade lignin. Similar patterns in activity are observed for peak 7,

though its maximum specific activity towards ABTS in the presence of H₂O₂ is significantly lower at 398 mAU min⁻¹ mg⁻¹.

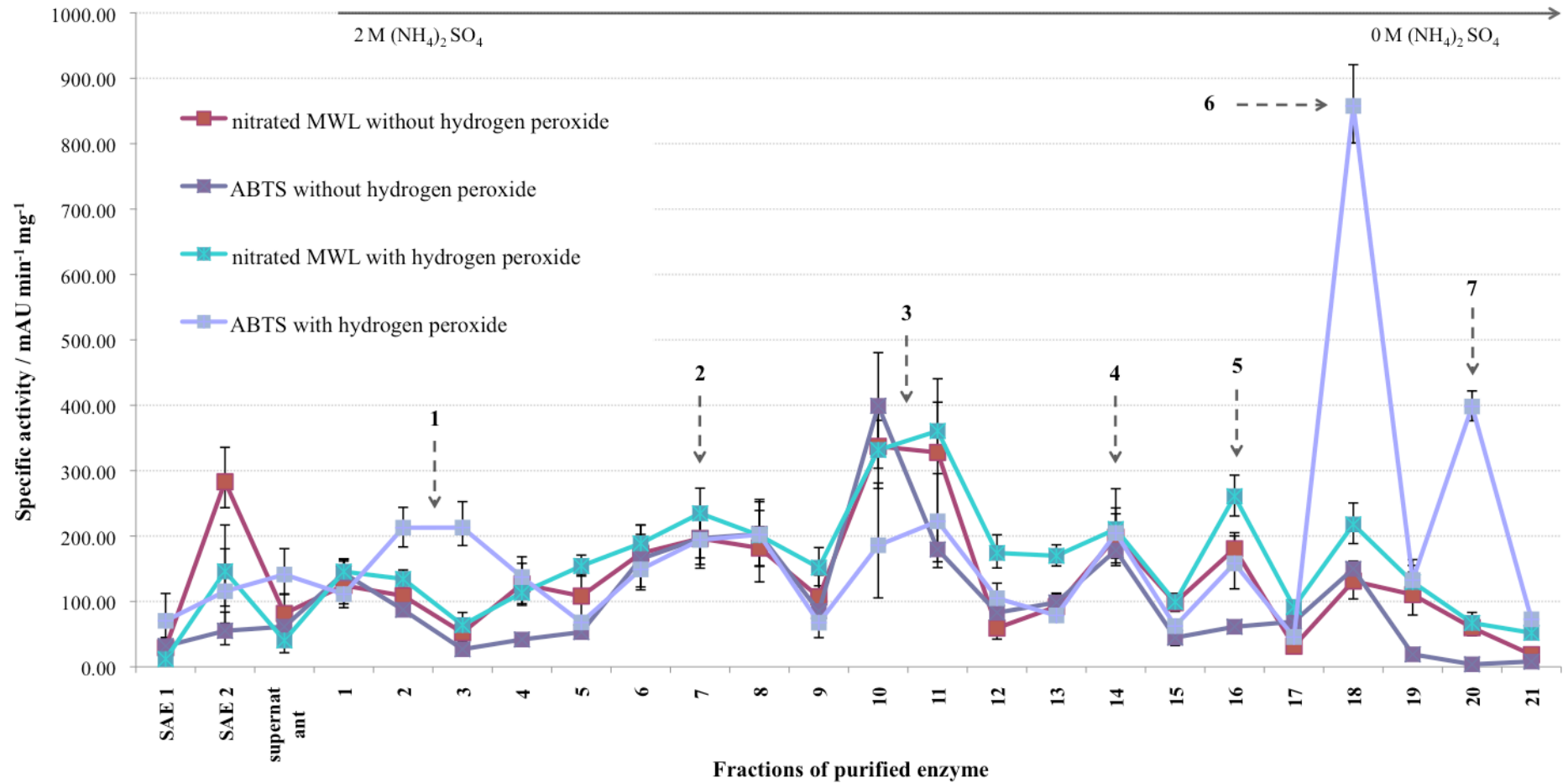


Figure 4.9. Specific activity of the un-purified extracellular enzymes from *Spingobacterium sp.*, SAE 1, SAE 2 and fractionated enzyme samples from SAE 2 of differing hydrophobic strength. Fractions 1–21 were eluted over a [(NH₄)₂SO₄] gradient of 2 M (Fr 1) to 0 M (Fr 21). A peak in activity is generally defined as any sample(s) of purified enzyme that exhibit a specific activity of at least 200 units mg⁻¹ in one or more assays. Assays were performed in the presence and absence of 2 mM H₂O₂, and carried out in technical triplicate. Peaks 1 (Fr 2, 3), 2 (Fr 6–8), 3 (Fr 10, 11), 4 (Fr 14), 5 (Fr 16), 6 (Fr 18) and 7 (Fr 20) are discussed in the text.

4.3.3.1. Purification of SAE 2 fraction 18 via gel filtration FPLC

Fraction 18, which appears to be the most active sample of purified enzyme from SAE 2 towards ABTS (Fig. 4.9) was purified further by gel filtration FPLC, using a Superdex 200 column.

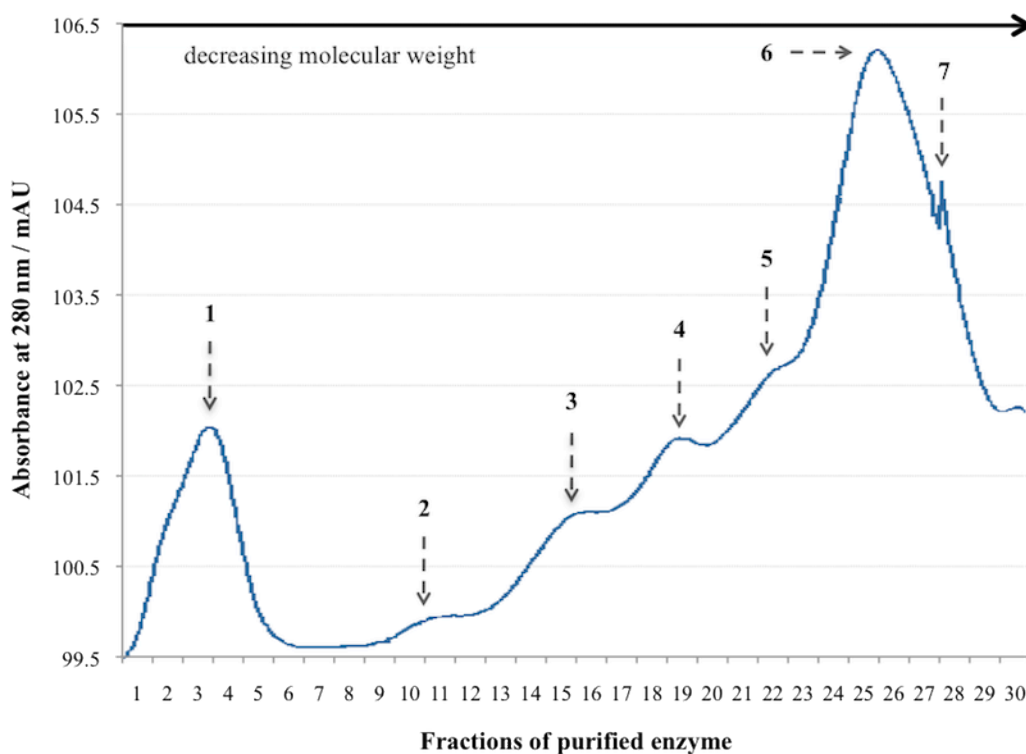


Figure 4.10. Absorbance of fractions 1 – 29 at 280 nm, purified from SAE 2 fraction 18 via gel filtration FPLC, using a Superdex 200 column. Absorbance peaks 1 – 7, which correspond to proteins of different molecular weight, are discussed in the text.

The variation in absorbance of fractions 1 – 29 suggests that several different enzymes exist at different concentrations in SAE 2 fraction 18. The gel filtration FPLC analysis (Fig. 4.10) is defined by the presence of six peaks in absorbance at 280 nm, indicating a similar number of different enzymes: peak 1 (Fr 2 – 4), peak 2 (Fr 10, 11), peak 3 (Fr 15, 16), peak 4 (Fr 19), peak 5 (Fr 23) and peak 6 (Fr 25, 26) and peak 7 (Fr 28).

Due to the very low volume of each sample following concentration and de-salting, there was insufficient substrate for estimation of protein concentration via the Bradford method and for evaluation of activity towards ABTS and nitrated lignin. Since fraction 18, purified from SAE 2, exhibited a much higher activity towards ABTS than nitrated lignin enzyme activity was evaluated by monitoring the time-dependent change in absorbance at 430 nm following the reaction of each enzyme fraction with ABTS rather than nitrated lignin solution.

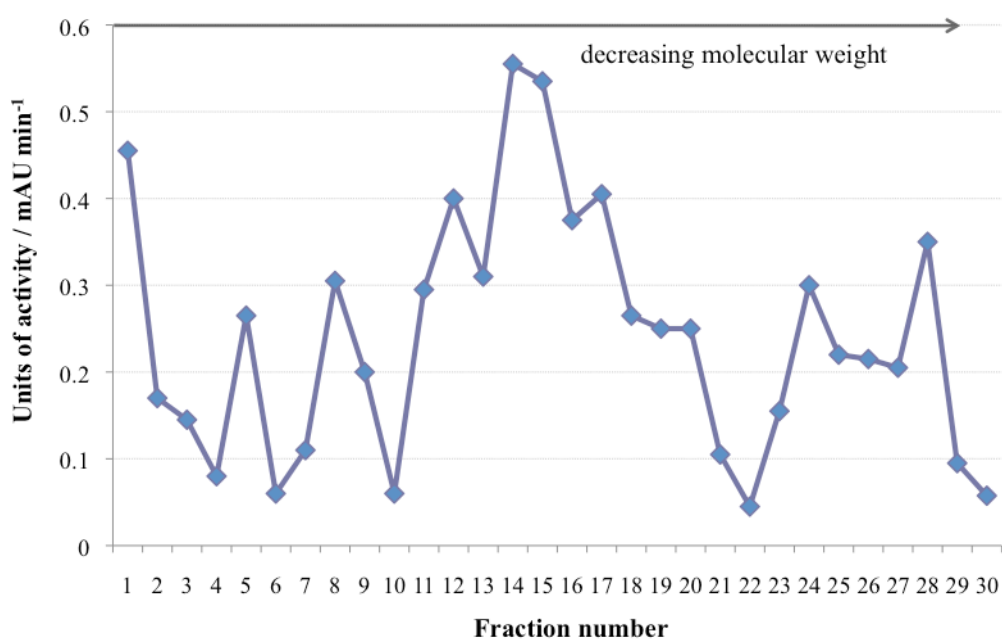


Figure 4.11. Change in absorbance at 430 nm over 20 min for purified enzyme fractions 1 – 29 (45 % v/v) in the presence of ABTS (50 % v/v) and 2 mM H₂O₂ (5 % v/v). Activity peaks 1 (Fr 1), 2 (Fr 5), 3 (Fr 8), 4 (Fr 11), 5 (Fr 14, 15), 6 (Fr 16, 17), 7 (Fr 18–20), 8 (Fr 24) and 9 (Fr 28) are discussed in the text. Fraction 30 is a control, containing 20 mM Tris buffer (pH 7.4) rather than a sample of enzyme.

Since there were insufficient volumes of each sample available to carry out the assays in duplicate, the level of accuracy of the ABTS assay data (Fig. 4.11) is relatively low, although the highest activity matches fractions 14 and 15.

On the basis of molecular weight and activity towards ABTS, fractions of similar properties were pooled to create 14 different samples: 1 (Fr 1), 2 (Fr 2–

4), 3 (Fr 5), 4 (Fr 11), 5 (Fr 12), 6 (Fr 13), 7 (Fr 14, 15), 8 (Fr 16, 17), 9 (Fr 18–20), 10 (Fr 22), 11 (Fr 24), 12 (Fr 25–27), 13 (Fr 28) and 14 (Fr 29). With the exception of sample 1, which was less than 5 μ l in volume, each sample was concentrated to a final volume of 50–100 μ l.

Following concentration, samples 2 – 14 were analyzed by SDS–PAGE and the gels stained with Coomassie Brilliant Blue–R250. Since no bands were visible in any of the samples, the gel was silver-stained and faint bands were revealed in sample 6 (Fig. 4.12), and several bands to low to moderate intensity in samples 9, 11, 12, 13 and 14 (Fig. 4.13).

Several proteins appear to be present in sample 6, the most dominant being ~ 30 kDa in molecular weight. Other proteins present in lower concentrations are indicated by the faint bands around 15 kDa and in the range 40 – 130 kDa. Proteins of similar molecular weight appear to be present in sample 5, indicated by the bands at 30 and 45 kDa.

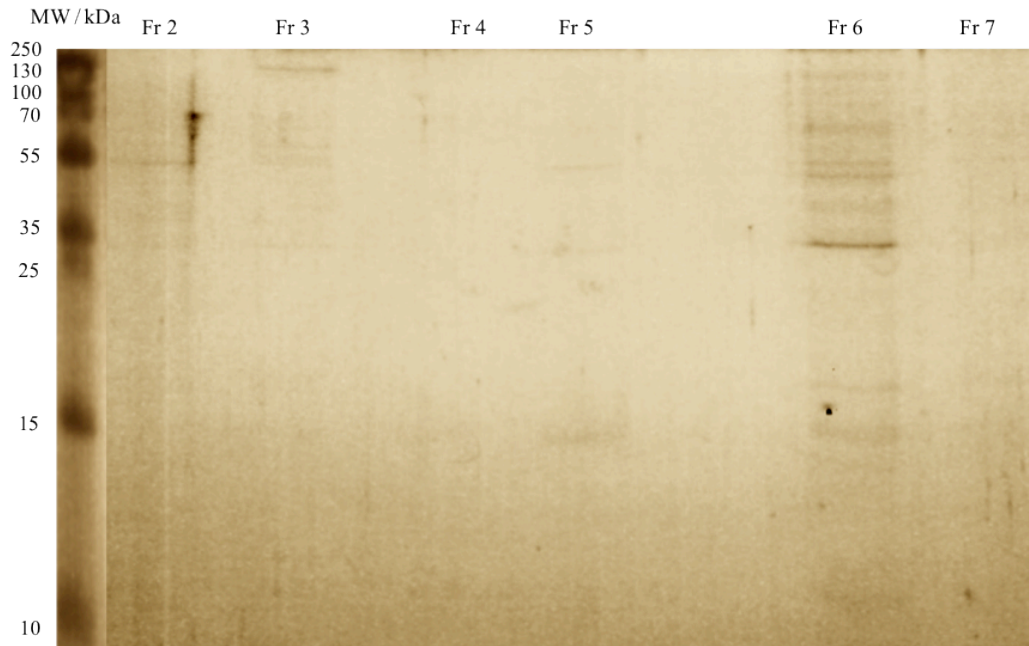


Figure 4.12. Silver-stained SDS-PAGE gel loaded with enzyme samples 2 – 7, purified from SAE 2 Fr 18 via gel filtration FPLC.

Unfortunately, few bands of very low intensity were visible in sample 7 (Fr 14, 15), which exhibited the greatest activity towards ABTS (Fig. 4.12). Identification of the protein corresponding to the most intense band in sample 6 (30 kDa) was attempted via tryptic digest, though no results were obtained due to the very low concentration of protein.

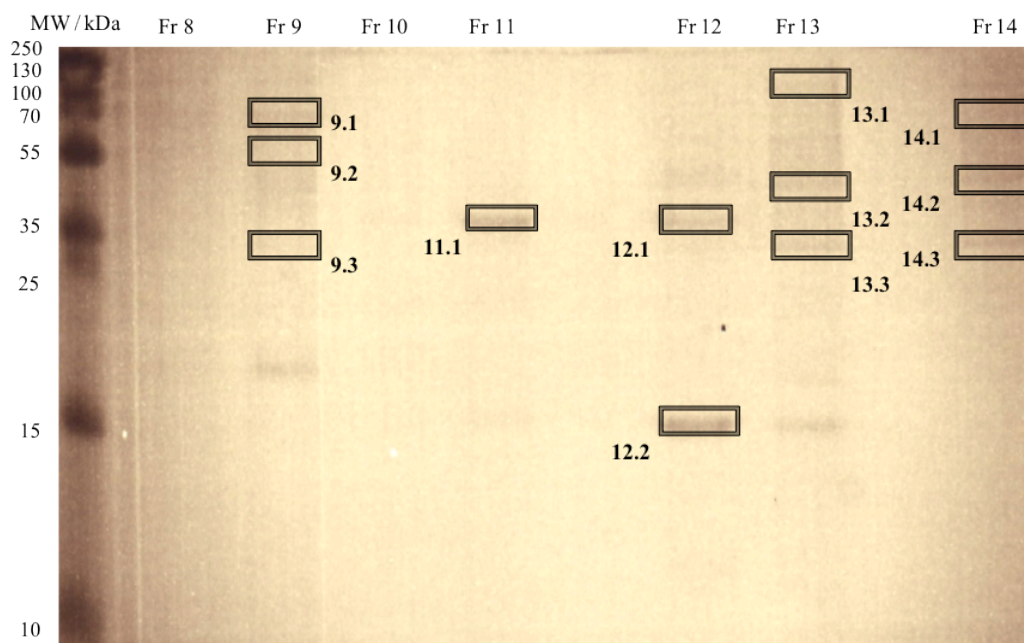


Figure 4.13. Coomassie Brilliant Blue–R250-stained SDS–PAGE gel loaded with enzyme samples 8 – 14, purified from SAE 2 Fr 18 via gel filtration FPLC. Bands 9.1 – 14.3 are discussed in the text.

Coomassie Brilliant Blue–R250-staining revealed the presence of several different proteins in samples 9, 11, 12, 13 and 14 (Fig. 4.13), indicating a much higher concentration of protein in these samples. The ABTS analysis for samples 8 – 14 (Fig. 4.12) suggests that samples 8, 11 and 14 are the most active in this group, exhibiting time-dependent absorbance increases in the range 0.3 – 0.4 mAU. Although no bands were visible in sample 8, a single band of moderate intensity was observed in sample 11, corresponding to a protein of ~ 35 kDa molecular weight. In contrast, 3 – 4 very faint bands were visible in the SDS–PAGE analysis of sample 14, indicating the presence of proteins in the molecular weight range of 25 – 100 kDa. Since the reliability of the assay data is limited by the lack of repeat experiments, bands of sufficient intensity from all samples were used for protein identification.

Identification of the proteins present in samples 9, 11, 12, 13 and 14 via tryptic digest and nano LC–ESI–MS/MS revealed a variety of proteins ranging from 14–73 kDa in molecular weight (Table 4.4).

Table 4.4. Identity and predicted molecular weight of proteins identified in enzyme fractions 9, 11, 12, 13 and 14, purified from SAE 2 fraction 18 via gel filtration chromatography. Samples 9.4 and 13.1 contained keratin, and identical peptides were observed in 14.3 and 14.4, therefore they were not considered.

Band ID	Protein name	Parent strain	Predicted MW / kDa	MW on gel / kDa
9.1	Unnamed protein product	<i>Leadbetterella byssophila</i> DSM 17132	24.93	68
9.2	TPR (tetratricopeptide) repeat-containing protein	<i>Sphingobacterium spiritivorum</i> ATCC 33300	63.80	63
9.3	C56 family peptidase	<i>Sphingobacterium spiritivorum</i> ATCC 33300	20.96	45
11.1	DNA polymerase III beta chain	<i>Sphingobacterium spiritivorum</i> ATCC 33861	41.41	38
12.1	Tetratricopeptide repeat family protein	<i>Sphingobacterium spiritivorum</i> ATCC 33861	43.26	38
12.2	Putative uncharacterized protein (Precursor)	<i>Leadbetterella byssophila</i> DSM 17132	14.57	15
13.2	OmpA/MotB family protein	<i>Sphingobacterium spiritivorum</i> ATCC 33300	52.86	45
13.3	Oligoendopeptidase F	<i>Uncultured bacterium</i> 66 PE=4 SV=1	57.08	25
14.1	Glucosamine-6-phosphate deaminase family protein	<i>Sphingobacterium spiritivorum</i> ATCC 33861	72.82	70
14.2	Gfo/Idh/MocA family oxidoreductase	<i>Sphingobacterium spiritivorum</i> ATCC 33861	42.87	48
	Oxidoreductase-dehydrogenase	<i>Sphingobacterium spiritivorum</i> ATCC 33300		
	Oxidoreductase domain protein	<i>Sphingobacterium</i> sp. (strain 21)		
14.5	Metal-dependent hydrolase	<i>Sphingobacterium spiritivorum</i> ATCC 33300	25.49	25
	Metallo-beta-lactamase	<i>Sphingobacterium spiritivorum</i> ATCC 33861		

With the exception of bands 9.1, 9.3 and 13.3 the predicted molecular weights of most proteins are similar to the approximate molecular weights of the corresponding Coomassie Brilliant Blue–R250-stained bands from which they were identified. It is interesting that most of the proteins are also produced by *Sphingobacterium spiritivorum*, an observation consistent with many of the proteins purified from SAE 1.

4.4. Conclusions

Attempts have been made to purify extracellular lignin-degrading enzymes from the culture supernatant of *M. phyllosphaerae* and *Sphingobacterium sp.*, both of which were hindered by low protein concentration and loss of enzyme activity vs. time. Limited progress was made towards the purification of extracellular enzymes from *M. phyllosphaerae* since the concentration of protein in the purified enzyme samples of highest activity after the first two chromatographic purification stages was insufficient to observe single Coomassie Brilliant Blue–R250-stained SDS–PAGE bands and hence identify purified enzymes. More extensive progress was made towards the purification of extracellular enzymes from *Sphingobacterium sp.*, mostly due to the greater concentration of purified enzymes. Several enzymes produced by this organism have been identified in samples of partially purified enzyme, which exhibited high activity towards nitrated lignin and ABTS. Enzymes of particular interest include up to three different forms of superoxide dismutase, an oxidoreductase, a peroxiredoxin, a metallohydrolase and dehydrogenases. The detection of multiple enzyme activities detected by the ABTS and nitrated lignin assays suggests that

Sphingobacterium sp. produces several enzymes of variable properties that degrade lignin via a collaborative process.

It is interesting that up to four different forms of superoxide dismutase have been identified in fractions of partially purified enzymes from *Sphingobacterium sp.*, particularly manganese peroxidase (MnSOD), since previous studies have found MnSOD to be a highly efficient enzyme with rate constants of MnSOD enzymes from thermophiles to be near the diffusion limit [196, 197], though it has also been discovered that the formation of a dead-end peroxide complex under the conditions of stopped flow kinetics significantly reduces the activity of this enzyme by approximately twenty-fold. It has been suggested that the efficiency of MnSOD is highly dependent on the balance between the rates of the oxidative and reductive half reactions, which form the catalytic cycle (Fig. 4.14).

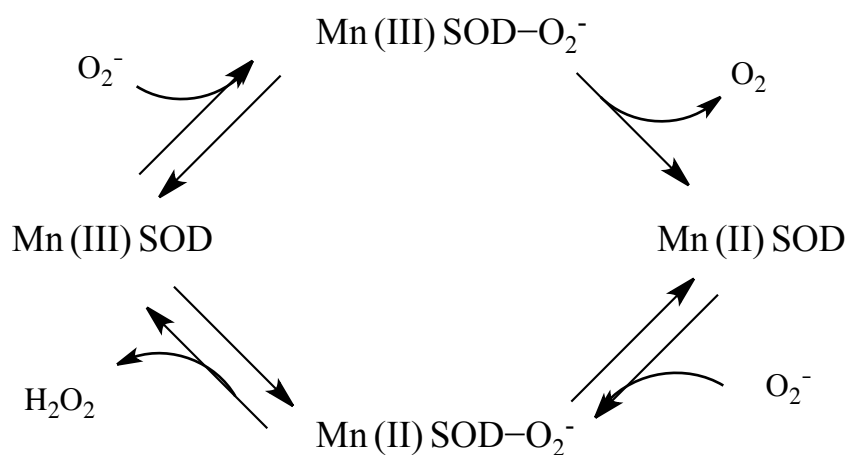


Figure 4.14. Conversion of the superoxide anion radical to O₂ and H₂O₂ by manganese superoxide dismutase (MnSOD) [196].

The literature reports of significantly reduced activity resulting from the formation of dead-end peroxide complexes are particularly interesting since the UV/visible nitrated lignin analysis for *Sphingobacterium sp.*, which seems to secrete manganese superoxide dismutase, showed significantly reduced activity in the presence of H₂O₂ (see Chapter 2).

Previous studies have also found that superoxide dismutase enhances the rate of oxidation of veratryl alcohol by LiP via prevention of the formation of compound III, an inactive compound formed by the reduction of the compound II form of LiP in the catalytic cycle [198]. Manganese superoxide dismutase has also been detected in cell extracts of *P. chrysosporium*, one of the most extensively studied lignin-degrading fungi [199]. The combination of the literature reports and the observations in this thesis suggests that superoxide dismutase enzymes may indirectly degrade lignin.

The identification of an oxidoreductase, also secreted by *Sphingobacterium spiritivorum*, is also of particular interest since LiP belongs to this family of proteins and cellobiose oxidoreductase has been found to inhibit LiP-catalyzed polymerization of Kraft lignin, decarboxylation of vanillic acid by laccase and the oxidation of veratryl alcohol and 1, 2, 4, 5-tetramethoxybenzene by lignin peroxidase [200].

Chapter 5: Conclusions and future work

Over the course of the PhD two recently developed assay methods have been optimized for the high-throughput screening of environmental bacteria for activity towards lignin degradation. Seven mesophilic lignin-degrading strains have been isolated from woodland and heathland soils, and three moderately thermotolerant strains from composted wheat straw. All of these isolates exhibited activities similar to, or greater than previously studied lignin-degrading bacteria *R. jostii* RHA1 and *P. putida* mt-2 [159] and the most active was *Sphingobacterium sp.*, which is approximately ten-fold more active than the other strains. The two nitrated lignin assay methods were found to give consistent results and since they were very effective in selecting strains that were active towards lignin degradation, this screening protocol may be used in future projects, and will shortly be used by collaborators at Monash University (Melbourne, Australia) to isolate lignin-degrading bacteria from Australian soils.

With the exception of the *Ochrobactrum* strains, the strains isolated in this project were found to be capable of depolymerizing high-molecular weight forms of Kraft lignin into lower-molecular weight material, and the metabolism of the lignin degradation products with the exception of *Sphingobacterium sp.* Significant variations between the abilities of the different strains to metabolise selected aromatic carbon sources and cellulose were observed: *Sphingobacterium sp.* and *R. erythropolis* were found to grow well on biphenyl, vanillic acid and veratryl alcohol whilst most of the other strains appeared to be more selective, growing well on only one or two of the carbon sources (see Chapter 3). *Sphingobacterium sp.*, *R. erythropolis* and *M. phyllosphaerae* were

found to be capable of breaking down wheat straw, Organosolv lignin and Kraft lignin into soluble and insoluble phenolic compounds, and several structural modifications were detected by FT-IR.

Although limited progress was made towards the purification of extracellular lignin-degrading enzymes from the culture supernatants of *M. phyllosphaerae* and *Sphingobacterium sp.*, the detection of several peaks in enzyme activity at different anionic strengths and hydrophobicities suggests that these organisms each produce a variety of enzymes that are directly or indirectly linked to lignin degradation. Proteins of interest have been identified in 'active' samples of partially purified enzymes from the culture supernatant of *Sphingobacterium sp.*, and include up to four different forms of superoxide dismutase and an oxidoreductase. The detection of multiple superoxide dismutases in the most active enzyme samples suggests that enzymes from this family are possibly highly efficient towards the depolymerization of lignin. Since superoxide dismutase has not previously been linked to lignin degradation, it could be classed as a novel lignin-degrading bacterial enzyme and its thermostability and high activity are advantages for future industrial use of this enzyme. However, future work is required to develop our understanding of this enzyme in the context of lignin degradation. Cloning and expression of genes for superoxide dismutase is currently being carried out by another researcher in the Bugg group, and the activity of the purified enzyme will be compared to that of other lignin-degrading enzymes, e.g. DyP B.

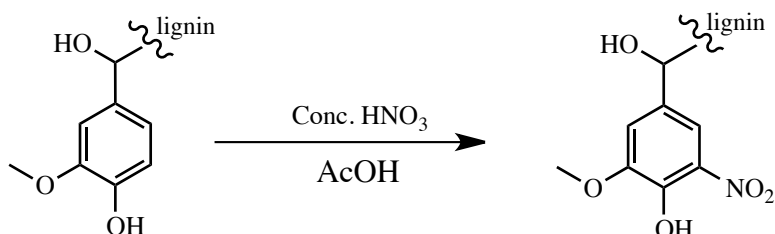
Ultimately, purified lignin-degrading enzymes from the strains isolated in this project may be commercially applied to the pre-treatment of lignocellulosic biomass and more specifically the degradation of lignin, which may yield an

array of renewable aromatic chemicals for use in a range of applications in green chemistry and biotechnology.

Chapter 6: Experimental

6.1. Screening for environmental lignin-degrading bacteria

6.1.1. Preparation of nitrated MWL solution



Milled wood lignin (MWL) from wheat straw (5 mg, supplied by M. Ahmad [159]) and glacial acetic acid (1 ml) were mixed and then filtered to remove insoluble material. Concentrated nitric acid (200 μ l) was added and the reaction mixture stirred at ~ 5 $^{\circ}$ C for 1 hr. Distilled H₂O (2 ml) was then added and the pH adjusted to 7.0 with 1 M NaOH, using a Hanna HI 110 series pH meter, calibrated at pH 4.0 and 10.0. The resulting solution was separated into 1 ml fractions, which were used as stock solutions for the nitrated lignin assay.

Data: UV/visible maximum: 300 nm. The degree of nitration was estimated from the ratio of A_{300} to A_{280} , using the extinction coefficients for lignin model compounds 5-nitrovanillyl alcohol ($\epsilon_{300} = 3255 \text{ mol dm}^{-3} \text{ cm}^{-1}$) and vanillyl alcohol ($\epsilon_{300} = 2544 \text{ mol dm}^{-3} \text{ cm}^{-1}$).

ESI-MS: m/z 540 – 1500 (envelope), 446.3.

6.1.2. Sourcing and enrichment of cultures

Soil samples were collected from six woodland sites in Hampshire and Warwickshire, United Kingdom. Each sample (25 mg) was used to set up enrichment cultures (5 ml) in M9 salt solution (Na₂HPO₄: 12.8 g l⁻¹, KH₂PO₄: 3.0 g l⁻¹, NaCl: 0.5 g l⁻¹, NH₄Cl: 1.0 g l⁻¹) supplemented with wheat straw (2.0 g l⁻¹) at

30 °C for 21 days, with shaking at 180 rev min⁻¹. Wheat straw was processed through a 5 mm mesh using a rotary mill (CRN laboratory). In the isolation of thermotolerant strains lignocellulosic enrichment cultures were set up from composted wheat straw (25 mg), obtained from the solid-state fermentation of wheat straw amended with chicken manure (1 % w/w), operating at 60 – 65 °C (Dr. K. Burton, Warwick HRI), and the enrichment was carried out at 45 °C for 21 days. Enriched samples were diluted 1000-fold in 20 mM Tris buffer (pH 7.4) and aliquots of each sample (200 µl) were then spread onto plates containing granulated agar, solidifying agent (Fisher Scientific UK ltd, Loughborough, UK; BP 1423) and M9 salts supplemented with wheat straw (2 % w/v) and incubated for 144 hr at 30 °C for the soil samples and 45 °C for samples from composted wheat straw. The number of CFUs per ml in each enriched sample was estimated by dividing the number of colonies observed on each agar-plated culture by 0.2 ml, and then multiplying by 1000 (the dilution factor).

6.1.3. UV/visible nitrated lignin assay for nitrated MWL samples A, B and C

UV/visible nitrated lignin assays were carried out using the method described by Ahmad *et al.* Liquid cultures of each isolate/strain were grown in Miller's LB broth (Fisher BioReagents BP 1426500, containing tryptone: 10.0 g l⁻¹, yeast extract: 5.5 g l⁻¹, NaCl: 10 g l⁻¹ and Tris buffer: 1.5 g l⁻¹) for 12 – 24 hr at 30 °C, and cell density monitored by OD₆₀₀. The culture supernatant was then prepared via centrifugation of 1 ml of each culture (10, 000 rev min⁻¹, 4 min) in Caccu™ Spin Micro centrifuge (Fisher Scientific Uk ltd) followed by decanting.

Nitrated MWL solution (sample C) was diluted 25-fold in dH₂O. Assays were performed on 96-well Nunclon D surface clear plates from Nunc, using a TECAN GENios plate reader. The total volume of each well (200 μ l) was filled with the culture supernatant (30 μ l), diluted nitrated MWL solution (160 μ l) and 40 mM H₂O₂ (10 μ l). Assays were repeated in the absence of H₂O₂, whereby the volume was made up to 200 μ l with 750 mM Tris buffer (pH 7.4, 37.5 mM final concentration) containing 50 mM NaCl. The absorbance at 430 nm was monitored over 20 min, with readings taken every 60 s, and the change in absorbance over this period was calculated by subtracting the absorbance reading taken after 1 min from the reading taken after 21 min. Assays were carried out in triplicate and control experiments were performed in which the culture supernatant had been replaced with 750 mM Tris buffer (pH 7.4) containing 50 mM NaCl.

6.1.4. Media Recipes

The M9 salts were prepared by adding Na₂HPO₄ (30.5 g, 215 mmol), KH₂PO₄ (15 g, 110 mmol), NaCl (2.5 g, 43 mmol) and NH₄Cl (5 g, 93 mmol) to dH₂O (800 ml). The solution was stirred and the volume made up to 1 l with dH₂O following dissolution. Granulated agar (15 g) was added when preparing agar plates. The solution was sterilized by autoclaving.

The medium was then prepared by adding M9 salts (200 ml), 1 M MgSO₄ (2 ml), a source of carbon (e.g. wheat straw) and 1 M CaCl₂ (100 μ l) to dH₂O (700 ml). The volume was adjusted to 1 l with dH₂O. For the preparation of M9 salts supplemented with glucose and yeast extract, 20 % v/v glucose (20 ml) and yeast extract (5 g) were added to the solution instead of wheat straw (20 g l⁻¹).

Solutions of 1 M MgSO₄ and 1 M CaCl₂ were added to the medium following autoclaving, and were filter-sterilized.

6.1.5. Nitrated lignin spray assay

Nitrated MWL solution was diluted 10- or 25-fold in 750 mM Tris buffer (pH 7.4) containing 50 mM NaCl, 20 mM Tris buffer (pH 7.4) or dH₂O. Cultures of each strain were streaked onto agar plates containing LB and sprayed with nitrated MWL solution (500 µl) and incubated at 30 or 45 °C for 48 hr. The colonies that were more yellow in appearance were labelled and then re-streaked onto plates containing M9 salts supplemented with glucose (2 % v/v), yeast extract (0.5 % w/v) and nutrient agar (OXOID ltd, Basingstoke, Hampshire, England; CMOOOJ 'lab-lemco' powder: 1.0 g ml⁻¹, yeast extract: 2.0 g ml⁻¹, peptone: 5.0 g ml⁻¹, NaCl: 5.0 g ml⁻¹, agar: 15.0 g ml⁻¹) in an attempt to isolate different bacterial strains and eliminate fungal species. The growth of the isolated colonies was monitored after 24 hr, and the incubation process was continued for a further 24 hr until rapid growth had occurred on all of the plates. Since very few plates contained visible single colonies, a cluster of colonies from each plate was re-streaked and incubated at 30 °C for 48 hr, and the agar plates were divided into 4 sections, each containing a cluster of colonies from a different sample.

All samples were incubated for a further 48 hr to promote any further growth in order to distinguish between the different isolates. Each isolate was then given a different sample ID, re-streaked and duplicate plates were prepared for each sample: one for use in the spray assay, and the other as an unsprayed control. Each plate was then sprayed with nitrated MWL solution (500 µl) and incubated along with the control at 30 or 45 °C for 48–96 hr.

6.1.6. UV/visible nitrated lignin assays for environmental lignin-degrading bacteria

UV/visible nitrated lignin assays were carried out using a similar procedure to that described in 6.1.3. To each well (200 μ l total volume) was added nitrated MWL solution (160 μ l), culture supernatant of each bacterial isolate (30 μ l) and 40 mM H₂O₂ (10 μ l). Assays were repeated in the absence of H₂O₂, whereby 750 mM Tris buffer (7.4) containing 50 mM NaCl was added instead. Assays were carried out in quadruplet, with a control experiment in which the culture supernatant was replaced with 750 mM Tris buffer (pH 7.4) containing 50 mM NaCl. In contrast to the method described in 6.1.3, nitrated MWL solution was prepared via 25-fold dilution of the stock solution in sterile dH₂O rather than 750 mM Tris buffer (pH 7.4) containing 50 mM NaCl. All assays were carried out in quadruplet.

6.1.7. Identification of environmental lignin-degrading bacteria

The similarity of isolates to known bacterial strains was examined by analysis of 16S rRNA gene sequences. Gene fragments of isolated strains were amplified by colony PCR using forward (5'–AGAGTTTGATCMTGGCTCAG–3') and reverse (5'–TACGGYTACCTTGTTACGACTT–3') primers. A single colony of each isolate (circa. 1 ml) was mixed with MgCl₂ (5 μ l), 5 μ l *Taq* reaction buffer (Sigma-Aldrich D 1806), dNTPs (0.4 μ l), 0.25 μ l *Taq* DNA polymerase from *Thermus aquaticus* (Sigma-Aldrich D 1806), forward primer (1 μ l) and reverse primer (1 μ l) at 4 °C. PCR products (approximately 1.5 kb fragments) were sequenced and investigated using the BLAST algorithm on the EBI web-server (www.ebi.ac.uk).

6.2. Characterization of environmental lignin-degrading bacteria

6.2.1. Growth in liquid media

Liquid cultures of selected strains were grown with regular shaking (180 rev min⁻¹) in LB broth and M9 salt solution supplemented with yeast extract (0.5 % w/v) and glucose (2 % v/v) and/or 2 % w/v Kraft lignin (Sigma-Aldrich 471003, average MW ~ 10000 g mol⁻¹). Aliquots of each culture (1 ml) were removed every 24 hr and the OD₆₀₀ monitored using a Biomate 3 (335 – 904 P – O4, Thermo Electron Corporation, Madison, WI, USA). All readings were taken in triplicate and cultures exhibiting readings above 0.5 OD₆₀₀ were diluted 2 – 5-fold in the appropriate culture medium.

6.2.2. Growth on aromatic carbon sources and cellulose

Selected strains were streaked onto agar-solidified M9 salts supplemented with the following carbon sources, at the final concentrations indicated: biphenyl (1.0 g l⁻¹), *m*-cresol (0.22 g l⁻¹), *p*-cresol (0.22 g l⁻¹), ferulic acid (1.0 g l⁻¹), vanillic acid (1.0 g l⁻¹), veratryl alcohol (0.84 g l⁻¹), and microgranular cellulose (0.5 g l⁻¹). Cultures of the mesophilic soil isolates were grown at 30 °C and thermotolerant isolates at 45 °C for 7 – 10 days, with the growth classed as good (10³ – 10⁴ colonies), moderate (10² – 10³ colonies), poor (< 50 colonies) or no growth.

6.2.3. Temperature-dependent growth of thermotolerant strains

Sphingobacterium sp. and *Rhizobiales sp.* were streaked onto agar plates containing LB and incubated at 30, 37, 45, 50 and 55 °C for 168 hr. Growth was monitored after 48 hr and 168 hr, and was classed as good (10³ – 10⁴ colonies), moderate (10² – 10³ colonies), poor (< 50 colonies) or no growth.

6.2.4. Transmission Electron Microscopy

Liquid cultures of *Sphingobacterium sp.*, grown in LB broth at 45 °C, were coated onto formvar-carbon grids and negatively stained with uranium acetate (2 % w/v). TEM images were obtained using a Jeol 2011 LaB 6 microscope with a Gatan ultra-scan 1000 camera.

6.2.5. Fractionation of Kraft lignin by aqueous gel filtration chromatography

A solution of Kraft lignin (Sigma-Aldrich 471003) in dH₂O (20 mg ml⁻¹, 5 ml) was loaded onto and Ultrogel ACA-44 gel filtration column (25 ml) and eluted with dH₂O, collecting 16 fractions, each 16 ml in volume, over 14 hr. Each fraction was analyzed by UV/visible spectroscopy at 280 nm, using a Cary 50 Bio UV/visible Spectrophotometer, and divided into three fractions eluted sequentially from the column, which correspond to high-, medium- and low-molecular weight Kraft lignin. In order to measure the absorbance at 280 nm, a sample of each fraction was diluted 80-fold in dH₂O.

6.2.6. Incubation of size-fractionated Kraft lignin with lignin-degrading bacteria

Solutions of high-, medium- and low-molecular weight size-fractionated Kraft lignin were incubated at 30 or 45 °C (for *Sphingobacterium sp.*) in 2 ml M9 salt solution (Na₂HPO₄: 12.8 g l⁻¹, KH₂PO₄: 3.0 g l⁻¹, NaCl: 0.5 g l⁻¹, NH₄Cl: 1.0 g l⁻¹) with each bacterial strain. Aliquots of each sample (200 µl) were collected after 72 and 192 hr, which were centrifuged (10,000 rev min⁻¹, 5 min). Growth of each strain in M9 salts supplemented with size-fractionated Kraft lignin was monitored qualitatively after 72 and 192 hr by comparing the volume of the cell

pellet following centrifugation of each aliquot. The supernatant from each sample (200 μ l) was analyzed using size-exclusion HPLC, using a BioSep SEC S-3000 column, eluting with water at a flow rate of 0.5 ml min⁻¹, with UV detection at 280 nm.

6.2.7. Bioconversion of lignin and lignocellulose

Wheat straw (processed through a 5 mm mesh using a rotary mill, CRN laboratory), Kraft lignin or Organosolv lignin (6.25 g) and 2.5 g of either fish meal (Sigma-Aldrich F 6381, containing protein: 62 %, ash: 18 % and fat 9 %) or corn steep solids (Sigma-Aldrich C 8160) were added to M9 salt solution (250 ml). 1 M MgSO₄ (500 μ l) and 1 M CaCl₂ (25 μ l) were added following autoclaving. Organosolv lignin, also known as BioligninTM, was supplied by CIMV (Champagne-Ardenne, France).

Starter cultures (5 ml) of *Sphingobacterium sp.*, *R. erythropolis* and *M. phyllosphaerae* were grown in LB broth over 48 hr to and OD₆₀₀ of 0.9 – 1.3. Each culture was centrifuged (5,000 rev min⁻¹, 30 min) and the cells washed twice with 20 mM potassium phosphate buffer (pH 7.0). The cells (0.9 g) were then re-suspended in fresh 20 mM phosphate buffer (10 ml).

Re-suspended cells of each strain were added to each different medium, containing wheat straw, Kraft lignin or Organosolv lignin (6.25 g, 2.5 % w/v) and fish meal or corn steep solids (2.5 g, 10 % w/v). The cultures were then incubated at 30 °C, or 45 °C for *Sphingobacterium sp.*, with regular shaking at 180 rev min⁻¹. Aliquots of each culture (10 ml) were removed after 48, 96, 168, 240 and 336 hr.

6.2.7.1. Estimation of CFU composition of each sample

Samples of each liquid fraction were diluted 10,000-fold in 20 mM potassium phosphate buffer (pH 7.0) and aliquots (100 μ l) spread onto agar plates containing LB and incubated at 30 °C, or 45 °C for *Sphingobacterium sp.*, for 96 hr. The number of colonies formed on each plate was noted, divided by the volume of the aliquot (0.1 ml) and then multiplied by 10,000 (the dilution factor) to give the number of CFUs per ml of culture.

6.2.7.2. Determination of soluble phenolic content

The soluble phenolic content of each liquid fraction was determined by Folin-Ciocalteu (FC) colorimetry [185, 186].

Reagent Preparation: FC reagent (Sigma-Aldrich F 9252) was prepared via 10-fold dilution in dH₂O and Na₂CO₃ solution was prepared by dissolution of anhydrous Na₂CO₃ (200 g) in dH₂O (800 ml), which was brought to boil and then cooled. Following cooling a few crystals of Na₂CO₃ were added and the resulting mixture left stationary at 20 °C for 24 hr. The solution was then filtered using filter paper (Whatmann no. 1) and dH₂O added to 1 l. The solution was stored indefinitely at 20 °C.

Gallic acid solution (10 μ g μ l⁻¹) was prepared via dissolution of 1.0 g gallic acid (Sigma–Aldrich G 7384) in 10 ml ethanol and dilution to 100 ml in dH₂O.

Standard curve: A series of calibration solutions were prepared by mixing solutions of varying gallic acid concentration (500 μ l) with FC reagent (100 μ l).

Table 6.1. Volumes of gallic acid solution ($10 \mu\text{g } \mu\text{l}^{-1}$) and dH_2O used in the preparation of each calibration standard solution.

<i>Volume of gallic acid solution / μl</i>	<i>Volume of dH_2O / μl</i>
0	500
100	400
200	300
300	200
400	100
500	0

Assay protocol: The liquid fraction of each sample ($20 \mu\text{l}$) was mixed with dH_2O (1.58 ml) in a plastic cuvette and FC reagent ($100 \mu\text{l}$) was then added. The solution was vortexed and incubated at $20 \text{ }^\circ\text{C}$ for 8 min. Na_2CO_3 ($300 \mu\text{l}$) was then added, the solution vortexed and then incubated at $20 \text{ }^\circ\text{C}$ for 2 hr. The absorbance of the sample at 765 nm was measured and all assays carried out in technical triplicate.

6.2.7.3. Determination of total reducing sugar content

The total reducing sugar content of each liquid fraction was determined via the 3,5-dinitrosalicylic acid (DNS) method [187].

Reagent preparation: DNS solution (1 \% w/v) was prepared by mixing separate solutions of DNS, NaOH and sodium potassium tartrate. DNS (Sigma-Aldrich D 0550) was dissolved in dH_2O (10 ml), NaOH (2 g) dissolved in dH_2O (10 ml) and sodium potassium tartrate (Sigma-Aldrich S 2377, 20 g) in dH_2O (50 ml). The solutions of DNS and sodium potassium tartrate (Reagent Plus®, Sigma-Aldrich S 2377) were mixed and the NaOH solution then added slowly. Glucose (1 mg ml^{-1}) was also prepared.

Standard curve: Six calibration solutions of varying glucose concentration were prepared by mixing varying volumes of glucose (1 mg ml^{-1}) and dH_2O .

Table 6.2. Volumes of glucose (1 mg ml^{-1}) and dH_2O used in the preparation of each calibration solution.

<i>Volume of glucose / μl</i>	<i>Volume of dH_2O / μl</i>
0	250
50	200
100	150
150	100
200	50
250	0

Assay protocol: DNS solution ($750 \mu\text{l}$) was added to each calibration solution and the absorbance at 540 nm measured using a Biomate 3 (Thermo Electron Corporation) spectrophotometer. For determining the reducing sugar content of samples from the bioconversion experiments, DNS solution ($750 \mu\text{l}$) was added to the culture supernatant of each sample ($250 \mu\text{l}$), which was prepared by centrifugation ($10,000 \text{ rev min}^{-1}$, 5 min), using a micro-centrifuge (accu Spin™ Micra, Fisher Scientific UK ltd). All assays were carried out in triplicate.

6.2.7.4. pH measurements

The pH of each sample was measured using a Hanna HI 110 series pH meter, calibrated at pH 4.0 and 10.0. All measurements were carried out in technical triplicate.

6.2.7.5. FT–IR measurements

FT–IR measurements of the liquid fractions were performed on 96–well silicon plates. Acetone (2:1 ratio) was added to the samples, which were then vortexed for 5 s and centrifugation ($10,000 \text{ rev min}^{-1}$, 3 min) in an Eppendorf 580 L microfuge. Each sample ($5 \mu\text{l}$) was spotted onto a well and the plate dried on an inverted hot block ingot at $30 \text{ }^\circ\text{C}$ for 10 min .

Analysis of the solid fractions was performed via attenuated total reflectance (ATR) from 4,000–600 cm^{-1} , using an Equinox 55 FT-IR Spectrometer (Bruker Optik GmbH, Germany) fitted with a Golden Gate ATR accessory (Specac, UK). Each sample was dried at 50 °C for 1 hr using a CHRIST 2 – 18 RVC vacuum concentrator at 5,000 rev min^{-1} , and then pressed onto a diamond crystal mounted as a window in a tungsten base plate. All spectra were averaged over 32 scans at a resolution of 4 cm^{-1} and corrected for background absorbance by subtracting the spectrum of the empty ATR crystal. Absorbance spectra were initially processed using Opus version 4.2 (Bruker Optik GmbH, Germany) and saved as text files.

6.3. Purification of extracellular enzymes

6.3.1. Collection of culture supernatant for enzyme purification

Cultures of the parent bacterial strain (1.5 – 3.0 l) were grown in LB broth at 30 °C or 45 °C (for *Sphingobacterium sp.*) at 180 rev min^{-1} for 24 – 48 hr, to and OD_{600} of 0.9 – 1.2. Aliquots of each culture (200 ml) were then centrifuged (SORVALL® RC 6 plus) at 4 °C (5,000 rev min^{-1} , 20 min) to remove solids.

6.3.2. Ammonium sulfate precipitation

The induction medium was prepared by adding $(\text{NH}_4)_2\text{SO}_4$ (675 g and 1.35 kg) to the culture supernatant (1.5 l and 3 l) for *M. phyllosphaerae* and *Sphingobacterium sp.* respectively, to achieve a saturation level of 70 % (w/v). The required mass of $(\text{NH}_4)_2\text{SO}_4$ in relation to the volume of culture supernatant was calculated using the ammonium sulfate calculator provided by EnCor Biotechnology Inc., Gainesville, Florida, USA

(<http://www.encorbio.com/protocols/AM-SO4.htm>). The crude enzyme was precipitated after gentle stirring at 4 °C for 1 hr, and aliquots were then centrifuged (5,000 rev min⁻¹, 20 min) at 4 °C to remove the liquid. Pellets were then re-suspended in the minimum required volume of 20 mM potassium phosphate buffer (pH 7.4).

6.3.3. Q-sepharose anion exchange column chromatography

The purification of enzyme by Q-sepharose column chromatography was carried out using 20 mM Tris (pH 7.4) as the binding buffer. Q-sepharose fast-flow, pre-swollen, 45 – 165 µm (wet), exclusion limit ~ 4000 kDa (Sigma-Aldrich Q 1126) was washed with 3 column volumes of 20 mM Tris buffer (pH 7.4, 300 ml) and the crude enzyme then loaded onto the column, with further washing (300 ml). A gradient of 0 – 2 M NaCl in the above buffer was applied (150 ml) at a constant flow rate of 1.6 ml min⁻¹, with a series of fractions (circa. 10 ml) collected at intervals of 5 min. Fractions were assayed for activity using the nitrated lignin and ABTS assays, with and without 2 mM H₂O₂. The resin was stored in ethanol (20 % v/v) when not in use. The process was carried out at 4 °C.

6.3.4. TCA precipitation

100 % w/v trichloroacetic acid (Sigma-Aldrich T 9159) was added to 1 ml of each fraction of partially purified enzyme and left standing for 15 min at 4 °C. The reaction mixture was then centrifuged (10,000 rev min⁻¹, 5 min) at 4 °C and the culture supernatant then removed followed by the addition of 20 mM Tris buffer (pH 7.4, 20 µl).

6.3.5. Concentration and desalting of protein samples

Samples of purified enzyme were concentrated using an Amicon regenerated Cellulose 10, 000 MWCO Ultracel 10 k membrane (Millipore ltd, Tullagreen, Carrigtwohill, Co. Cork, Ireland; UFC 901024) at 5, 000 rev min⁻¹ for 20 – 30 min at 4 °C, to a final volume of approximately 1 – 1.5 ml, achieving approximately a ten-fold concentration. Samples were desalted using a spin column (3 kDa NMWCO membrane), involving repeated concentration and dilution with 20 mM Tris buffer (pH 7.4). The process was carried out three times to ensure that a reduction in salt concentration of approximately 1, 000-fold.

6.3.6. UV/visible nitrated lignin assays for samples of partially purified enzyme

Nitrated lignin assays [159] were carried out following the procedure described in 6.1.3, though nitrated Organosolv lignin, which was prepared following the same procedure described in 6.1.1, was also used. Assays performed on purified extracellular enzyme samples from *M. phyllosphaerae* involved a higher volume of purified enzyme since individual samples were not concentrated: 100 µl of nitrated lignin solution was reacted with 90 µl partially purified enzyme and 10 µl 40 mM H₂O₂ (2 mM final concentration). In wells containing no H₂O₂, the volume was made up to 200 µl with 750 mM Tris buffer (pH 7.4.). Assays on partially purified enzymes from *Sphingobacterium sp.* were performed using the same parameters described in 6.1.3. All assays were carried out in technical

triplicate unless otherwise stated and control experiments were performed in which the enzyme sample had been replaced by 20 mM Tris buffer (pH 7.4).

6.3.7. ABTS assays

The solutions required for ABTS assays [195] include 50 mM sodium phosphate buffer (pH 6.0), 10 mM ABTS and 20 mM H₂O₂. Sodium phosphate buffer was prepared by dissolution of NaH₂PO₄·2H₂O (11.64 g) in dH₂O (500 ml), and the pH adjusted to 6.0 with conc. HCl (3 M), using a Hanna HI 110 series pH meter, calibrated at pH 4.0 and 10.0. ABTS solution (10 mM) was prepared by dissolving 258 mg ABTS (Sigma-Aldrich A 1888) in 50 ml of 50 mM sodium phosphate buffer (pH 6.0). H₂O₂ was prepared by mixing 30 wt % H₂O₂ (230 µl) with sodium phosphate buffer (100 ml). All assays were carried out in technical triplicate unless otherwise stated and control experiments were performed in which the enzyme sample had been replaced by 20 mM Tris buffer (pH 7.4).

6.3.8. Protein characterization by SDS–PAGE

6.3.8.1. Preparation of polyacrylamide gels

1x running gel solution (12 % v/v bis-acrylamide) was prepared by mixing dH₂O (10.2 ml) with 1.5 M Tris–HCl (pH 8.8, 7.5 ml), 20 % (w/v) sodium dodecyl sulfate (SDS, 150 µl), 0.8 % (w/v) bis-acrylamide (12.0 ml), 10 % (w/v) ammonium persulfate (APS, 150 µl) and tetramethylethylenediamine (TEMED, 20 µl). SDS (Electrophoresis grade) was supplied from Fisher Scientific (BP 166), TEMED (Electrophoresis reagent) from Sigma-Aldrich T 9281, APS (98 + % A.C.S. reagent) from Sigma-Aldrich (7727) and bis-acrylamide (30 % solution Electrophoresis reagent) from Sigma-Aldrich (A 3574).

Stacking gel solution (4 % v/v bis-acrylamide) was prepared by mixing dH₂O (3.075 ml) with 0.5 M Tris-HCl (pH 6.8, 1.25 ml), 20 % (w/v) SDS (25 µl), 0.8 % (w/v) bis-acrylamide (670 µl), 10 % (w/v) APS (125 µl) and TEMED (7.5 µl).

6.3.8.2. Preparation of protein samples

Each protein (20 µl) was mixed with 5x sample buffer (5 µl) and then boiled for 5 – 10 min. 5x sample buffer was prepared by mixing 10 % (w/v) SDS with 10 mM 2-mercaptoethanol, electrophoresis reagent (Sigma-Aldrich M 7154), 20 % (v/v) glycerol, 0.2 M Tris-HCl (pH 6.8) and 0.5 % (w/v) bromophenolblue, A.C.S. reagent (Sigma--Aldrich 114391).

6.3.8.3. Electrophoresis

The gel was clamped and both chambers filled with running buffer. Each protein sample (20 µl) and 10 µl of molecular weight marker, Page Ruler™ Plus pre-stained protein ladder (Thermo Scientific, Rockford, IL, USA; 26619) were loaded onto the gel, which was then run at + 150 V for 30 min, and then + 200 V, at 4 °C until the blue dye front reached the bottom of the gel. 1x running buffer was prepared using 25 mM Tris-HCl, 200 mM glycine and 0.1 % (w/v) SDS.

6.3.8.4. Coomassie Brilliant Blue-R250 staining

The reagents used for Coomassie staining include fixing solution (50 % v/v methanol and 10 % v/v glacial acetic acid), staining solution (0.1 % v/v Coomassie Brilliant Blue-R250, 50 % v/v methanol and 10 % v/v glacial acetic acid), destaining solution (40 % v/v methanol and 10 % v/v glacial acetic acid) and storage solution (5 % v/v glacial acetic acid). Coomassie Brilliant Blue-R250 was supplied from Bio-rad Laboratories, Hercules, CA, USA (161-0435).

The gel was fixed in fixing solution with gentle agitation for 2 hr, with replacement of the solution after 1 hr. The gel was then stained in staining solution with gentle agitation for 30 min, followed by destaining. Replacement of destaining solution was carried out several times until the background of the gel became fully destained, and the gel then stored in storage solution

6.3.8.5. Silver Staining

Prior to silver staining, several pre-requisite solutions were prepared including fixing solution, pre-stain, staining solution, developing solution, stopping solution, 50 % v/v acetone and 1 % v/v acetic acid. Fixing solution was prepared by mixing 50 % v/v trichloroacetic acid (TCA, 1.5 ml) and 37 % v/v formaldehyde (25 μ l) with 50 % v/v acetone (60 ml). Pre-stain solution was prepared by dissolving $\text{Na}_2\text{S}_2\text{O}_3$ (10 mg) in dH_2O (60 ml). Staining solution was prepared by dissolving AgNO_3 (160 mg) and formaldehyde (600 μ l) in dH_2O (60 ml). Developing solution was prepared by dissolution of Na_2CO_3 (1.2 g), 37 % v/v formaldehyde (25 μ l) and $\text{Na}_2\text{S}_2\text{O}_3$ (2.5 mg) in dH_2O (60 ml). Stopping solution (1 % v/v acetic acid) was also prepared.

The procedure was initiated by placing the gel in fixing solution with gentle agitation for 15 min. The gel was then washed with dH_2O for 5 min, followed with washing in acetone for 5 min. The gel was then placed in pre-stain solution with gentle agitation for 1 min, quickly washed with dH_2O and then placed in staining solution for 8 min. Following two quick washes with dH_2O , the gel was developed for 10 – 20 s and stopping solution added for 1 – 2 min after bands appeared. The gel was then rinsed with, and stored in, dH_2O .

6.3.9. Phenyl-sepharose hydrophobic interaction chromatography

Further purification of extracellular enzymes by phenyl-sepharose column chromatography was carried out at 4 °C, using 20 mM sodium phosphate (pH 7.4) containing 2 M (NH₄)₂SO₄ as the binding buffer. Phenyl-sepharose 6, fast-flow, 40 μ mol ml⁻¹ (Sigma-Aldrich P 2459) was washed with buffer (3 column volumes, 300 ml) and the enzyme then loaded onto the column. After further washing of the enzyme with buffer (3 column volumes, 300 ml), a gradient of 2 – 0 M (NH₄)₂SO₄ in the above buffer was applied (150 ml) at a constant flow rate of 1.6 ml min⁻¹, with a series of fractions (circa. 10 ml) collected at intervals of 5 min. Fractions were assayed for activity using the nitrated lignin and ABTS assays in the presence and absence of 2 mM H₂O₂. The resin was stored in ethanol (20% v/v) at 4 °C when not in use.

6.3.10. Gel filtration FPLC

Gel filtration FPLC was carried out using a Superdex™ 200 column (25 ml in volume) over 30 min at a flow rate of 0.5 ml min⁻¹ at 4 °C, using 20 mM Tris buffer (pH 7.4). Superdex™ 200 was supplied from Bio-rad Laboratories. Fractions were assayed for activity towards ABTS in the presence of H₂O₂.

6.3.11. Determination of protein concentration

Bradford protein assays [194] were carried out in 96-well Nunclon D Surface clear plates, using a TECAN GENios plate reader. To each well 150 μl of Bio-rad protein dye concentrate (Bio-rad laboratories, 500 – 0006) and 0 – 25 μl of 1 mg ml⁻¹ Quick-start bovine serum albumin (BSA) standard (Bio-rad laboratories, 500 – 0206), a stable protein standard, was added. Prior to each assay, a

calibration graph was constructed by monitoring the absorbance at 595 nm over a concentration range of 0–25 $\mu\text{g } \mu\text{l}^{-1}$ 1 mg ml^{-1} BSA (see Table 6.3).

Table 6.3. Volumes of Bio-rad protein dye concentrate and 1 mg ml^{-1} BSA used in the construction of the calibration graph. All measurements were carried out in triplicate.

Bio-rad protein dye concentrate / μl	1 mg ml^{-1} BSA / μl
150	5
150	10
150	15
150	20

The amount of protein in each enzyme fraction (150 μl) was then determined by using this graph to indicate the corresponding mass of protein to the absorbance of the enzyme at 595 nm. Assays were carried out in technical triplicate.

6.3.12. Identification of proteins by tryptic digest and nano LC-ESI-MS/MS

The Coomassie-stained gel bands were processed and tryptically digested. The extracted peptides from each sample were analyzed by nano LC-ESI-MS/MS using Nano Acquity/Ultima Global Instrumentation (Waters), using a 30-min LC gradient. All MS and MS/MS data were corrected for mass drift using reference data collected from [Glc']-fibrinopeptide B (human-F 3261 Sigma), which was sampled at each one-minute interval during data collection.

The data were processed to generate peak list files using Protein Lynx Global Server v 2.5.1.

6.3.13. Solution-based tryptic digest and protein identification by nano LC-ESI-MS/MS

Each sample was solubilized and a solution containing Rapigest surfactant (Waters corp. -186001861) was added to the sample to give a final concentration of 0.2 % Rapigest. Each solution was then concentrated using an Amicon Ultra-0.5 Centrifugal Filter Unit with Ultracel 3 kDa membrane (Millipore-UFC500396) at 12, 000 g to a final volume of ~ 25 μ l, and subsequently heated at 80 °C for 15 min. Dithiothreitol (5 μ l, 100 mM) was then added and the solution incubated at 60 °C for 15 min, followed by the addition of iodoacetamide (5 μ l, 200 mM) and the solutions left in the dark at room temperature for 30 min. Trypsin solution (2 μ l of 1 μ g μ l⁻¹) was then transferred to each sample, which was incubated overnight at 37 °C. The surfactant was hydrolyzed by the addition of conc. formic acid (2 μ l) at 37 °C for 20 min, and each sample was then filtered through a 0.22 μ m Costar[®] Spin-X[®] centrifuge tube filter.

References

1. N. Sarkar, S.K. Ghosh, S. Bannerjee, K. Aikat. *Renewable Energy*, 2012, **37**, 19–27.
2. Biomass Energy Center. <http://www.biomassenergycentre.org.uk>.
3. Anon. Survey of energy resources, World energy council. 20th ed. Oxford: Elsevier Ltd; 2004. p. 267.
4. J.Y. Zhu, X.S. Zhuang. *Prog. Energy Combust. Sci*, 2012, **38**, 583–598.
5. EC (European Commission, directorate general for research). *Towards a European knowledge-based bio-economy workshop conclusions on the use of plant biotechnology for the production of industrial bio-based products*. EUR 21459, Brussels, Belgium; 2004. Available from: http://ec.europa.eu/research/agriculture/library_en.htm.
6. F. Cherubini. *Energy Convers. Manage.*, 2010, **51** (7), 1412–1421.
7. F. Cherubini, S. Ulgiati. *Appl. Energy*, 2010, **87**, 47–57.
8. National Renewable Energy Laboratory: <http://www.nrel.gov/biomass/biorefinery.html>.
9. F. Wei, N.U.Nair, H. Zhao. *Curr. Biotechnol.*, 2009, **20**: 412–419.
10. R.E.H. Sims, W. Mabee, J.N. Saddler, M. Taylor. *Biores. Technol.*, 2010, **101**: 1570–1580.
11. P. Abdeshahian, M.G. Dushti, M.S. Kalil, W.M.W. Yusoff. *Biotechnol.*, 2010, **9** (3): 274–282.
12. ‘Sustainable biofuels: prospects and challenges’, policy document, RSC, 2008, London.
13. L. Cadoche, G.D. Lope. *Biology of Wastes*, 1989, **30**, 153–157.
14. P. Binod, R. Sindhu, R.R. Singhanian, S. Vikram, L. Devi, S. Nagalakshmi. *Biores. Technol.*, 2010, **101** (4), 767–774.
15. S.J.B. Duff, W.D. Murray. *Biores. Technol.*, 1996, **55**, 1–33.
16. N. S. Mosier, C. Wyman, B. Dale B. *Biores. Technol.*, 2005; **96**: 673–686.
17. G. Peiji, Q. Yinbo, Z. Xin, Z. Mingtian, D. Yongcheng. *Enzyme Microb. Technol.*, 1997, **20**; 581–584.
18. http://www.life.ku.dk/forskning/online_artikler/artikler/marken_en_stor_solfanger.asp
19. D. Crawford, M.J. Barder, A.L. Pometto, R.L. Crawford. *Arch. Microbiol.*, 1982, **131**: 140–145.
20. S. Reshamwala, B.T. Shawky, B.E. Dale, *Appl. Biochem. Biotechnol.*, 1995, **51/52**, 43–55.

21. S.W. Cheung, B.C. Anderson, *Biores. Technol.*, 1997, **59**, 81–96.
22. M. Laser, D. Schulman, S.G. Allen, J. Lichwa, M.J. Antal, L.R. Lynd, *Biores. Technol.*, 2002, **81**; 33–44.
23. M.J. Negro, P. Manzanares, I. Ballesteros, J.M. Oliva, A. Cabanas, M. Ballesteros, *Appl. Biochem. Biotechnol.*, 2003, **105**; 87–100.
24. H. Olivier-Bourbigou, L. Magna, D. Morvan. *Appl. Catal.*, 2010, **373**; 1–56.
25. G. Muralikrishna, M.V.S.S.T. Subba Rao, *Crit. Rev. Food Sci. Nutrition*, 2007, **47**; 599.
26. J.P. Joseleau, J. Conlrat, K. Ruel. *Prog. Biotechnol.*, 1992, **7**; 1–15.
27. D. Shallom, Y. Shoham. *Curr. Microbiol.*, 2003, **6** (3); 219–228.
28. K.V. Sarkanen, H.L. Hergert, in *Lignins: Occurrence, Formation, Structure and Reactions*, 1971, **43**.
29. R. Hayatsu, R.E. Winans, R.L. McBeth, R.G. Scott, L.P. Moore, M.H. Studier. *Nature*, 1979, **278**; 41–43.
30. K.E.L. Eriksson, H. Bermek. *Appl. Microbiol.*, 2009, 373–384.
31. W. Boerjan, J. Ralph, M. Baucher. *Annu. Rev. Plant Physiol.*, 2003, **54**; 519–546.
32. F. Chen, R.A. Dixon. *Nat. Biotechnol.*, 2007, **25**; 759.
33. H.R. Bjørsvik, L. Liguori. *Org. Process Res. Dev.*, 2002, **6** (3); 279–290.
34. N.J. Walton, M.J. Mayer, A. Narbad. *Phytochemistry*, 2003, **63**; 505–515.
35. J.D.P. Araujo, C.A. Grande, A.E. Rodrigues. *Chem. Eng. Res. Des.*, 2010, doi: 10.1016/j.cherd.2010.01.021.
36. V. Chang, M. Holtzapfle. *Appl. Biochem. Biotechnol.*, 2000, **84/86**; 5–37.
37. B.S. Dien, M.A. Cotta, T.W. Jeffries. *Appl. Microbiol. Biotechnol.*, 2003, **63**; 258–266.
38. F. Wei, N.U. Nair, H. Zhao. *Curr. Biotechnol.*, 2009, **20**; 412–419.
39. R.E.H. Sims, W. Mabee, J.N. Saddler, M. Taylor. *Biores. Technol.*, 2010, **101**: 1570–1580.
40. A. Demirbas. *Energy Sources*, 2005, **27**; 327–33.
41. Y. Zheng, Z. Pan, R. Zhang. *Int. J. Agric. & Biol. Eng.*, 2009), **2** (3); 51–68.
42. H. Zhao, G.A. Baker, Z. Song, O. Olubajo, T. Crittle, D. Peters, *Green Chem.*, 2008, **10**; 696–705.
43. R.P. Chandra, R. Bura, W.E. Mabee, A. Berlin, X. Pan, J.N. Saddler. *Biofuels*, 2007, **108**; 67–93.

44. O.J. Sanchez, C.A. Cardona. *Biores. Technol.*, 2008, **99**; 5270–5295.
45. S. Prasad, A. Singh, H.C. Joshi. *Resour. Conserv. Recycl.*, 2007, **50**; 1–39.
46. G.Y.S. Mtui. *Afr. J. Biotechnol.*, 2009, **8 (8)**; 1398–1415.
47. P. Das, A. Ganesha, P. Wangikar. *Biomass Bioenergy*, 2004, **27**; 445–457.
48. Fan, M.M. Gharpuray, Y.H. Lee. *Cellulose hydrolysis biotechnology monographs*, 1987; 57.
49. Y. Sun, J. Cheng. *Biores. Technol.*, 2002, **96**; 673–686.
50. A.B. Bjerre, A.B. Olesen, T. Fernqvist. *Biotechnol. Bioeng.*, 1996, **49**; 568–577.
51. A. Pandey. *Handbook of plant-based biofuels. 2009, New York: CRC Press.*
52. F. Talebnia, D. Karakashev, I. Angelidaki. *Biores. Technol.*, 2010, **101 (13)**; 4744–4753.
53. X.J. Pan, C. Arato, N. Gilkes, D. Gregg, W. Mabee, K. Pye, Z. Xiao, X. Zhang, J. Saddler, J. *Biotechnol. Bioeng.*, 2005, **90**; 473–481.
54. X.J. Pan, N. Gilkes, J. Kadla, K. Pye, S. Saka, D. Gregg, K. Ehara, D. Xie, D. Lam, J. Saddler. *Biotechnol. Bioeng.*, 2006, **94**; 851–861.
55. X.J. Pan, D. Xie, R.W. Yu, J.N. Saddler. *Biotechnol. Bioeng.*, 2008, **101**; 39–48.
56. R. Solar, E. Gajdos, D. Kacikova, F. Kacik. *Cell. Chem. Technol.*, 2000, **34**; 571–580.
57. L. Jimenez, M.J. de la Torre, J.L. Ferrer, J.C. Garcia. *Proc. Biochem.*, 1999, **35 (1–2)**; 143–148.
58. R.C. Remsing, R.P. Swatloski, R.D. Rogers, G. Moyna. *Chem. Commun.*, 2006, 1271.
59. L. Kilpelainen, H. Xie, A. King, M. Granstrom, S. Heikkinen, D.S. Argyropoulos. *J. Agric. Food Chem.*, 2007, **55**; 9142.
60. Y. Pu, N. Jiang, A.J. Ragauskas. *J. Wood Chem. Technol.*, 2007, **27**; 23.
61. A. Dadi, S. Varanasi, C. Schall. *Biotechnol. Bioeng.*, 2006, **95 (5)**; 904–910.
62. Z.C. Zhang. *Adv. Catal.*, 2006, **49**; 153.
63. H. Olivier-Bourbigou, L. Magna, D. Morvan. *Appl. Catal.*, 2010, **373**; 1.
64. T.V. Doherty, R.J. Linhardt, J.S. Dordick JS. *Biotechnol. Bioeng.*, 2009, **102 (5)**; 1368 – 1376.
65. G.A. Smook. *Handbook for Pulp and Paper Technologists*, 1992, **11 (2)**; 163–183.
66. G. Gellerstedt, E. Lindfors. *Svensk Papperstidning*, 1984, **9**; 61–67.
67. J. Gierer. *Wood Sci. Technol.*, 1980, **14**; 241–266.

68. J. Gierer. *Wood Sci. Technol.*, 1985, **19**; 289–312.
69. J. Gierer. *Svensk Papperstidning*, 1970, **18**; 571–596.
70. J. Gierer. *Holzforschung*, 1982, **36**; 43–51.
71. M. Kurakake, N. Ide, T. Komaki. *Curr. Microbiol.*, 2007, **54**; 424–428.
72. J.W. Lee, K.S. Gwak, J.Y. Park. *J. Microbiol.*, 2007, **45**: 485–491.
73. P. Singh, A. Suman, P. Tiwari. *World J. Microbiol. Biotechnol.*, 2008, **24**; 667–673.
74. E. Sjostrom. *Wood Chemistry Fundamentals and Applications*, 1993, **2**; 54–89.
75. K.E.L. Eriksson, H. Bermek. *Appl. Microbiol.*, 2009; 373–384.
76. R. Vicuna. *Enzyme Microbiol. Technol.*, 1988, **10**; 646–655.
77. H.H. Nimtz, J. Tappi. New York, 1971, **56**; 124.
78. J. Ralph, J. Peng, F. Lu, R.D. Hatfield. *J. Agric. Food Chem.*, 1999, **47 (8)**; 2991–2996.
79. E. Adler. *Wood Sci. Technol.*, 1977, **11**; 169–218.
80. E. Sjostrom. *Wood Chemistry: Fundamentals and Applications*, 1981; 68–82.
81. K.V. Sarkanen, C.H. Ludwig. *Occurrence, Formation, Structure and Reactions*, 1971; 95–240.
82. P. Karhunen, P. Rummakko, G. Brunow. *Tetrahedron Lett.*, 1995, **36 (25)**; 4501–4504.
83. P. Karhunen, P. Rummakko, J. Sipila, G. Brunow. *Tetrahedron Lett.*, 1995, **36 (1)**; 169–170.
84. R. Vanholme, B. Demedts, K. Morreel, J. Ralph, W. Boerjan. *Plant Physiol.*, 2010, **153**; 895–905.
85. R. Hayatsu, R.E. Winans, R.L. McBeth, R.G. Scott, L.P. Moore, M.H. Studier. *Nature*, 1979, **278**: 41–43.
86. W. Boerjan, J. Ralph, M. Baucher. *Ann. Rev. Plant Biol.*, 2003, **54**; 519–546.
87. H. Hisano, R. Nandakumar, Z-Y. Wang. *Dev. Biol. Plant.*, 2009, **45**; 306.
88. T. Liitia, S.L. Maunu, B. Hortling. *J. Pulp. Pap. Sci.*, 2000, **26**; 323–330.
89. T. Liitia, S.L. Maunu, B. Hortling. *Holzforschung*, 2001, **55**; 503–510.
90. B. Hortling, E. Turunen, J. Sundquist. *Nord. Pulp. Pap. Res. J.*, 1992, **7**; 144–151.
91. W.F. Manders. *Holzforschung*, 1987, **41**; 13–18.
92. G.E. Hawkes, C.Z. Smith, J.H.P. Utley, R.R. Vargas, H. Viertler. *Holzforschung*, 1993, **47**; 302–312.

93. K.M. Holtman, H. Chang, H. Jameel. *J. Wood. Chem. Technol.*, 2006, **26**; 21 – 34.
94. O. Faix, S.Y. Lin, C.W. Dence. *Methods in Lignin Chemistry*, 1992, 83 – 109.
95. K.K. Pandey. *J. Appl. Polym. Sci.*, 1999, **71**; 1969 – 1975.
96. C-M. Popescu, G.H. Singwel, C. Vasile, D.S. Argyropoulos, S. Willfor. *Appl. Spectrosc.*, 2009, **61**, 1168 – 1177.
97. O. Faix, J. Bremner, O. Schmidt, T. Stevanovic. *J. Anal. Appl. Pyrol.*, 1993, **21**; 147 – 162.
98. I. Korner, O. Faix, O. Wienhaus. *Holz. Roh. Werkst.*, 1992, **50**; 363 – 367.
99. M.P.C. Conrad, G.D. Smith, G. Fernlund, *Wood Fiber Sci.*, 2003, **35**; 570.
100. D.B. Johnson, W.E. Moore, and L.C. Zank. *Tappi*, 1961, **44**: 793 – 798.
101. R.S. Fukushima, B.A. Dehority. *J. Anim. Sci.*, 2000, **78**, 3135 – 3143.
102. R.S. Fukushima, R.D. Hatfield. *J. Agric. Food Chem.*, 2001, **46**, 3133 – 3139.
103. R.S. Fukushima, R.D. Hatfield. *J. Agric. Food Chem.*, 2004, **52**, 3713 – 3720.
104. A.T. Martinez, F. Ruiz-Duenas, M. Jesus Martinez, J.Rio, A. Gutierrez. *Curr. Opin. Biotechnol.*, 2009, **20**; 348 – 357.
105. W. Zimmermann. *J. Biotechnol.*, 1988, **10**; 646 – 655.
106. K. Haider, J. Trojanowski, V. Sundman. *Arch. Microbiol.*, 1978, **119**; 103 – 106.
107. F. Perestelo, A. Rodrigues, R. Perez, A. Carnicero, G. De La Fuente, M. Falcon. *World J. Microbiol. Biotechnol.*, 1996, **12**; 111 – 112.
108. A. Raj, R. Chandra, M.K. Reddy, H.J. Purohit, A. Kapley. *World J. Microbiol. Biotechnol.*, 2007; **23**; 793 – 799.
109. G. Singh, N. Capalash, R. Goel, P. Sharma. *Enzyme Microb. Technol.*, 2007, **41**, 794 – 799.
110. V. Antonopoulos, M. Hernandez, M. Arias, E. Mavrakos, A. Ball. *Appl. Microbiol. Biotechnol.*, 2001, **57**, 92 – 97.
111. L. Bandounas, N.J.P. Wierckx, J. H. de Winde, H. J. Ruijssenaars. *BMC Biotechnology*, 2011,**11**; 94.
112. C.R.Taylor, E.M. Hardiman, M. Ahmad, P.D. Sainsbury, P.R. Norris, T.D.H. Bugg. *J. Appl. Microbiol.*, 2012, **3**; 521 – 530.
113. M.H. Gold, M. Alic. *Microbiol. Rev.*, 1993, **57**; 605 – 622.
114. W. Blodig, A.T. Smith, W.A. Doyle, K. Piontek. *J. Mol. Biol.*, 2000, **305**; 851 – 861.

115. T. Higuchi. *Proceedings of the Japan Academy Series B- Physical and Biological Sciences*, 2004, **80**; 204 – 214.
116. R.C. Bonguli-Santos, L.R. Durrant, M. Da Silva, L.D. Sette. *Enz. And Microb. Tech.*, 2010, **46**; 32 – 37.
117. E.I. Solomon, U.M. Sundaram, T.E. Machonkin. *Chem. Rev.*, 1996, **96**; 2563 – 2605.
118. N.T. Dimmer, M.R. Kanost. *Insect Biochem. And. Mol. Biol.*, 2010, **40**; 179 – 188.
119. D. L. Crawford. *Enzyme Microb. Technol.*, 1980, **2**; 11 – 22.
120. B.M. Lahtinen, K. Kruus, H. Boer, M. Kernell, M. Andberg, L. Viikani, J. Sipila. *J. Mol. Cat. B: Enz.*, 2009, **57**; 204 – 210.
121. J-A. Majeau, S.K. Brar, R.D. Tyagi. *J. Biores. Technol.*, 2010, **101**; 2331 – 2350.
122. N. Hakulinen, L-L. Kiiskinen, K. Kruus, M. Saloheimo, A. Koivula, J. Rouvinen. *Nature Struct. Biol.*, 2002, **9**; 601 – 605.
123. U. Urzua, P. J. Kersten, R. Vicuna. *Appl. Environ. Microbiol.*, 1998, **64**; 68 – 73.
124. M. Hofrichter, D. Ziegenhagen, T. Vares, M. Friedrich, M. G. Jager, W. Fritsche, A. Hatakka. *FEBS Lett.*, 1998, **434**; 362 – 366.
125. C. Hofer, D. Schlosser. *FEBS Lett.*, 1999, **451**; 186 – 190.
126. V. Gomez-Toribio, A. T. Martínez, M. J. Martínez, F. Guillen. *Eur. J. Biochem.*, 2001, **268**; 4787 – 4793.
127. C. Munoz, F. Guillen, A. T. Martínez, and M. J. Martínez. *Appl. Environ. Microbiol.*, 1997, **63**; 2166 – 2174.
128. F.S. Archibald, I. Fridovich. *Arch. Biochem. Biophys.*, 1982, **214**; 452 – 463.
129. U. Urzua, P. J. Kersten, R. Vicuna. *Arch. Biochem. Biophys.*, 1998, **360**; 215 – 222.
130. D. Crawford, R. Crawford, A. Pometto. *Appl. Environ. Microbiol.*, 1983, **45**; 898 – 904.
131. Y. Sugano. *Cell. Mol. Life Sci.*, 2009, **66**; 1387 – 1403.
132. M. Ahmad, J.N. Roberts, E.M. Hardiman, R. Singh, L.D. Eltis, T.D.H. Bugg. *Biochemistry*, 2011, **50**; 5096 – 5107.
133. T. Nilsson, G. Daniel. *International Symposium of Wood and Pulping Chemistry, Technical papers, Vancouver*, 1985; 175.
134. G.F. Daniel, T. Nilsson. *Wood Preservation*, 1986; 1283.

135. T. Nilsson, G. Daniel. *Biodegradation*, 1988, **7**; 739 – 742.
136. T. Sonok, Y. Limura, E. Masai, S. Kajita, Y. Katayama. *J. Wood Sci.*, 2002, **48**; 429 – 433.
137. E. Masai, Y. Katayama, M. Fukuda. *Biosci. Biotechnol. Biochem.*, 2007, **71**; 1 – 15.
138. M. Seeger, K.N. Timmis, B. Hofer. *Marine Chem.*, 1997, **58**; 327 – 333.
139. F. Furukawa, H. Suenaga, M. Goto. *J. Bacteriol.*, 2004, **186 (16)**; 5189 – 5196.
140. Q. Hong, X. Dong, L. He, X. Jiang, S. Li. *Int. Biodeter. & Biodeg.*, 2009, **63**; 365 – 370.
141. J. Van der Meer. *J. Gen. Mol. Microbiol.*, 1997, **71**; 159 – 178.
142. G.M. Klecka, D.T. Gibson. *Appl. Environ. Microbiol.*, 1981, **41**; 1159 – 1165.
143. E. Schmidt, I. Bartels, H. Knackmuss. *FEMS Microbiol. Ecol.*, 1985, **31**; 381 – 389.
144. J. Davis, J. Sello. *Appl. Microbiol. Biotechnol.*, 2010, **86**; 921 – 929.
145. B. Karmakar, R.M. Vohra, H. Nandanwar, P. Sharma, K.G. Gupta, R.C. Sobti. *J. Biotechnol.*, 2000, **80**; 195 – 202.

146. J.P.N. Rosazza, Z. Huang, L. Dostal. *J. Ind. Microbiol.* 1995, **15**; 457 – 471.
147. A. Toms, J.M. Wood. *J. Biochem.*, 1970, **9**; 337 – 343.
148. A. Narbad, M.J. Gasson. *J. Microbiol.*, 1998, **144**; 1397 – 1405.
149. G. Singh, N. Ahuja, M. Batish, N. Capalash, P. Sharma. *Biores. Technol.*, 2008, **99**; 7472 – 7479.
150. A. Unall, N. Kolankaya. *Turk. J. Biol.*, 2001, **41**; 67 – 72.
151. M.E. Brown, M.C. Walker, T.G. Nakashige, A.T. Iavarone, M.C.Y. Chang. *J. Am. Chem. Soc.*, 2011, **133 (45)**; 18006 – 18009.
152. F. Niehaus, C. Bertoldo, M. Kaehler, G. Antranikian. *Appl. Microbiol. Biotechnol.*, 1999, **51**; 711 – 729.

153. J.L. Yang, K.E.L. Eriksson. *Holzforschung*, 1992, **46**; 481 – 488.
154. C.C. Chen, R. Adolphson, F.D.J. Dean, K.E.L. Eriksson, M.W.W. Adamas, J. Westpheling. *Enzyme Microbiol. Technol.*, 1997, **20**; 39 – 45.
155. K. Haider, J. Trojanowski, V. Sundman. *Arch. Microbiol.*, 1978, **119**; 103 – 106.
156. M. Tien, T. K. Kirk. *Burds. Science*, 1983, **221**; 661 – 663.
157. M. Tien, T. K. Kirk. *Proc. Natl. Acad. Sci.*, 1984, **81**; 2280 – 2284.

158. F.S. Archibald. *Appl. Environ. Microbiol.*, 1992; 3110 – 3116.
159. M. Ahmad, C.R. Taylor, D. Pink, K. Burton, D. Eastwood, G.D. Bending, T.D.H. Bugg. *Mol. Biosyst.*, 2010, **6**, 815 – 821.
160. K. Kato, S. Kozaki, M. Sakuranaga. *Biotechnol. Lett.*, 1998, **20**; 459 – 462.
161. S.M. Geib, T.R. Filley, P.G. Hatcher, K. Hoover, J.E. Carlson, M. Jimenez-Gasco, A. Nakagawa-Izumi, R.L. Sleighter, M. Tien. *Proc. Natl. Acad. Sci.*, 2008, **105**; 12932 – 12937.
162. T.D.H. Bugg, M. Ahmad, E.M. Hardiman, R. Singh. *Curr. Opin. Biotechnol.*, 2011, **22**; 394 – 400.
163. T.D.H. Bugg, M. Ahmad, E.M. Hardiman, R. Rahmanpour. *Nat. Prod. Rep.*, 2011, **28**, 1883 – 1896.
164. M. Kosa, A.J. Ragauskas. *Appl. Microbiol. Biotechnol.*, 2012, **93**; 891 – 900.
165. D.O. Rybkina, E.G. Plotnikova, L.V. Dorofeeva, Y.L. Mironenko, and V.A. Demakov. *Microbiology*, 2003, **72**; 672 – 677.
166. H.M. Zhang, A. Kallimanis, A.I. Koukkou, and C. Drainas. *Appl. Microbiol. Biotech.*, 2004, **65**; 124 – 131.
167. M. Wenzel, I. Schönig, M. Berchtold, P. Kämpfer, H. König. *J. Appl. Microbiol.*, 2002, **92**; 32 – 40.
168. L.N. Ten, Q-M. Liu, W-T. Im, Z. Aslam, and S-T. Lee. *J. Microbiol. Biotech.*, 2006, **16**; 1728 – 1733.
169. M.L. Suihko, E. Skytta. *J. Ind. Microbiol. Biotech.*, 2009, **36**; 53 – 64.
170. D.P. Dhawal, P. Tamboli, A.A. Telke, V.V. Dawkar, S.B. Jadhav, S.P. Govindwar. *Biotechnol. Bioproc. Eng.*, 2011, **16**; 661 – 668.
171. P. Ander, L. Marzullo. *J. Biotechnol.*, 1997, **53**; 115 – 131.
172. A. Telke, D. Kalyani, J. Jadhav, and S. Govindwar. *Acta Chim. Slov.*, 2008, **55**; 320 – 329.
173. A. Lykidis, K. Mavromatis, N. Ivanova, I. Anderson, M. Land, G. Di Bartolo, M. Martinez, A. Lapidus. *J. Bacteriol.*, 2007, **189**; 2477 – 2486.
174. A. Saeed, P. Fatehi, Y. Ni. *Biotechnol. Prog.*, 2012, **28** (4); 998 – 1004.
175. M.B. Prieto, A. Hidalgo, J.L. Serra. *J. Biotechnol.*, **97** (2002) 1 – 11.
176. M. Vesely, M. Patek, J. Nesvera, A. Cejkova, J. Masak, V. Jirku. *Appl. Microbiol. Biotechnol.*, 2003, **61** (5 – 6); 523 – 527.

177. M. Seto, K. Kimbara, M. Shimura, T. Hatta, M. Fukuda, K. Yano. *Appl. Environ. Microbiol.*, 1995, **6**; 3353 – 3358.
178. J.A. Zermeno-Equia Liz, J. Jan-Roblero, J. Zavala-Diaz de la Serna, A. Vera-Once de Leon, C. Nernandez-Rodriguez. *World J. Microbiol. Biotech.*, 2009, **25**; 165 – 170.
179. D. Ghosal, J. Chakraborty, P. Khara, and T.K. Dutta. *FEMS Microbiol. Lett.*, 2010, **313**; 103 – 110.
180. Faix, O., Lange, W., Salud, E.C. *Holzforschung*, 1981, **35**; 3 – 9.
181. D. Feldman. Ed. Hu, T.Q. Kluwer *Academic, New York*, 2002; 81 – 99.
182. S. Baumberger. *Academic, New York*, 2002; 1 – 20.
183. D. Robert, M. Bardet, G. Gellerstedt, E-L. Lindfors. *J. Wood Chem. Technol.*, 1984, **4**; 239 – 263.
184. B. Hortling, M. Ranua. *Pap. Res. J.*, 1990, **5**; 33 – 37.
185. V.L. Singleton, J.A. Rossi. *Am. J. Enol. Vitic.*, 1965, **16**; 144 – 158.
186. V.L. Singleton, R. Orthofer, R.M. Lamuela-Raventos. *Methods Enzymol.*, 1999, **299**; 152 – 178.
187. G.L. Miller. *Anal. Chem.*, 1959, **31 (3)**; 426 – 428.
188. R. Winston Liggett, H. Koffler. *Bacteriol. Rev.*, 1948, **12 (4)**; 297.
189. A. Ruiter. *Schmidtdorff, W. ed.*, 1995; 347 – 376.
190. B-W. Koo, N. Park, H-S. Jeong, J-W. Choi, H. Yeo, I-G. Choi. *J. Ind. Eng. Chem.*, 2011, **17 (1)**; 18 – 24.
191. T. Todorciuc, A-M. Capraru, I. Kratochvilova, V.I. Popa. *Cellulose Chem. Technol.*, 2009, **43 (9 –10)**; 399 – 408.
192. R. Rana, R. Langenfeld-Heyser, R. Finkeldey, A. Polle. *Wood Sci. Technol.*, 2010, **44**; 225 – 242.
193. P.S. Parker. Plenum press, New York, 1983; 21 – 25.
194. M.M. Bradford. *Anal. Biochem.*, 1976, **72**; 248 – 254.
195. J. Pütter, R. Becker. *Methods of Enzymatic Analysis*, 1983, **3 (3)**; 286 – 293.
196. C. Bull, E.C. Niederhoffer, T. Yoshida, J.A. Fee. *J. Am. Chem. Soc.*, 1991, **113**; 4069 – 4076.

197. M.L. Ludwig, A.L. Metzger, K.A. Pattridge, W.C. Stallings. *J. Mol. Biol.*, 1991, **219**; 335 – 358.
198. D.P. Barr, S.D. Aust. *Arch. Biochem. Biophys.*, 1994, **311 (2)**; 378 – 382.
199. P.A. Belinky, N. Flikshtein, C.G. Dosoretz. *Enz. Microb. Technol.*, 2006, **39**; 222 – 228.
200. P. Ander, C. Mishra, R.L. Farrell, K-E.L. Eriksson. *J. Biotechnol.*, DOI:10.1016/0168-1656(90)90104-J.